MODELING AND ROBUST CONTROL OF TWO COLLABORATIVE ROBOT MANIPULATORS HANDLING A FLEXIBLE OBJECT

BALASUBRAMANIAN ESAKKI

A THESIS

IN THE DEPARTMENT OF

MECHANICAL AND INDUSTRIAL ENGINEERING

PRESENTED IN PARTIAL FULFILLMENT OF THE REQUIREMENTS

FOR THE DEGREE OF DOCTOR OF PHILOSOPHY

CONCORDIA UNIVERSITY

MONTRÉAL, QUÉBEC, CANADA

MARCH 2011

CONCORDIA UNIVERSITY

SCHOOL OF GRADUATE STUDIES

This is to certify that the thesis prepared

By: **Balasubramanian Esakki**

Entitled: **Modeling and Robust Control of Two Collaborative Robot Manipulators Handling a Flexible Object**

and submitted in partial fulfillment of the requirements for the degree of

DOCTOR OF PHILOSOPHY (Mechanical Engineering)

complies with the regulations of the University and meets the accepted standards with respect to originality and quality.

Signed by the final examining committee:

_____ Chair
Dr. O. Ormandjieva

_____ External Examiner
Dr. G. Liu

_____ External to Program
Dr. S. Williamson

_____ Examiner
Dr. R. Sedaghati

_____ Examiner
Dr. Y. Zhang

_____ Thesis Co-Supervisor
Dr. R. Bhat

_____ Thesis Co-Supervisor
Dr. C.Y. Su

Approved by _____
Dr. W-F. Xie, Graduate Program Director

March 24, 2011

_____
Dr. Robin A.L. Drew, Dean
Faculty of Engineering & Computer Science

ABSTRACT

Modeling and Robust Control of Two Collaborative Robot Manipulators Handling a Flexible Object

Balasubramanian Esakki, Ph.D.

Concordia University, 2011

Robots are often used in industry to handle flexible objects, such as frames, beams, thin plates, rubber tubes, leather goods and composite materials. Moving long flexible objects in a desired path and also precise positioning and orienting the objects need a collaborative action between two robot arms. Most of the earlier studies have dealt with manipulation of rigid objects and only a few have focused on the collaborative manipulators handling flexible objects. Such studies on handling of flexible objects generally used finite element method or assumed mode method for deriving the dynamic model of the flexible objects. These approximation methods require more number of sensors to feedback the vibration measurements or require an observer. Unlike in the earlier studies, this thesis concerns with development of a dynamic model of the flexible object in partial differential equation (PDE) form and design of a robust control strategy for collaborative manipulation of the flexible objects by two rigid robot arms.

Two planar rigid manipulators each with three links and revolute joints handling a flexible object is considered during the model development. Kinematic and dynamic equations of the flexible object are derived without using any approximation techniques. The

resulting dynamic equation of the flexible object together with the manipulator dynamic equations form the combined dynamic model of the system. The developed complete system of dynamic equations is described by the PDE's having rigid as well as flexible parameters coupled together. Such a coupled system must be controlled without using any form of approximation techniques and this is accomplished using the singular perturbation approach. By utilizing this technique, slow and fast subsystems are identified in two different time scales and controller is designed for each subsystem. The key issue in developing a control algorithm is that, it should be robust against uncertain parameters of the manipulators and the flexible object and it should also achieve the exponential convergence. Hence, for the slow subsystem, sliding mode control algorithm is developed and for the fast subsystem, a simple feedback control algorithm is designed. In general, usage of singular perturbation technique necessitates exponential stability of the slow and fast subsystems, which is evaluated by satisfying the Tikhnov's theorem. Hence, the exponential stability analysis for both the subsystems is performed. Simulation results are presented to validate the composite control scheme.

As a further consideration in the improvement of control law for the slow subsystem, two modified control algorithms are suggested. The first one focused on the avoidance of velocity signal measurement which is useful to eliminate the need of velocity sensors and the second controller aims at avoiding the complex regressor in the control law. The capability of those controllers is illustrated through simulation studies. The extension of earlier analysis has been carried out by developing the complete system of dynamic equations in joint space.

ACKNOWLEDGEMENTS

I would like to express my deepest gratitude to Dr. B. V. A. Rao, for showing me the way to Concordia University.

I am very much thankful to my supervisors Prof. Rama Bhat and Prof. Chun-Yi Su for their continuous support and encouragement during my research. Their help, patience and guidance enabled me to complete this thesis. I benefited greatly from their encouragement and care throughout my course of studies.

I wish to acknowledge the financial assistance provided by Government of India through High Commission of India, Ottawa and very much thankful for their support.

I also thank Dr. Vivek, Dr. Vasudevan, Dr. Alfin, Dr. Krishna Prasad, Mr. Wijendra and all my friends for their constant support and encouragement throughout the course of this work.

I would like to thank particularly my wife Mrs. Priyalakshmi whose continuous support and patience throughout my Ph.D. program have enabled me to produce this thesis. I also thank my child Miss. Lakshitaa for her patience and understanding.

Finally, I sincerely thank my parents Mr. Esakki and Mrs. Saroja and my uncle and aunty Mr. Navaneethakrsihnan and Mrs. Amsavalli for their support.

Contents

LIST OF FIGURES **xi**

LIST OF TABLES **xvi**

LIST OF SYMBOLS **xvii**

1 Introduction **1**

1.1 Motivation 1

1.2 Literature Review 4

1.2.1 Collaborative manipulation of rigid objects 5

1.2.2 Collaborative manipulation of flexible objects 8

1.3 Scope and Objectives 12

1.4 Thesis Overview 14

2 Kinematics and Dynamics of Manipulators - Flexible Object System **16**

2.1 Introduction 16

2.2 Manipulators - flexible object system description 17

2.3 Kinematics and dynamics of the flexible object 19

2.3.1 Kinematics of the flexible object 19
2.3.2 Dynamics of the flexible object 22
2.4 Kinematics and dynamics of the manipulator 28
2.4.1 Kinematics of the manipulator 28
2.4.2 Dynamics of the manipulator 33
2.5 Combined dynamics 37
2.6 Summary 39

3 Singular Perturbation Model **40**

3.1 Need for singular perturbation analysis 40
3.2 Outline of singular perturbation approach 41
3.2.1 Singularly perturbed analysis of linear systems 42
3.2.2 Singularly perturbed analysis of nonlinear systems 43
3.2.3 Features of singularly perturbed solutions 47
3.3 Validity of singular perturbation approach 47
3.4 Singular perturbed model of the manipulators - flexible object system . . . 50
3.5 Slow and fast dynamic models 53
3.5.1 Slow subsystem 54
3.5.2 Fast subsystem 57
3.6 Summary 62

4 Controller Design **63**

4.1 Introduction 63
4.1.1 Adaptive control 64

4.1.2 Robust control 67
4.1.2.1 Sliding mode control 68
4.2 Composite control for the manipulators - flexible object system 70
4.2.1 Robust control design for slow subsystem 71
4.2.2 Control design for fast subsystem 72
4.3 Stability analysis 74
4.3.1 Stability analysis for slow subsystem 74
4.3.2 Stability analysis for fast subsystem 76
4.4 Simulation of composite controller 78
4.4.1 Avoidance of chattering in the slow subsystem control law 93
4.5 Special case as manipulators handling a rigid object 94
4.6 Summary 96

5 Further Studies on Controller Design 98

5.1 Introduction 98
5.2 Control design without velocity measurements 99
5.2.1 Stability analysis 101
5.2.2 Simulation results 103
5.3 Control design without regressor 107
5.3.1 Stability analysis 109
5.3.2 Simulation results 111
5.4 Summary 112

6 Manipulators - Flexible Object System in Joint Space 116

6.1 Introduction 116

6.2 Modeling of manipulators - flexible object system in joint space 117

6.2.1 Combined dynamics in joint space 118

6.3 Singular perturbation modeling in joint space 120

6.3.1 Slow subsystem in joint space 121

6.3.2 Fast subsystem in joint space 122

6.4 Composite control for the manipulators - flexible object system in joint space 123

6.4.1 Robust control for slow subsystem in joint space 124

6.4.1.1 Stability analysis 125

6.4.2 Feedback control for fast subsystem in joint space 126

6.4.3 Simulation results 127

6.5 Further improvements on the controller design of slow subsystem in joint space 132

6.5.1 Controller design without velocity measurements in joint space . . 134

6.5.1.1 Stability analysis 139

6.5.1.2 Simulation results 140

6.5.2 Controller design without regressor in joint space 144

6.5.2.1 Stability analysis: 145

6.5.2.2 Simulation results 147

6.6 Summary 149

7 Conclusions and Recommendations for Future Works 152

7.1 Summary 152

7.2 Major Contributions 155

7.3 Conclusions 155

7.4 Future Works 157

Bibliography **159**

Appendices **174**

A Dynamics of Beam **174**

B Regressor for Manipulator - Flexible Object System in Cartesian Space **180**

B.1 Time dependent parameters 180

B.2 Time independent parameters 196

C Regressor for Manipulators - Flexible Object System in Joint Space **199**

C.1 Time dependent parameters 199

C.2 Time independent parameters 207

List of Figures

1 A Planar manipualtor 18

2 Two planar rigid manipulators grasping a flexible object 18

3 Beam rigid body motion and deflection 20

4 Flexible beam with boundary forces 25

5 A manipulator with link-frame assignments 29

6 Two Coordinate frames A and B 30

7 Sliding surface and various initial conditions 69

8 X-Position tracking-Sliding control in CS 82

9 Y-Position tracking-Sliding control in CS 82

10 Orientation of the beam-Sliding control in CS 83

11 Circular trajectory 83

12 J1M1-Sliding control in CS 84

13 J2M1-Sliding control in CS 84

14 J3M1-Sliding control in CS 85

15 J1M2-Sliding control in CS 85

16 J2M2-Sliding control in CS 85

17 J3M2-Sliding control in CS 85
18 SV 1-Sliding control in CS 86
19 SV 2-Sliding control in CS 86
20 SV 3-Sliding control in CS 87
21 CT of J1M1-Sliding control in CS 87
22 CT of J2M1-Sliding control in CS 87
23 CT of J3M1-Sliding control in CS 88
24 CT of J1M2-Sliding control in CS 88
25 CT of J2M2-Sliding control in CS 88
26 CT of J3M2-Sliding control in CS 88
27 Structural damping characteristics $\beta = -0.5$ 89
28 Strong damping characteristics $\beta = 0$ 90
29 Deflection of the beam for Damping ratio=0.1 90
30 Deflection of the beam for Damping ratio=0.4 91
31 Deflection at 0.1 m from the left end of the beam 91
32 Deflection at mid point of the beam for E=71GPa 92
33 Deflection at mid point of the beam for E=150GPa 92
34 Deflection at mid point of the beam for E=200GPa 93
35 X-Position tracking-Without velocity measurement in CS 104
36 Y-Position tracking-Without velocity measurement in CS 104
37 Orientation of the beam-Without velocity measurement in CS 105
38 J1M1-Without velocity measurement in CS 106
39 J2M1-Without velocity measurement in CS 106

40 J3M1-Without velocity measurement in CS 106
41 J1M2-Without velocity measurement in CS 106
42 J2M2-Without velocity measurement in CS 107
43 J3M2-Without velocity measurement in CS 107
44 X-Position tracking-Without regressor in CS 112
45 Y-Position tracking-Without regressor in CS 113
46 Orientation of the beam-Without regressor in CS 113
47 J1M1-Without regressor in CS 114
48 J2M1-Without regressor in CS 114
49 J3M1-Without regressor in CS 114
50 J1M2-Without regressor in CS 114
51 J2M2-Without regressor in CS 115
52 J3M2-Without regressor in CS 115
53 X movement-Sliding control in JS 128
54 Y movement-Sliding control in JS 128
55 Orientation-Sliding control in JS 129
56 J1M1-Sliding control in JS 130
57 J2M1-Sliding control in JS 130
58 J3M1-Sliding control in JS 131
59 J1M2-Sliding control in JS 131
60 J2M2-Sliding control in JS 131
61 J3M2-Sliding control in JS 131
62 SV 1 with chattering in JS 132

63 SV 2 with chattering in JS 132
64 SV 3 with chattering in JS 132
65 SV 4 with chattering in JS 132
66 SV 5 with chattering in JS 133
67 SV 6 with chattering in JS 133
68 CT of J1M1 with chattering in JS 133
69 CT of J2M1 with chattering in JS 133
70 CT of J3M1 with chattering in JS 134
71 CT of J1M2 with chattering in JS 134
72 CT of J2M2 with chattering in JS 134
73 CT of J3M2 with chattering in JS 134
74 SV 1 without chattering in JS 135
75 SV 2 without chattering in JS 135
76 SV 3 without chattering in JS 135
77 SV 4 without chattering in JS 135
78 SV 5 without chattering in JS 136
79 SV 6 without chattering in JS 136
80 CT of J1M1 without chattering in JS 136
81 CT of J2M1 without chattering in JS 136
82 CT of J3M1 without chattering in JS 137
83 CT of J1M2 without chattering in JS 137
84 CT of J2M2 without chattering in JS 137
85 CT of J3M2 without chattering in JS 137

86 X movement-Without velocity measurement in JS 141
87 Y movement-Without velocity measurement in JS 142
88 Orientation-Without velocity measurement in JS 142
89 J1M1-Without velocity measurement in JS 143
90 J2M1-Without velocity measurement in JS 143
91 J3M1-Without velocity measurement in JS 143
92 J1M2-Without velocity measurement in JS 143
93 J2M2-Without velocity measurement in JS 144
94 J3M2-Without velocity measurement in JS 144
95 X movement-Without regressor in JS 148
96 Y movement-Without regressor in JS 148
97 Orientation-Without regressor in JS 149
98 J1M1-Without regressor in JS 150
99 J2M1-Without regressor in JS 150
100 J3M1-Without regressor in JS 150
101 J1M2-Without regressor in JS 150
102 J2M2-Without regressor in JS 151
103 J3M2-Without regressor in JS 151

List of Tables

1 Parameters of the manipulator 81

2 Parameters of the flexible beam 84

3 Control parameters-sliding control in CS 84

4 Control parameters-without velocity measurements in CS 105

5 Parameters of the manipulator 127

6 Parameters of the beam 129

7 Control parameters-sliding control in JS 130

8 Control parameters-without velocity measurements in JS 141

List of Symbols

A	Differential operator in Hilbert space.
A_{jf}	Transverse vibration parameter matrix.
a	Arbitrary constant to satisfy the equality.
a_c	Non-negative constant.
b_c	Non-negative constant.
C_i	Coriolis and centrifugal components of a i^{th} manipulator.
C_o	Semigroup.
C_r	Coriolis and centrifugal components of two manipulators in assembled form.
C_{or}	Coriolis and centrifugal components of combined dynamics for the case of manipulator handling rigid beam.
C_{rd}	Coriolis components of the beam with only rigid parameters.
C_{cs}	Coriolis and centrifugal components of slow subsystem in CS.
C_{js}	Coriolis and centrifugal components of slow subsystem in JS.
C_{rf}	Centrifugal components of the beam with flexible and rigid parameters.

C_{jsf}	Coriolis and centrifugal components of combined rigid motion dynamics of the system in JS.
C_{orf}	Coriolis and centrifugal components of combined rigid motion dynamics of the system in CS.
c_0	Mass center of the beam.
$c_1,\ c_2$	Arbitrary constants for fast subsystem stability analysis.
$D(A)$	Domain of the operator A.
E	Young's modulus of the beam.
$E(v)$	Energy function.
$e_1,\ e_2$	Left and right end position and orientation of the beam.
e_r	Tracking error of CS slow subsystem.
e_{rr}	Tracking error of JS slow subsystem.
$\dot{e}_1, \dot{e}_2$	Left and right end effectors velocities of the beam.
$\dot{e}$	End-effectors velocity.
F	Linear bounded operator in Hilbert space.
F^*	Adjoint of F
$F_{1x},\ F_{1y}$	Force applied by the manipulator at the left end of the beam.
$F_{2x},\ F_{2y}$	Force applied by the manipulator at the right end of the beam.
F_{ff}	Force transformation matrix in the transverse vibration.
F_{rd}	Force transformation matrix with rigid parameters.
F_{rf}	Force transformation matrix with flexible and rigid parameters.
f	Forces/moments at the two ends of the manipulator.

f_f	Interaction force between a manipulator and the flexible beam in the fast subsystem.
f_i	Interaction force between i^{th} manipulator and the flexible beam.
f_p	Continuously differentiable function.
f_s	Interaction force between a manipulator and the flexible beam in the slow subsystem.
G_i	Gravitational components of a i^{th} manipulator.
G_r	Gravitational components of two manipulators in assembled form.
G_{cs}	Gravitational components of slow subsystem in CS.
G_{js}	Gravitational components of slow subsystem in JS.
G_{or}	Gravitational components of combined dynamics for the case of manipulator handling rigid beam.
G_{rd}	Gravitational components of the beam with only rigid parameters.
G_{rf}	Gravitational components of the beam with flexible and rigid parameters.
G_{jsf}	Gravitational components of combined rigid motion dynamics of the system in JS.
G_{orf}	Gravitational components of combined rigid motion dynamics of the system in CS.

g	Gravitational constant.
g_p	Continuously differentiable function.
H	Hilbert space.
I	Moment of inertia of the beam.
I_d	Identity matrix.
J	Jacobian matrix of the manipulators in assembled form.
J_i	Jacobian matrix of a i^{th} manipulator.
K	Dimensionless parameter.
K_D	Control gain in sliding control for CS slow subsystem.
K_d	Control gain in adaptive control.
K_{D1}	Control gain in sliding control for JS slow subsystem.
k	Control gain in fast feedback control.
L	Length of the beam.
L_a	Lagrangian function.
l_{ij}	Length of each link of the manipulator.
M_i	Inertia matrix of a i^{th} manipulator.
M_r	Inertia matrix of two manipulators in assembled form.
M_{cs}	Inertia matrix of slow subsystem in CS.
M_{js}	Inertia matrix of slow subsystem in JS.
M_{or}	Inertia matrix of combined dynamics for the case of manipulator handling rigid beam.
M_{rd}	Inertia matrix of the beam only with rigid parameters.

M_{rf}	Inertia matrix of the beam with flexible and rigid parameters.
M_{jsf}	Inertia matrix of combined rigid motion dynamics of the system in JS.
M_{orf}	Mass matrix of combined rigid motion dynamics of the system in CS.
m	Mass of the beam.
$P_1,\ P_v$	Positive definite matrices.
p	Constant varies between 1 to ∞.
Q	An operator in Hilbert space.
$Q_1,\ Q_v$	Positive definite matrices.
$q_1,\ q_2$	Vector of joint angles of manipulators 1 and 2.
$\dot{q}_1,\ \dot{q}_2$	Vector of joint velocities of manipulators 1 and 2.
q_d	Desired trajectory.
q_r	Reference trajectory.
$\tilde{q}$	Position tracking error.
$\dot{q}$	Vector of joint velocities of two manipulators.
$\ddot{q}$	Vector of joint accelerations of two manipulators.
q_{ij}	Joint angle i^{th} manipulator of j^{th} link.
R	Transformation matrix to relate end-effector and object velocities with flexible parameters.

R_1	Transformation matrix to relate end-effector and object velocities without flexible parameters.
$S_1(t)$	Sliding surface in adaptive control.
$S_2(t)$	Sliding surface in sliding control.
S_{cs}	Sliding surface in CS.
S_{js}	Sliding surface in JS.
S_ϕ	Measure of algebraic distance of the current state to the boundary layer in CS.
$S_{\phi 1}$	Measure of algebraic distance of the current state to the boundary layer in JS.
T	Kinetic energy of the beam.
T_s	Fast time scale variable.
T_{iB}^{iA}	Denavit-Hartenberg transformation matrix between the two successive coordinate frames of the manipulator.
$t_1,\ t_2$	Arbitrary time interval.
U	Potential energy of the beam.
U_e	Potential energy due to elasticity of the beam.
U_g	Potential energy due to gravitational force of the beam.
u	Composite control input.
u_s	Slow subsystem control input in CS.
u_f	Fast subsystem control input in CS.

u_{cs}	Vector of input forces for the slow subsystem in CS.
u_{or}	Vector of input forces in the combined dynamics for the case of manipulator handling rigid beam.
u_{ss}	Slow subsystem control input in JS.
u_{sf}	Fast subsystem control input in JS.
u_{orf}	Vector of input forces in the combined dynamics of the system.
V_i	Lyapunov function candidate.
W	Work done due to the external forces of the beam.
$w(x,t)$	Arbitrary variable.
w_f	Fast variable in the fast subsystem.
$\hat{w_f}$	Differentiating fast variable with respect to fast time scale.
$\hat{\hat{w}}_f$	Differentiating fast variable with respect to fast time scale in two times
w_s	Slow variable in the slow subsystem.
X, Y	Any point on the beam.
X_1Y_1	Fixed coordinate frame of manipulator 1.
X_2Y_2	Fixed coordinate frame of manipulator 2.
$X_{e_1}Y_{e_1}$	End-effector coordinate frame of manipulator 1.
$X_{e_2}Y_{e_2}$	End-effector coordinate frame of manipulator 2.
$\dot{X}_r$	Auxiliary trajectory for CS slow subsystem.
$\dot{X}_{rf}$	Velocity of the mass center of the object.
$\ddot{X}_{rf}$	Acceleration of the mass center of the object.

X_{rfd}	Desired trajectory for CS slow subsystem.
x	Spatial coordinate ranging from $\frac{-L}{2}$ to $\frac{+L}{2}$.
$\tilde{x}$	Tracking error in sliding control.
xy	Moving coordinate frame.
x_i, y_i, θ_i	Position and orientation of the end-effector.
x_s	Slow subsystem variable.
x_v	State vector in CS.
x_1	State vector in JS.
Y_a	Regressor for CS slow subsystem with desired velocity.
Y_{cs}	Regressor for CS slow subsystem.
Y_{js}	Regressor for JS slow subsystem.
Y_{im}	Regressor of a manipulator.
y_d	Distance from the neutral axis of the beam.
z_s	Slow subsystem variable.
z_f	Fast subsystem variable.
σ_{xx}	Bending stress.
ε_{xx}	Bending strain.
δ	Variational operator.
δ_1	Arbitrary constant.
τ_i	Vector of input joint torque of i^{th} manipulator.
τ	Vector of input joint torques of manipulators.
$\mu_1,\ \mu_2$	Constants of lower and upper bounds of inertia matrix.
Θ_i	Parameters vector of i^{th} manipulator.

ε	Perturbation parameter.
φ_i	Solutions of slow subsystem.
ν	Fast time scale.
α_o	Parameter vector of manipulators.
α_{cs}	Parameter vector of slow subsystem in CS.
α_{js}	Parameter vector of slow subsystem in JS.
Π	Unbounded operator.
λ_i	Eigen values of fast subsystem.
ϕ_i	Eigen vectors of fast subsystem.
υ	m-dimensional vector.
$\tilde{\upsilon}$	Parameter estimation error.
$\beta_1,\ \beta_2$	Positive constants.
λ_{cs}	Positive definite matrix in CS.
λ_{js}	Positive definite matrix in JS.
ψ	Switching functions in CS.
ψ_{js}	Switching functions in JS.
β	Damping factor.
β_{cs}	Upper bound based upon α_{cs}.
β_{js}	Upper bound based upon α_{js}.
κ	Least eigenvalue of the system in CS.
κ_1	Least eigenvalue of the system in JS.
ε_f	A constant parameter varies between 0 to 1.
ε_1	Arbitrary constant.

τ	Arbitrary time.
$\Upsilon,\ \Upsilon_1$	Positive definite matrices.
$\Omega,\ \Omega_1$	Control gain for without velocity feedback.
$\rho,\ \rho_1$	Control gain for without velocity feedback.
$\zeta,\ \zeta_1$	Control gain for without velocity feedback.
$\lambda_p,\ \lambda_q$	Eigenvalues of P_v and Q_v.
$\lambda_{p1},\ \lambda_{q1}$	Eigenvalues of P_1 and Q_1.
$\vartheta,\ \vartheta_1$	Arbitrary constant.
$\Omega,\ \Omega_1$	Arbitrary constant.
$\omega,\ \bar{\omega}$	Intermediate vectors.
$\omega_1,\ \bar{\omega}_1$	Intermediate vectors.
$\rho_i,\ \rho_{ii}$	Adaptive control gains.
$\beta_i,\ \beta_{ii}$	Control gains.
γ, γ_1	Arbitrary constant.
ϕ	Boundary layer.
$(\cdot)''$	Differentiating two times with respect to spatial coordinate.
$(\cdot)^{iv}$	Differentiating four times with respect to spatial coordinate.
$\dot{(\cdot)}$	Differentiating one time with respect to time.
$\ddot{(\cdot)}$	Differentiating two times with respect to time.
$< \cdot >$	Dot product.
$(\cdot)^{-1}$	Inverse of a matrix.
$(\cdot)^T$	Transpose of a matrix or a vector.
$(\cdot)^\dagger$	Pseudo inverse of a matrix.

$\check{(\cdot)}$	Estimate of a parameter.
$\|\| \cdot \|\|$	Appropriate norm.
$sat(\cdot)$	Saturation function.
$sgn(\cdot)$	Signum function.
sup	Supremum.

Chapter 1

Introduction

1.1 Motivation

A tremendous growth of the use of robots in automobile, electronics, construction, manufacturing and medical equipment industry has evolved in the past four decades. Robotic systems relieved humankind from boring repetitive tasks, dangerous environments in space, underwater and high radiation environments. They are used for a large variety of tasks such as material handling, welding, paint spraying, part deburring, pick and place operations and machining at high speeds with high precision. A robot can work in hazardous environments replacing humans and also minimizing the production cost. In addition to that, robot needs little environmental control compared to the humans performing the same task in hazardous environments. In general, the robots are effectively used in the industry and in the near future, the use of robots will be increasing significantly.

In the past, a single robot alone was not able to grasp and move a long object in a safe

and efficient way. Owing to the single arm structure, present day robots are called "handicapped operators" for performing complex tasks. Most tasks in assembly / disassembly, handling large or heavy objects are done efficiently with two robot arms. Collaborative manipulators have the following advantages compared to single arm manipulators:

- increased load carrying capacity by sharing the loads between the manipulators.
- greater dexterity and manipulability in handling flexible objects.
- reduced need for extra auxiliary equipments.
- efficient use of available workspace.
- increased productivity by operating each robot in parallel to achieve different tasks at the same time.

Considering these advantages, two manipulator system is employed in wide range of tasks and the first master/slave teleoperated manipulator was used in the nuclear industry in the 1940's at Oak Ridge and Argonne National Laboratories [1] which led to the need for two robots. In the 1970's, Nakano *et al.* [2] reported on their research on multi robot coordination where they recognized the need for two arms. Luh [3] categorized the two robot arm co-ordinated motion into two types: loosely coordinated motion and tightly coordinated motion. In the former, two robots share a common workspace and execute independent tasks. The failure of one robot will not affect the other. In the latter case, movement of one robot depends on the other and also, failure of one of the robot affects the other.

Two robots handling a rigid object have been studied by many researchers whereas manipulating a flexible object was studied in the 1990's [4]. A modern automobile body assembly has more than 200 sheet metal parts which must be assembled in a precise way. Handling them needs special equipment and skilled operation. Two robots can grasp a flexible sheet metal and force them together for assembly. Also, in industry, many deformable objects such as rubber tubes, sheet metals, cords and leather products are handled by special equipment or human operators. In aerospace industry, composite materials which have high flexibility are used to replace metals. In the shipbuilding industry long flexible frames and plates can be assembled with the help of two manipulators. Many of these applications need vibration free motion especially in robot assisted surgery. In order to effectively manipulate complex flexible objects and bend them in a desired manner, for example, the insertion of a flexible beam into a hole and assembling sheet metal in the required place, two robot arms are needed. In real time applications, motor torque requirements can be shared between two robots when handling long and heavy objects. In the case of a single manipulator a large torque is required to handle heavy loads which increases the cost of the motor, whereas the use of dual robotic arms may be able to reduce the torque requirements of the individual motors.

The dynamics and control problem of two manipulators handling flexible materials collaboratively is complex compared with handling the rigid parts. In order to develop an efficient control algorithm a precise dynamic model is necessary and the unprecise models may create problems such as control and observation spill over. In most of the applications, beams, plates and shells are considered to represent the flexible system. Many researchers

approximated the dynamics of a flexible object using the finite element model or the finite assumed mode model which converts the Partial Differential Equation (PDE) of the beam into the Ordinary Differential Equation (ODE). The control design for PDE based systems is very few compared with ODE based systems. Further, the controlling of these systems are of utmost importance in real time applications because of its complexity and high demand in various industries. This dissertation involves, dynamic modeling of the manipulators-flexible object system without using any approximation or discretization and development of suitable robust control approach to achieve the desired motion and simultaneously suppressing the vibration of the flexible object. In order to review the relevant studies in terms of various dynamic modeling and control approaches for these kind of systems, a detailed survey is conducted in the next section.

1.2 Literature Review

Many of the tasks in various industrial applications need at least two robots. Two robots performing a single task can have a significant advantage over a single robot performing similar task. It is quite obvious that a human being using two arms has more advantage than using a single arm. The main application of such type of robots can be realized from the transportation of massive and/or bulky objects, assembling of automotive parts and also handing non-rigid payloads. As a result, considerable amount of work has been done for the coordinated control of two manipulators or multiple manipulators in the recent past. There are many pioneering studies related to collaborative motion of robots manipulating a common rigid object and non-rigid object. Considering this, the literature survey is divided

into two parts. Firstly, some of the important works related to two manipulators handling a rigid object are reviewed and secondly a detailed review on manipulation of the flexible objects including different approaches of modeling and control of the flexible object is presented.

1.2.1 Collaborative manipulation of rigid objects

In the past decades a number of control methods for the coordinated motion of manipulators have been developed. Nakino *et al.* [2] used force sensors for the coordination and control of two arms. Luh and Zheng [3] formulated a closed loop kinematic chain where the position and orientation of two robots had satisfied the necessary constraints. In their master-slave approach, if the trajectory of the master arm is planned and executed, the slave arm trajectory was derived from the constrained relations and correspondingly the coordination was achieved. Ishida [5] proposed a force control algorithm which uses a PID controller to move the object in a parallel and rotational mode. The master-slave principle was employed and interactive forces between the two arms were measured using a wrist force sensor. The master robot arm was position controlled and slave arm was position and/or force controlled based upon the information given by the master arm. Alford and Belyeu [6] utilized the concept of Ishida [5] for the position control of two arms. In their case, given the trajectory of the master arm, the slave arm trajectory is modified in run time. Zheng and Sias [7] studied the collision effects between the end-effectors which caused changes in joint velocities, and impulsive force generated at the end-effectors was used to detect the position and orientation of the two arms. Tarn *et al.* [8, 9] developed a nonlinear feedback

control method to control two Puma robot arms and also the position/velocity errors and force/torque errors were reduced. However, the master-slave approach failed due to the kinematic and dynamic uncertainties in an un-calibrated slave robot joint measurements. In order to resolve this issue, hybrid position/force control algorithm was developed.

The Hybrid position/force control scheme developed by Raibert and Craig [10] created a new arena for controlling the manipulators in non - deterministic environments. In the case of hybrid position/force control, the position and force information are separately fed back and compared with the desired value. The corrective action is taken separately by applying position and force control laws, and then converting it into joint torques using the Jacobian. By selecting 0's and 1's in the matrices, the position and force control action is determined. However, it was only applied to a single arm robot. As far as the two robot coordination was concerned, Hayati [11] proposed a control architecture based on the Raibert hybrid control strategy [10] for multi arm robots grasping a rigid object. Uchiyama *et al.* [12, 13] and Dauchez *et al.* [14] have used Hayati's [11] algorithm for their applications and further investigations to control the coordination between two robot arms. They have considered the static force relationship and it can be used only for low speed operations [15]. Experimental results of Kopf and Yabuta [16] showed that the hybrid control law achieves better coordination than master-slave control scheme. However, Duffy [17] identified some fallacies in the hybrid position/force control scheme. In the master-slave and hybrid control approach, the controllers need the accurate information of the dynamic parameters. However, in the real time applications, industrial manipulators have uncertainties while grasping the load which cannot be handled by master-slave and hybrid position/force control methods. Hence, nonlinear control algorithms have to be adopted.

In order to adapt to the uncertainties, an adaptive scheme [18] which controls the motion of the object, internal force and contact force with respect to the environment was developed and simulated. Several adaptive based control schemes [19]-[21] have been proposed by various researchers. However, these methods use structure information of the robot. Furthermore, object dynamics can lack robustness to unmodeled dynamics such as arm or object flexibility, actuator lags, and sensor noise. Although many of them proposed and simulated the various control algorithms without friction and neglecting gravitation effects, they provided a great insight into further development. A few of them had implemented their control strategy in the experiments. Bonitz and Hsia [22, 23] introduced a robust internal force based impedance control for the manipulators coordination. Under this control scheme, nonlinear dynamic terms of the robot are compensated. The developed controller was implemented through experiments by using the two Puma robots. Uzmaya *et al.* [24] performed the simulation considering uncertainties such as contact and friction constraints for grasp, bearing conditions and structural flexibility using adaptive, robust and inverse dynamics controllers. Gueaieb *et al.* [25] proposed a hybrid (combination of a conventional adaptive controller and an adaptive fuzzy controller) intelligent controller to handle unwanted parametric and modeling uncertainties. The simulation was carried out and it was evident from the results that the controller was very effective. Caccavale *et al.* [26] developed centralized impedance control which was aimed at conferring the compliant behavior of the object and decentralized impedance control to avoid large internal loading of the object. These control algorithms were implemented in the two 6 Degrees of Freedom (DOF) manipulators test bed. Moosavian and Papadopoulos [27] also incorporated

impedance control to achieve the free motions and contact tasks without changing the control modes. The simulation results confirm that the two manipulators achieve good tracking performance. In order to handle load transportation of two robots, a sliding mode control [28] has been implemented. The comparative study on PID and sliding mode controllers through simulation results showed that, the tracking error is minimized in sliding control.

1.2.2 Collaborative manipulation of flexible objects

Earlier studies dealt with coordinated control of multiple robots handling a rigid object. However, the manipulation of flexible objects is more challenging in terms of dynamics and control. Mills [4] considered the vibrations of flexible sheet metal parts in the fixtureless assembly case. The sheet metal bending was modeled as a lumped spring - damper system. In his work, the two robots were used to carry the negligible payload and the robots were always in contact with the payload. Due to this assumption, a set of kinematic constraints are imposed in certain directions. The computed torque control law regulates the constraint forces in the constrained directions, the bending forces in the bending directions of the payload and positions in the free motion directions of the payload. This problem was intended only for parts having small mass but in the case of large payloads dynamics can not be ignored. Later, he modeled the sheet metal as approximated model using assumed mode method [29] and also discretized the model using finite element method [30]. The control law proposed by him assumes that the sheet metal parts exhibit rigid body motion in certain directions while deforming elastically in remaining directions.

Zheng *et al.* [31] studied the deflection behavior of beams in connection with a single

robot arm and the beam was assembled into a rigid hole. Zheng and Chen [32] extended their work on single arm manipulation to two robot arm manipulation, for the alignment of flexible sheets in printed circuit boards. In their two methods, the first method was used to position the flexible beam but not the orientation, and the second method to position and orient the object. The bending angle of the beam is considered as a variable and the positions of two end-effectors are taken as functions of bending angle. Piece - wise linear approximation is considered for trajectory tracking based on bending angle and minimizing force and moment on end-effectors. Dellinger and Anderson [33] developed a mathematical model for interactive forces and torque generated, when the two manipulators handle a pair of pliers. Yukawa *et al.* [34] developed the beam dynamic model by assuming mode functions in the state space form. They proposed a position control algorithm to achieve total system stability and they also suppressed the vibration at the intermediate points of the flexible beam. Kosuge *et al.* [35] derived FE models for bending and twisting sheet metal. The relationship between them and static deformations of sheet metal was also developed. Their control algorithm was implemented experimentally and the deformation was reduced. Nguyen and Mills [36] derived combined dynamics of the system utilizing finite element method, considering the rigid body dynamics of robots and payloads. They proposed the force control algorithm which was implemented in the real time for assembling auto body sheet metal parts.

Kraus and McCarragher [37] used kinematic redundancy resolution to achieve the coordination between two robot arms. They also used [38] the force field information caused by elastic deformations of the load for force guided control of end-effector motions. His innovative concept was demonstrated using their experimental setup for inserting a flexible

beam into a hole. By minimum-effort optimality criteria, the controlled variable in each direction was determined. They continued their work [39] for two case studies, namely, the bending of sheet metal and the insertion of a beam into a hole by employing a hybrid position/force controller in their experiments. Yukawa *et al.* [40] proposed a handling system to transform the flexible object in 2D space and also investigated the stability and robustness of the proposed system. Sun *et al.* [41] developed a dynamic model of the object using finite element method. They also formulated a PD plus gravity compensation algorithm for the position control of multiple robots handling a flexible material while suppressing the vibrations of the payload at each contact. Sun and Liu [42] developed a mathematical model of the beam using assumed mode method. They proposed a hybrid impedance controller which was used to stabilize the system while suppressing the vibrations and controlling internal forces. Asymptotic stability was analyzed for various boundary conditions of the beam using assumed mode functions. In the previous work of Sun *et al.* [42], vectors containing vibration parameters and states were hard to be compensated using the feedback controllers. Hence, a new compensation scheme [43] and [44], with saturation controller was proposed in order to achieve the desired trajectory. To control the interaction forces between the manipulators and the beam and also to stabilize the total system, hybrid position and force controller was developed. The proposed controllers are simulated and their results validated the proposed control algorithms. They also extended their work [45] for the two manipulator handling of a general flexible object and also developed a hybrid control algorithm.

Ji and Park [46] developed a computational scheme which determines the optimal trajectory and vibration was also suppressed. In their analysis, assumed mode method

has been utilized to develop the dynamic model of the flexible object. Zoe and John [47] modeled the flexible object as a spring - mass - damper system. The complete system kinematics and dynamics equations were formulated and a feedback control was proposed. Simulation results showed that the proposed controller achieved the desired pose of the object and also the deformation is minimized. Al-Yahmadi and Hsia [48] considered a spring-mass system as the object model and developed an internal force based impedance controller in which the internal force was controlled to deform the object in order to reach a desired shape. By controlling the contact forces between the object and the fixture, the deformed object was assembled into the fixture. They [49] also derived flexible beam dynamic model using spline approximation. The proposed sliding mode control algorithm was designed in such a way that it provides robustness against the model imperfection and uncertainty and suppresses the vibration. The stability of the system was proved and the simulation results were presented. Ali *et al.* [50] also used assumed mode method to derive the dynamic model of the beam. Their two time scale controllers such as, PD control scheme for rigid motion and pole placement technique for flexible motion were designed to track the desired trajectory for the rigid body motion and to suppress the vibration. In order to avoid the external measurement equipment to measure the displacement of a beam, a linear observer was designed. Tang and Li [51] used finite element method to derive the dynamic equations of motion of the object. By using singular perturbation approach, the slow and fast subsystems were identified. For the slow subsystem, an adaptive sliding mode control was proposed and for fast subsystem, a robust optimal control was suggested.

1.3 Scope and Objectives

From the review of the relevant studies, it is evident that, collaborative manipulation of two robots handling a flexible object is a complex and challenging task. However, from the reported studies related to collaborative robots manipulating the flexible objects, some of them considered lumped spring-mass-damper system as the flexible object model and many of them obtained the dynamic model of the flexible object either by discretizing using finite element method or by approximations using assumed mode method.

The truncation of the original model with infinite degrees of freedom of a flexible model to a finite dimensional model poses the following issues such as [52]:

1. Requirement of a higher order controller to achieve greater performance in terms of accuracy of tracking. This results in increase in the number of flexible modes to be assumed.

2. Presence of control and observation spill over due to the ignored high frequency dynamics.

3. Unambiguous consideration of number of modes while constructing the discretized ODE model.

4. Destabilization of the system due to the negligence of the higher order modes.

5. Requirement of as many sensors as the locations of the measurement of vibration and the difficulty in implementation.

Alternatively, PDE based systems were proved to be effective in eliminating above mentioned issues. It can also be seen from the review of literature that several control algorithms are available for the ODE based systems compared to the PDE based systems. Control engineers have more challenge due to the complexity involved in developing the control algorithm for the PDE based systems. Moreover, the two manipulators collaboratively handling the flexible object involve more intricacy in developing the dynamics of the system and a suitable control scheme to achieve the desired motion of the object and reducing the vibration. Furthermore to improve the controller design

Considering the aforementioned reasons and unlike in the earlier available studies, this thesis concerns with an overall objective of development of a dynamic model of manipulators-flexible object system without using any approximation methods and design of a robust control scheme. The purpose of the robust control system design is to use the two planar three link manipulators to move the flexible object in the prescribed trajectory (tracking problem) and simultaneously to suppress the vibration of the flexible object with unknown manipulator and beam parameters. In addition, this thesis also considers to improve the controller design in terms of avoiding the need for velocity sensor and also alleviate the computation burden. Furthermore, to avoid online inverse kinematic calculations and corresponding singularity problems, joint space dynamic system will be derived and similar analysis will also be carried out.

The above mentioned objectives would be achieved in different sequential steps. The specific objectives of each step of this dissertation research can be summarized as follows:

- Develop a mathematical model of manipulators - flexible object system in Cartesian

space without any approximation and discretization techniques.

- Implement singular perturbation approach to identify the slow subsystem that depicts the rigid body motion and the fast subsystem that describes the transverse vibration of the flexible object.

- Develop a robust control scheme that would achieve the desired tracking performance while suppressing the vibration of flexible object being handled when the parameters of the system are unknown.

- Extend the analysis by developing the complete system of dynamic model in joint space.

1.4 Thesis Overview

This dissertation is organized into 7 Chapters. The outline of the thesis is as follows.

Chapter 1 summarizes the relevant reported studies on collaborative manipulators handling rigid and flexible objects. The scope and objectives of the dissertation is subsequently formulated on the basis of the reviewed studies.

Chapter 2 presents the kinematics and dynamics of flexible object as well as those of the manipulators. Dynamic equations of motion of the flexible object are derived using Hamilton's principle. The resulting equation is combined with manipulator dynamic equations forming the combined dynamics.

After a brief introduction to singular perturbation approach and using these concepts, the two sub systems, namely, slow subsystem which deals with rigid body motion of the beam

and also fast subsystem which accounts the transverse vibration of beam are derived in Chapter 3.

Regressor based control scheme for slow subsystem to control the rigid motion of the beam and a simple feedback control algorithm for the fast subsystem to suppress the vibration is developed in Chapter 4. The stability analysis for each subsystem has been analyzed. Simulation results are presented so as to validate the composite control scheme.

Chapter 5 proposes an adaptive control law for the slow subsystem with only position feedback to avoid the measurements of velocity feedback and the corresponding stability analysis is also carried out. Furthermore, a non-regressor based adaptive robust control algorithm is implemented to the slow subsystem to avoid the regressor and its stability results are also discussed. The effectiveness of different control schemes are illustrated through simulation studies.

In Chapter 6, the extension of earlier analyses has been carried out by developing the complete system of dynamic equations in joint space. The composite control strategies, stability analysis and corresponding simulation results are discussed.

The major conclusions drawn from the dissertation research are summarized in Chapter 7 together with a few recommendations and suggestions for further studies.

Chapter 2

Kinematics and Dynamics of Manipulators - Flexible Object System

2.1 Introduction

Handling flexible objects using robot manipulators is of growing interest in industry. For example, assembly of automotive parts involves manipulation of deformable parts and also air craft assembly involves joining flexible structural components. In order to handle these objects effectively, and precisely positioning them in the required location, at least two robot arms are necessary. Two robots collaboratively manipulating a flexible object is a complex and challenging problem compared to that of handling a rigid object. Control of this kind of problem requires precise mathematical model of the flexible object. However, it is evident from the literature that the solution of the dynamic equation of motion of the

flexible object is implemented by using assumed mode or finite element method. These approximations cause many problems which are mentioned in Chapter 1, for example, measurement difficulties. Hence, in this Chapter the dynamic equation of motion of flexible object is derived by using Hamilton's principle and solved directly without approximation. Then, the kinematic relations for the flexible object and the manipulators are formulated. By utilizing these relations, the general manipulators dynamics and flexible object dynamics are combined. The resulting combined dynamics derived in Cartesian space is coupled with rigid and flexible parameters where the flexible parameters are not approximated with the modes unlike the existing methods in the literature.

2.2 Manipulators - flexible object system description

In this study, two planar rigid manipulators each with three links are considered. Fig. 1 shows schematic representation of a manipulator with corresponding joint angles q_{ij}, link lengths l_{ij} and also its end-effector which is used to grasp the object. where, $i = 1,2$ represents the two manipulators and $j = 1,2,3$ represents the links of each manipulator. Here, in this thesis two manipulators are considered to be identical.

In order to analyze the rigid body and flexible body motion of two planar manipulators handling a flexible object shown in Fig. 2, five coordinate frames are considered. Frames X_1Y_1 and X_2Y_2 are two fixed coordinate frames for each manipulator attached at the base. Frames $X_{e_1}Y_{e_1}$ and $X_{e_2}Y_{e_2}$ are end-effector coordinate frames attached at the contact points of the object and xy is a moving frame attached at the mass center of the flexible object. All the kinematic relations are written with respect to the fixed frame X_1Y_1.

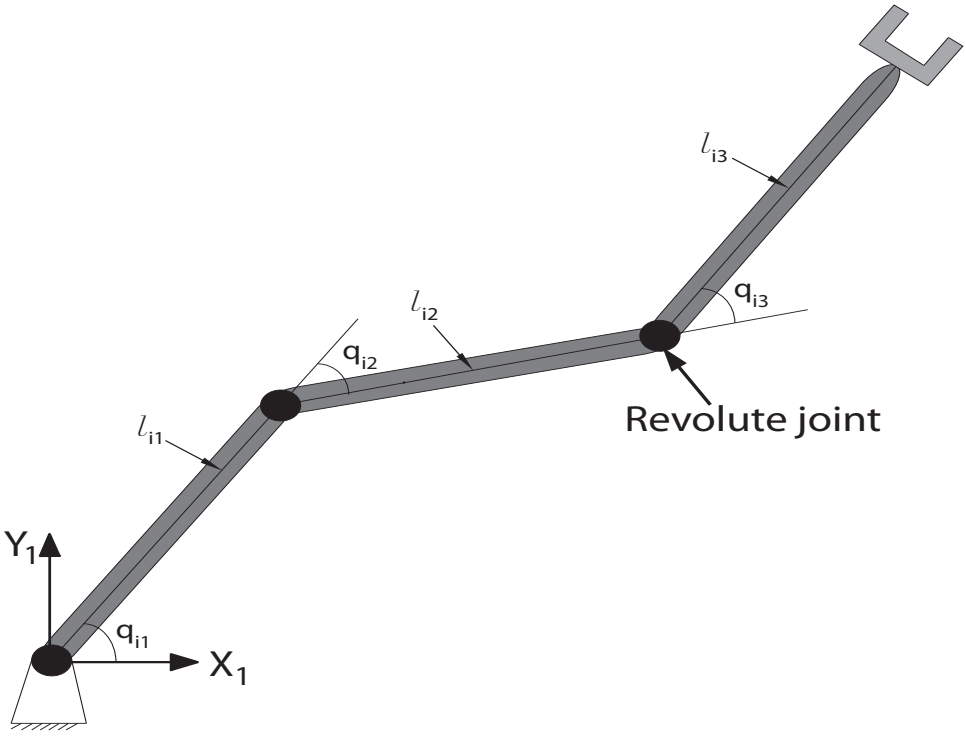

Figure 1: A Planar manipualtor

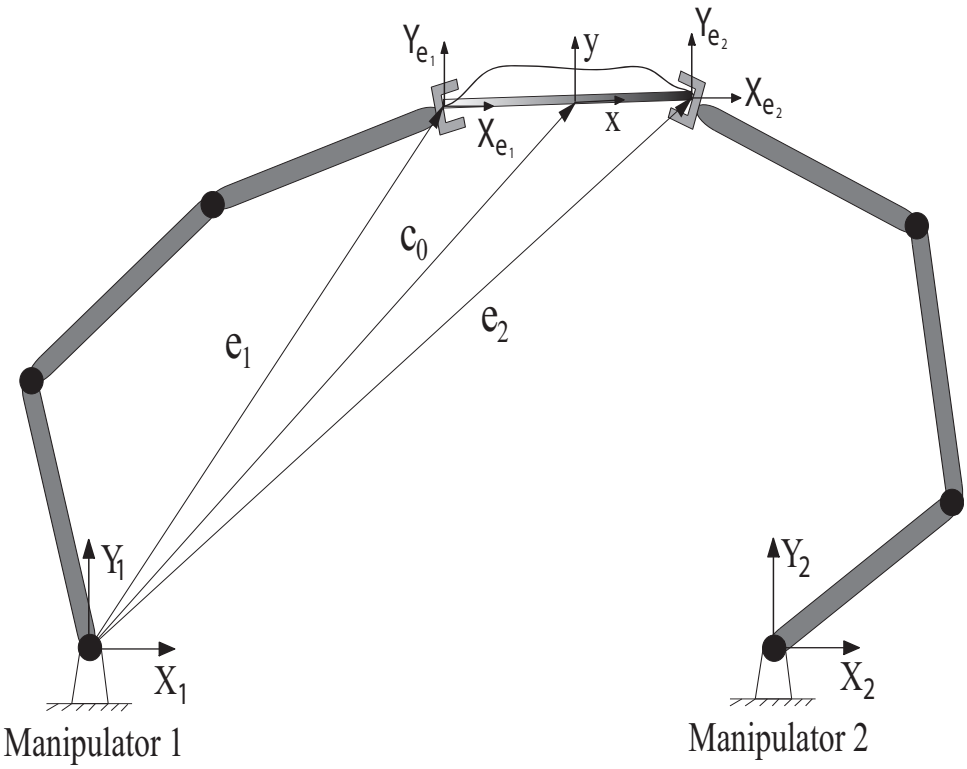

Figure 2: Two planar rigid manipulators grasping a flexible object

2.3 Kinematics and dynamics of the flexible object

In the manufacturing and automobile industries, many components to be assembled can be modeled as beams. Various applications such as, turbine rotor blades, spacecrafts with flexible appendages, flexible robot arms and aerospace systems, are essentially beams which are flexible bodies. Therefore, in this thesis the flexible object is considered as an Euler-Bernoulli beam. Since the two manipulators are used to move the object to a desired position and orientation which necessitates rotation at the two ends of the beam, simply supported end conditions are considered for deriving the dynamic equations of motion of the beam. Certainly, other end boundary conditions can be included for the derivation of the beam dynamics. However, with the aim of illustrating the essential features of the controller design and to avoid complex mathematical expressions, simply supported boundary conditions are considered.

2.3.1 Kinematics of the flexible object

A flexible beam can be modeled with discretized finite elements [30] or approximated with assumed modes [42]. In view of the disadvantages mentioned in Chapter 1 and also stated in [52], exact PDE based model is developed in this section without resorting to approximate discretized model is used in this thesis.

Consider a beam of length L, mass $m = \rho L$, where ρ is mass per unit length. The mass center position and orientation of the beam with respect to X_1Y_1-frame are given by $\{c_0\} = \{x_0,\, y_0,\, \theta\}^T$. F_{1x}, F_{1y}, F_{2x}, F_{2y} are the forces applied by the manipulator at the two

ends of the beam. The transverse displacement $\eta(x,t)$ is measured with respect to xy-frame and deformation in the longitudinal direction is neglected. For simplicity, argument (x,t) will be omitted further in this thesis.

Any point on the beam can be written as,

$$X = x_0 + x\cos\theta - \eta\sin\theta \quad (1)$$

$$Y = y_0 + x\sin\theta + \eta\cos\theta \quad (2)$$

where, x is the spatial coordinate ranging from $\frac{-L}{2}$ to $\frac{+L}{2}$.

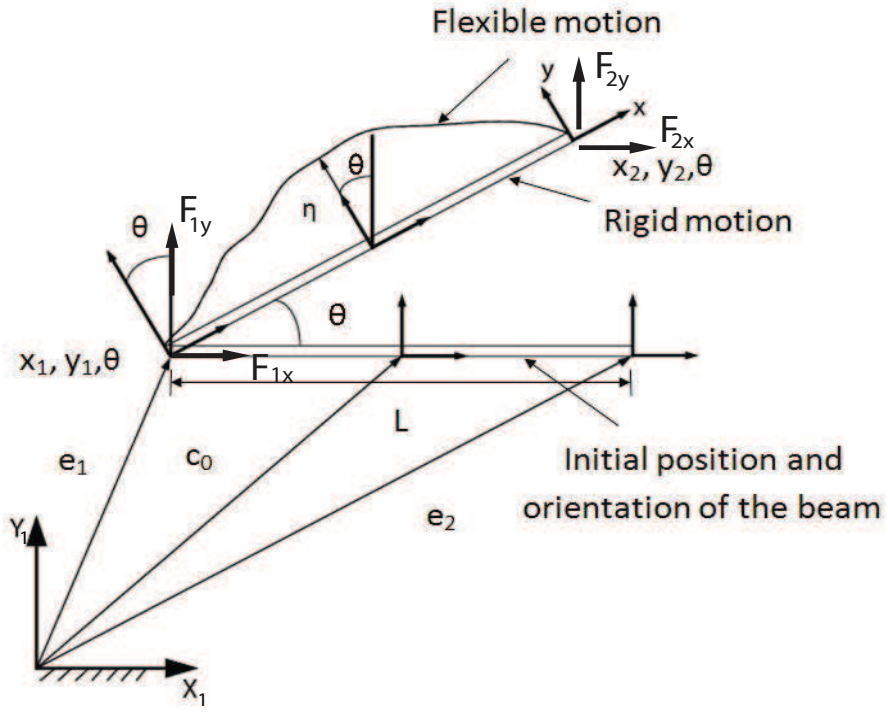

Figure 3: Beam rigid body motion and deflection

In general, the beam has rigid body motion on which the flexible motion or vibration of beam is superimposed. It is evident from the Fig. 2 that the left and right end points of the beam sharesthe left and right end-effector grasping point of the two end-effectors. The

slope due to transverse deflection is small compared to the orientation of the beam and is neglected at the two ends of the beam. The following kinematic relations are obtained from Fig. 3.

The left end pose (position and orientation) of the beam is given by,

$$\{e_1\} = \{c_o\} - \{\frac{L}{2}cos\theta \quad \frac{L}{2}sin\theta \quad 0\}^T + \{-\eta \sin\theta \quad \eta\cos\theta \quad 0\}^T \tag{3}$$

The right end pose of the beam is given by,

$$\{e_2\} = \{c_o\} + \{\frac{L}{2}cos\theta \quad \frac{L}{2}sin\theta \quad 0\}^T + \{-\eta \sin\theta \quad \eta\cos\theta \quad 0\}^T \tag{4}$$

Differentiating (3) and (4) results in,

$$\{\dot{e}_1\} = \begin{Bmatrix} \dot{x}_0 + \frac{L}{2}sin\theta\dot{\theta} - \eta\cos\theta\dot{\theta} - \dot{\eta}\sin\theta \\ \dot{y}_0 - \frac{L}{2}cos\theta\dot{\theta} - \eta\sin\theta\dot{\theta} + \dot{\eta}\cos\theta \\ \dot{\theta} \end{Bmatrix}$$

$$\{\dot{e}_2\} = \begin{Bmatrix} \dot{x}_0 - \frac{L}{2}sin\theta\dot{\theta} - \eta\cos\theta\dot{\theta} - \dot{\eta}\sin\theta \\ \dot{y}_0 - \frac{L}{2}cos\theta\dot{\theta} - \eta\sin\theta\dot{\theta} + \dot{\eta}\cos\theta \\ \dot{\theta} \end{Bmatrix}$$

where $\dot{(\cdot)}$ represents differentiation with respect to time.

Above relations can be written in compact form with respect to the Cartesian co-ordinates as,

$$\{\dot{e}\} = [R]\{\dot{X}_{rf}\} \tag{5}$$

where $\{\dot{X}_{rf}\} = \{\dot{x}_0,\ \dot{y}_0,\ \dot{\theta}\}^T$ denotes the velocity of the mass center of the object, and

$$R = \begin{bmatrix} 1 & 0 & \frac{L}{2}sin\theta - \eta\cos\theta \\ 0 & 1 & -\frac{L}{2}cos\theta - \eta\sin\theta \\ 0 & 0 & 1 \\ 1 & 0 & -\frac{L}{2}sin\theta - \eta\cos\theta \\ 0 & 1 & \frac{L}{2}cos\theta - \eta\sin\theta \\ 0 & 0 & 1 \end{bmatrix}$$

Differentiating (5) gives the acceleration,

$$\{\ddot{e}\} = [\dot{R}]\{\dot{X}_{rf}\} + [R]\{\ddot{X}_{rf}\} \tag{6}$$

where $\ddot{X}_{rf}$ describes the acceleration of the mass center of the object.

The resulting equations (5) and (6) will be used latter to obtain the manipulator dynamics in the Cartesian space.

2.3.2 Dynamics of the flexible object

The equation of motion of the dynamic systems can be derived using principle of virtual displacements, Euler-Lagrange equations or Hamilton's principle. The Hamilton's principle provides an elegant approach to describe the equations of motion because the boundary conditions are derived simultaneously. Hamilton's principle describes that, the dynamic system can be moved from one point to another point in time for the given time interval in all of the possible paths, but, the actual path followed is determined by minimizing the time integral between the kinetic and potential energy. The Hamilton's principle [53] is

stated as follows, “The actual path in configuration space followed by a dynamical system during the fixed time interval t_1 to t_2 is such that the integral $\int_{t_1}^{t_2} L_a \, dt$ where, L_a= kinetic energy - potential energy, is stationary with respect to path variations and vanishes at the end points”.

The Hamilton’s principle is mainly used for rigid bodies. A flexible body has infinite degrees of freedom and the states of the systems are described by continuous functions of time and space. The Extended Hamilton’s principle is developed for such bodies and it is given by [53],

$$\int_{t_1}^{t_2} (\delta T - \delta U + \delta W) dt = 0 \tag{7}$$

where δ represents the variational operator, T is kinetic energy and U is potential energy. Further, t_1 to t_2 are any two instances of time with $t_2 > t_1 > 0$. In order to determine the dynamic equations of motion of beam, the kinetic energy, potential energies due to elasticity of the beam and due to gravity must be obtained. In the following, these energy expressions are obtained.

Kinetic energy of the beam is defined as,

$$T = \frac{1}{2} \int_{\frac{-L}{2}}^{\frac{L}{2}} \rho (\dot{X}^2 + \dot{Y}^2) dx \tag{8}$$

Differentiating (1) and (2) gives,

$$\dot{X} = \dot{x}_0 - [x sin\theta + \eta cos\theta]\dot{\theta} - sin\theta \dot{\eta} \tag{9}$$

$$\dot{Y} = \dot{y}_0 + [x cos\theta - \eta sin\theta]\dot{\theta} + cos\theta \dot{\eta} \tag{10}$$

Squaring (9) and (10) and substituting into (8) yields,

$$
\begin{aligned}
T &= \frac{1}{2}\int_{\frac{-L}{2}}^{\frac{L}{2}} \rho[\dot{x}_0^2+\dot{y}_0^2+\dot{\theta}^2\eta^2+(x\dot{\theta}+\dot{\eta})^2-2\dot{\theta}\eta(\dot{x}_0 cos\theta+\dot{y}_0 sin\theta) \\
&\quad +2(\dot{\theta}x+\dot{\eta})(\dot{y}_0 cos\theta-\dot{x}_0 sin\theta)]dx \qquad (11)
\end{aligned}
$$

Neglecting the shear deformation and considering the bending of the beam, potential energy of the beam due to elasticity can be obtained as,

$$
U_e = \frac{1}{2}\int_V \sigma_{xx}\varepsilon_{xx}dV \qquad (12)
$$

where,

$$
\sigma_{xx} = E\varepsilon_{xx}, \quad \varepsilon_{xx} = -y_d\eta'', \quad dV = dxdydz \qquad (13)
$$

where $(\cdot)'$ represents differentiation with respect to space.

Further, σ_{xx}, ε_{xx}, dV and E denote the stress, strain component, infinitesimal volume and Young's Modulus of a beam element, respectively. Bending strain is measured at a distance y_d from the neutral axis of the beam.

Substituting (13) into (12) gives,

$$
\begin{aligned}
U_e &= \frac{1}{2}\int_V E\varepsilon_{xx}^2 dV \\
&= \frac{1}{2}\int_{\frac{-L}{2}}^{\frac{L}{2}} \left[\eta''^2 E \int_0^A y_d^2 dA\right] dx \\
U_e &= \frac{1}{2}\int_{\frac{-L}{2}}^{\frac{L}{2}} \left[EI\eta''^2\right] dx \qquad (14)
\end{aligned}
$$

where, $I = \int_0^A y_d^2 dA$.

Potential energy due to the gravitational force can be obtained as,

$$
U_g = \rho g\int_{\frac{-L}{2}}^{\frac{L}{2}} (y_0+xsin\theta)dx = mgy_0 \qquad (15)
$$

Total potential energy can be calculated by the following,

$$U = U_g + U_e \tag{16}$$

The manipulator will exert forces, namely, F_{1x}, F_{1y}, F_{2x} and F_{2y} at the two ends of the

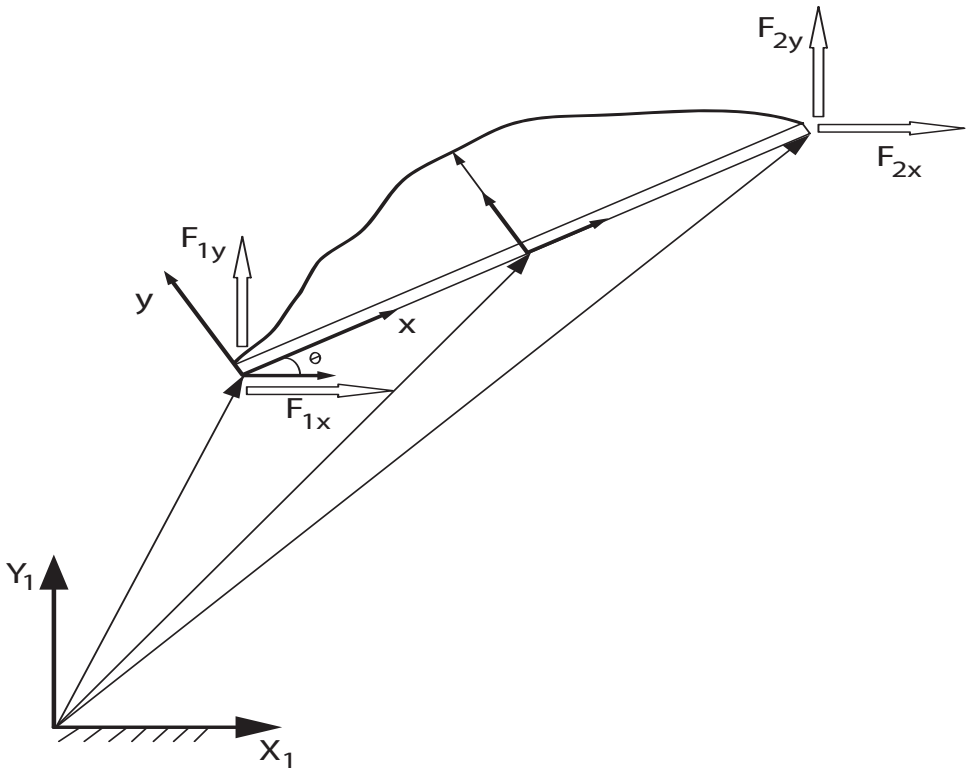

Figure 4: Flexible beam with boundary forces

beam which is shown in Fig. 4.

Work done due to the external forces are formulated as,

$$W = F_{1x}(x_0 - \frac{L}{2}\cos\theta) + F_{1y}(y_0 - \frac{L}{2}\sin\theta) + F_{2x}(x_0 + \frac{L}{2}\cos\theta) + F_{2y}(y_0 + \frac{L}{2}\sin\theta) + (F_{2y} + F_{1y})\eta\cos\theta - (F_{1x} + F_{2x})\eta\sin\theta \tag{17}$$

By applying Extended Hamilton's Principle (7), the following equations of motion of beam along X, Y and Z directions are obtained.

The detailed derivations are given in Appendix A. Based upon these derivations, the following are obtained:

The equation of motion for translation along the X - direction is obtained as,

$$\begin{aligned} m\ddot{x}_0 - (\rho\cos\theta\int_{\frac{-L}{2}}^{\frac{L}{2}}\eta\,dx)\ddot{\theta} - \rho\sin\theta\int_{\frac{-L}{2}}^{\frac{L}{2}}\ddot{\eta}\,dx \\ -2\rho\dot{\theta}\cos\theta\int_{\frac{-L}{2}}^{\frac{L}{2}}\dot{\eta}\,dx + \dot{\theta}^2\rho\sin\theta\int_{\frac{-L}{2}}^{\frac{L}{2}}\eta\,dx &= F_{1x}+F_{2x} \end{aligned} \tag{18}$$

The translation in the Y - direction is described by the equation,

$$\begin{aligned} m\ddot{y}_0 - (\rho\sin\theta\int_{\frac{-L}{2}}^{\frac{L}{2}}\eta\,dx)\ddot{\theta} + \rho\cos\theta\int_{\frac{-L}{2}}^{\frac{L}{2}}\ddot{\eta}\,dx \\ -2\rho\dot{\theta}\sin\theta\int_{\frac{-L}{2}}^{\frac{L}{2}}\dot{\eta}\,dx - \dot{\theta}^2\rho\cos\theta\int_{\frac{-L}{2}}^{\frac{L}{2}}\eta\,dx + mg &= F_{1y}+F_{2y} \end{aligned} \tag{19}$$

Rotation about the Z axis is described by,

$$\begin{aligned} (-\rho\cos\theta\int_{\frac{-L}{2}}^{\frac{L}{2}}\eta\,dx)\ddot{x}_0 - (\rho\sin\theta\int_{\frac{-L}{2}}^{\frac{L}{2}}\eta\,dx)\ddot{y}_0 + (\frac{mL^2}{12}+\rho\int_{\frac{-L}{2}}^{\frac{L}{2}}\eta^2dx)\ddot{\theta} + \rho\int_{\frac{-L}{2}}^{\frac{L}{2}}x\ddot{\eta}\,dx \\ +2\rho\dot{\theta}\int_{\frac{-L}{2}}^{\frac{L}{2}}\eta\dot{\eta}\,dx = F_{1x}(\frac{L}{2}\sin\theta-\eta\cos\theta)+F_{1y}(-\frac{L}{2}\cos\theta-\eta\sin\theta)+ \\ F_{2x}(-\frac{L}{2}\sin\theta-\eta\cos\theta)+F_{2y}(\frac{L}{2}\cos\theta-\eta\sin\theta) \end{aligned} \tag{20}$$

The differential equation of motion of transverse vibration of beam is derived as,

$$\begin{aligned} -\sin\theta\ddot{x}_0+\cos\theta\ddot{y}_0+x\ddot{\theta}+\ddot{\eta}-\eta\dot{\theta}^2+\frac{EI}{\rho}\eta^{iv} \\ = -F_{1x}\sin\theta+F_{1y}\cos\theta-F_{2x}\sin\theta+F_{1y}\cos\theta \end{aligned} \tag{21}$$

Hence, from (18), (19) and (20) the beam dynamics with respect to Cartesian coordinates $\{x_0,\ y_0,\ \theta\}^T$ can be written in a compact form as,

$$M_{rf}\ddot{X}_{rf}+C_{rf}+\eta_{rf}+G_{rf}=F_{rf}(-f) \tag{22}$$

where,

$$M_{rf} = \begin{bmatrix} m & 0 & -\rho\cos\theta\int_{\frac{-L}{2}}^{\frac{L}{2}}\eta\,dx \\ 0 & m & -\rho\sin\theta\int_{\frac{-L}{2}}^{\frac{L}{2}}\eta\,dx \\ -\rho\cos\theta\int_{\frac{-L}{2}}^{\frac{L}{2}}\eta\,dx & -\rho\sin\theta\int_{\frac{-L}{2}}^{\frac{L}{2}}\eta\,dx & \frac{mL^2}{12}+\rho\int_{\frac{-L}{2}}^{\frac{L}{2}}\eta^2dx \end{bmatrix}$$

$$C_{rf} = \begin{Bmatrix} \dot\theta^2(\rho\sin\theta\int_{\frac{-L}{2}}^{\frac{L}{2}}\eta\,dx) \\ -\dot\theta^2(\rho\cos\theta\int_{\frac{-L}{2}}^{\frac{L}{2}}\eta\,dx) \\ 0 \end{Bmatrix};\quad \eta_{rf} = \begin{Bmatrix} -\rho\sin\theta\int_{\frac{-L}{2}}^{\frac{L}{2}}\ddot\eta\,dx - 2\rho\dot\theta\cos\theta\int_{\frac{-L}{2}}^{\frac{L}{2}}\dot\eta\,dx \\ \rho\cos\theta\int_{\frac{-L}{2}}^{\frac{L}{2}}\ddot\eta\,dx - 2\rho\dot\theta\sin\theta\int_{\frac{-L}{2}}^{\frac{L}{2}}\dot\eta\,dx \\ \rho\int_{\frac{-L}{2}}^{\frac{L}{2}}x\ddot\eta\,dx + 2\rho\dot\theta\int_{\frac{-L}{2}}^{\frac{L}{2}}\eta\dot\eta\,dx \end{Bmatrix};$$

$$F_{rf} = \begin{bmatrix} 1 & 0 & 0 & 1 & 0 & 0 \\ 0 & 1 & 0 & 0 & 1 & 0 \\ \frac{L}{2}\sin\theta-\eta\cos\theta & -\frac{L}{2}\cos\theta-\eta\sin\theta & 0 & -\frac{L}{2}\sin\theta-\eta\cos\theta & \frac{L}{2}\cos\theta-\eta\sin\theta & 0 \end{bmatrix}$$

$$G_{rf} = \begin{Bmatrix} 0 \\ mg \\ 0 \end{Bmatrix};\quad \ddot X_{rf} = \begin{Bmatrix} \ddot x_0 \\ \ddot y_0 \\ \ddot\theta \end{Bmatrix};\quad f = \begin{Bmatrix} F_{1x} \\ F_{1y} \\ Mo_1 \\ F_{2x} \\ F_{2y} \\ Mo_2 \end{Bmatrix}$$

and also the flexible motion is the transverse vibration of beam dynamics which can be rewritten as,

$$-\sin\theta\ddot x_0 + \cos\theta\ddot y_0 + x\ddot\theta + \ddot\eta - \eta\dot\theta^2 + \frac{EI}{\rho}\eta^{iv} = F_{ff}(f) \tag{23}$$

where, $F_{ff} = [-\sin\theta \;\; \cos\theta \;\; 0 \;\; -\sin\theta \;\; \cos\theta \;\; 0]$

Equation (22) is written in compact form in which the rigid as well as flexible parameters are coupled together as also in (23). The above beam dynamic equations will be combined with the manipulator dynamics to form complete system dynamics.

2.4 Kinematics and dynamics of the manipulator

2.4.1 Kinematics of the manipulator

The study of manipulator kinematics gives us the geometrical and time-based properties of the motion of a manipulator. It provides information about the locations of frames attached to each link when the manipulator is performing a given task. It is classified into forward and inverse kinematics [54]. In the former case, given the manipulator joint angles of each link, the end-effector pose is determined. In the latter case, for the desired pose of the end-effector, one can find joint angles which will achieve the given pose. In general, velocity of each end-effector of the manipulator is related to joint velocity of the manipulator through Jacobian matrix [54]. The Jacobian matrix can be obtained with the help of position and orientation relations of the end-effector. Here in this section, the Jacobian matrix for a three link manipulator will be obtained which holds for another manipulator too. In general manipulators are considered to be identical in order to achieve the desired Cartesian space motion. However, by proper selection of different configuration of manipulator to achieve the similar Cartesian space motion is also possible. In that case, the manipulators Jacobian, inertia matrix, centrifugal and coriolis components and gravitational components

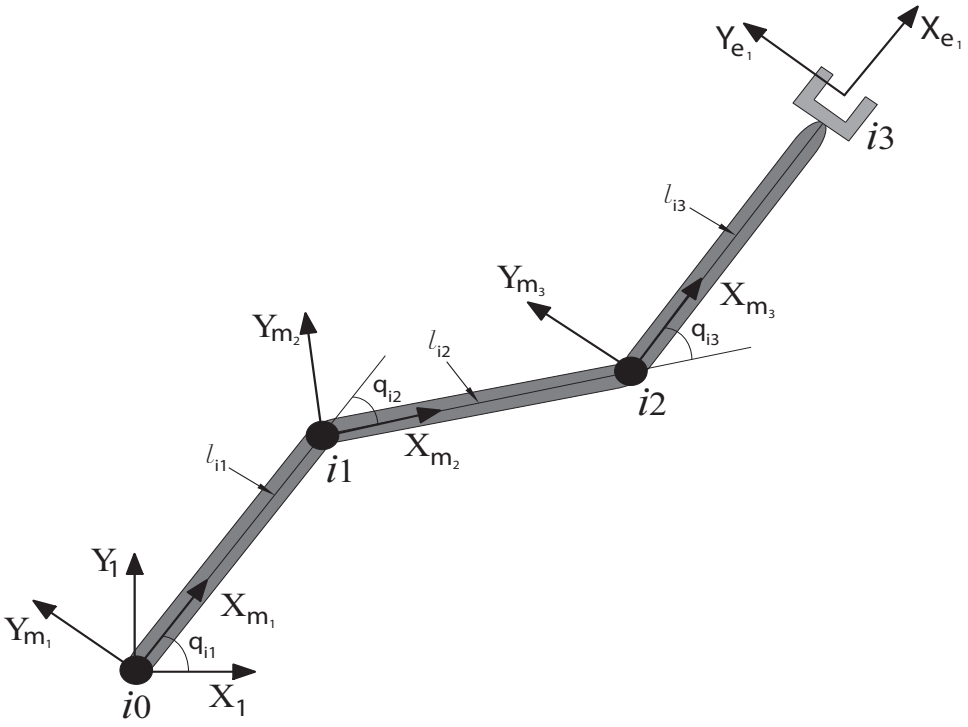

Figure 5: A manipulator with link-frame assignments

have to be derived separately.

Consider the position and orientation of end-effector $\{e_i\} = \{x_i,\, y_i,\, \theta\}^T$ with respect to a fixed coordinate frame (Refer Fig. 2). Each manipulator joint angles are represented by a vector $\{q_i\} = \{q_{i1},\, q_{i2},\, q_{i3}\}^T$. To compute the end-effector position and orientation of a manipulator, a local coordinate frame at each joint of a manipulator is considered. $X_{m_1}Y_{m_1}$ represents a coordinate frame attached at the base of the first link and similarly other coordinate frames are shown in Fig. 5. For example, the relationship between two coordinate frames A and B that are shown in Fig. 6 can be described by Denavit-Hartenberg notation [54] and this transformation matrix is denoted as T_{iB}^{iA}. Similarly, the transformation matrix between each links of manipulator is obtained. Finally, these transformation matrices are multiplied in a certain order which gives the transformation between the end-effector frame

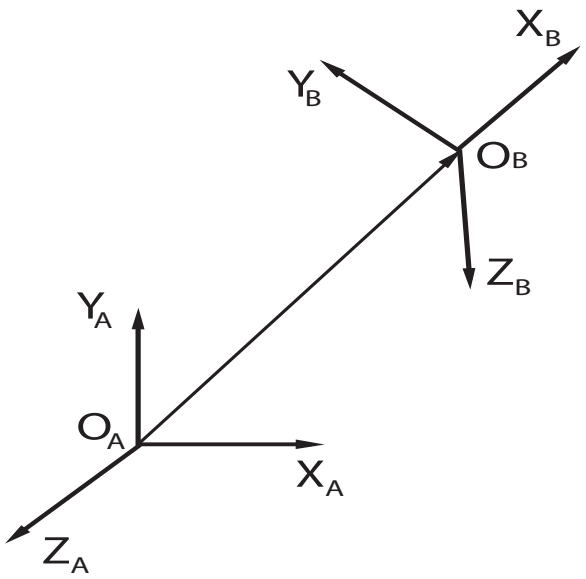

Figure 6: Two Coordinate frames A and B

and fixed frame of a manipulator.

The transforation matrix between each joint coordinate frame is as follows,

$$T_{i1}^{i0} = \begin{bmatrix} \cos(q_{i1}) & -\sin(q_{i1}) & 0 & l_{i1}\cos(q_{i1}) \\ \sin(q_{i1}) & \cos(q_{i1}) & 0 & l_{i1}\sin(q_{i1}) \\ 0 & 0 & 1 & 0 \\ 0 & 0 & 0 & 1 \end{bmatrix}$$

$$T_{i2}^{i1} = \begin{bmatrix} \cos(q_{i2}) & -\sin(q_{i2}) & 0 & l_{i2}\cos(q_{i2}) \\ \sin(q_{i2}) & \cos(q_{i2}) & 0 & l_{i2}\sin(q_{i2}) \\ 0 & 0 & 1 & 0 \\ 0 & 0 & 0 & 1 \end{bmatrix}$$

$$T_{i3}^{i2} = \begin{bmatrix} \cos(q_{i3}) & -\sin(q_{i3}) & 0 & l_{i3}\cos(q_{i3}) \\ \sin(q_{i3}) & \cos(q_{i3}) & 0 & l_{i3}\sin(q_{i3}) \\ 0 & 0 & 1 & 0 \\ 0 & 0 & 0 & 1 \end{bmatrix}$$

The transformation matrix of the manipulator can be obtained by,

$$T_{i3}^{i0} = T_{i1}^{i0}\ T_{i2}^{i1}\ T_{i3}^{i2} \tag{24}$$

$$T_{i3}^{i0} = \begin{bmatrix} c_{i123} & -s_{i123} & 0 & l_{i1}c_{i1} + l_{i2}c_{i12} + l_{i3}c_{i123} \\ s_{i123} & c_{i123} & 0 & l_{i1}s_{i1} + l_{i2}s_{i12} + l_{i3}s_{i123} \\ 0 & 0 & 1 & q_{i1} + q_{i2} + q_{i3} \\ 0 & 0 & 0 & 1 \end{bmatrix}$$

where, $c_{ij} = cos(q_{ij})$; $s_{ij} = sin(q_{ij})$; $c_{i12} = cos(q_{i1} + q_{i2})$; $s_{i12} = sin(q_{i1} + q_{i2})$;

$c_{i123} = cos(q_{i1} + q_{i2} + q_{i3})$; $s_{i123} = sin(q_{i1} + q_{i2} + q_{i3})$.

From the above transformation, the end-effector position and orientation are obtained, which are given by,

$$x_i = l_{i1}c_{i1} + l_{i2}c_{i12} + l_{i3}c_{i123} \tag{25}$$

$$y_i = l_{i1}s_{i1} + l_{i2}s_{i12} + l_{i3}s_{i123} \tag{26}$$

$$\theta_i = q_{i1} + q_{i2} + q_{i3} \tag{27}$$

In general, Jacobian matrix of a manipulator can be calculated by [54],

$$J_i = \begin{bmatrix} \frac{\partial x_i}{\partial q_{i1}} & \frac{\partial x_i}{\partial q_{i2}} & \frac{\partial x_i}{\partial q_{i3}} \\ \frac{\partial y_i}{\partial q_{i1}} & \frac{\partial y_i}{\partial q_{i2}} & \frac{\partial y_i}{\partial q_{i3}} \\ \frac{\partial \theta_i}{\partial q_{i1}} & \frac{\partial \theta_i}{\partial q_{i2}} & \frac{\partial \theta_i}{\partial q_{i3}} \end{bmatrix}$$

After partial differentiation, the Jacobian matrix can be derived as,

$$J_i = \begin{bmatrix} -l_{i1}s_{i1} - l_{i2}s_{i12} - l_{i3}s_{i123} & -l_{i2}s_{i12} - l_{i3}s_{i123} & -l_{i3}s_{i123} \\ l_{i1}c_{i1} + l_{i2}c_{i12} + l_{i3}c_{i123} & l_{i2}c_{i12} + l_{i3}c_{i123} & l_{i3}c_{i123} \\ 1 & 1 & 1 \end{bmatrix}$$

Above matrix is used to map the end-effector velocities which is in the Cartesian space to joint velocities which is represented in joint space. Since we have two manipulators with their Jacobian matrices denoted by J_1 and J_2, corresponding vectors of joint angles are denoted as q_1 and q_2, respectively.

A well known kinematic relation between the end-effector velocity and joint velocity gives [54],

$$\{\dot{e}_i\} = [J_i]\{\dot{q}_i\} \tag{28}$$

For the two manipulators,

$$\{\dot{e}_1\} = [J_1]\{\dot{q}_1\}, \quad \{\dot{e}_2\} = [J_2]\{\dot{q}_2\} \tag{29}$$

Equation (29) in an assembled form is given by,

$$\{\dot{e}\} = [J]\{\dot{q}\} \tag{30}$$

where,

$$\{\dot{e}\} = \begin{Bmatrix} \dot{e}_1 \\ \dot{e}_2 \end{Bmatrix}; \quad J = \begin{bmatrix} J_1 & 0 \\ 0 & J_2 \end{bmatrix}$$

Equation (30) can be rewritten as,

$$\{\dot{q}\} = [J^{-1}]\{\dot{e}\} \tag{31}$$

Differentiating (31) gives,

$$\{\ddot{q}\} = [J^{-1}]\{\ddot{e}\} + [\dot{J}^{-1}]\{\dot{e}\} \tag{32}$$

The above relations representing joint velocities (31) and joint acceleration (32) will be used in the next section to convert the manipulator dynamics represented in joint space to Cartesian space.

2.4.2 Dynamics of the manipulator

The dynamics of manipulator plays a vital role in developing the control algorithm and also simulating the motions of the manipulator. In general, dynamics of manipulator can be classified into inverse and forward dynamics. In the first case, given joint motion trajectories, one has to determine the required joint torques in order to achieve the desired joint motion. In the second case, given joint torques, the joint motions such as joint angles, its velocities and accelerations are calculated. The dynamic equations of motion of manipulator can be represented in a generalized joint coordinate space or in a generalized Cartesian coordinate space. In many of the assembly tasks, manipulator may require the geometrical information of the environment in task space and the dynamic equations of motion in that space is helpful in designing the control method. However, depending upon the applications and for the development of various control algorithms, the dynamics can be presented in any one of these spaces. In this section, the manipulator dynamics will be converted into Cartesian space because of the fact that it should be combined with beam dynamics which is already available in Cartesian space.

Dynamic equations of manipulator can be derived using Newton-Euler recursive

method or Euler - Lagrange method. The Euler-Lagrange equations are generally used to obtain the dynamic equations of manipulator [55] because, it gives good insight to understand the nonlinear characteristics of the manipulator.

The following are the assumptions to be considered while deriving the dynamic equations of manipulator.

1. Each link of the manipulator is assumed to be rigid and exhibits no structural compliance.

2. Compliance at each joint of the manipulator is ignored.

General manipulator dynamic equation can be written in joint space as [55],

$$M_i(q_i)\ddot{q}_i + C_i(q_i,\dot{q}_i)\dot{q}_i + G_i(q_i) = \tau_i + J_i^T f_i \qquad where\ i = 1,2 \tag{33}$$

where,

q_i is the vector of joint angles.

M_i represents inertia matrix.

C_i is the matrix due to coriolis and centrifugal components.

G_i represents the vector of gravitational components.

τ_i is the vector of input torque applied at each joints of the manipulator.

f_i is the interaction force between the manipulator and the flexible beam.

J_i is the Jacobian matrix of a manipulator.

Although, Equation (33) is complex and possesses highly nonlinear terms, is has a few important properties which will be useful for the control design purpose. These properties are given in [55] and [56] which are stated as follows:

Property 1:

The inertia matrix $M_i(q_i)$ is symmetric and positive definite. If all of the joints are revolute then,

$$\mu_1 I_d \leq M_i(q_i) \leq \mu_2 I_d$$

where, the bounds μ_1 and μ_2 are constants and I_d is identity matrix. Since q appears in $M_i(q_i)$ only through sine and cosine terms, their magnitudes are bounded by 1.

Similarly, the inverse of inertia matrix, $M_i^{-1}(q_i)$, is also bounded

$$\frac{1}{\mu_2} I_d \leq M_i^{-1}(q_i) \leq \frac{1}{\mu_1} I_d$$

Property 2:

The matrix $V(q, q_i) = \dot{M}_i(q_i) - 2C_i(q_i, \dot{q}_i)$ is skew symmetric, i.e, the components V_{jk} of V satisfy $V_{jk} = -V_{kj}$

If V is skew-symmetric, the following should also be satisfied and the detailed proof is found in [57].

$$\dot{q}_i^T [\dot{M}_i(q_i) - 2C_i(q_i, \dot{q}_i)]\dot{q}_i = 0$$

Property 3:

Since $C_i(q_i, \dot{q}_i)$ is quadratic in $\dot{q}_i$, it can also be bounded by quadratic function of $\dot{q}_i$. That is,

$$C_i(q_i, \dot{q}_i) \leq v_b(q)\|\dot{q}_i\|^2$$

where $v_b(q)$ is known scalar function and $\|\cdot\|$ denotes any appropriate norm.

Property 4:

$$M_i(q_i)\ddot{q}_i + C_i(q_i,\dot{q}_i)\dot{q}_i + G_i q_i =: Y_{im}(q_i,\dot{q}_i,\ddot{q}_i)\Theta_{im}$$

The function Y_{im} is called Regressor [58] of i^{th} manipulator which has time dependant variables and Θ_{im} is the parameter vector of i^{th} manipulator which contains time independent variables such as link masses, moments of inertia, etc., that must be determined for a particular manipulator.

Assembling the dynamic equations (33) of the two manipulators in joint space gives,

$$M_r\ddot{q} + C_r\dot{q} + G_r = \tau + J^T f \tag{34}$$

where,

$$M_r = \begin{bmatrix} M_1 & 0 \\ 0 & M_2 \end{bmatrix};\ C_r = \begin{bmatrix} C_1 & 0 \\ 0 & C_2 \end{bmatrix};\ G_r = \begin{Bmatrix} G_1 \\ G_2 \end{Bmatrix};\quad \tau = \begin{Bmatrix} \tau_1 \\ \tau_2 \end{Bmatrix}$$

$$J = \begin{bmatrix} J_1 & 0 \\ 0 & J_2 \end{bmatrix};\quad f = \begin{Bmatrix} f_1 \\ f_2 \end{Bmatrix};\quad q = \begin{Bmatrix} q_1 \\ q_2 \end{Bmatrix}$$

It can be seen that the beam dynamics in (22) is represented with respect to Cartesian coordinates, $\{x_0,\ y_0,\ \theta\}^T$, whereas the manipulator dynamics (34) is represented with respect to joint space coordinates. In order to formulate a complete system of dynamic equations in Cartesian space, the manipulator dynamics will be converted into Cartesian space and the result will be combined with the beam dynamics to form the combined dynamics.

Substituting (5) into (31) yields,

$$\{\dot{q}\} = [J^{-1}][R]\{\dot{X}_{rf}\} \tag{35}$$

Differentiating (35) gives,

$$\{\ddot{q}\} = J^{-1}\dot{R}\dot{X}_{rf} + J^{-1}R\ddot{X}_{rf} + \dot{J}^{-1}R\dot{X}_{rf} \tag{36}$$

For simplicity, parentheses for vectors and square brackets for matrices are omitted in the following.

Substituting (35) and (36) into (34), we obtain the manipulator dynamics in Cartesian space,

$$M_r J^{-1}R\ddot{X}_{rf} + (M_r\dot{J}^{-1}R + M_r J^{-1}\dot{R} + C_r J^{-1}R)\dot{X}_{rf} + G_r = \tau + J^T f \tag{37}$$

2.5 Combined dynamics

The dynamics of manipulators and beam represented with respect to Cartesian coordinates are combined to formulate the kinematically closed loop system.

Premultiplying (37) by $R^T J^{-T}$ gives,

$$R^T J^{-T} M_r J^{-1} R\ddot{X}_{rf} + R^T J^{-T}(M_r\dot{J}^{-1}R + M_r J^{-1}\dot{R} + C_r J^{-1}R)\dot{X}_{rf} + R^T J^{-T} G_r = R^T J^{-T}\tau + R^T J^{-T} J^T f \tag{38}$$

In view of the assumption of simply supported beam boundary conditions, the moments at the two ends are zero. However, in reality manipulators experience forces as well as moments at the two ends of the beam [59]. Utilizing this fact, the moments at the two ends of the beam is included in the matrix F_{rf} of (22). So, F_{rf} becomes R^T and is given by,

$$F_{rf} = \begin{bmatrix} 1 & 0 & 0 & 1 & 0 & 0 \\ 0 & 1 & 0 & 0 & 1 & 0 \\ \frac{L}{2}\sin\theta - \eta\cos\theta & -\frac{L}{2}\cos\theta - \eta\sin\theta & 1 & -\frac{L}{2}\sin\theta - \eta\cos\theta & \frac{L}{2}\cos\theta - \eta\sin\theta & 1 \end{bmatrix}$$

Since $R^T = F_{rf}$, (42) becomes,

$$R^T J^{-T} M_r J^{-1} R\ddot{X}_{rf} + R^T J^{-T}(M_r \dot{J}^{-1} R + M_r J^{-1}\dot{R} + C_r J^{-1} R)\dot{X}_{rf} + R^T J^{-T} G_r = R^T J^{-T}\tau + F_{rf} f \quad (39)$$

Substituting (22) into (39) yields,

$$R^T J^{-T} M_r J^{-1} R\ddot{X}_{rf} + R^T J^{-T}(M_r \dot{J}^{-1} R + M_r J^{-1}\dot{R} + C_r J^{-1} R)\dot{X}_{rf} + R^T J^{-T} G_r = R^T J^{-T}\tau - (M_{rf}\ddot{X}_{rf} + C_{rf} + \eta_{rf} + G_{rf}) \quad (40)$$

The above combined rigid motion dynamic equation can be rewritten as,

$$M_{orf}\ddot{X}_{rf} + C_{orf}\dot{X}_{rf} + G_{orf} + \eta_{orf} = u_{orf} \quad (41)$$

where,

$$M_{orf} = R^T J^{-T} M_r J^{-1} R + M_{rf}$$

$$C_{orf} = R^T J^{-T}(M_r \dot{J}^{-1} R + M_r J^{-1}\dot{R} + C_r J^{-1} R) + C_{rf}$$

$$G_{orf} = R^T J^{-T} G_r + G_{rf}$$

$$\eta_{orf} = \eta_{rf}$$

$$u_{orf} = R^T J^{-T}\tau$$

The above combined rigid motion dynamic equation (41) represented in the Cartesian coordinate space has coupling between rigid and flexible parameters and there is no approximation or discretization involved.

Taking into account the transverse vibration of beam dynamics (23), the complete manipulator-beam system dynamics is represented as

$$M_{orf}\ddot{X}_{rf} + C_{orf}\dot{X}_{rf} + G_{orf} + \eta_{orf} = u_{orf} \quad (42)$$

$$-\sin\theta\ddot{x}_0+\cos\theta\ddot{y}_0+x\ddot{\theta}+\ddot{\eta}-\eta\dot{\theta}^2+\frac{EI}{\rho}\eta^{iv}=F_{ff}(f) \tag{43}$$

The above system of dynamic equations are used further to design a control algorithm without using any approximate methods.

2.6 Summary

This Chapter focuses on the development of mathematical model of manipulator-flexible object system. Kinematic relations of manipulators and the flexible object were obtained. The dynamic model of the flexible object was obtained without involving any approximations or discretizations. Furthermore, the derived object dynamics has been combined with the manipulators dynamics, which yields the combined dynamics in Cartesian space without using any assumption of number of modes. The resulting combined dynamic equation and also the transverse vibration of beam equation are coupled with rigid as well as flexible parameters which are in PDE form. In order to develop control strategy for such a PDE based system without using any approximate method is tedious. The control of such a coupled rigid and flexible body motion is normally achieved by employing singular perturbation technique. In the next Chapter, the system of dynamic equations (23) and (41) will be decoupled into rigid and flexible dynamics by using singular perturbation technique. Then, they will form a slow and fast subsystem, in two different time scales, respectively.

Chapter 3

Singular Perturbation Model

3.1 Need for singular perturbation analysis

The system of dynamic equations obtained from the previous chapter involves rigid and flexible body motions. These two motions can be also controlled without using any approximation or discretization. Moreover, the assumption of number of modes causes increase in the order of the control algorithm and also neglecting the higher order frequencies would destabilize the system. It is necessary to implement a suitable control strategy for the developed PDE based systems which is a more challenging task. It can be possible by separating the system dynamics into rigid and flexible dynamics by means of singular perturbation approach. The main purpose of the singular perturbation approach is to alleviate the high dimensionality and ill-conditioning resulting from the interaction of slow and fast dynamic modes. Utilizing this approach, the system of dynamic equations is decoupled into slow and fast subsystems in two different time scales, respectively. Then, one can design a control algorithm for each subsystem that together forms a composite control input to achieve

the desired rigid body motion of the object and also suppressing the vibration. This thesis considers a similar approach to decouple the system into slow and fast subsystems.

In this Chapter, before proceeding into the development of rigid and flexible dynamic model an outline of singular perturbed approach for linear and nonlinear systems is reviewed. Then, the typical steps of singularly perturbed analysis of nonlinear systems is implemented into the system dynamics (23) and (41) (manipulator-beam system) under some specific requirements. It yields into slow subsystem which corresponds to rigid body motion of the object and fast subsystem that signifies the vibration of the object. Furthermore, based upon the concept of differential operators, the infinite dimensional partial differential model of the fast subsystem is further modified into abstract differential equation which will avoid the issues due to approximation or discretization techniques.

3.2 Outline of singular perturbation approach

For the control engineer, the first task is to mathematically model the given physical system. While simplifying the given model, the presence of small "parasitic" parameters such as time constants, masses, capacitances, inductances, resistances, moments of inertia, Reynolds number and other parameters may increase the order and also stiffness of the systems. In order to alleviate these problems, singular perturbation approach is employed commonly. These problems are dealt in many fields of applied mathematics, various disciplines of engineering, electrical and electronics circuits and systems, electrical power systems, aerospace systems, nuclear reactors and ecology. This approach would also be

helpful for analytical investigations of robustness of system properties, behavior of optimal controls near singular arcs and other order reduction models. Some of the well known applications are in aircraft and rocket flight models and chemical reaction diffusion theory.

Singular perturbation introduces multitime-scale behavior of dynamical systems, namely, slow and fast phenomena due to the external stimuli. It is stated in [60] as, "Singular perturbation approach lowers the model order by first neglecting the fast phenomena. It then improves approximation by reintroducing their effect as boundary layer corrections calculated in separate time scales". In most of the classical and modern control schemes, singular perturbation analysis plays a role in the order reduction of the model which disregard high frequency parasitics [61]. This leads to the development of time scale methods for various control algorithms such as state feedback, output feedback, filter and observer design. It is also useful for the analysis of high-gain feedback systems, control of dynamic networks and other class of linear and nonlinear dynamic systems. The complete survey on singular perturbations and time scales in control theory and applications can be seen in [60]-[63]. After brief review on the concepts of singular perturbation analysis for the case of linear and nonlinear systems, they will be employed in the manipulator-flexible beam system.

3.2.1 Singularly perturbed analysis of linear systems

In order to illustrate the basics of singularly perturbed systems, the second order initial value problem presented in [62] is reproduced here.

The standard singularly perturbed linear second order problem is given by,

$$\varepsilon\ddot{x}(t,\varepsilon)+\dot{x}(t,\varepsilon)+x(t,\varepsilon)=0$$

$$x(t_0) = x(0), \quad \dot{x}(t_0) = \dot{x}(0) \tag{44}$$

where, the small parameter ε multiplying into the highest derivative term defines the singularly perturbed problem. The degenerate problem or reduced-order problem can be obtained by setting $\varepsilon = 0$ in (44) which is given by,

$$\dot{x}^{(0)}(t) + x^{(0)}(t) = 0 \tag{45}$$

where $x^{(0)}(t_0) = x(0)$ and the solution to (45) is,

$$x^{(0)}(t) = x(0)e^{-t} \tag{46}$$

The reduced order problem in (45) is only of first order which may not satisfy both of the initial conditions given in (44) and hence, $\dot{x}(t_0)$ is sacrificed during the degeneration process.

3.2.2 Singularly perturbed analysis of nonlinear systems

Now let us analyze singularly perturbed time varying nonlinear system which is given by [64],

$$\dot{x} = f_p(x, z, \varepsilon, t), \quad x(t_0) = x_0, \quad x \in R^{n_1} \tag{47}$$

$$\varepsilon \dot{z} = g_p(x, z, \varepsilon, t), \quad z(t_0) = z_0, \quad z \in R^{m_1} \tag{48}$$

where, f_p and g_p are many times continuously differentiable functions of their arguments x, z, ε and t. If the functions f_p and g_p are having same order of magnitude then, the perturbation parameter ε represents the ratio of two time scales. When ε approaches zero,

the dynamics of z becomes faster than x and also the above n_1+m_1 dimensional model will reduce to n_1 dimensional model, because, (48) degenerates into the algebraic or transcendental equation,

$$0 = g_p(x_s, z_s, 0, t) \tag{49}$$

where the subscript "s" indicates the slow subsystem when ε approaches zero. On solving (49) we have $k_1 \geq 1$ distinct or isolated real roots given by,

$$z_s = \varphi_i(x_s, t), \quad i = 1, 2, ..., k_1 \tag{50}$$

Substituting (50) into (47) gives,

$$\dot{x_s} = f_p(x_s, \varphi_i(x_s, t), 0, t), \quad x_s(t_0) = x_0 \tag{51}$$

The above model given in (51) is called as quasi-steady-state model or reduced-order model. The multi-time-scale behavior occurs due to this model, (i.e) the slow response is obtained from the reduced order model. The discrepancy between the response of the reduced order model (51) and that of the given nonlinear model (47) and (48) is the fast response or transient behavior. Due to this behavior, the quasi-steady-state variable z_s would not start at the prescribed initial condition z_0 of the original variable z and there may be small or large order of magnitude difference which is specified by $O(\varepsilon)$ [64]. Due to this error, z_s cannot be a uniform approximation of z and it can be approximated as

$$z = z_s(t) + O(\varepsilon), \quad t \in [t_1, T] \quad \text{where } \mathrm{t_1} > \mathrm{t_0} \tag{52}$$

However, the slow variable x_s can be constrained to start from the pre-specified initial condition x_0. Hence, the approximation of x by the quasi-steady-state variable x_s will be

uniform and is given by

$$x = x_s(t) + O(\varepsilon), \quad t \in [t_0, T] \tag{53}$$

The above way of approximating the solution is called degeneration. It can be seen from (52) that, in the initial interval (boundary layer) $[t_0,\ t_1]$ the original variable z approaches z_s and after that it remains close to z_s.

In order to study the fast parts of x and z, let us define new time scale variable,

$$\nu = \frac{t - t_0}{\varepsilon}, \quad \nu = 0 \ at \ t = t_0 \tag{54}$$

Then, (47) and (48) can be rewritten with respect to fast time scale as,

$$\frac{dx}{d\nu} = \varepsilon f_p(x, z, \varepsilon, t_0 + \varepsilon\nu) \tag{55}$$

$$\frac{dz}{d\nu} = g_p(x, z, \varepsilon, t_0 + \varepsilon\nu) \tag{56}$$

When $\varepsilon \to 0$ then,

$$\frac{dx}{d\nu} = 0 \tag{57}$$

which means that, x = constant in the fast time scale. However, the deviations of z from its quasi-steady-state z_s plays a role in the fast time scale. In order to obtain the behavior of z as a function of ν, the boundary layer correction has to be obtained which is given by,

$$z_f = z - z_s \tag{58}$$

Using (58) and letting $\varepsilon = 0$ in (56), the fast subsystem or boundary layer system can be obtained as,

$$\frac{dz_f}{d\nu} = g_p(x_0, z_s(t_0) + z_f(\nu), 0, t_0), \quad z_f(\nu_0) = z_0 - z_s(t_0) \tag{59}$$

The solution of (59), (i.e) $z_f(v)$ is considered as boundary layer correction of (52) for a uniform approximation of z which is given by,

$$z = z_s(t) + z_f(v) + O(\varepsilon) \tag{60}$$

It is evident from (60) that, $z_s(t)$ is slow transient of z and $z_f(v)$ is the fast transient of z. The corrected approximation (60) has to converge in a short period to the slow approximation in (52) and the correction term $z_f(v)$ must decay as $v \to \infty$. The stability of boundary layer system given in (59) has to account for the approximations made in (52), (53) and (60). Hence, valid stability properties should be stated. The stability properties are provided as assumptions in [64] which are given below.

Assumption 1:

The equilibrium $z_f(v) = 0$ of (59) is asymptotically stable uniformly in x_0 and t_0 and $z_0 - z_s(t_0)$ belongs to its domain of attraction and hence, $z_f(v)$ exists for all $v \geq 0$.

If this assumption is satisfied, then

$$\lim_{v \to \infty} z_f(v) = 0 \tag{61}$$

uniformly in x_0, t_0; that is, z will come close to its quasi-steady-state z_s at some time $t_1 > t_0$. To ensure that z stays close to z_s the following assumption is considered.

Assumption 2:

The eigenvalues of $\frac{\partial g_p}{\partial z}$ evaluated, for $\varepsilon = 0$, along $x_s(t)$ and $z_s(t)$, have real parts smaller than a fixed negative number, i.e.

$$Re\lambda\{\frac{\partial g_p}{\partial z}\} \leq -c < 0 \tag{62}$$

The above mentioned two assumptions describe strong stability property of the boundary layer system (59).

3.2.3 Features of singularly perturbed solutions

The important characteristics of singular perturbation problems are summarized below:

- In any given mathematical model, the highest derivative of the model is multiplied by the small parameter ε and is called singularly perturbed model if the order of model is reduced when $\varepsilon = 0$.
- The singularly perturbed problem has two phenomena namely slow and fast in its solution which occurs in two different time scales.
- The degenerate problem of reduced order model will not satisfy all the given boundary conditions of the original given problem.
- In the boundary layer, solution changes rapidly.
- In order to approximate the fast solution, boundary layer correction is incorporated with the help off stretching transformation such as $v = \frac{t-t_0}{\varepsilon}$.

3.3 Validity of singular perturbation approach

The use of singular perturbation approach for the non-linear systems necessitates the satisfaction of Tikhnov's theorem. Hence, based upon the background material presented earlier on standard singularly perturbed model of the non-linear systems, the Tikhnov's theorem

given in Khalil [65] is reproduced for the different cases of time intervals.

Theorem 1 (for the case of finite time interval):

Consider the singular perturbation problem (47) and (48) and let $z = \vartheta(x,t)$ be an isolated root of (49). Assume that the following conditions are satisfied for all

$$[x,t,z-\vartheta(x,t),\varepsilon] \in [0,T] \times B_r \times B_p \times [0,\varepsilon_0]$$

1. The functions f_p, g_p and their first partial derivatives with respect to (x,z,ε) are continuous. The function $\vartheta(x,t)$ and the Jacobian $\partial g(x,z,0,t)/\partial z$ have continuous first partial derivatives with respect to their arguments.

2. The reduced problem (51) has a unique solution $x_s(t)$, defined on $[t_0,t_1]$ and $\|x_s(t)\| \leq r_1 < r$ for all $t \in [t_0,T]$.

3. The origin of the boundary layer model (59) is exponentially stable, uniformly in (x,t).

Then, there exist positive constants μ and $\varepsilon^\star$ such that for all $\|z(0)-\phi(t_0,x(0)\| < \mu$ and $0 < \varepsilon < \varepsilon^\star$, the singular perturbation problem (47) and (48) has a unique solution $x(t,\varepsilon)$, $z(t,\varepsilon)$ on $[t_0,T]$ and

$$\begin{aligned} x - x_s(t) &= O(\varepsilon) \\ z - \vartheta(x_s,t) - z_f(\nu) &= O(\varepsilon) \end{aligned}$$

hold uniformly for $t \in [t_0,T]$, where $z_f(\nu)$ is the solution of the boundary layer model (59). Moreover, given any $t_1 > t_0$, there is $\varepsilon^{\star\star} \leq \varepsilon^\star$ such that,

$$z - \vartheta(x_s,t) = O(\varepsilon)$$

holds uniformly for $t \in [t_1, T]$ whenever $\varepsilon < \varepsilon^\star$

The above theorem holds good for finite time intervals. This is because, the error estimate $O(\varepsilon)$ is not uniform in for all $t \geq 0$. In order to extend this theorem to infinite time intervals, additional stability requirement on reduced model (47) must be met. To be precise, the reduced order model should also be exponentially stable for the infinite time interval. Hence, Tikhnov extended the previous theorem to the infinite interval which is as follows.

Theorem 2 (for the case of infinite time interval):

Consider the singular perturbation problem (47) and (48) and let $z = \vartheta(x,t)$ be an isolated root of (49). Assume that the following conditions are satisfied for all

$$[x, t, z - \vartheta(x,t), \varepsilon] \in [0, \infty] \times B_r \times B_p \times [0, \varepsilon_0]$$

1. The functions f_p, g_p and their first partial derivatives with respect to (x, z, ε) are continuous and bounded. The function $\vartheta(x,t)$ and the Jacobian $\partial g(x,z,0,t)/\partial z$ have bounded continuous first partial derivatives with respect to their arguments.

2. The Jacobian $\partial f(x, \vartheta(t,x), 0, t)/\partial x$ has bounded first partial derivatives with respect to x.

3. The origin of the reduced problem (51) is exponentially stable.

4. The origin of the boundary layer model (59) is exponentially stable, uniformly in (x,t).

Then, there exist positive constants μ_{11}, μ_{22} and $\varepsilon^\star$ such that for all

$$\|x(0)\| < \mu_{11}, \quad \|z(0) - \phi(t_0, x(0)\| < \mu_{22} \quad \text{and} \quad 0 < \varepsilon < \varepsilon^\star$$

the singular perturbation problem (47) and (48) has a unique solution $x(\varepsilon,t)$ and $z(\varepsilon,t)$ defined for all $T \geq t_0 \geq 0$, and

$$x - x_s(t) = O(\varepsilon)$$

$$z - \vartheta(x_s,t) - z_f(v) = O(\varepsilon)$$

hold uniformly for $t \in [t_0,\infty]$. Moreover, given any $t_1 > t_0$, there is $\varepsilon^{\star\star} \leq \varepsilon^{\star}$ such that,

$$z - \vartheta(x_s,t) = O(\varepsilon)$$

holds uniformly for $t \in [t_1,\infty]$ whenever $\varepsilon < \varepsilon^{\star\star}$.

Hence, it is evident from the above theorem that, for the validation of use of singular perturbation approach, the slow subsystem or reduced order model and fast subsystem or boundary layer model must be exponentially stable for the infinite time interval.

3.4 Singular perturbed model of the manipulators - flexible object system

Singular perturbation approach is not straightforward to apply to the manipulator-beam system. There are some requirements to be met to apply this technique into the system of dynamic equations (42) and (43) which will be discussed later. In this section, initially the control task will be stated and based upon this task singularly perturbed model will be developed.

The control task is stated as follows: For any given desired bounded trajectories of the mass center of the beam X_{rfd} and $\dot{X}_{rfd}$, with some or all of the manipulator and beam

parameters unknown, derive a controller for the manipulators τ such that the beam center X_{rf} tracks X_{rfd} while suppressing the vibration of the flexible object, η, to zero.

The system dynamics derived without using any approximation methods given in (42) and (43) have rigid as well as flexible parameters that are coupled together. To achieve the above control objective for such a complicated nonlinear system, a possible control approach is the two-time scale theory which considers the high frequency phenomenon of flexible motion in different time scales. The basic idea for the two-time scale theory is to identify the slow and fast subsystems in separate time scales by employing singular perturbation approach [64]. Then, a control algorithm for each subsystem is designed, which will be combined to yield the composite control strategy for the original system. However, the challenge is such that the designed sub-controllers satisfy the so-called Tikhnov's theorem in order to guarantee that the composite controller can be applied to the original system, especially when the parameters of the system are unknown.

It is evident from the complete system of dynamic equations that, the inertia matrix M_r, Coriolis and Centrifugal matrix C_r, Gravitational vectors G_r and Jacobian matrix J do not have any flexible parameters, because the manipulators are considered to be rigid. However, in M_{rf}, C_{rf}, η_{rf} and in R, rigid as well as flexible parameters are coupled together. These flexible parameters have to be uncoupled from the above matrices and vectors by using singular perturbation technique. It is to noted that, in order to avoid confusion, these parameters are separated from the complete system of dynamic equations and typical steps of singular perturbation approach is applied. This technique also accounts for the neglected high frequency characteristics when the beam undergoes vibration [66]. Using a perturbation parameter, say ε^2, order of the system dynamics can be changed and this small

parameter depends upon the system variable. Keeping that in mind, the term EI/ρ in (43), which has large magnitude compared to other coefficients [66], can be re-defined as,

$$\frac{EI}{\rho} = a \; . \; K \tag{63}$$

where K is a dimensionless parameter which has large value for the different materials [64] and [66] and its order is equal to EI/ρ and also the variable "a" satisfies the equalities. For example, an aluminium rod with a diameter of 0.05m, E = 71 GPa and $\rho = 2700\ kg/m^3$ has the value of the co-efficient $EI/\rho \cong 4.1 \times 10^3$ and therefore $a = 4.1$ and $K = 10^3$. However, the beam has rigid motion with respect to the state variables $X_{rf} = \{x_0,\ y_0,\ \theta\}^T$ and also the transverse vibration η with respect to the state variable occurs in different time scales. Then, one need to introduce a new variable $w(x,t)$ in the same order of the state variable by the following,

$$\eta(x,t) = \varepsilon^2 . w(x,t) \tag{64}$$

where $\varepsilon^2 = 1/K$ is the so-called perturbed parameter.

Using (64) one can re-write the rigid motion dynamics of the beam as follows:

The equation of motion (18) in the X-direction can be written in terms of perturbed parameter as,

$$m\ddot{x}_0 - (\rho \cos\theta\ \varepsilon^2 \int_{\frac{-L}{2}}^{\frac{L}{2}} w dx)\ddot{\theta} - \rho \sin\theta\ \varepsilon^2 \int_{\frac{-L}{2}}^{\frac{L}{2}} \ddot{w} dx - 2\rho\dot{\theta}\cos\theta\ \varepsilon^2 \int_{\frac{-L}{2}}^{\frac{L}{2}} \dot{w} dx + \dot{\theta}^2 \rho \sin\theta\ \varepsilon^2 \int_{\frac{-L}{2}}^{\frac{L}{2}} w dx = F_{2x} + F_{1x} \tag{65}$$

The equation of motion (19) in the Y-direction can be written in terms of perturbed parameter as,

$$m\ddot{y}_0 - (\rho \sin\theta\ \varepsilon^2 \int_{\frac{-L}{2}}^{\frac{L}{2}} w dx)\ddot{\theta} + \rho \cos\theta\ \varepsilon^2 \int_{\frac{-L}{2}}^{\frac{L}{2}} \ddot{w} dx - 2\rho\dot{\theta}\sin\theta\ \varepsilon^2 \int_{\frac{-L}{2}}^{\frac{L}{2}} \dot{w} dx$$

$$-\dot{\theta}^2\rho\cos\theta\ \varepsilon^2\int_{\frac{-L}{2}}^{\frac{L}{2}} w dx + mg = F_{2y} + F_{1y} \tag{66}$$

Rotation about the Z axis described in equation of motion (20) in terms of perturbed parameter is,

$$(-\rho\cos\theta\ \varepsilon^2\int_{\frac{-L}{2}}^{\frac{L}{2}} w dx)\ddot{x}_0 - (\rho\sin\theta\ \varepsilon^2\int_{\frac{-L}{2}}^{\frac{L}{2}} w dx)\ddot{y}_0 + (\frac{mL^2}{12} + \rho\ \varepsilon^4\int_{\frac{-L}{2}}^{\frac{L}{2}} w^2 dx)\ddot{\theta}$$
$$+\rho\ \varepsilon^2\int_{\frac{-L}{2}}^{\frac{L}{2}} x\ddot{w}dx 2\rho\dot{\theta}\ \varepsilon^4\int_{\frac{-L}{2}}^{\frac{L}{2}} w\dot{w}dx = F_{1x}(\frac{L}{2}\sin\theta - \varepsilon^2 w\cos\theta)$$
$$+F_{1y}(-\frac{L}{2}\cos\theta - \varepsilon^2 w\sin\theta) + F_{2x}(-\frac{L}{2}\sin\theta - \varepsilon^2 w\cos\theta) + F_{2y}(\frac{L}{2}\cos\theta - \varepsilon^2 w\sin\theta) \tag{67}$$

Correspondingly, using (63) and (64), the equation of motion for transverse vibration of the beam can be rewritten as,

$$-\sin\theta\ddot{x}_0 + \cos\theta\ddot{y}_0 + x\ddot{\theta} + \varepsilon^2\ddot{w} - \varepsilon^2 w\dot{\theta}^2 + aw^{iv} = F_{ff}(f) \tag{68}$$

The equations (65), (66), (67) and (68) represent the singularly perturbed form which will be incorporated into the system of dynamic equations (42) and (43) to form the singularly perturbed model of the complete system.

3.5 Slow and fast dynamic models

In this section, the two subsystems, namely slow and fast, are obtained by following the typical steps of singular perturbation approach which were discussed earlier in this Chapter. Due to the presence of perturbed parameter ε^2, the complete system has two motions in the different time scales. Initially, the singularly perturbed model of rigid motion dynamics of the beam will be converted into the rigid dynamic model without involving any flexible parameter and finally it will be incorporated into (42) which forms the slow subsystem.

Similarly, after following the usual procedure of the singular perturbation approach, the fast subsystem will be obtained from (68).

3.5.1 Slow subsystem

When the perturbation parameter ε approaches zero, the equivalent quasi-steady-state system [67] represents the slow subsystem. By setting $\varepsilon = 0$, (65), (66) and (67) forms the rigid dynamic model of the beam which is given in compact form as,

$$M_{rd}\ddot{X}_{rf} + C_{rd} + \eta_{rd} + G_{rd} = F_{rd}(-f) \tag{69}$$

$$M_{rd} = \begin{bmatrix} m & 0 & 0 \\ 0 & m & 0 \\ 0 & 0 & \frac{mL^2}{12} \end{bmatrix};\ \ddot{X}_{rf} = \begin{Bmatrix} \ddot{x}_0 \\ \ddot{y}_0 \\ \ddot{\theta} \end{Bmatrix};\ C_{rd} = \{0\ 0\ 0\}^T;$$

$$\eta_{rd} = \{0\ 0\ 0\}^T;\ G_{rd} = \begin{Bmatrix} 0 \\ mg \\ 0 \end{Bmatrix};$$

$$F_{rd} = \begin{bmatrix} 1 & 0 & 0 & 1 & 0 & 0 \\ 0 & 1 & 0 & 0 & 1 & 0 \\ \frac{L}{2}\sin\theta & -\frac{L}{2}\cos\theta & 1 & -\frac{L}{2}\sin\theta & \frac{L}{2}\cos\theta & 1 \end{bmatrix}$$

The equation of motion for transverse vibration of the beam (68) becomes,

$$[-\sin\theta\ddot{x}_0 + \cos\theta\ddot{y}_0 + x\ddot{\theta} + aw^{iv}]_s \ = F_{ff}(f_s) \tag{70}$$

where f_s corresponds to f when ε approaches zero.

Again, substituting (64) into (5) and also setting $\varepsilon = 0$, R becomes R_1 which is given by,

$$R_1 = \begin{bmatrix} 1 & 0 & \frac{L}{2}sin\theta \\ 0 & 1 & -\frac{L}{2}cos\theta \\ 0 & 0 & 1 \\ 1 & 0 & -\frac{L}{2}sin\theta \\ 0 & 1 & \frac{L}{2}cos\theta \\ 0 & 0 & 1 \end{bmatrix}$$

Based upon the above results, the combined dynamic equation (42) becomes,

$$(M_o + M_{rd})\ddot{X}_{rf} + C_o\dot{X}_{rf} + G_o + G_{rd} = u_o \tag{71}$$

where,

$$M_o = R_1^T J^{-T} M_r J^{-1} R_1$$

$$C_o = R_1^T J^{-T}(M_r \dot{J^{-1}} R_1 + M_r J^{-1}\dot{R}_1 + C_r J^{-1} R_1)$$

$$G_o = R_1^T J^{-T} G_r$$

$$u_0 = R_1^T J^{-T}\tau$$

The above equation can be rewritten as,

$$M_{cs}\ddot{X}_{rf} + C_{cs}\dot{X}_{rf} + G_{cs} = u_{cs} \tag{72}$$

where,

$$M_{cs} = M_o + M_{rd}$$

$$C_{cs} = C_o$$

$$G_{cs} = G_o + G_{rd}$$

$$u_{cs} = u_o$$

The slow subsystem given in (72) represents the rigid body motion without involving any flexible parameters. It will be used further to design a control algorithm to track a desired trajectory of the object.

The slow subsystem has following properties which are important to the stability analysis.

Property 1 in Cartesian Space(CS): M_{cs} is a symmetric positive definite matrix [59] and [68].

Property 2 in CS: The matrix M_{cs} and C_{cs} in (72) must satisfy

$$\mathbf{X}^T(\dot{M}_{cs} - 2C_{cs})\mathbf{X} = 0, \quad \forall X \neq 0 \tag{73}$$

where, **X** is any arbitrary vector. Hence $(\dot{M}_{cs} - 2C_{cs})$ is a skew-symmetric matrix [59] and [68].

Property 3 in CS: There exists a vector $\alpha_{cs} \in \mathbf{R}^{v\times 1}$ which solely depends on manipulators and beam dynamic parameters (link lengths, masses and moments of inertia etc.) such that

$$M_{cs}\ddot{X}_{rf} + C_{cs}\dot{X}_{rf} + G_{cs} = Y_{cs}(\ddot{X}_{rf}, \dot{X}_{rf}, \dot{q}, q)\alpha_{cs} \tag{74}$$

where $Y_{cs} \in \mathbf{R}^{u\times v}$ is called regressor matrix of manipulator-beam systems in Cartesian space. The regressor for the Cartesian space slow subsystem Y_{cs} and also α_{cs} is given in Appendix B.

Property 4 in CS: Since the matrices M_{cs}, C_{cs} and G_{cs} in (72) are the functions of sine and cosine of manipulator joint angles and velocities, they are bounded. Then, there exist arbitrary positive constants ρ_i (i=1, 2, 3), the boundedness [69] of each matrices can be described as follows:

$$\| M_{cs} \| \leq \rho_1$$

$$\| C_{cs} \| \leq \rho_2 \| \dot{X}_{rf} \|$$

$$\| G_{cs} \| \leq \rho_3$$

3.5.2 Fast subsystem

Equation (68) represents the perturbed flexible model obtained with perturbation parameter ε which is very small and solely depends upon the E, I and ρ.

In order to study the dynamic behavior of fast system, the so called boundary layer phenomenon [64] and [67] must be obtained. This can be identified by ensuring that the slow variables are kept constant in the fast time scale $\nu = \frac{t-t_0}{\varepsilon}$. From the typical steps of singular perturbation [64], one can define the fast variable w_f

$$w_f = w - w_s \tag{75}$$

Differentiating the fast time scale,

$$\begin{aligned} d\nu &= \frac{dt}{\varepsilon} \\ \frac{d\nu}{dt} &= \frac{1}{\varepsilon} \end{aligned} \tag{76}$$

Differentiating (75) gives,

$$\dot{w} = \dot{w}_s + \frac{d}{dt} w_f = \dot{w}_s + \frac{d\nu}{dt}\frac{d}{d\nu} w_f = \dot{w}_s + \frac{1}{\varepsilon}\hat{w}_f \tag{77}$$

where $\hat{w}_f$ denotes differentiating fast variable with respect to fast time scale.

Differentiating (77) again yields,

$$\ddot{w} = \ddot{w}_s + \frac{d\nu}{dt}\frac{d}{d\nu}\hat{w}_f = \ddot{w}_s + \frac{1}{\varepsilon^2}\hat{\hat{w}}_f \tag{78}$$

Using (75), (68) can be rewritten as,

$$-\sin\theta\ddot{x}_0+\cos\theta\ddot{y}_0+x\ddot{\theta}+\ \varepsilon^2\ddot{w}-\ \varepsilon^2(w_s+w_f)\dot{\theta}^2+a(w_s^{iv}+w_f^{iv})=F_{ff}(f) \tag{79}$$

Using (70) and (78), (79) becomes,

$$F_{ff}(f_s)+\hat{\hat{w}}_f+\varepsilon^2\ddot{w}_s-\varepsilon^2(w_s+w_f)\dot{\theta}^2+a{w_f}^{iv}=F_{ff}(f) \tag{80}$$

By defining $F_{ff}(f_f)=F_{ff}(f)-F_{ff}(f_s)$, the above equation can be rewritten as,

$$\hat{\hat{w}}_f+\varepsilon^2\ddot{w}_s-\varepsilon^2(w_s+w_f)\dot{\theta}^2+a{w_f}^{iv}=F_{ff}(f_f) \tag{81}$$

However, in the boundary layer system, the slow variable w_s is constant which implies $\ddot{w}_s=0$ and also $\varepsilon=0$ [67]. Then, the fast dynamics can be represented as,

$$\hat{\hat{w}}_f+a{w_f}^{iv}=F_{ff}(f_f) \tag{82}$$

The above equation (82) represents the fast subsystem in the fast time scale which connotes the vibration of the flexible object.

Thus it is evident from the above analysis that, singular perturbation approach establishes slow and fast system in two different time scales. The slow or the quasi-steady-state response is obtained from the reduced order model (72) and the fast transient is nothing but the discrepancy between the original complete system dynamics (42) and (43) and the reduced order model. However, the fast subsystem (82) is still in the form of infinite dimensional partial differential model and it should not be approximated using finite element method or assumed mode method. Luo [70] and [71] introduced some of the operators and its properties to avoid the issues related to approximation and discretization for such a PDE based systems. These operators will be useful to form the abstract differential model of the

fast subsytem without any approximation. Following are some of the important definitions and terms used by Luo [70] for developing the abstract differential equation from the infinite dimensional model of the beam.

Hilbert Space [72]:

A Hilbert space is a space which satisfies the following axioms [72]:

- It is a vector space, in which the operations such as addition and multiplication of the vector elements by a scalar can be done. Also, the usual commutative, associative and distributive properties are satisfied.
- For every pair of elements x, y there is associated a scalar product also called inner product denoted by $< x \,.\, y >$ exists.
- It has an infinite number of dimensions, i.e., the number of linearly independent elements has no bound.
- It is a complete space which means that every Cauchy sequence converges.
- It is of countable type. There exists one sequence $\Upsilon = (x_1 .... x_n)$ which is everywhere dense in H. i.e., for every x in H and every small $\Delta > 0$, there is atleast one x_n which satisfies $\|x - x_n\| < \Delta$.

Bounded Operator [72]:

The operator A is bounded in the Hilbert space and then, there exists a positive number α such that,

$$\|Ax\| \leq \alpha \|x\| \qquad \forall x \in H$$

Adjoint Operator [72]:

Consider a linear bounded operator F and the product $< Fx \,.\, y >$, where y is fixed and x ranges over H. Then, there exists an element F^*y such that,

$$< Fx \,.\, y > \;=\; < x \,.\, F^*y > \qquad \forall x \in H$$

The operator F^* is linear and bounded and called as adjoint of F.

Self-Adjoint Operator [73]:

The linear bounded operator F on a Hilbert space H is said to be self adjoint, if $F^* = F$. Then,

$$< Fx \,.\, y > \;=\; < x \,.\, Fy > \qquad \forall x \in H$$

By utilizing above definitions, an operator A [71] is defined as,

$$D(A) = \{w_f | w_f^{iv} \in H, w_f(0) = w_f''(0) = w_f(L) = w_f''(L) = 0\} \tag{83}$$

$$Aw_f = aw_f^{iv}, \quad \forall w_f \in D(A) \tag{84}$$

where, $D(A)$ denotes the domain of the operator A and H denotes the Hilbert space.

The important properties of operator A has been introduced by Sakawa and Luo [74] which are as follows:

- A is closed, self-adjoint, and positive definite operator
- The inverse (A^{-1}) of A exists and is compact on H

They also provided [74] the detailed proof for each of the above properties.

In addition to those properties, the operator A has the eigenvalues λ_i and the corresponding eigenfunctions ϕ_i satisfying the following conditions [75].

1. $0 < \lambda_1 < \lambda_2 ....., \ \ lim\ \lambda_i = \infty$

2. $A\phi_i = \lambda_i \phi_i, \ \ i = 1, 2 ....\infty$

3. The set of the eigenfunctions forms a complete orthonormal system in the Hilbert space.

Luo [71] defined another unbounded operator Π with $D(\Pi) \supset D(A)$. The following are some of the important assumptions that has to be satisfied by the operator Π:

1. Π is A-bounded. i.e., $\forall u \in D(A)$, there exist nonnegative constants a_c and b_c such that $\|\Pi u\| \leq a_c \|u\| + b_c \|Au\|$.

2. Π is A-symmetric. i.e., $\forall u, v \in D(A)$, there holds $(\Pi u, Av) = (Au, \Pi v)$.

3. Π is A-positive semidefinite. i.e., $\forall u \in D(A)$, there holds $(\Pi u, Au) \geq 0$.

The operator Π is called as *A-dependant operator* when it satisfies all of the above assumptions. If Π is A-positive definite, then, we call Π as *strict A-dependant operator*. Some of the A-dependant operators are $\Pi = I_d$, the identity operator on H, $\Pi = A^{\frac{1}{2}}$ and also $\Pi = A$. It is also shown by Luo [70] that, the operator Π can be expressed as,

$$\Pi = \Pi A^{-1} A = QA \tag{85}$$

where, $Q = \Pi A^{-1}$ and it has the following properties:

- It is a bounded operator on H
- It is a symmetric operator on H
- It is a positive semidefinite operator on H

These operators are useful for stability analysis in the next Chapter. The complete proof for the above mentioned properties can be found in [70].

Using (84), the partial differential equation (82) can be rewritten as an abstract differential equation on H as,

$$\hat{\dot{w}}_f(v) + Aw_f(v) = F_{ff}(f_f) \tag{86}$$

$$w_f(0) = w_{f0}, \qquad \dot{w}_f(0) = w_{f1}$$

Equation (86) represents the fast subsystem in the abstract differential equation form, which will be used for designing fast feedback control.

3.6 Summary

Fundamental concepts of singular perturbation method have been reviewed in this Chapter. Based upon these concepts, the coupled rigid-flexible dynamics have been separated into slow subsystem which corresponds to rigid body motion and fast subsystem that describes transverse vibration of flexible object. The separation of these two subsystems occurred in two different time scales. In addition, the fast subsystem is further modified into abstract differential equation by using various differential operators. Therefore one can develop control scheme for each subsystem and combining them together to form a composite control input for the manipulator-beam system. The next Chapter deals with the development of composite control scheme and its stability analysis. Simulation studies will be performed to evaluate the proposed composite control scheme.

Chapter 4

Controller Design

4.1 Introduction

From a review of literature in Chapter 1 it becomes evident that majority of the studies on manipulating flexible objects have focused on the development of linear control algorithms such as PD controller [41], [43] and [50] and hybrid impedance controller [45] and [48] . Even though the linear control algorithms had been generally successful in industrial applications, it has a few drawbacks while handling structured and unstructured uncertainties, external disturbances and also in linearizing large operating ranges.

The key issue in developing a control algorithm is that, it should handle the uncertain parameters of the manipulators and beam and it must give exponential convergence of both slow and fast subsystems to satisfy the validity of singular perturbation approach by means of Tikhnov's theorem. Considering these facts, in this Chapter, a regressor based sliding mode control is developed for the slow subsystem and as a part of the composite control

law; a simple feedback control algorithm is proposed for the fast subsystem. The justification of a composite control scheme is achieved by presenting the exponential stability analysis for the slow and fast subsystems. Simulation results are also presented to validate the proposed composite controller. In order to reduce the chattering on the slow subsystem, a smoothing control law is considered. A special case of two manipulators handling a rigid object has been derived by keeping the flexible parameter zero and the modulus of elasticity assumed to be infinite. Since, this thesis makes use of the basic notions of adaptive and robust control algorithm, they are reviewed initially and consequently the composite control law will be presented.

4.1.1 Adaptive control

Adaptive controllers were developed in the 1950's with the aim of designing autopilots for high performance aircraft when difficulties were encountered implementing PID controllers. Adaptive control laws are determined from the given desired control objective and the feedback signal derives the parameter update law. Basically, it has adaptation law which is used to learn the uncertain parameters of the system and the learned parameters are used further in the designed control law. Several adaptive schemes related to control of robot manipulators can be seen in the literature. A comprehensive survey of adaptive control of rigid robots is reported in [57]. These controllers use parametric formulation of robot dynamics resulting in better performance. Also, adaptive control is useful in various applications [76] such as aircraft control, process control, ship steering and robot manipulation control.

The following example will illustrate the overview of the adaptive controller proposed by Slotine and Li [58] for a rigid manipulator with n_1 number of links which is as follows.

General manipulator dynamic equation can be written in joint space as [55],

$$M(q)\ddot{q}+C(q,\dot{q})\dot{q}+G(q)=\tau \tag{87}$$

For the given initial joint position of rigid manipulator with some or all of the manipulator unknown parameters, control law for the input joint torques will be derived to track the desired trajectory $q_d \in \mathbf{R}^{n_1}$, $\dot{q}_d \in \mathbf{R}^{n_1}$ and $\ddot{q}_d \in \mathbf{R}^{n_1}$. The manipulator will track the desired path after an initial adaptation process.

Let $\upsilon = [\upsilon_1 \ldots\ldots \upsilon_{m_1}]^T$ be an m_1-dimensional vector containing the unknown manipulator and load parameters, and $\check{\upsilon}$ is its estimate. Correspondingly, $\check{M}$, $\check{C}$ and $\check{G}$ are the estimates of M, C and G and are obtained by substituting $\check{\upsilon}$ for actual υ. Utilizing the linear parameterized property 4 of the dynamics of manipulator mentioned in Chapter 2, one can have,

$$\tilde{M}(q)\ddot{q}_r+\tilde{C}(q,\dot{q})\dot{q}_r+\tilde{G}(q):=Y(q,\dot{q},\dot{q}_r,\ddot{q}_r)\tilde{\upsilon} \tag{88}$$

where, $Y(q,\dot{q},\dot{q}_r,\ddot{q}_r) \in \mathbf{R}^{n_1 \times m_1}$ is the regressor matrix which is independent of dynamic parameters and $\tilde{\upsilon}=\check{\upsilon}-\upsilon$ is the parameter estimation error.

Considering a positive definite matrix λ_1 and the position tracking error $\tilde{q}=q-q_d$, the reference trajectory velocity can be written as,

$$\dot{q}_r=\dot{q}_d-\lambda_1\tilde{q} \tag{89}$$

Then, the sliding surface can be defined as,

$$S_1=\dot{q}-\dot{q}_r=\dot{\tilde{q}}+\lambda_1\tilde{q} \tag{90}$$

Using above relations, the control law becomes,

$$\tau = Y(q, \dot{q}, \dot{q}_r, \ddot{q}_r)\check{\upsilon} - K_d S_1(t) \tag{91}$$

and the adaptation law is given by,

$$\dot{\check{\upsilon}} = -\Phi^{-1} Y^T(q, \dot{q}, \dot{q}_r, \ddot{q}_r) S_1(t) \tag{92}$$

where Φ is a constant positive definite matrix and K_d is a symmetric positive definite matrix usually diagonal. The vector $S_1(t)$ is the measure of tracking accuracy.

By choosing the following Lyapunov function candidate,

$$V(t) = \frac{1}{2}[S_1^T(t) M S_1(t) + \tilde{\upsilon}^T \Phi \tilde{\upsilon}] \tag{93}$$

it was shown that, the control and the adaptation laws achieve global convergence of the positional and velocity tracking error to zero. Hence, the sliding surface (90) converged asymptomatically to zero which in turn guarantees that $\tilde{q}$ and $\dot{\tilde{q}}$ also converge to zero. An advantage of this type of controller is that there is no need of measurement of joint accelerations to feed back or inverting the estimated inertia matrix. However, the given adaptation law (92) is of gradient type and the convergence of tracking errors to zero does not mean that the convergence of estimated parameters to the exact values. In order to achieve the asymptotic convergence of estimated parameters to the true parameters, the matrix $Y_d(q_d, \dot{q}_d, \ddot{q}_d)$ should be persistently exciting and uniformly continuous. If the matrix $Y_d(q_d, \dot{q}_d, \ddot{q}_d)$ is not persistently exciting, it means that, the following relation does not hold good for all time [77]. There exist positive constants δ, β_1 and β_2 such that,

$$\beta_1 I_d \leq \int_{t_1}^{t_1+\delta} Y_d^T Y_d dt \leq \beta_2 I_d \tag{94}$$

Also, if the above condition is not satisfied then the estimator may become unstable i.e., the estimated parameters will diverge. It is also shown in [78] that, without persistent excitation, system may not be able to achieve uniform adaptation transient because $\check{\upsilon}$ is away from υ and also convergence of vector $S_1(t)$ or $\tilde{\upsilon} = \check{\upsilon} - \upsilon$ is very slow. In addition, adaptive controllers deal with the case of constant or slowly varying parametric uncertainties only. However, various parametric and unparametric uncertainties are occurring frequently in robot models. In order to handle these uncertainities, robust control algorithms came into picture.

4.1.2 Robust control

In the robust controllers, the controller has a fixed structure with known bounds of uncertainty and no learning behavior takes place. The robust controllers have attractive features compared to adaptive controllers, which are [76]

- ability to deal with disturbances.
- ability to handle quickly varying parameters and unmodeled dynamics.
- they are easy to implement.

These controllers can achieve desired transient response and also convergence of their tracking error is uniform and bounded [79]. The survey on robust control strategies [80] and [81] shows that these kind of controllers are well known and very useful for different applications. This thesis considers, one of the robust control scheme, namely, sliding mode control which is reviewed in the following section.

4.1.2.1 Sliding mode control

One of the robust schemes to control the nonlinear systems is by means of Variable Structure Control (VSC) and it is a high-speed switching feedback control. The high-speed switching gain and advancement of computer technology increases interest in the practical implementation of VSC. A simple approach to robust control is the so-called sliding mode control. Here, in this section an overview of sliding mode control is provided [76].

A single input dynamic system is given by,

$$x^{(n)} = f_s(\mathbf{x}) + b_s(\mathbf{x})u \tag{95}$$

where the scalar x is the output, u is the control input and $\mathbf{x} = [x,\ \dot{x},\ ....\ ,x^{(n-1)}]^T$ is the vector of state variables. The nonlinear function $f_s(\mathbf{x})$ is known by its upper bound and the control gain $b_s(\mathbf{x})$ is also bounded with known sign. The control objective is to track the desired state $\mathbf{x}_d = [x_d,\ \dot{x}_d\ ....\ x_d^{(n-1)}]$ in the presence of model uncertainities on $f_s(\mathbf{x})$ and $b_s(\mathbf{x})$. The tracking error vector can be defined as,

$$\tilde{\mathbf{x}} = \mathbf{x} - \mathbf{x}_d = [\tilde{x},\ \dot{\tilde{x}},\ ....\ ,\tilde{x}^{(n-1)}] \tag{96}$$

and the sliding surface is given by,

$$S_2 = (\frac{d}{dt} + \lambda_2)\tilde{x} \tag{97}$$

where λ_2 is a positive constant and $\tilde{x}$ is the tracking error in the variable x.

For the given initial condition $\mathbf{x}_d$ = $\mathbf{x}(0)$, the sliding control will track the desired trajectory $\mathbf{x}_d$ which is equivalent to the state variables remaining on the surface $S_2(t)$ for all $t > 0$. Fig. 7 shows that for the different Initial Conditions (IC), the state variables

are converge to $S_2(t) = 0$. It is also observed from (97) that, the sliding surface is related to tracking error $\tilde{x}$ and therefore the sliding variable S_2 is the true measure of tracking performance. We need to keep $S_2(t)$ at zero when tracking is outside of $S_2(t)$. This can

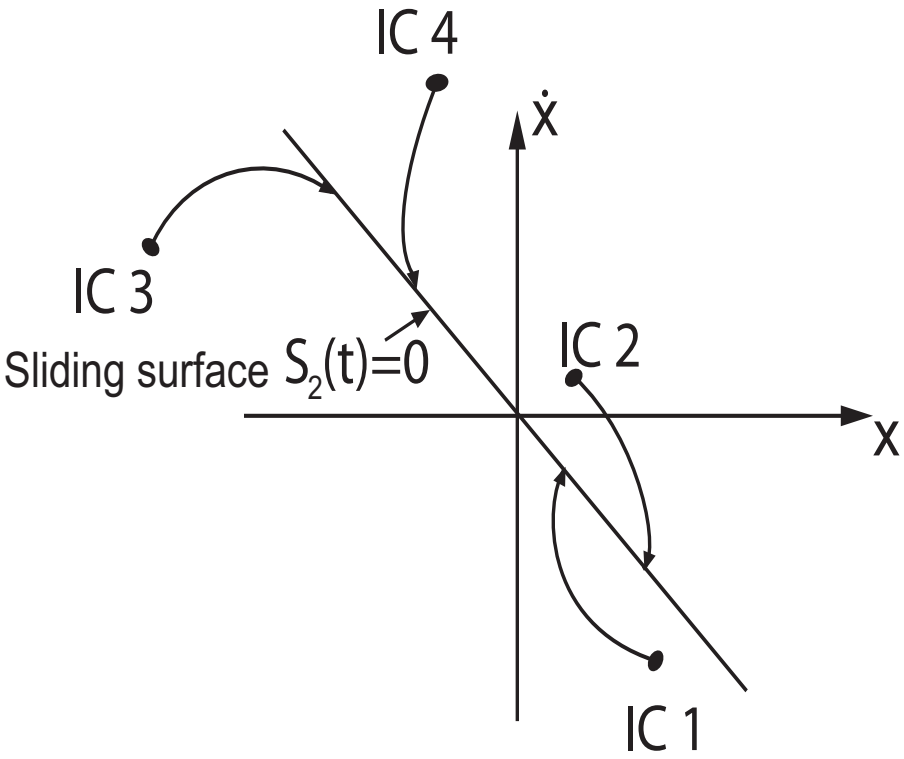

Figure 7: Sliding surface and various initial conditions

be achieved by choosing the control law of u of (95) such that the outside of $S_2(t)$ should satisfy the following,

$$\frac{1}{2}\frac{d}{dt}S_2^2(t) \leq -\Upsilon|S_2(t)| \tag{98}$$

where Υ is a strict positive constant and (98) describes that the system trajectories will converge towards the sliding surface which is an important conclusion for the existence of sliding mode and satisfying this condition is called as sliding condition.

In this technique, a nonlinear system state trajectory will be driven onto a specified and user-chosen sliding or switching surface. If the system trajectory will be “above” the

surface, then the control path has one gain and a different gain if the trajectory drops "below" the surface. The state trajectories of the system maintained in this surface indicate that the system is controlled. In this approach, the tracking error will reach a switching surface and afterwards the system will be in sliding mode. The sliding behavior causes the system to slide along or in the vicinity of sliding surface. Then, the system will not be affected by any model uncertainty i.e., it is robust and insensitive to disturbances. By designing a proper sliding surface, VSC can achieve the goals such as, stabilization, regulation and tracking in control perspective. Sliding mode control has been applied to various applications [76] such as robot manipulators, underwater vehicles, automotive transmissions and engines, high performance electric motors and power systems. This thesis also considers sliding mode approach for the control of slow subsystem.

4.2 Composite control for the manipulators - flexible object system

Singular perturbation approach produces a multi-time-scale model of manipulator-flexible beam system. Due to the end-effector force, the flexible beam has to move in the desired trajectory and simultaneously, vibration of the object must be suppressed. In order to achieve these objectives, a composite control algorithm will be designed. A composite control for the manipulator-flexible object system is, by definition, a controller of the form

$$u = u_s(\dot{X}_{rf}, X_{rf}, t) + u_f(\hat{w}_f, v)$$

where u_s is designed based on slow subsystem (72) and u_f is designed to stabilize the fast subsystem (86). The slow control for the rigid nonlinear subsystem can be designed by utilizing sliding mode control theory. In case of fast subsystem, a feedback control law with special damping term will be introduced. Utilizing the various operators mentioned in Chapter 3, a control law for the fast subsystem will be developed.

4.2.1 Robust control design for slow subsystem

The key issue in developing a control algorithm is that, with the unknown manipulators and beam parameters, the design of $u_s(\dot{X}_{rf}, X_{rf}, t)$ can not be arbitrary. It has to guarantee the exponential tracking of the desired trajectories so that the Tikhnov's theorem can be satisfied, which will be clear in the later development. For that purpose, a sliding mode control approach will be adopted.

The tracking error is defined as,

$$e_r = X_{rf} - X_{rfd} \tag{99}$$

where X_{rfd} is the desired trajectory, and the auxiliary trajectory as,

$$\dot{X}_r = \dot{X}_{rfd} - \lambda_{cs} e_r \tag{100}$$

where λ_{cs} is a positive definite matrix whose eigenvalues are strictly in the right half complex plane.

The sliding surface can be chosen as,

$$S_{cs} = \dot{X}_{rf} - \dot{X}_r = \dot{e}_r + \lambda_{cs} e_r \tag{101}$$

The sliding mode controller can be given as,

$$u_s = u_{cs} = Y_{cs}\psi - K_D\, S_{cs} \tag{102}$$

where K_D is a positive definite gain matrix, $Y_{cs}(\ddot{X}_r,\ \dot{X}_r,\ \dot{q}, q)$ is the regressor matrix given in property 3 in CS (74) where the dynamic parameters of manipulators and beam are excluded and $\psi = [\psi_1 .... \psi_m]^T$ are the switching functions which are given by,

$$\psi = -\beta_{cs} \frac{Y_{cs}^T\, S_{cs}}{\|Y_{cs}^T\, S_{cs}\|} \tag{103}$$

where $\beta_{cs} \geq \|\alpha_{cs}\|$ is upperbound of α_{cs} which is known though it could be conservatively selected. The advantages of the suggested control scheme is, exact knowledge of the manipulator parameters or the beam are not required; it avoids the need for parameter estimation unlike in the adaptive control; it gives the desired transient response and also robustness to uncertainties are guaranteed; and it satisfies the Tikhnov's theorem.

4.2.2 Control design for fast subsystem

The objective of the controller is to suppress the vibration of the flexible object by incorporating following feedback control law,

$$u_f = (f_f) = -F_{ff}^{\dagger} \Pi \hat{w}_f(v) \tag{104}$$

where $F_{ff}^{\dagger}$ can be found using pseudo inverse. The operator Π is neither selfadjoint nor positive definite and is also shown in [70] and [71] that, it is A-symmetric and A-positive semidefinite. This operator was formulated in [71] as $\Pi = kQA$ where Q is a bounded and positive definite operator. Also, the velocity signal $\hat{w}_f(v)$ can be measured using velocity

sensor. It is to be noted that, there are some established results available using the velocity feedback for example [82] and [83]. However, they have considered assumed modes while in this control algorithm no form of approximation is used. In addition, compared to other recent boundary control methods available in the literature [66] and [84] where the velocity and slope of fast state variable are used as feedback and they are dependant upon the boundary conditions of the beam. Also, the feedback of slope of the beam is not easy to measure in real time applications. However, the presented control algorithm uses only velocity feedback which is irrespective of boundary conditions and it does not need the information of modes. This controller is simple to implement in real time and reduces the need for number of sensors.

Substituting (104) into (86) gives closed loop system which is given by,

$$\hat{\dot{w}}_f(v) + \Pi \hat{w}_f(v) + A w_f(v) = 0 \tag{105}$$

Using the operators Π and Q, (105) can be rewritten as,

$$\hat{\dot{w}}_f(v) + kQA\hat{w}_f(v) + A w_f(v) = 0 \tag{106}$$

$$w_f(0) = w_{f0}, \quad \dot{w}_f(0) = w_{f1}$$

where k is the positive gain and the term $QA\hat{w}_f(v)$ is a special damping term [71]. This damping has been studied by various researchers especially [85]-[88]. The two operators Q and A are related by $Q = A^{\beta}$ and β varies between $[\frac{-1}{2}, 0]$. It is shown analytically by Huang [86] when $\beta = \frac{-1}{2}$, the damping term $QA\hat{w}_f(v)$ becomes $A^{\frac{1}{2}}\hat{w}_f(v)$. This corresponds to structural damping which can also be seen in [88]. If $\beta = 0$, then damping term exhibits strong damping or overdamping characteristics which is shown in [86] and [87].

4.3 Stability analysis

The stability of the closed loop system is essential to show the ability of the suggested control algorithms for slow and fast subsystems. The development of slow and fast subsystem with the help of singular perturbation technique insists on to satisfy the Tikhnov's theorem. It is evident from the Tikhnov's theorem for the infinite time interval presented in Chapter 3 that, the slow and fast subsystems must be exponentially stable. Therefore, the rigorous exponential stability proof for slow and fast subsystem will be presented in the following.

4.3.1 Stability analysis for slow subsystem

The Tikhnov's theorem requires the slow subsystem to be exponentially stable. Hence, the following analysis will illustrate the exponential stability of the slow subsystem.

Differentiating the sliding surface (101) with respect to time results in,

$$\dot{S}_{cs} = \ddot{X}_{rf} - \ddot{X}_r \tag{107}$$

Mutiplying both sides of (107) by M_{cs} and using (72), (107) can be rewritten as,

$$M_{cs}\dot{S}_{cs} = u_{cs} - C_{cs}\dot{X}_{rf} - G_{cs} - M_{cs}\ddot{X}_r \tag{108}$$

Adding and subtracting $C_{cs}\dot{X}_r$ in (108) results in,

$$M_{cs}\dot{S}_{cs} = u_{cs} - (M_{cs}\ddot{X}_r + C_{cs}\dot{X}_r + G_{cs}) + C_{cs}\dot{X}_r - C_{cs}\dot{X}_{rf} \tag{109}$$

Using (101), (109) can be rewritten as,

$$M_{cs}\dot{S}_{cs} = u_{cs} - Y_{cs}(\ddot{X}_r, \dot{X}_r, \dot{q}, q)\alpha_{cs} - C_{cs}S_{cs} \tag{110}$$

where,

$$(M_{cs}\ddot{X}_r + C_{cs}\dot{X}_r + G_{cs}) = Y_{cs}(\ddot{X}_r, \dot{X}_r, \dot{q}, q)\alpha_{cs}$$

Consider a Lyapunov function candidate as,

$$V_1(t, S_{cs}) = \frac{1}{2} S_{cs}^T M_{cs} S_{cs} \tag{111}$$

Differentiating (111) with respect to time gives,

$$\dot{V}_1(t, S_{cs}) = S_{cs}^T M_{cs} \dot{S}_{cs} + \frac{1}{2} S_{cs}^T \dot{M}_{cs} S_{cs} \tag{112}$$

Substituting (110) into (112) and also using property 2 in CS (73), above equation yields,

$$\dot{V}_1(t, S_{cs}) = S_{cs}^T [u_{cs} - Y_{cs}(\ddot{X}_r, \dot{X}_r, \dot{q}, q)\alpha_{cs}] \tag{113}$$

Substituting the control law given in (102) and (103) into (113) results in,

$$\dot{V}_1(t, S_{cs}) \leq -S_{cs}^T K_D S_{cs} - \beta \|Y_{cs}^T \, S_{cs}\| + \|S_{cs}^T Y_{cs}\| \|\alpha_{cs}\| \tag{114}$$

Taking transpose of $\|S_{cs}^T Y_{cs}\|$ and also $\beta \geq \|\alpha_{cs}\|$ gives,

$$\dot{V}_1(t, S_{cs}) \leq -S_{cs}^T K_D S_{cs} \tag{115}$$

It is known that [89] $K_D = M_{0r}\kappa$ where κ can be considered as a least eigenvalue. Hence, (115) can be rewritten as,

$$\frac{dV_1(t, S_{cs})}{dt} \leq -S_{cs}^T M_{cs} \kappa S_{cs} \tag{116}$$

Using (111), (116) can be rewritten as,

$$\frac{dV_1(t, S_{cs})}{dt} \leq -2\kappa V_1(t, S_{cs}) \tag{117}$$

The solution of the above equation is,

$$V_1(t, S_{cs}) \leq V_1(0, S_{cs}(0))e^{-2\kappa t} \tag{118}$$

It is evident from the above equation that the sliding surface will converge exponentially to zero. Thus the sliding surface is related to the tracking error e_r in (101) which also converges exponentially to zero which satisfies the Tikhnov's theorem.

4.3.2 Stability analysis for fast subsystem

Tikhnov's theorem requires that for the infinite time interval, the fast subsystem or the boundary layer model also must be exponentially stable. The energy multiplier method used by [71] is followed to prove the exponential stability under the following theorem [90], [theorem 4.1] which guarantees exponential stability.

Theorem 3:

Let A be the infinitesimal generator of a C_o semigroup $T(t)$. If for some p, $1 \leq p \leq \infty$

$$\int_0^\infty \|T(t)\|^p dt < \infty \tag{119}$$

then there are constants $M \geq 1$ *and* $\mu > 0$ *such that* $\|T(t)\| \leq Me^{-\mu t}$.

Note: It is also shown in [71] and [91] that the property of L^p stability and exponential stability for a strongly continuous semigroup must satisfy the following,

$$\int_0^\infty \|E(v)\|^2 dv < \infty \tag{120}$$

Proof:

Let the energy function for (106) be of the form,

$$E(v) = \frac{1}{2}\|Aw_f(v)\|^2 + \frac{1}{2}\|A^{\frac{1}{2}}\hat{w}_f(v)\|^2 \tag{121}$$

where $E(\nu)$ is weakly monotonically decreasing function with respect to fast time scale ν [91]. The fast time scale derivative of $E(\nu)$ from the above equation will be,

$$\hat{E}(\nu) = -k\langle QA\hat{w}_f(\nu) \,.\, A\hat{w}_f(\nu)\rangle \leq 0 \tag{122}$$

Let us choose $0 < \varepsilon_f < 1$ and the Lyapunov function candidate is given by,

$$V_2(\nu) = 2(1-\varepsilon_f)\nu E(\nu) + \langle \hat{w}_f(\nu) \,.\, Aw_f(\nu)\rangle \tag{123}$$

We have the following relation,

$$\langle \hat{w}_f(\nu) \,.\, Aw_f(\nu)\rangle \leq \frac{1}{2}(\|Aw_f(\nu)\|^2 + \|A^{\frac{-1}{2}}\|^2 \|A^{\frac{1}{2}}\hat{w}_f(\nu)\|^2)$$

There exists a constant c_1 such that,

$$[2(1-\varepsilon_f)\nu - c_1]E(\nu) \leq V_2(\nu) \leq [2(1-\varepsilon_f)\nu + c_1]E(\nu) \tag{124}$$

For $\nu > \nu_1$, the Lyapunov function is positive and ν_1 is found from,

$$2(1-\varepsilon_f)\nu_1 - c_1 = 0 \tag{125}$$

The derivative of $V_2(\nu)$ in (123) with respect to fast time scale is given by,

$$\hat{V}_2(\nu) = (2-\varepsilon_f)\|A^{\frac{1}{2}}\hat{w}_f(\nu)\|^2 - \varepsilon_f\|Aw_f(\nu)\|^2 - 2k(1-\varepsilon_f)\nu\langle QA\hat{w}_f(\nu) \,.\, A\hat{w}_f(\nu) - k\langle QA\hat{w}_f(\nu) \,.\, Aw_f(\nu)\rangle \tag{126}$$

For any arbitrary constant, say, $c_2 > 0$ we have,

$$-\langle QA\hat{w}_f(\nu) \,.\, Aw_f(\nu)\rangle \leq \frac{1}{2}\lambda_{max}(Q)[c_2^2(\|A\hat{w}_f(\nu)\|^2 + \frac{1}{{c_2}^2}\|Aw_f(\nu)\|^2 \tag{127}$$

Using (127), (126) can be rewritten as,

$$\hat{V}_2(\nu) = [(2-\varepsilon_f)\|A^{-\frac{1}{2}}\|^2 + \frac{c_2^2 k}{2}\lambda_{max}(Q) - 2k\nu(1-\varepsilon_f)\lambda_{min}(Q)]\|A\hat{w}_f(\nu)\|^2 - (\varepsilon_f - \frac{k}{2c_2^2}\lambda_{max}(Q))\|Aw_f(\nu)\|^2 \tag{128}$$

where $\lambda_{max}(Q) = max_{w_f \in H}\langle Qw_f \,.\, w_f\rangle$ *and* $\lambda_{min}(Q) = min_{w_f \in H}\langle Qw_f \,.\, w_f\rangle$.

If c_2 can be chosen as large then $(\varepsilon_f - \frac{k}{2c_2^2}\lambda_{max}(Q)) > 0$,

$$\hat{V}_2(v) \leq 0 \qquad \forall v > v_2 \tag{129}$$

where v_2 be found from the following is satisfied,

$(2-\varepsilon_f)\|A^{-\frac{1}{2}}\|^2 + \frac{c_2^2 k}{2}\lambda_{max}(Q) - 2kv_2(1-\varepsilon_f)\lambda_{min}(Q) = 0$

The above result in (129) shows that derivative of Lyapunov function has decreasing trend for $v > v_2$ and it is also evident from (122) that the energy will also be dissipating for $v > 0$. Using these facts, for $v > T_s := max\{v_1, v_2\}$ and also from (124) $E(v)$ can be estimated as,

$$E(v) \leq \frac{V(T_s)}{2(1-\varepsilon_f)v - c_1} \leq \frac{[2(1-\varepsilon_f)T_s + c_1]E(0)}{2(1-\varepsilon_f)v - c_1} \tag{130}$$

Then, (130) can be rewritten as,

$$\int_{T_s}^{\infty} E(v)^2 dv \leq \int_{T_s}^{\infty} \frac{[2(1-\varepsilon_f)T_s + c_1]^2 E(0)^2}{2(1-\varepsilon_f)v - c_1} < \infty \tag{131}$$

which confirms the exponential stability as given in (119) and hence it is proved.

4.4 Simulation of composite controller

In many manufacturing and automobile industries various operations on flexible components such as assembling, welding, picking and placing are efficiently done using two robot arms. In a typical car industry, number of sheet metal parts must be assembled in the required place. In order to avoid the collision between the parts and also to satisfy the ergonomic constraints, these parts must move in the prescribed trajectory (tracking problem). By defining effective desired path, the robots help us to perform repetitive tasks that

ultimately improve productivity. In order to illustrate the effectiveness of the proposed composite controller, simulation studies are performed.

The following are the time independent parameters of a manipulator dynamic equation which are used to formulate the regressor [68].

$$p_{i1} = m_{i1}l_{i1c}^2 + I_{i1} + m_{i2}(l_{i1}^2 + l_{i2c}^2) + I_{i2} + m_{i3}(l_{i1}^2 + l_{i2}^2 + l_{i3c}^2) + I_{i3}$$

$$p_{i2} = m_{12}l_{i1}l_{i2c} + m_{i3}l_{i1}l_{i2}$$

$$p_{i3} = m_{i3}l_{i2}l_{i3c}; \quad p_{i4} = m_{i3}l_{i1}l_{i3c}$$

$$p_{i5} = m_{i2}l_{i2c}^2 + I_{i2} + m_{13}(l_{i2}^2 + l_{i3}^2) + I_{i3}$$

$$p_{i6} = m_{i3}l_{i3c}^2 + I_{i3}; \quad p_{i7} = m_{i1}gl_{i1c} + m_{i2}gl_{i1} + m_{i3}gl_{i1}$$

$$p_{i8} = m_{i2}gl_{i2c} + m_{i3}gl_{i2}; \quad p_{i9} = m_{i3}gl_{i3c}$$

Each manipulator inertia matrix is given by,

$$M_i = \begin{bmatrix} m_{i11} & m_{i12} & m_{i13} \\ m_{i21} & m_{i22} & m_{i23} \\ m_{i31} & m_{i32} & m_{i33} \end{bmatrix}$$

where,

$$m_{i11} = p_{i1} + 2p_{i2}\cos(q_{i2}) + 2p_{i3}\cos(q_{i3}) + 2p_{i4}\cos(q_{i2} + q_{i3})$$

$$m_{i12} = p_{i5} + p_{i2}\cos(q_{i2}) + 2p_{i3}\cos(q_{i3}) + p_{i4}\cos(q_{i2} + q_{i3})$$

$$m_{i13} = p_{i6} + p_{i3}\cos(q_{i3}) + p_{i4}\cos(q_{i2} + q_{i3})$$

$$m_{i21} = m_{i12}; \quad m_{i31} = m_{i13}; \quad m_{i22} = p_{i5} + 2p_{i3}\cos(q_{i3})$$

$$m_{i23} = p_{i6} + p_{i3}\cos(q_{i3}); \quad m_{i32} = m_{i23}; \quad m_{i33} = p_{i6}$$

The centrifugal and coriolis matrices for each manipulator are given by,

$$C_i = \begin{bmatrix} c_{i11} & c_{i12} & c_{i13} \\ c_{i21} & c_{i22} & c_{i23} \\ c_{i31} & c_{i32} & c_{i33} \end{bmatrix}$$

where,

$$c_{i11} = -p_{i2}\sin(q_{i2})\dot{q}_{i2} - p_{i3}\sin(q_{i3})\dot{q}_{i3} - p_{i4}\sin(q_{i2}+q_{i3})(\dot{q}_{i2}+\dot{q}_{i3})$$

$$c_{i12} = -p_{i2}\sin(q_{i2})(\dot{q}_{i1}+\dot{q}_{i2}) - p_{i3}\sin(q_{i3})\dot{q}_{i3} - p_{i4}\sin(q_{i2}+q_{i3})(\dot{q}_{i1}+\dot{q}_{i2}+\dot{q}_{i3})$$

$$c_{i13} = -p_{i3}\sin(q_{i3})(\dot{q}_{i1}+\dot{q}_{i2}+\dot{q}_{i3}) - p_{i4}\sin(q_{i2}+q_{i3})(\dot{q}_{i1}+\dot{q}_{i2}+\dot{q}_{i3})$$

$$c_{i21} = p_{i2}\sin(q_{i2})\dot{q}_{i1} - p_{i3}\sin(q_{i3})\dot{q}_{i3} + p_{i4}\sin(q_{i2}+q_{i3})\dot{q}_{i1}$$

$$c_{i22} = -p_{i3}\sin(q_{i3})\dot{q}_{i3}$$

$$c_{i23} = -p_{i3}\sin(q_{i3})(\dot{q}_{i1}+\dot{q}_{i2}+\dot{q}_{i3})$$

$$c_{i31} = p_{i3}\sin(q_{i3})(\dot{q}_{i1}+\dot{q}_{i2}) + p_{i4}\sin(q_{i2}+q_{i3})\dot{q}_{i1}$$

$$c_{i32} = p_{i3}\sin(q_{i3})(\dot{q}_{i1}+\dot{q}_{i2});\;\; c_{i33} = 0$$

Each manipulator gravity vector is given by,

$$G_i = \begin{Bmatrix} g_{i1} \\ g_{i2} \\ g_{i3} \end{Bmatrix}$$

where,

$$g_{i1} = p_{i7}\cos(q_{i1}) + p_{i8}\cos(q_{i1}+q_{i2}) + p_{i9}\cos(q_{i1}+q_{i2}+q_{i3})$$

$$g_{i2} = p_{i8}\cos(q_{i1}+q_{i2}) + p_{i9}\cos(q_{i1}+q_{i2}+q_{i3})$$

$$g_{i3} = p_{i9}\cos(q_{i1}+q_{i2}+q_{i3})$$

Each manipulator Jacobian matrix is given by,

$$J_i = \begin{bmatrix} J_{i11} & J_{i12} & J_{i13} \\ J_{i21} & J_{i22} & J_{i23} \\ 1 & 1 & 1 \end{bmatrix}$$

where,

$$J_{i11} = -l_{i1}\sin(q_{i1}) - l_{i2}\sin(q_{i1}+q_{i2}) - l_{i3}\sin(q_{i1}+q_{i2}+q_{i3})$$

$$J_{i12} = -l_{i2}\sin(q_{i1}+q_{i2}) - l_{i3}\sin(q_{i1}+q_{i2}+q_{i3})$$

$$J_{i13} = -l_{i3}\sin(q_{i1}+q_{i2}+q_{i3})$$

$$J_{i21} = l_{i1}\cos(q_{i1}) + l_{i2}\cos(q_{i1}+q_{i2}) + l_{i3}\cos(q_{i1}+q_{i2}+q_{i3})$$

$$J_{i22} = l_{i1}\cos(q_{i1}) + l_{i2}\cos(q_{i1}+q_{i2})$$

$$J_{i23} = l_{i3}\cos(q_{i1}+q_{i2}+q_{i3})$$

In the tracking problem, desired circular trajectory of the object is specified by,

$$X_{rfd} = \begin{bmatrix} sin(t) \\ cos(t) \\ 0 \end{bmatrix}$$

Table 1: Parameters of the manipulator

Link	Length (m)	Mass (kg)	Moment of inertia (kgm^2)
1	0.6	1.5	0.50
2	0.6	1.5	0.50
3	0.2	1.5	0.25

The parameters of identical manipulators [68] are given in Table 1. The flexible beam parameters are given in Table 2.

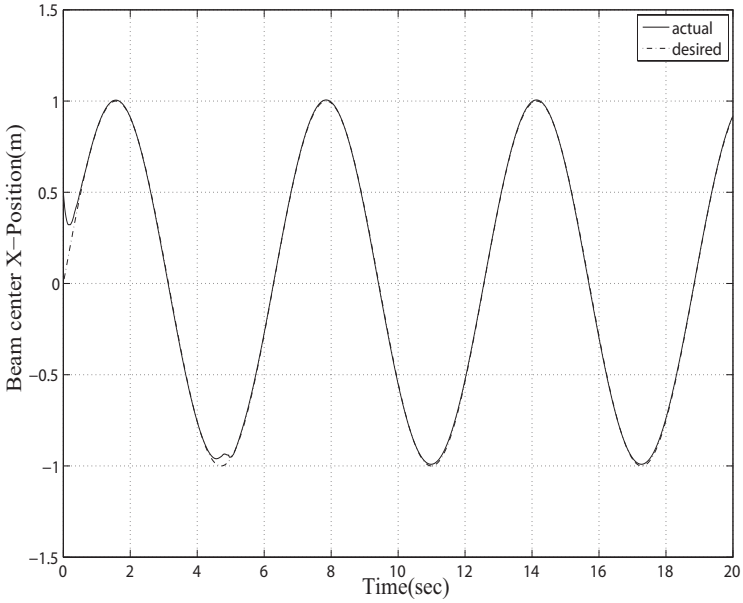

Figure 8: X-Position tracking-Sliding control in CS

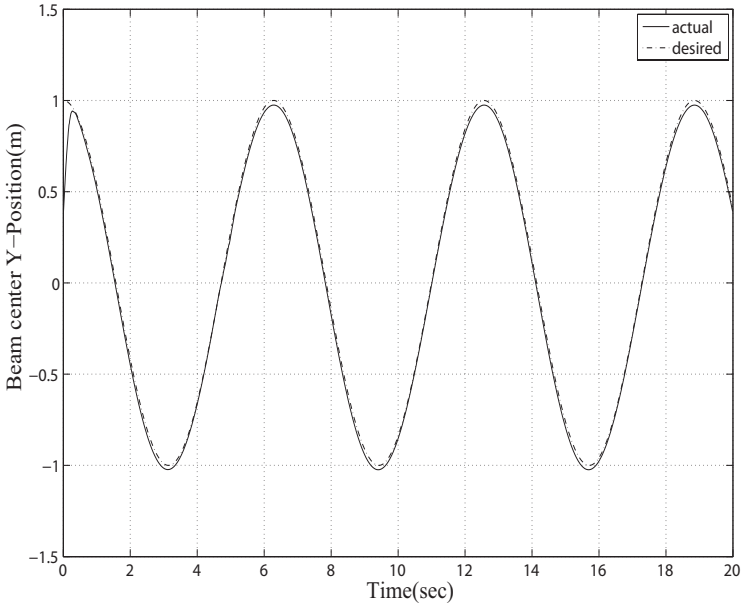

Figure 9: Y-Position tracking-Sliding control in CS

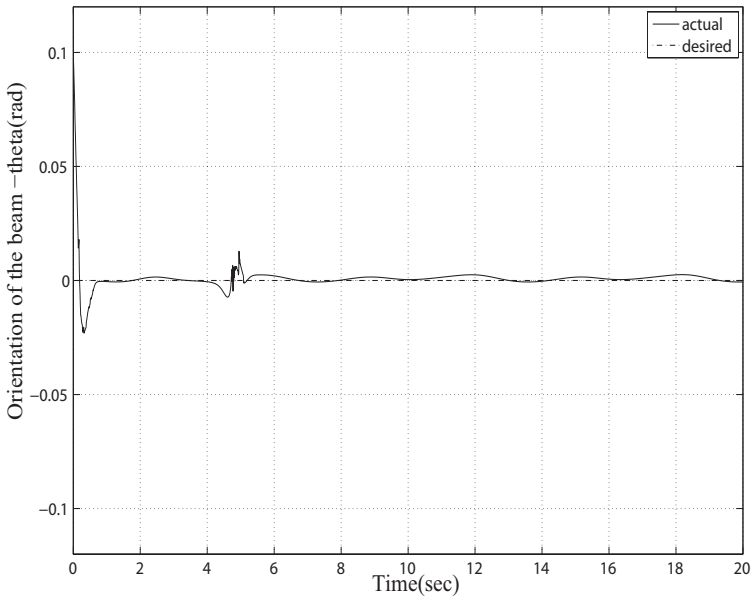

Figure 10: Orientation of the beam-Sliding control in CS

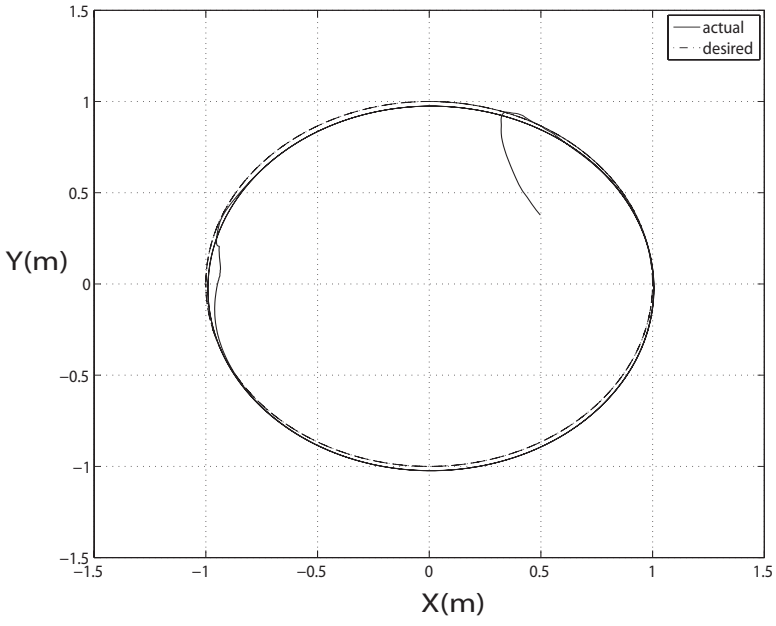

Figure 11: Circular trajectory

Table 2: Parameters of the flexible beam

Parameter	Value
Mass (m)	1.5 kg
Length (L)	1 m
Radius of the object	0.05 m
Density	2700kg/m^3
Young's modulus (E)	71 GPa

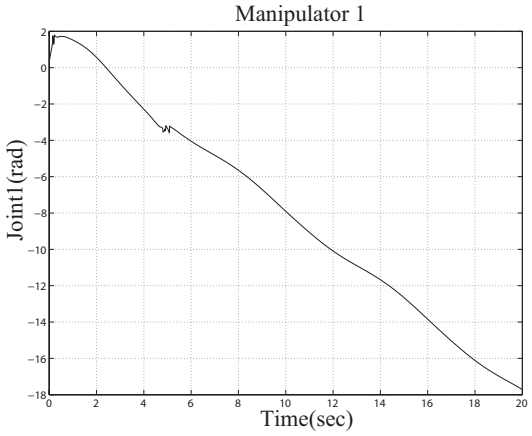

Figure 12: J1M1-Sliding control in CS

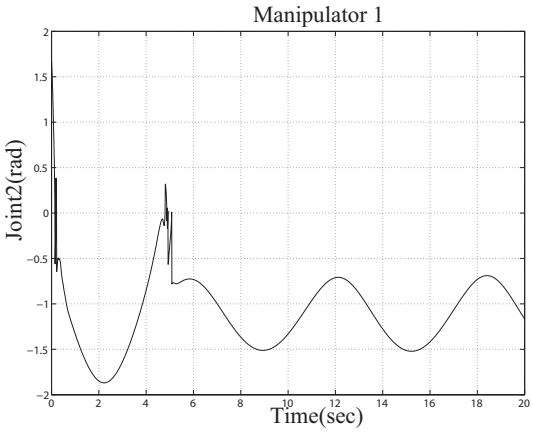

Figure 13: J2M1-Sliding control in CS

The beam initial position and orientation are $X_{rf} = \{0.51, 0.36, 0.1\}^T$ and initial velocity and acceleration are considered to be zero. Initial joint angles of manipulator are q_{11} = 0.2974 rad, q_{12} = 1.6974 rad, q_{13} = -1.6948 rad, q_{21} = 0.2149 rad, q_{22} = 1.4886 rad and q_{23} = -1.4306 rad, respectively. The initial joint velocities of all the joints of manipulators are 0.001 rad/sec and joint accelerations are assumed to be zero. The simulation is carried

Table 3: Control parameters-sliding control in CS

Parameter	Value
K_D	diag(424.2)
λ_{cs}	diag(7.9)
β_{cs}	0.004
k	1

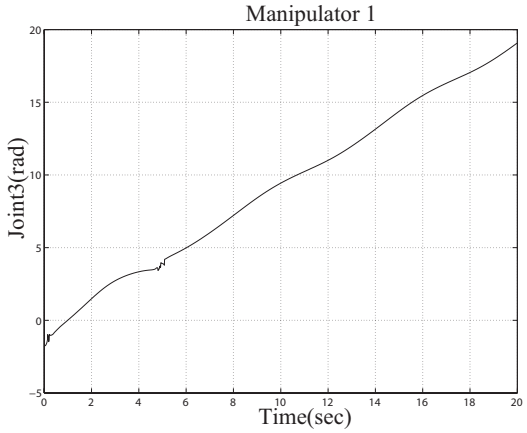

Figure 14: J3M1-Sliding control in CS

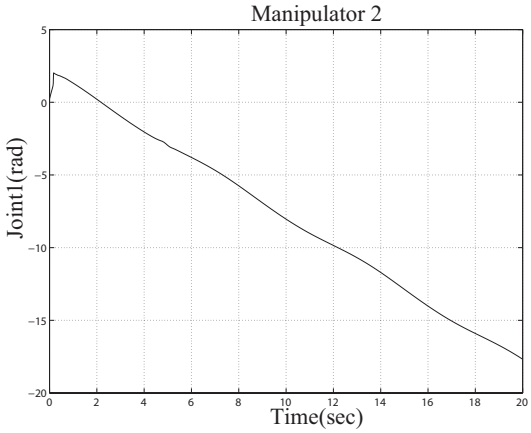

Figure 15: J1M2-Sliding control in CS

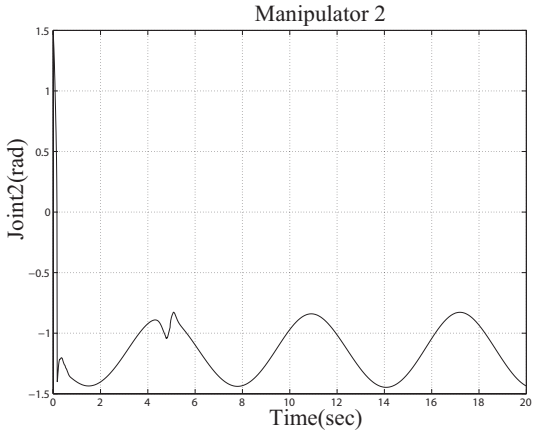

Figure 16: J2M2-Sliding control in CS

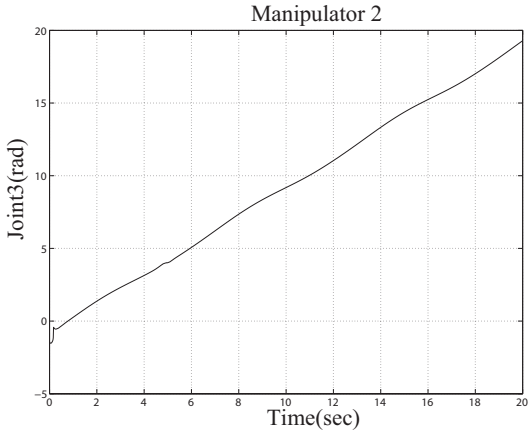

Figure 17: J3M2-Sliding control in CS

out with a sampling period of 0.01sec. The control parameters are tuned and are given in Table 3.

The value of Γ was chosen based on the L_∞ norm of the time independent parameters of the regressor in this case, vector α_{or}. Figs. 8 - 10 show the tracking of planar motion of center of the object along X, Y directions and also rotation about Z axis, respectively. It can be observed that, tracking of position and orientation is achieved within 1 sec, which shows the effectiveness of the controller. It can be seen from the Fig. 11 that the desired circular motion is achieved. In order to achieve the desired circular trajectory of the object,

each joint of the manipulator are moved in a smooth manner which are shown in Figs. 12 - 17. In all the figure captions, “JjMi” the j-th Joint of i-th Manipulator where (i=1, 2), (j=1, 2, 3) and “CS” represents the Cartesian Space.

It is also observed from the Figs. 18 - 20 that the sliding variables (SV) approach zero. Once the system reaches the sliding surface it becomes stable and it will try to maintain in the sliding surface which can also be inferred from these figures. Hence, it is evident from (101) that, the tracking error will also converge exponentially to zero. The control torques (CT) of each joints of manipulators are shown in Figs. 21 - 26. In all of these results around 4.5 secs there is a sudden increase in the value and afterwards it is stabilized. This is due to the joint 2 of manipulator 1 approaches towards the singularity point which can be seen in Fig. 13. These singularity problems can be avoided with the help of careful path planning techniques.

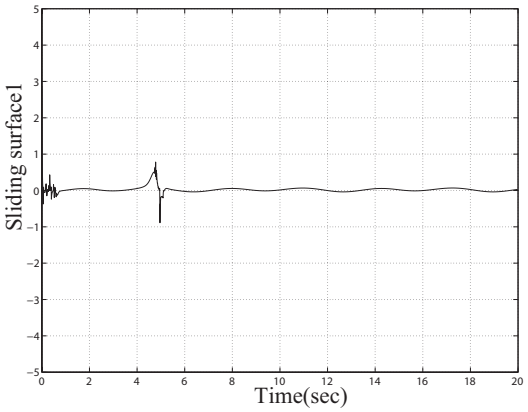

Figure 18: SV 1-Sliding control in CS

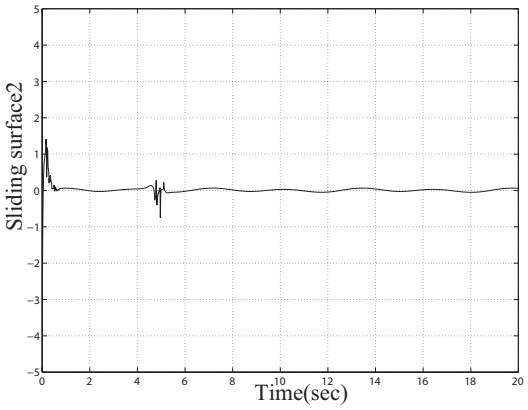

Figure 19: SV 2-Sliding control in CS

In the case of fast subsystem, the initial disturbance of 5 mm with zero initial velocity is considered for the simulation. Even though the flexible object is neither approximated nor discretized, for the simulation purpose first few natural frequencies of the beam are

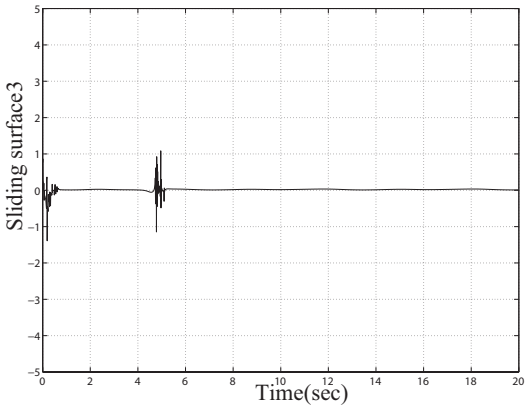

Figure 20: SV 3-Sliding control in CS

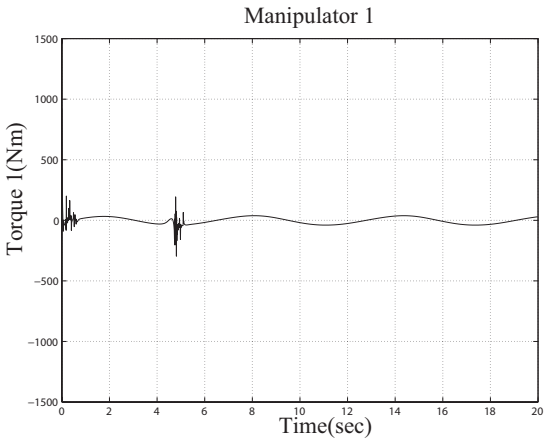

Figure 21: CT of J1M1-Sliding control in CS

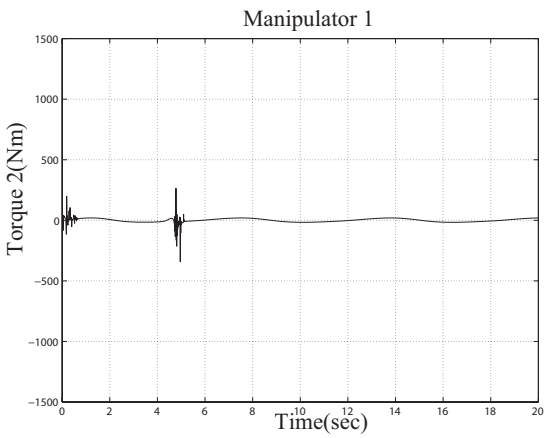

Figure 22: CT of J2M1-Sliding control in CS

considered. Since the first few modes are dominant yielding higher amplitude of vibration, first four modes of vibration are taken into account for the simulation studies. For the case of structural damping characteristics when $\beta = -0.5$, the vibration initially yields oscillatory motion and is completely suppressed around 1 second which is shown in Fig. 27. It is also observed from the Fig. 28 that exponential decay occurs at $\beta = 0$ which corresponds to over damping behavior of the fast subsystem which is same for all modes.

Simulations are also performed with different damping ratios of 0.1 and 0.4. Figures 29 and 30 show that, with increasing damping ratio, the amplitude of vibration has been

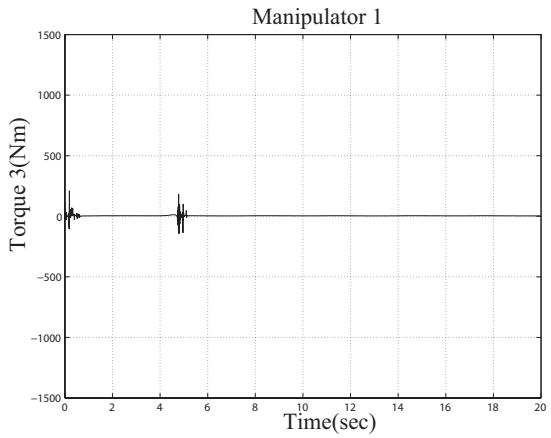

Figure 23: CT of J3M1-Sliding control in CS

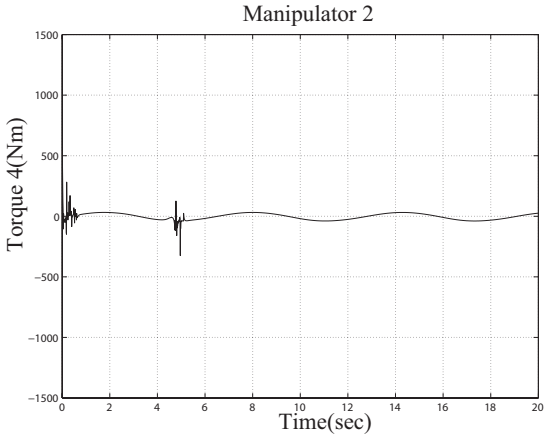

Figure 24: CT of J1M2-Sliding control in CS

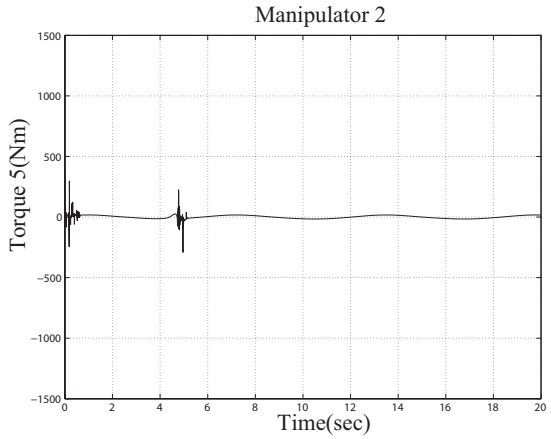

Figure 25: CT of J2M2-Sliding control in CS

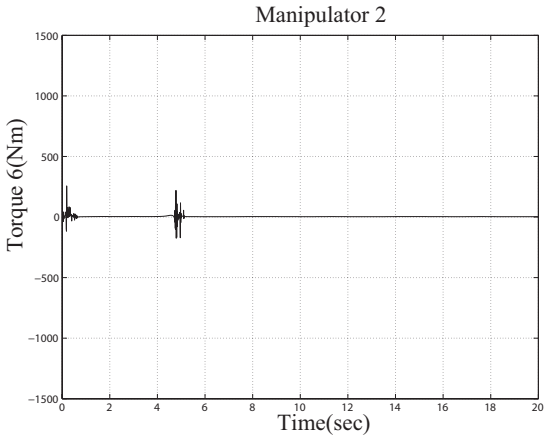

Figure 26: CT of J3M2-Sliding control in CS

significantly suppressed. Furthermore, the transverse displacement under simply supported end condition of the beam with damping ratio of 0.1 is evaluated at various locations of the beam using the modal summation method. Due to symmetry boundary conditions, the deflections at 0.1 m from the left end and at the middle of the beam are considered. It can be observed from the Figs. 31 and 32 that, the center of the beam yields more deflection than any other point on the beam. The simulation results are compared with the existing available results [44] and [50], where, assumed modes are considered. It can be

seen from those results that, the proposed controller suppresses the vibration with limited information compared with the existing controller, which shows the effectiveness of the proposed controller.

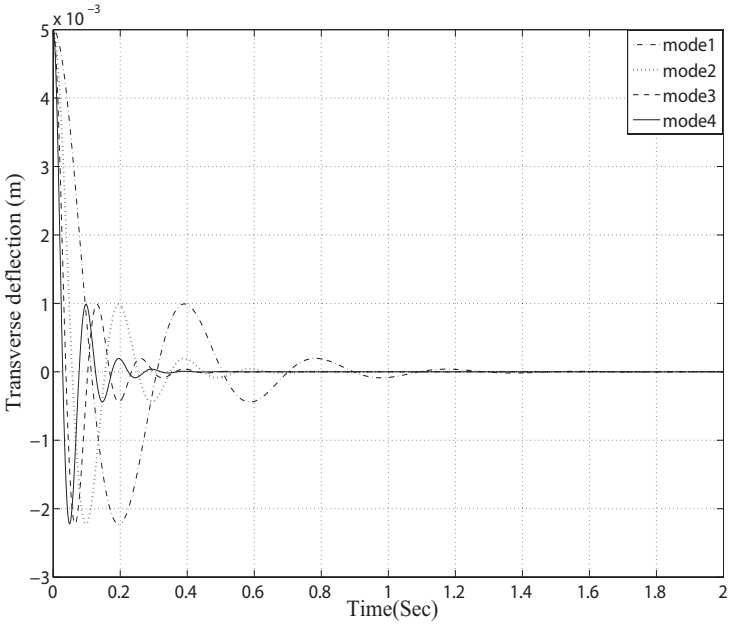

Figure 27: Structural damping characteristics $\beta = -0.5$

Further simulation analysis is being carried by increasing the modulus of elasticity which resembles the rigid beam. Initially, the Young's modulus (E) of aluminium is considered as 71GPa and the transverse deflection at the mid point of the beam is suppressed around 0.2 secs which is shown in Fig. 32. Then, E is increased around two times to show the rigid nature of the beam. By considering the E as 150 GPa simulations are performed again. It is shown in Fig. 33 that the vibration is suppressed comparatively in less time than in the previous case. Finally, the E value is increased to 200 GPa that is close to that of steel, and simulation is carried out. Compared to the above mentioned two cases here, the vibration is suppressed within 0.15 secs which shows that the increase in modulus of

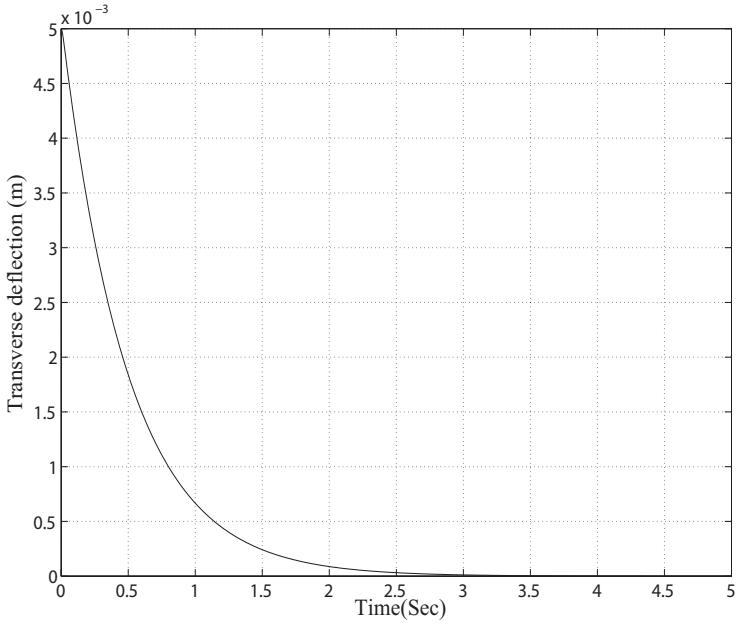

Figure 28: Strong damping characteristics $\beta = 0$

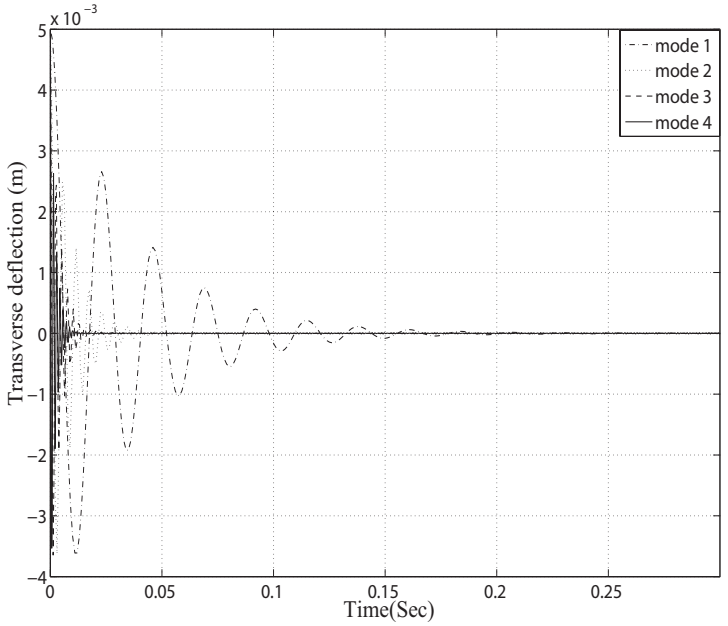

Figure 29: Deflection of the beam for Damping ratio=0.1

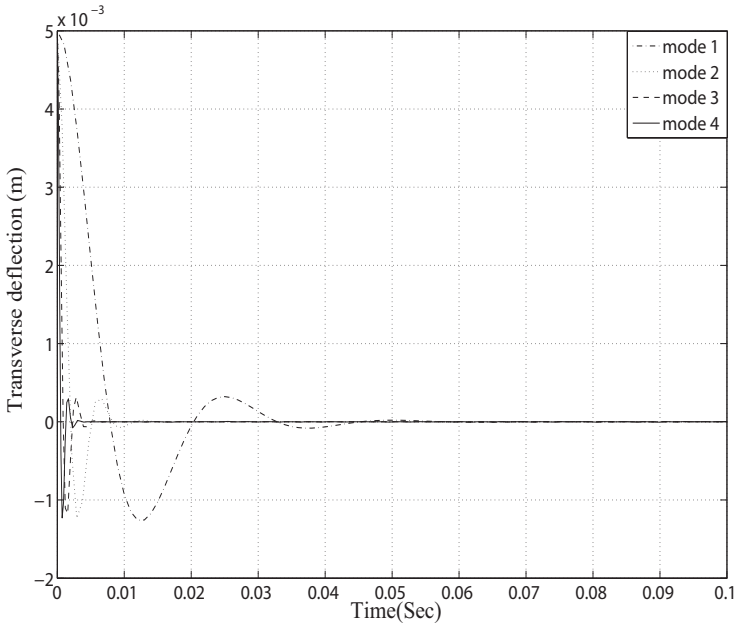

Figure 30: Deflection of the beam for Damping ratio=0.4

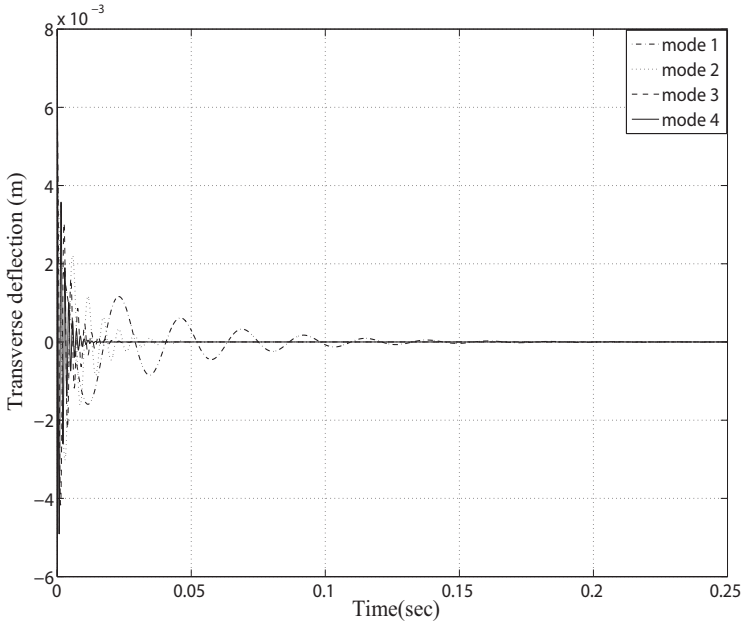

Figure 31: Deflection at 0.1 m from the left end of the beam

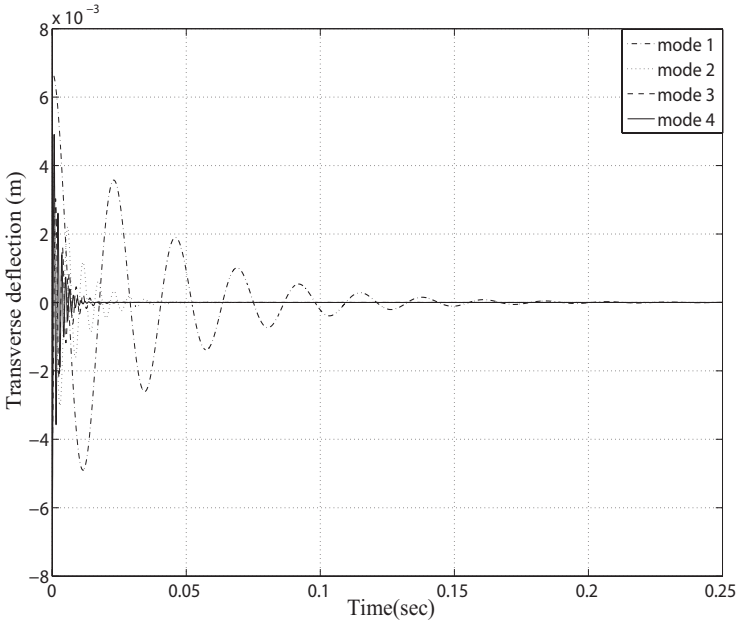

Figure 32: Deflection at mid point of the beam for E=71GPa

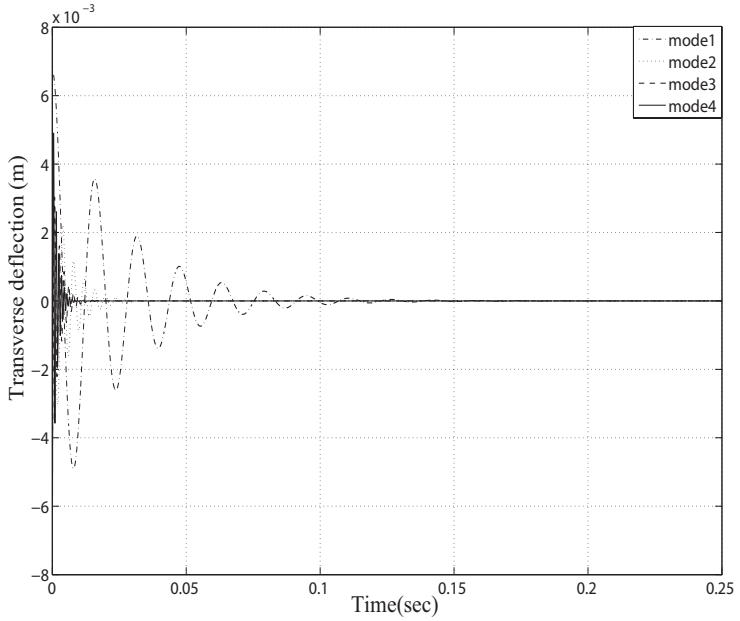

Figure 33: Deflection at mid point of the beam for E=150GPa

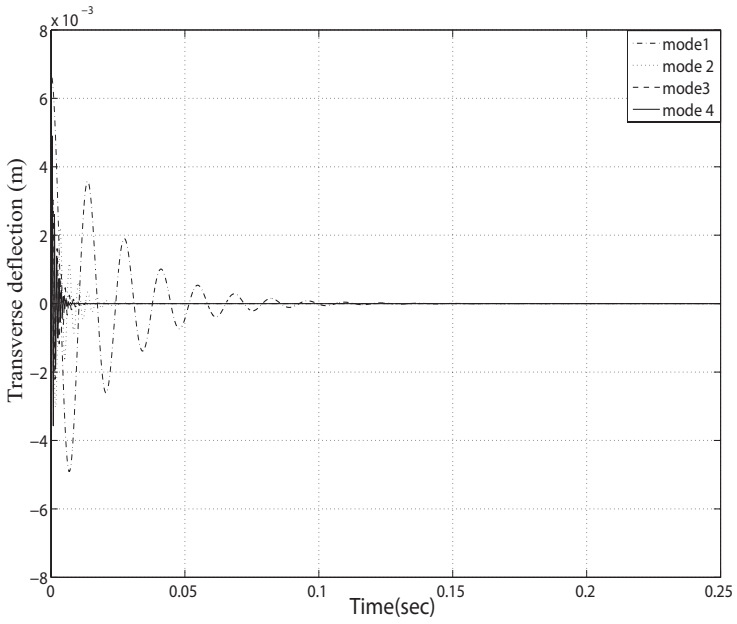

Figure 34: Deflection at mid point of the beam for E=200GPa

elasticity has made the beam rigid and correspondingly vibration is suppressed faster.

4.4.1 Avoidance of chattering in the slow subsystem control law

Since the control law (102) and (103) is discontinuous across the sliding surface, such a control law leads to chattering. Chattering is undesirable in practice because it involves high control activity. To remedy this drawback, we usually use $\frac{x}{|x|+\delta_1}$ to replace $sgn(x)$ in the control law (102), where δ_1 is a constant. Let the switching function ψ in the control law (102) be replaced by,

$$\psi = -\beta_{cs}\frac{Y_{cs}^T S_{cs}}{\|Y_{cs}^T S_{cs}\| + \delta_1} \tag{132}$$

where β_{cs} becomes $\beta_{cs} \geq (1+\frac{\delta_1}{\varepsilon_1})\|\alpha_{cs}\|$ and ε_1 is a design constant. Following the analysis given in [77], it can be proved that e_r will exponentially converge to a small bound, which depends on selection of δ_1. Based on the Tikhnov's theorem, the stability analysis given

in [77] is still valid. However, in such a case, tracking error e_r will not tend to zero but is uniformly bounded. The admissible amplitude of the tracking error can be achieved by choosing a suitable δ_1. By incorporating the suggested switching function in the control law, the chattering can be avoided.

4.5 Special case as manipulators handling a rigid object

When we consider the object as rigid, then the flexible parameter η in the dynamic equations of motion of the object (22) will be considered to be zero and the modulus of elasticity is assumed to be infinite in (23). Hence, one can have the dynamic model for the rigid object as,

$$M_{rd}\ddot{X}_{rf} + C_{rd} + \eta_{rd} + G_{rd} = F_{rd}(-f) \tag{133}$$

$$M_{rd} = \begin{bmatrix} m & 0 & 0 \\ 0 & m & 0 \\ 0 & 0 & \frac{mL^2}{12} \end{bmatrix};\ \ddot{X}_{rf} = \begin{Bmatrix} \ddot{x}_0 \\ \ddot{y}_0 \\ \ddot{\theta} \end{Bmatrix};\ C_{rd} = \{0\ 0\ 0\}^T;\ \eta_{rd} = \{0\ 0\ 0\}^T;\ G_{rd} = \begin{Bmatrix} 0 \\ mg \\ 0 \end{Bmatrix}$$

Including the moments at the two ends of the beam,

$$F_{rd} = \begin{bmatrix} 1 & 0 & 0 & 1 & 0 & 0 \\ 0 & 1 & 0 & 0 & 1 & 0 \\ \frac{L}{2}\sin\theta & -\frac{L}{2}\cos\theta & 1 & -\frac{L}{2}\sin\theta & \frac{L}{2}\cos\theta & 1 \end{bmatrix}$$

Also R becomes R_1

$$R_1 = \begin{bmatrix} 1 & 0 & \frac{L}{2}sin\theta \\ 0 & 1 & -\frac{L}{2}cos\theta \\ 0 & 0 & 1 \\ 1 & 0 & -\frac{L}{2}sin\theta \\ 0 & 1 & \frac{L}{2}cos\theta \\ 0 & 0 & 1 \end{bmatrix}$$

The obtained dynamic equation of rigid object (133) is equivalent to the rigid object model presented in [68].

Then, the manipulator equation derived in Cartesian space (37) can be rewritten as,

$$M_r J^{-1} R_1 \ddot{X}_{rf} + (M_r \dot{J}^{-1} R_1 + M_r J^{-1} \dot{R}_1 + C_r J^{-1} R_1)\dot{X}_{rf} + G_r = \tau + J^T f \tag{134}$$

Premultiplying (134) by $R_1^T J^{-T}$ and also $R_1^T = F_{rf}$ gives,

$$R_1^T J^{-T} M_r J^{-1} R_1 \ddot{X}_{rf} + R_1^T J^{-T} (M_r \dot{J}^{-1} R_1 + M_r J^{-1} \dot{R}_1 + C_r J^{-1} R_1)\dot{X}_{rf} + R_1^T J^{-T} G_r = R_1^T J^{-T} \tau + F_{rf} f \tag{135}$$

Substituting (133) into (135) yields,

$$R_1^T J^{-T} M_r J^{-1} R_1 \ddot{X}_{rf} + R_1^T J^{-T} (M_r \dot{J}^{-1} R_1 + M_r J^{-1} \dot{R}_1 + C_r J^{-1} R_1)\dot{X}_{rf} + R_1^T J^{-T} G_r = R_1^T J^{-T} \tau - (M_{rd} \ddot{X}_{rf} + G_{rd}) \tag{136}$$

The above combined dynamic equation formulated in Cartesian space is described by,

$$(M_o + M_{rd})\ddot{X}_{rf} + C_o \dot{X}_{rf} + G_o + G_{rd} = u_o \tag{137}$$

where,

$$M_o = R_1^T J^{-T} M_r J^{-1} R_1$$

$$C_o = R_1^T J^{-T} (M_r \dot{J^{-1}} R_1 + M_r J^{-1} \dot{R}_1 + C_r J^{-1} R_1)$$

$$G_o = R_1^T J^{-T} G_r$$

$$u_0 = R_1^T J^{-T} \tau$$

The above equation can be rewritten as,

$$M_{or} \ddot{X}_{rf} + C_{or} \dot{X}_{rf} + G_{or} = u_{or} \tag{138}$$

where,

$$M_{or} = M_o + M_{rd}$$

$$C_{or} = C_o$$

$$G_{or} = G_o + G_{rd}$$

$$u_{or} = u_o$$

which is same as the slow subsystem presented in (72). Then, the control algorithm and stability analysis presented for the slow subsystem earlier in this Chapter will be valid for the case of two manipulators rigidly grasping and moving the rigid object.

4.6 Summary

In this Chapter, basic idea of adaptive and robust control algorithms were reviewed. Based on those concepts, a regressor based sliding mode control algorithm was developed for the slow subsystem. In case of fast subsystem, as a part of the composite control law, a simple feedback control algorithm was derived. Exponential stability analysis was carried out to satisfy the Tikhnov's theorem which validated the singular perturbation approach.

The simulation results showed that the proposed composite controller yields good tracking performance and simultaneously suppresses the vibration of the beam. In addition, to reduce the chattering effect on the slow subsystem control law, a smoothing control law was suggested. Furthermore, as a special case, combined dynamic model for the two manipulators handling a rigid object was presented. In the next Chapter, two more control strategies will be developed to improve the slow subsystem control law and corresponding simulations will be performed to demonstrate the efficiency of the controller.

Chapter 5

Further Studies on Controller Design

5.1 Introduction

In the previous Chapter, the detailed investigation and advantages of regressor based control algorithm was carried out for the slow subsystem. However, further improvement on the control law for the slow subsystem can be made without the use of velocity feedback and also disregarding the regressor. In some of the real time applications, velocity measurement may require additional instrumentation and also measured feedback signal may be contaminated with noise. Also, the inclusion of regressor matrix in the control algorithm increases the computational effort needed and implementing them in real time application is also tedious. This Chapter addresses these issues by providing suitable controllers to the slow subsystem. The stability analysis is performed and the corresponding simulation studies are carried out. The simulation results show that the proposed controllers can achieve good tracking performance.

5.2 Control design without velocity measurements

In most of the control algorithms, it is assumed that the velocity feedback signal is available. However, in some applications it may not be possible to measure the velocity or may not even be desirable to do it. Furthermore, the use of noisy velocity signal in the control algorithm may creates the instability in the system [92]. In practice, the joint velocity is measured by means of tachometers or by differentiating the position measurements which are obtained from encoders or resolvers. This necessitates additional sensors which increases the cost and also the velocity signals are contaminated by severe noise [93]. This section, focuses on the development of an adaptive control law without measuring the velocity signal.

By using desired velocity and acceleration trajectory of the object, the slow subsystem given in (72) can be described based on the parameterizations technique [76] which is given by,

$$M_{cs}\ddot{X}_{rfd} + C_{cs}\dot{X}_{rfd} + G_{cs} = Y_a(X_{rf}, \dot{X}_{rfd}, \ddot{X}_{rfd})\alpha_{cs} \tag{139}$$

where $Y_a(X_{rf}, \dot{X}_{rfd}, \ddot{X}_{rfd})$ is the regressor matrix which is dependent on desired trajectory and independent of dynamic parameters. α_{cs} is the constant vector of manipulator and beam inertia parameters.

The control law can be formulated as [94],

$$u_{cs} = Y_a(X_{rf}, \dot{X}_{rfd}, \ddot{X}_{rfd})\breve{\alpha}_{cs} - \Omega^2\Upsilon(\omega + \rho e_r) \tag{140}$$

and the intermediate vectors ω and $\bar{\omega}$ can be calculated by,

$$\omega = \bar{\omega} + \Omega^2 e_r \tag{141}$$

$$\dot{\bar{\omega}} = -2\Omega\bar{\omega} - 2\Omega^3 e_r \tag{142}$$

Also, the adaptive law is defined as,

$$\dot{\breve{\alpha}}_{cs} = \dot{\hat{\alpha}}_{cs} = -\zeta Y_a^T z \tag{143}$$

and z is given by,

$$z = \dot{e}_r - \frac{\omega}{\Omega} + \frac{\rho}{\Omega} e_r \tag{144}$$

where $e_r = X_{rf} - X_{rfd}$ is the tracking error; $\breve{\alpha}_{cs}$ is the estimate of α_{cs}, then, the parameter error vector can be defined as $\tilde{\alpha}_{cs} = \breve{\alpha}_{cs} - \alpha_{cs}$; Υ is constant positive definite matrix; Ω, ρ and ζ are positive constants. It should be noted here that the control law given in (140) and the adaptive parameter $\breve{\alpha}_{cs}$ can be found using adaptive law given in (143) do not involve any velocity measurement as feedback. Thus, it avoids the velocity sensors and the controller needs only position measurements.

Substituting (140) into (72) gives,

$$\ddot{e}_r = M_{cs}^{-1}(-\Omega^2\Upsilon\omega - \rho\Omega^2\Upsilon e_r - C_{cs}\dot{e}_r + Y_a\tilde{\alpha}_{cs} - C_d\dot{e}_r) \tag{145}$$

where $C_d\dot{e}_r = C_{cs}(X_{rf}, \dot{X}_{rf})\dot{X}_{rfd} - C_{cs}(X_{rf}, \dot{X}_{rfd})\dot{X}_{rfd}$.

With the introduction of state vector $x_v^T = [\dot{e}_r^T, \omega^T, {e_r}^T]$, using (141), (142) and (145), the state space form of the closed-loop equation is described by,

$$\dot{x}_v = -A_v x_v + C_v(-C_{cs}\dot{e}_r - C_d\dot{e}_r + Y_a\tilde{\alpha}_{cs}) \tag{146}$$

where the matrix A_v and C_v are given by,

$$A_v = \begin{bmatrix} 0 & \Omega^2 M_{cs}^{-1}\Upsilon & \rho\Omega^2 M_{cs}^{-1}\Upsilon \\ -\Omega^2 \mathrm{I} & 2\Omega\mathrm{I} & 0 \\ -\mathrm{I} & 0 & 0 \end{bmatrix}; \; C_v = \begin{bmatrix} M_{cs}^{-1} \\ 0 \\ 0 \end{bmatrix}$$

By arbitrarily selecting the matrices P_v and Q_v, one can show that $1/2(P_vA_v+A_v{}^TP_v) = Q_v$. One of the possible choice for the symmetric positive definite matrices P_v and Q_v are [95],

$$P_v = \begin{bmatrix} M_{cs} & -\frac{1}{\Omega}M_{cs} & \frac{\rho}{\Omega}M_{cs} \\ -\frac{1}{\Omega}M_{cs} & \Upsilon & 0 \\ \frac{\rho}{\Omega}M_{cs} & 0 & \rho\Omega^2\Upsilon \end{bmatrix};\ Q_v = \begin{bmatrix} (\Omega-\frac{\rho}{\Omega})M_{cs} & -M_{cs} & 0 \\ -M_{cs} & \Omega\Upsilon & 0 \\ 0 & 0 & \rho^2\Omega\Upsilon \end{bmatrix}$$

Also, the eigenvalues of P_v and Q_v satisfies the following bounds,

$$\lambda_p \parallel x_v \parallel^2 \leq x_v^T P_v x_v \qquad and \qquad \Omega\lambda_q \parallel x_v \parallel^2 \leq x_v^T Q_v x_v \tag{147}$$

The stability of closed loop system given in (143) and (146) will be proved in the following section.

5.2.1 Stability analysis

Stability analysis aims to show, by properly choosing a Lyapunov function candidate, that the proposed control algorithm can accomplish asymptotic tracking performance.

Theorem:

The closed-loop system described by (143) and (146) and all the signals are bounded and also $lim_{t\to\infty}\ x_v = 0$, provided the following condition satisfied,

$$\Omega\lambda_q > 3 \parallel C_d \parallel +2\vartheta[sup \parallel \dot{X}_{rfd} \parallel +\sqrt{\frac{2V_3(t)}{\lambda_p}}] \tag{148}$$

where λ_p and λ_q are the eigenvalues of P_v and Q_v and a function $V_3(t)$ is defined in (149).

Proof:

Consider a Lyapunov function candidate

$$V_3(t) = \frac{1}{2}x_v^T P_v x_v + \frac{1}{2\zeta}\tilde{\alpha}_{cs}^T\tilde{\alpha}_{cs} \tag{149}$$

Differentiating (149) gives,

$$\dot{V}_3(t) = x_v^T P_v\dot{x}_v + \frac{1}{2}x_v^T\dot{P}_v x_v + \frac{1}{\zeta}\dot{\tilde{\alpha}}_{cs}^T\tilde{\alpha}_{cs} \tag{150}$$

Using (146), the above equation can be rewritten as,

$$\dot{V}_3(t) = -x_v^T Q_v x_v + x_v^T P_v C_v(-C_{cs}\dot{e}_r - C_d\dot{e}_r + Y_a\tilde{\alpha}_{cs}) + \frac{1}{2}x_v^T\dot{P}_v x_v + \frac{1}{\zeta}\dot{\tilde{\alpha}}_{cs}^T\tilde{\alpha}_{cs} \tag{151}$$

When $\Omega \geq max(1,\rho)$, one can have the following,

$$\begin{aligned} -x_v^T P_v C_v C_d\dot{e}_r &= -(\dot{e}_r - \frac{\omega}{\Omega} + \frac{\rho}{\Omega}e_r)^T C_d\dot{e}_r \\ &\leq 3 \parallel C_d \parallel\parallel x_v \parallel^2 \end{aligned} \tag{152}$$

$$\begin{aligned} \frac{1}{2}x_v^T\dot{P}_v x_v - x_v^T P_v C_v C_{cs}\dot{e}_r = \frac{1}{2}\dot{e}_r^T\dot{M}_{cs}\dot{e}_r + \dot{e}_r\frac{\rho}{\Omega}\dot{M}_{cs}{e_r}^T - \dot{e}_r\frac{1}{\Omega}\dot{M}_{cs}\omega^T \\ -(\dot{e}_r - \frac{\omega}{\Omega} + \frac{\rho}{\Omega}e_r)^T C_{cs}\dot{e}_r \end{aligned} \tag{153}$$

Using the property ${\dot{e}_r}^T(1/2\dot{M}_{cs} - C_{cs})\dot{e}_r = 0$, above equation can be rewritten as,

$$\begin{aligned} \frac{1}{2}x_v^T\dot{P}_v x_v - x_v^T P_v C_v C_{cs}\dot{e}_r &= \frac{1}{\Omega}[\rho e_r - \omega][\dot{M}_{cs} - C_{cs}]\dot{e}_r \\ &\leq 2\vartheta \parallel \dot{X}_{rf} \parallel\parallel x_v \parallel^2 \end{aligned} \tag{154}$$

where $\vartheta \parallel \dot{X}_{rf} \parallel = \parallel \dot{M}_{cs} - C_{cs} \parallel$.

Substituting (147), (152) and (154) into (151) yields,

$$\begin{aligned} \dot{V}_3(t) &\leq -(\Omega\lambda_q - 3 \parallel C_d \parallel - 2\vartheta \parallel \dot{X}_{rf} \parallel) \parallel x_v \parallel^2 + (z^T Y_a + \frac{1}{\zeta}\dot{\tilde{\alpha}}_{cs}^T)\tilde{\alpha}_{cs} \\ &= -f(\parallel \dot{X}_{rf} \parallel) \parallel x_v \parallel^2 \end{aligned} \tag{155}$$

where $f(\| \dot{X}_{rf} \|) = \Omega\lambda_q - 3 \| C_d \| - 2\vartheta \| \dot{X}_{rf} \|$ and $x_v^T P_v C_v = z^T$ and also (143) is used to obtain the above equation. The right hand side of (155) is negative if $f(\| \dot{X}_{rf} \|) > 0$, which is true if (148) is satisfied.

When $\Omega\lambda_q$ is sufficiently large, (148) is satisfied. By induction with respect to t, $V_3(t)$ will be decreasing until $\| x_v \| = 0$ which shows that the closed-loop system (146) is asymptotically stable and hence the given theorem is proved.

5.2.2 Simulation results

To illustrate the performance of the proposed controller, simulations are carried out. The parameters of the identical manipulators and beam are given in Table 1 and 2. The beam initial position and orientation are $X_{rf} = \{0.51, 0.36, 0.1\}^T$ and it's initial velocity and acceleration are considered to be zero. Initial joint angles of manipulator are q_{11} = 0.2974 rad, q_{12} = 1.6974 rad, q_{13} = -1.6948 rad, q_{21} = 0.2149 rad, q_{22} = 1.4886 rad and q_{23} = -1.4306 rad respectively. The initial joint velocities of all the joints of manipulators are 0.001 rad/sec and joint accelerations are assumed to be zero. The simulation was carried out with a sampling period of 0.001sec to track the desired trajectory given by,

$$X_{rfd} = \begin{bmatrix} sin(t) \\ cos(t) \\ 0 \end{bmatrix}$$

The initial values of $\breve{\alpha}_{cs}(0)$ are chosen as=[0.11; 0.06; $6e^{-3}$; $6e^{-3}$; 0.11; 0.02; 0.073; 0.044; 0.16; 0.11; 0.06; $6e^{-3}$; $6e^{-3}$; 0.11; 0.02; 0.073; 0.044; 0.16; 0.16; 0.01]^T. The initial value of $\bar{\omega}(0)$ is chosen as zero. The control parameters are tuned and given in Table 4.

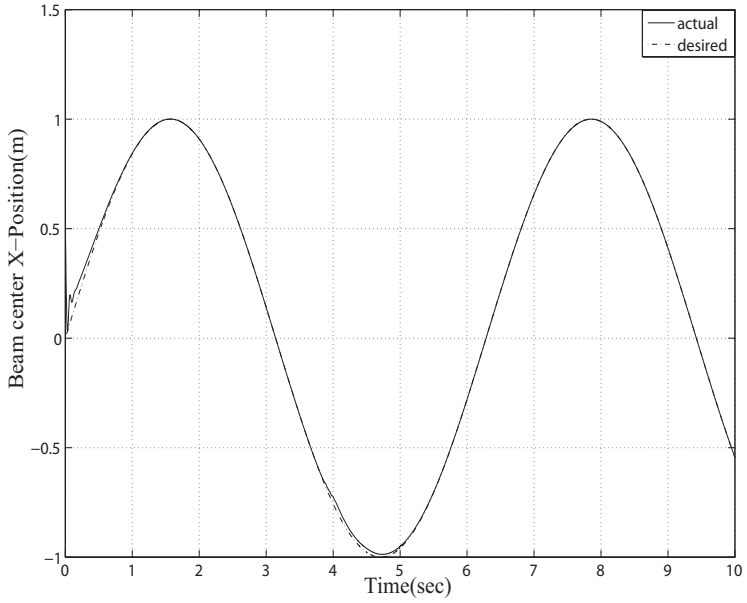

Figure 35: X-Position tracking-Without velocity measurement in CS

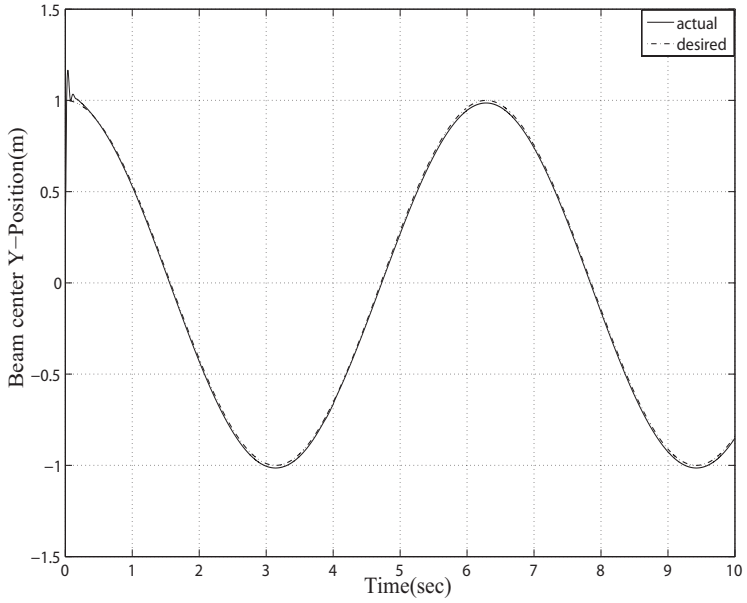

Figure 36: Y-Position tracking-Without velocity measurement in CS

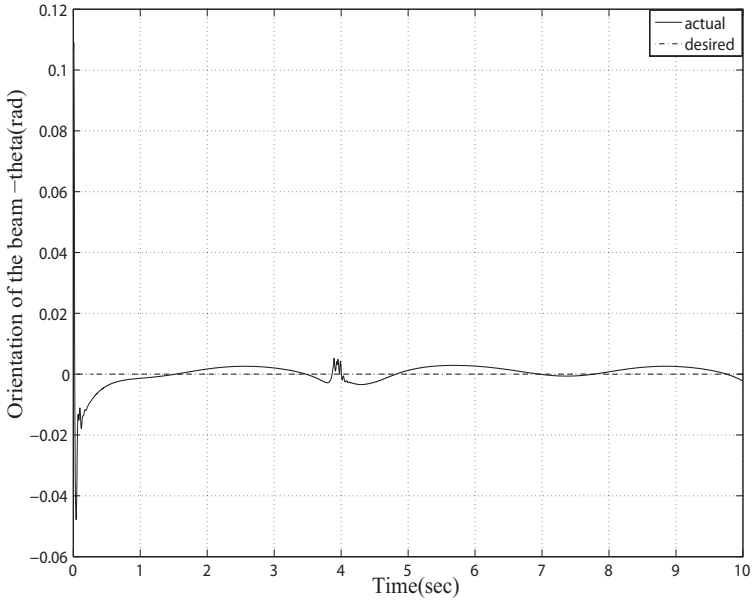

Figure 37: Orientation of the beam-Without velocity measurement in CS

Table 4: Control parameters-without velocity measurements in CS

Parameter	Value
Ω	31
ρ	27.8
Υ	diag(0.1)
ζ	0.1

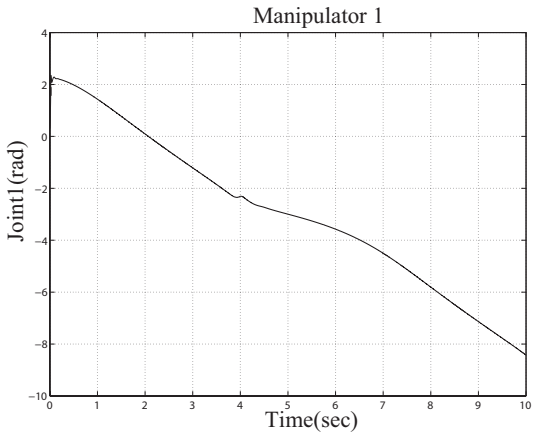

Figure 38: J1M1-Without velocity measurement in CS

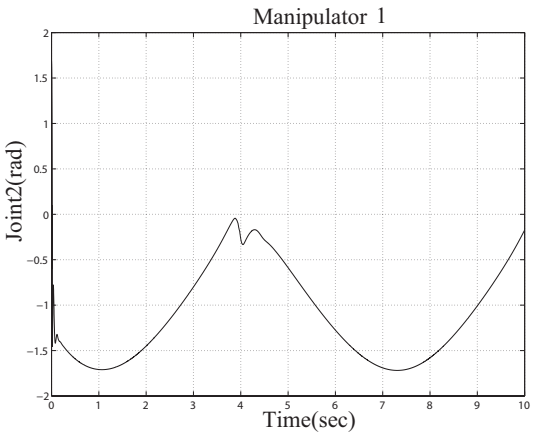

Figure 39: J2M1-Without velocity measurement in CS

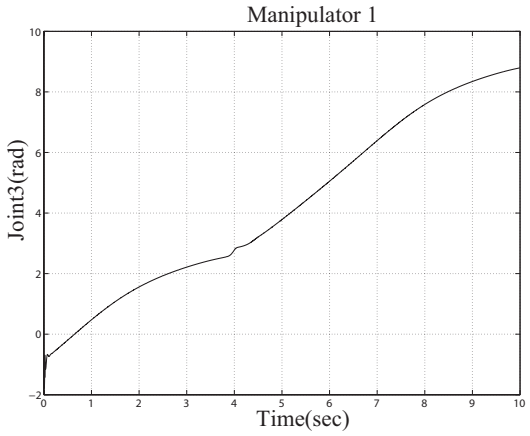

Figure 40: J3M1-Without velocity measurement in CS

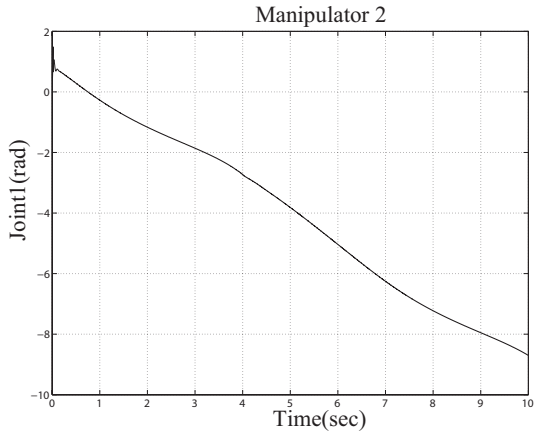

Figure 41: J1M2-Without velocity measurement in CS

It can be observed from the Figs. 35 - 37 that the control law without velocity measurement also yields good performance in tracking along X, Y directions and also reaches the desired orientation. It can be seen from the Figs. 38 - 43 that the manipulators also moved in a similar path as in the regressor based sliding control. Similarly, joint 2 of manipulator 1 approaches the singularity point around 4 secs which can also be seen in the previous section controller simulation results. It is evident from the simulation results that the suggested controller can track the desired trajectory without using velocity feedback

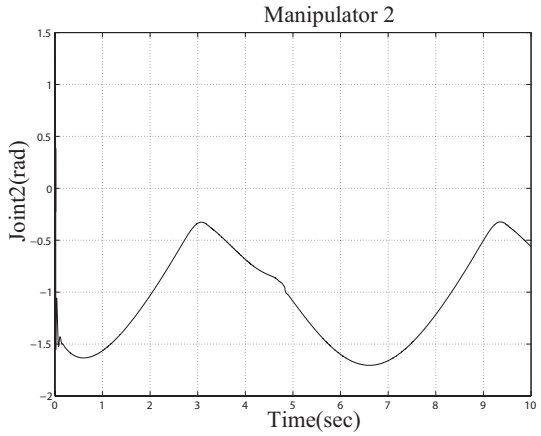

Figure 42: J2M2-Without velocity measurement in CS

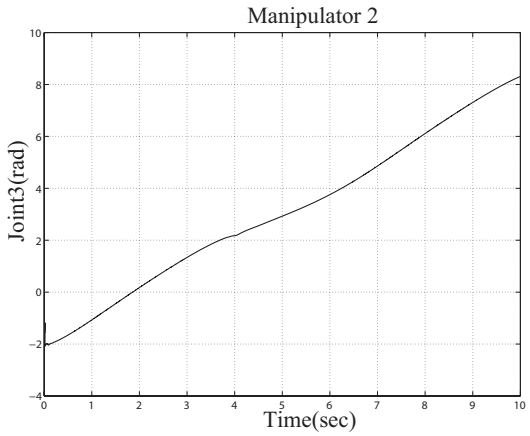

Figure 43: J3M2-Without velocity measurement in CS

signal. This avoids the need for necessary sensors and ultimately reduces the cost.

5.3 Control design without regressor

Many studies have been focused on the development and implementation of adaptive and robust control algorithms [18], [24], [25], [68], [86] and [96] for two manipulators handling an object. All of these studies need the use of the regressor matrix to simplify the control algorithm and help in achieving the stability proof for the linearized robot dynamics [58]. However, it should be noted that the regressor based approach has difficulties in implementing in practical problems as it involves more computations. Furthermore, the recomputation of the regressor at the servo control rates increases the computational effort in practical applications [97]. An off-line computational scheme of regressor is thus proposed to calculate the regressor [98] to reduce the on-line computational complexity which uses the position, velocity and acceleration information of the desired trajectory. However, the computation of regressor could not be avoided when there is a change in the robot

structures or desired trajectory.

Considering the aforementioned difficulties, for a single manipulator case various control strategies have been developed (see, for example, [69] and also [97] - [99]) which avoids the regressor. In particular, Leung and Su's adaptive [69] approach involves computation of simple scalar functions and it involves only four parameters to be estimated which is independent of number of robots. This control approach is also valid when more number of links are considered for each of the robot. Hence, the algorithm developed for the single manipulator is extended to the two manipulator-beam system. However, it is to be noted that the typical parameter adaptive algorithm requires atleast [68] ten parameters to be estimated for each robot.

The robust adaptive control law can be chosen as [69],

$$u_{cs} = -K_d M_{cs} S_\phi - (\check{\rho}_1 \parallel \ddot{X}_r \parallel + \check{\rho}_2 \parallel \dot{X}_{rf} \parallel \parallel \ddot{X}_r \parallel + \check{\rho}_3 + \check{\rho}_4 \parallel \dot{X}_{rf} \parallel) sat(\frac{S_{cs}}{\phi}) \qquad (156)$$

where K_d is the positive definite matrix and $\check{\rho}_i$, i=1,2,3,4, are the adaptive control gains. S_ϕ is the measure of the algebraic distance of the current state to the boundary layer which is given by,

$$S_\phi = S_{cs} - \phi \; sat(S_{cs}/\phi) \qquad (157)$$

where $\phi > 0$ is boundary layer thickness.

Also, the sat(S_{cs}/ϕ) is defined as follows,

$$\begin{aligned} sat(S_{cs}/\phi) &= \text{sgn}(\text{S}_{\text{cs}}) \quad \text{if} \mid \text{S}_{\text{cs}} \mid > \phi \\ &= S_{cs}/\phi \qquad \text{if} \mid \text{S}_{\text{cs}} \mid \leq \phi \end{aligned}$$

The adaptive parameters are given by,

$$\dot{\breve{\rho}}_1 = \beta_1 \parallel S_\phi \parallel \parallel \ddot{X}_r \parallel \tag{158}$$

$$\dot{\breve{\rho}}_2 = \beta_2 \parallel S_\phi \parallel \parallel \dot{X}_{rf} \parallel \parallel \ddot{X}_r \parallel \tag{159}$$

$$\dot{\breve{\rho}}_3 = \beta_3 \parallel S_\phi \parallel \tag{160}$$

$$\dot{\breve{\rho}}_4 = \beta_4 \parallel S_\phi \parallel \parallel \dot{X}_{rf} \parallel \tag{161}$$

where $\beta_i > 0$, i=1,2,3,4 are the arbitrary constants which determines rates of adaptation. The control law (156) has two terms. The first term is representing proportional and derivative control. The adaptive control gains $\dot{\breve{\rho}}_i$, i=1,2,3,4 are represented in the second term which are used to recover and cancel the unknown nonlinear dynamics. It should be emphasized here that the control laws (156) and (158)-(161) involve multiplication of simple scalar functions and the detailed description of model is not necessary. Therefore, the suggested controller will avoid the complex calculations of regressor, computationally fast, structurally simple and easy to implement in real time applications.

5.3.1 Stability analysis

In order to determine the stability of the closed loop system described by (72) and (156), the following analysis is being carried out.

Differentiating the sliding surface (101) with respect to time gives,

$$\dot{S}_{cs} = \ddot{X}_{rf} - \ddot{X}_r \tag{162}$$

Multiplying both sides of (162) by M_{cs} and using (72), (162) can be rewritten as,

$$M_{cs}\dot{S}_{cs} = u_{cs} - C_{cs}\dot{X}_{rf} - G_{cs} - M_{cs}\ddot{X}_r \tag{163}$$

Adding and subtracting $C_{cs}\dot{X}_r$ in (163) gives,

$$M_{cs}\dot{S}_{cs} = u_{cs} - M_{cs}\ddot{X}_r - C_{cs}S_{cs} - G_{cs} - C_{cs}\dot{X}_r \tag{164}$$

Consider a Lyapunov function candidate,

$$V_4(t) = \frac{1}{2}S_\phi^T M_{cs} S_\phi + \frac{1}{2}\Sigma\frac{(\rho_i - \check{\rho}_i)^2}{\beta_i} \tag{165}$$

Since $\dot{S_\phi} = \dot{S}_{cs}$ and differentiating (165) with respect to time gives ,

$$\dot{V}_4(t) = S_\phi^T M_{cs}\dot{S}_{cs} + \frac{1}{2}S_\phi^T \dot{M}_{cs} S_\phi + \Sigma\frac{(\rho_i - \check{\rho}_i)(-\dot{\check{\rho}}_i)}{\beta_i} \tag{166}$$

Using (156) and (164), (166) becomes,

$$\begin{aligned}\dot{V}_4(t) = S_\phi^T[-K_d M_{cs} S_\phi - (\check{\rho}_1 \parallel \ddot{X}_r \parallel + \check{\rho}_2 \parallel \dot{X}_{rf} \parallel\parallel \ddot{X}_r \parallel + \check{\rho}_3 + \check{\rho}_4 \parallel \dot{X}_{rf} \parallel)]sat(\frac{S_{cs}}{\phi}) \\ + S_\phi^T(-M_{cs}\ddot{X}_r - C_{cs}S_{cs} - G_{cs} - C_{cs}\dot{X}_r) + \frac{1}{2}S_\phi^T\dot{M}_{cs}S_\phi + \Sigma\frac{(\rho_i - \check{\rho}_i)(-\dot{\check{\rho}}_i)}{\beta_i}\end{aligned} \tag{167}$$

Since $\parallel S_\phi \parallel = S_\phi^T sat(S_{cs}/\phi)$ [69], using property 4 in CS given in Chapter 3 and after some algebraic manipulation, (167) results in,

$$\begin{aligned}\dot{V}_4(t) \leq -S_\phi^T K_d M_{cs} S_\phi - (\check{\rho}_1 \parallel \ddot{X}_r \parallel + \check{\rho}_2 \parallel \dot{X}_{rf} \parallel\parallel \ddot{X}_r \parallel + \check{\rho}_3 + \check{\rho}_4 \parallel \dot{X}_{rf} \parallel) \parallel S_\phi \parallel \\ + (\rho_1 \parallel \ddot{X}_r \parallel + \rho_2 \parallel \dot{X}_{rf} \parallel\parallel \ddot{X}_r \parallel + \rho_3) \parallel S_\phi \parallel + \frac{1}{2}S_\phi^T\dot{M}_{cs}S_\phi \\ + \Sigma\frac{(\rho_i - \check{\rho}_i)(-\dot{\check{\rho}}_i)}{\beta_i} - S_\phi^T C_{cs} S_\phi + \phi\rho_2 \parallel \dot{X}_{rf} \parallel\parallel S_\phi \parallel\end{aligned} \tag{168}$$

Since $S_\phi^T(\dot{M}_{cs} - 2C_{cs})S_\phi = 0$ (property 2 in CS) and define $\rho_4 = \phi\rho_2$ and also using the adaptive parameters (158)-(161), (168) yields into,

$$\dot{V}_4(t) = -S_\phi^T K_d M_{cs} S_\phi \tag{169}$$

Since $K_d M_{cs}$ is symmetric positive definite matrix then there exists a constant γ such that $\gamma I_d \leq K_d M_{cs}$. Hence, (169) can be rewritten as,

$$\dot{V}_4(t) \leq -\gamma \parallel S_\phi \parallel_2^2 \leq 0 \tag{170}$$

In order to achieve the stability of the system, it is necessary to show that $S_\phi \rightarrow 0$ as $t \rightarrow \infty$. This can be achieved by applying Barbalat's lemma to the following continuous non-negative function,

$$\begin{aligned} \dot{V}(t) &= V_4(t) - \int_0^t (\dot{V}_4(\tau) + \gamma \parallel S_\phi(\tau) \parallel_2^2) d\tau \quad \text{with} \\ \dot{V}(t) &= -\gamma \parallel S_\phi(\tau) \parallel_2^2 \end{aligned} \tag{171}$$

By definition, S_ϕ is related with S_{cs} in (157). Then, using the standard argument, since S_{cs} is bounded and correspondingly e_r and $\dot{e}_r$ are also bounded. Thus, all the feedback signals X_{rf}, $\dot{X}_{rf}$ and $\dot{X}_r$ are bounded. Therefore, it can seen from (164) that, $\dot{S}_{cs}$ is also bounded because M_{cs} is already given as bounded property (property 4 in CS) which proves $\dot{V}(t)$ to be uniformly continuous function of time. Since V is bounded below by 0 and $\dot{V}(t) \leq 0$ for all t, use of Barbalat's lemma proves that $\dot{V}(t) \rightarrow 0$ and from (171) that $\parallel S_\phi \parallel \rightarrow 0$ as $t \rightarrow \infty$.

5.3.2 Simulation results

To demonstrate the effectiveness of the controller, simulations are performed by considering the manipulators and beam parameters given in Table 1 and 2. The adaptive gains are chosen as β_1=β_2=β_3=2 and β_4=2.4. The initial adaptive parameters are taken as $\check{\rho}_1(0)$=$\check{\rho}_2(0)$=$\check{\rho}_3(0)$=$\check{\rho}_4(0)$=1. In order to reduce the chattering effect, the boundary layer thickness is chosen as ϕ=0.2. The control gain parameters are chosen as K_d = 50 and λ_{cs} = 19.94. The tracking performance along X and Y-directions are shown in the Figs. 44 and 45. The orientation of the beam reached its desired value within a sec as shown

in Fig. 46. The results show that, without incorporating the regressor, the proposed controller can achieve good tracking performance. Similarly, the joint angular motions of each manipulator follow a similar trend as in the case of other controllers.

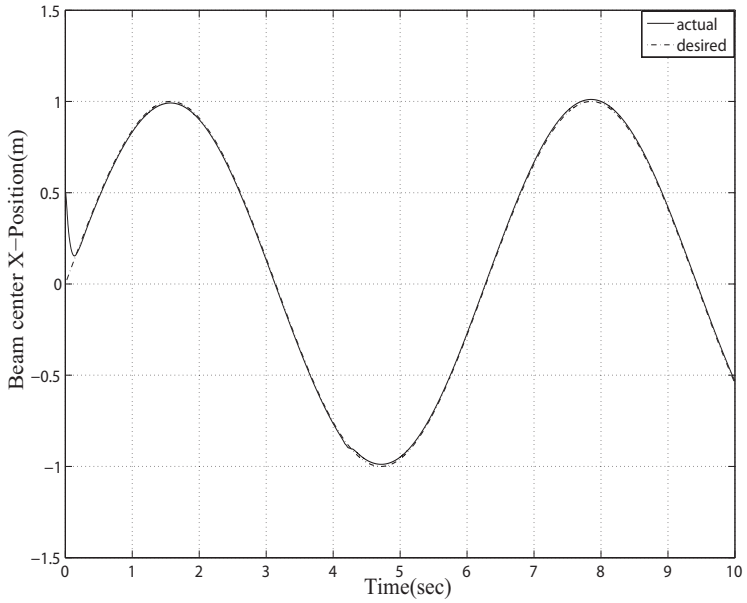

Figure 44: X-Position tracking-Without regressor in CS

5.4 Summary

This Chapter presented two control strategies to overcome the problems related to measurement of velocity feedback and inclusion of regressor matrix. Initially, in order to avoid the concerns associated with the measurement of velocity signal, an adaptive control law with only position feedback has been implemented to the slow subsystem, and corresponding stability analysis is also carried out. Simulation results confirm that, the presented control does not need any velocity feedback which avoids the velocity sensors and other associated practical difficulties. Finally, a non-regressor based adaptive robust

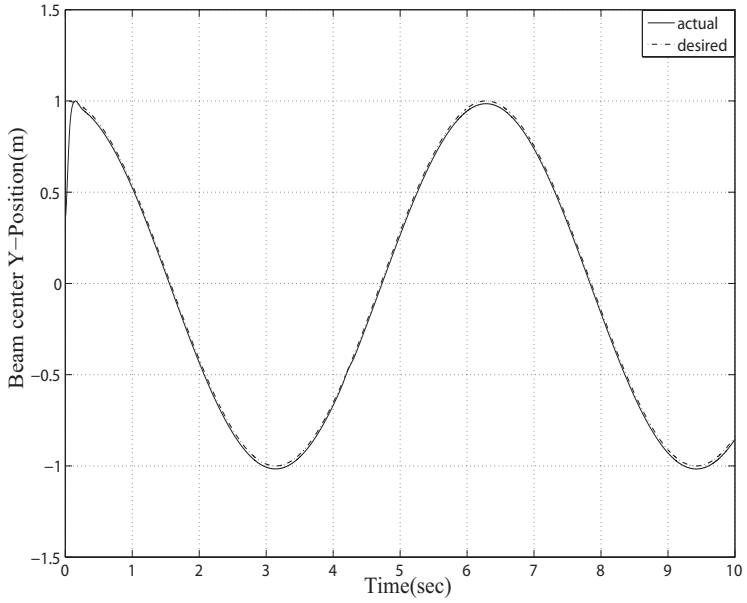

Figure 45: Y-Position tracking-Without regressor in CS

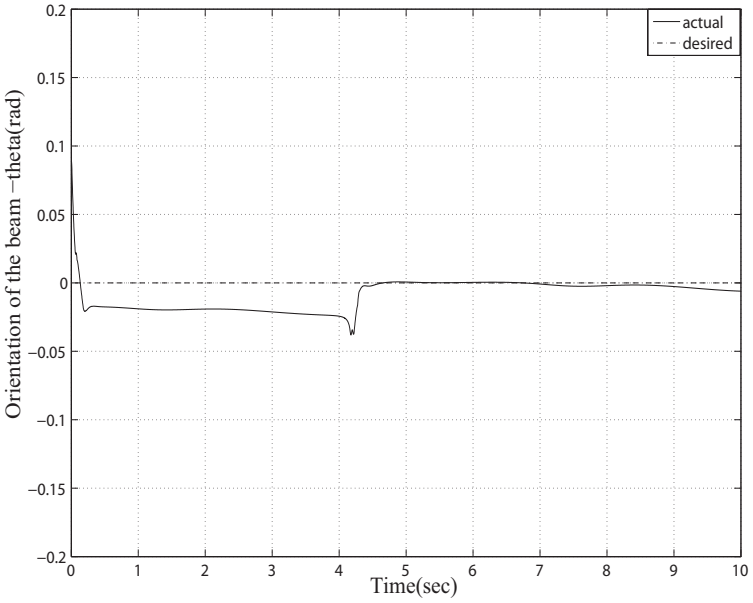

Figure 46: Orientation of the beam-Without regressor in CS

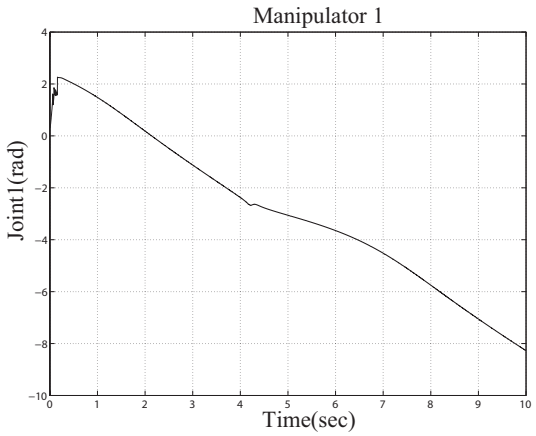

Figure 47: J1M1-Without regressor in CS

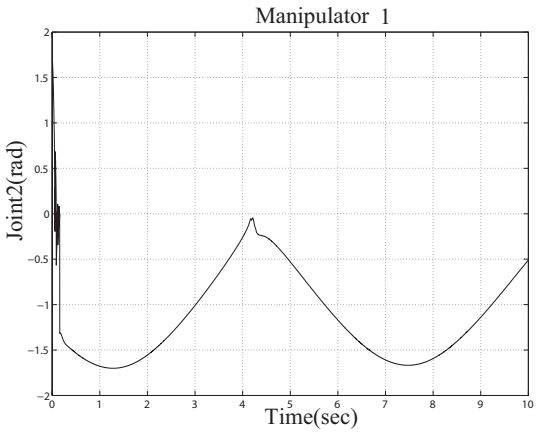

Figure 48: J2M1-Without regressor in CS

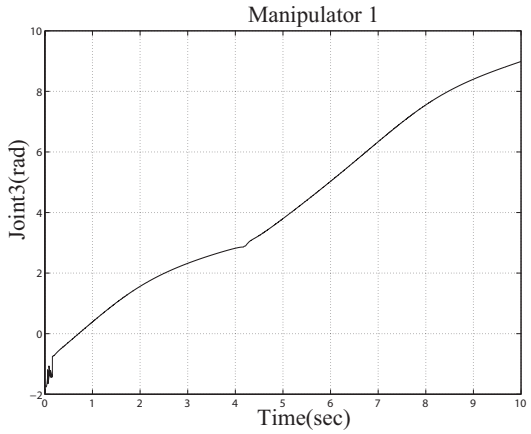

Figure 49: J3M1-Without regressor in CS

Figure 50: J1M2-Without regressor in CS

control algorithm was implemented to the slow subsystem to avoid the computation burden of the regressor. Stability analysis and simulation results reveal that the presented controller can track the desired trajectory effectively. Earlier Chapters discussed broadly the dynamics and control of manipulators-flexible object system in Cartesian space. In the next Chapter, further analysis will be carried out by developing the complete system of dynamic equations in joint space.

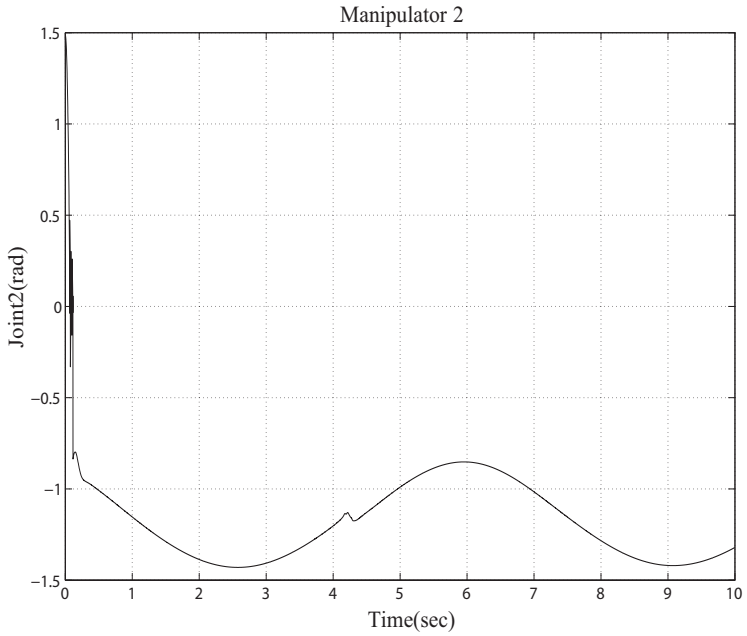

Figure 51: J2M2-Without regressor in CS

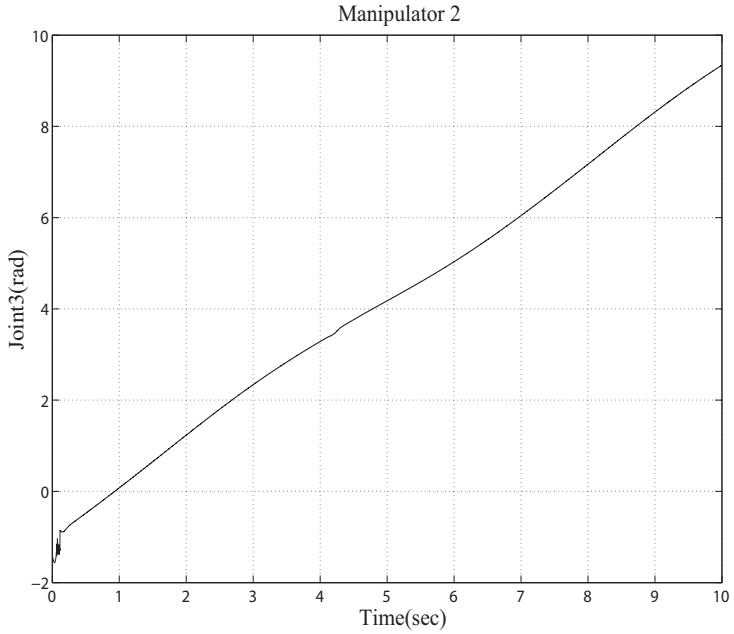

Figure 52: J3M2-Without regressor in CS

Chapter 6

Manipulators - Flexible Object System in Joint Space

6.1 Introduction

Depending on the nature of the problems and the intended control applications, the dynamic equations of motion of a manipulator-beam system can be expressed either in joint coordinate space or Cartesian coordinate space. Earlier Chapters have dealt with Cartesian space system. However, there are certain advantages in using joint space compared to the Cartesian space. The joint space motion planning can be achieved in two steps [101]: path planning and trajectory generation. In the path planning, robot motion is preplanned for the desired geometric path and the problems associated with geometric constraints and joint angle limits are taken care of. The trajectory generation determines how fast the robot should move along the desired geometric path and it considers other constraints such as limits of joints velocity, acceleration, jerk and torque. Many industrial robots utilize joint

space control schemes for the position control. Also, while defining the Cartesian trajectory, the inverse kinematics is used to transform the Cartesian variables to joint variables and there may be a chance of singularity problem. Furthermore, the inverse kinematic calculations are computationally expensive for complicated trajectories. Hence, defining the joint space motion can be an advantage. Moreover, classical joint space control schemes are not only simple to implement, but also stable and robust [102]. Considering these reasons, earlier analysis is further extended by developing the complete system of dynamic model in joint space. Then, by utilizing the typical steps of singular perturbation approach, slow and fast subsystem will be obtained. For each subsystem corresponding control law will be suggested and together they form a composite control input to the complete system. Stability analysis and simulation results are presented to illustrate the composite control strategy. It should be noted that some of the equations presented in the previous Chapters are reviewed here to formulate the complete system of dynamic equations in joint space.

6.2 Modeling of manipulators - flexible object system in joint space

In order to obtain the complete system of dynamic equations in joint space, the manipulators and beam dynamic equations obtained in Chapter 2 are reconsidered.

The two manipulators dynamic equation assembled in joint space (34) is rewritten as,

$$M_r\ddot{q} + C_r\dot{q} + G_r = \tau + J^T f \tag{172}$$

The beam dynamic equation derived in Chapter 2 for the rigid body motion can be reproduced as,

$$M_{rf}\ddot{X}_{rf} + C_{rf} + \eta_{rf} + G_{rf} = F_{rf}(-f) \tag{173}$$

and for the flexible beam equation of motion is rewritten in compact form as,

$$A_{jf}\ddot{X}_{rf} + \ddot{\eta} - \eta\dot{\theta}^2 + \frac{EI}{\rho}\eta^{iv} = F_{ff}(f) \tag{174}$$

where $A_{jf} = [-\sin\theta \quad \cos\theta \quad x]$.

It can be seen from (173) and (174) that, the beam dynamics is represented in Cartesian space and it should be converted into joint space. Then, the resulting equation can be combined with the manipulator dynamics (172) to yield the complete system of dynamic equations in joint space. The following section illustrates how to formulate the combined dynamics in joint space.

6.2.1 Combined dynamics in joint space

Following relations are taken into account again from Chapter 2 to formulate the combined dynamics in joint space.

The end-effector velocities and joint velocities of the manipulators are related by,

$$\{\dot{e}\} = [J]\{\dot{q}\} \tag{175}$$

and the end-effectors velocities are related to the object velocity as,

$$\{\dot{e}\} = [R]\{\dot{X}_{rf}\} \tag{176}$$

Using (175), (176) can be written as,

$$\dot{X}_{rf} = R^{\dagger}J\dot{q} \tag{177}$$

where $R^{\dagger}$ is the pseudo inverse of R.

Differentiating (177) gives,

$$\ddot{X}_{rf} = \dot{R^{\dagger}} J\dot{q} + R_1^{\dagger}(\dot{J}\dot{q} + J\ddot{q}) \tag{178}$$

Then incorporating (178) into (173) and (174) yields the beam rigid body motion in joint space,

$$M_{rf}R^{\dagger}J\ddot{q} + M_{rf}(\dot{R^{\dagger}}J + R^{\dagger}\dot{J})\dot{q} + C_{rf} + \eta_{rf} + G_{rf} = F_{rf}(-f) \tag{179}$$

and also flexible motion of beam in joint space can be written as,

$$A_{jf}R^{\dagger}J\ddot{q} + A_{jf}(\dot{R^{\dagger}}J + R^{\dagger}\dot{J})\dot{q} + \ddot{\eta} - \eta\dot{\theta}^2 + \frac{EI}{\rho}\eta^{iv} = F_{ff}(f) \tag{180}$$

Substituting for the force f from (179) into (172) gives the combined rigid motion dynamic equation in joint space,

$$M_{jsf}\ddot{q} + C_{jsf}\dot{q} + G_{jsf} + \eta_{jsf} = \tau_{jsf} \tag{181}$$

where,

$$M_{jsf} = (M_r + J^T F_{rf}^{\dagger} M_{rf} R^{\dagger} J)$$

$$C_{jsf} = C_r + J^T F_{rf}^{\dagger} M_{rf}(\dot{R^{\dagger}}J + R^{\dagger}\dot{J})$$

$$G_{jsf} = G_r + J^T F_{rf}^{\dagger} G_{rf}$$

$$\eta_{jsf} = \eta_{rf}$$

Since F_{rf} is not a square matrix, its inverse $F_{rf}^{\dagger}$ can be calculated by the pseudo inverse. Taking into account the transverse vibration of beam dynamics (180) and also above derived combined dynamics forms the complete manipulator-beam system dynamics in joint space given by,

$$M_{jsf}\ddot{q} + C_{jsf}\dot{q} + G_{jsf} + \eta_{rf} = \tau_{jsf} \tag{182}$$

$$A_{jf}R^{\dagger}J\ddot{q}+A_{jf}(\dot{R^{\dagger}}J+R^{\dagger}\dot{J})\dot{q}+\ddot{\eta}-\eta\dot{\theta}^2+\frac{EI}{\rho}\eta^{iv}=F_{ff}(f) \tag{183}$$

The above system of dynamic equations are coupled with rigid and flexible parameters. Without using any approximate methods, the coupled motions must be controlled. Therefore, singular perturbation approach can be applied to this system of dynamic equations as well.

6.3 Singular perturbation modeling in joint space

In order to develop a robust control algorithm for the system of dynamic equations (182) and (183), the following control task is considered.

Control task: For any given desired bounded trajectories q_d and $\dot{q}_d$, with some or all of the manipulator and beam parameters unknown, derive a controller for the manipulator control torque τ_{jsf} such that the manipulator q tracks q_d while suppressing the vibration of the flexible object, η, to zero.

The above control task can be achieved by developing the slow and fast subsystem in joint space. These subsystems can be obtained following a similar analysis as discussed in Chapter 3 by using singular perturbation approach. By incorporating $\eta=\varepsilon^2.\ w$ into (182) and (183) and also using (63), the singularly perturbed model of the complete system of dynamic equations is obtained as,

$$\tilde{M}_{jsf}\ddot{q}+\tilde{C}_{jsf}\dot{q}+\tilde{G}_{jsf}+\tilde{\eta}_{rf}=\tau_{jsf} \tag{184}$$

$$A_{jf}\tilde{R}^{\dagger}J\ddot{q}+A_{jf}(\dot{\tilde{R}^{\dagger}}J+\tilde{R}^{\dagger}\dot{J})\dot{q}+\ \varepsilon^2\ddot{w}-\ \varepsilon^2 w\dot{\theta}^2+aw^{iv}=F_{ff}(f) \tag{185}$$

where $\tilde{M}_{jsf}$, $\tilde{C}_{jsf}$, $\tilde{G}_{jsf}$, $\tilde{\eta}_{rf}$ and $\tilde{R}^{\dagger}$ are obtained by substituting w instead of η. Henceforth, the typical steps of singular perturbation approach will be followed to obtain the slow and fast subsystem from (184) and (185).

6.3.1 Slow subsystem in joint space

The slow subsystem in joint space is determined when $\varepsilon \to 0$ in (184) and (185). Therefore, the slow subsystem can be obtained as,

$$M_{js}\ddot{q} + C_{js}\dot{q} + G_{js} = \tau_{js} \tag{186}$$

where,

$$M_{js} = (M_r + J^T F_{rd}^{\dagger} M_{rd} R_1^{\dagger} J)$$

$$C_{js} = C_r + J^T F_{rd}^{\dagger} M_{rd} (\dot{R_1^{\dagger}} J + R_1^{\dagger} \dot{J})$$

$$G_{js} = G_r + J^T F_{rd}^{\dagger} G_{rd}$$

and the transverse vibration of beam equation becomes,

$$[A_{jf} R_1^{\dagger} J\ddot{q} + A_{jf} (\dot{R_1^{\dagger}} J + R_1^{\dagger} \dot{J})\dot{q} + a w^{iv}]_s = F_{ff}(f_{js}) \tag{187}$$

Since the manipulators are considered to be rigid, the matrices related to the beam dynamics such as M_{rf}, G_{rf}, F_{rf} and R become M_{rd}, G_{rd}, F_{rd} and R_1 which are given in Chapter 3. The following properties describe the characteristics of slow subsystem in joint space which are useful for stability analysis:

Property 1 in Joint Space(JS): M_{js} is a symmetric positive definite matrix.

Property 2 in JS: The matrix M_{js} and C_{js} in (186) must satisfy

$$X^T(\dot{M}_{js} - 2C_{js})X = 0, \quad \forall X \neq 0 \tag{188}$$

where X is any arbitrary vector. That is $(\dot{M}_{js} - 2C_{js})$ is a skew-symmetric matrix.

Property 3 in JS: There exists a vector $\alpha_{js} \in \mathbf{R}^{v_2 \times 1}$ which solely depends on manipulator and beam dynamic parameters (lengths, masses and moment of inertias etc.) such that

$$M_{js}\ddot{q} + C_{js}\dot{q} + G_{js} = Y_{js}(\ddot{q}, \dot{q}, q)\alpha_{js} \tag{189}$$

where $Y_{js} \in \mathbf{R}^{u_2 \times v_2}$ is called regressor of the slow subsystem represented in joint space which is given in Appendix C.

Property 4 in JS: Since the matrices M_{js}, C_{js} and G_{js} in (186) are the functions of sine and cosine of manipulator joint angles and velocities, they are bounded. Then, there exist arbitrary positive constants ρ_{ii} (i=1,2,3), the boundedness of each matrices can be described as follows:

$$\| M_{js} \| \leq \rho_{11}$$

$$\| C_{js} \| \leq \rho_{22} \| \dot{q} \|$$

$$\| G_{js} \| \leq \rho_{33}$$

6.3.2 Fast subsystem in joint space

In order to obtain the fast subsystem in the different time scale $v = \frac{t-t_0}{\varepsilon}$, the fast variable $w_f = w - w_s$ is introduced into the flexible system (185). Following similar arguments as mentioned in Chapter 3 for the development of fast subsystem, (185) becomes,

$$A_{jf}\tilde{R}^{\dagger}J\ddot{q} + A_{jf}(\dot{\tilde{R}}^{\dagger}J + \tilde{R}^{\dagger}\dot{J})\dot{q} + \hat{w}_f + \varepsilon^2\ddot{w}_s - \varepsilon^2(w_s + w_f)\dot{\theta}^2 + a(w_s^{iv} + w_f^{iv}) = F_{ff}(f) \tag{190}$$

In the boundary layer system, the slow variable w_s is constant which implies $\ddot{w}_s = 0$ and also $\varepsilon = 0$. Then, the above equation yields into,

$$A_{jf}R_1^{\dagger}J\ddot{q} + A_{jf}(\dot{R}_1^{\dagger}J + R_1^{\dagger}\dot{J})\dot{q} + a(w_s^{iv} + w_f^{iv}) = F_{ff}(f) \tag{191}$$

Using (187) and also defining $F_{ff}(f_{jf}) = F_{ff}(f) - F_{ff}(f_{js})$, (191) becomes,

$$\hat{\hat{w}}_f + a{w_f}^{iv} = F_{ff}(f_{jf}) \tag{192}$$

After incorporating the operator A as mentioned in Chapter 3, the above partial differential equation (192) becomes,

$$\hat{\hat{w}}_f(v) + Aw_f(v) = F_{ff}(f_{jf}) \tag{193}$$

$$w_f(0) = w_{f0}, \quad \dot{w}_f(0) = w_{f1}$$

The above equation represents the fast subsystem which is similar to the one developed (82) in Chapter 3.

6.4 Composite control for the manipulators - flexible object system in joint space

In the previous section, singular perturbation analysis yielded the slow and fast subsystem in joint space. These two subsystems have to be controlled together to achieve the desired trajectory while suppressing the vibrations of the beam. Hence, a composite control law in the following form is conidered:

$$u = u_{ss}(\dot{q}, q, t) + u_{sf}(\hat{w_f}, v)$$

where u_{ss} is designed based on slow subsystem (186) and u_f signal is designed for the fast subsystem (193).

6.4.1 Robust control for slow subsystem in joint space

In order to handle non linear coupled dynamics and uncertain manipulators and beam parameters, a robust control scheme presented for the slow subsystem in Chapter 4 is considered here also. It is reformulated according to the dynamic model given in (186).

Define the tracking error as,

$$e_{rr} = q - q_d \tag{194}$$

and the auxiliary trajectory can also be defined as,

$$\dot{q}_r = \dot{q}_d - \lambda_{js} e_{rr} \tag{195}$$

where λ_{js} is a positive definite matrix whose eigenvalues are strictly in the right half of complex plane.

The sliding surface can be chosen as,

$$S_{js} = \dot{q} - \dot{q}_r = \dot{e}_{rr} + \lambda_{js} e_{rr} \tag{196}$$

The sliding mode controller can be given as,

$$u_{ss} = \tau_{js} = Y_{js}\psi_{js} - K_{D1} S_{js} \tag{197}$$

where K_{D1} is a positive definite gain matrix, $Y_{js}(\ddot{q}_r, \dot{q}_r, q)$ is regressor matrix and $\psi_{js} = [\psi_1 .... \psi_m]^T$ are the switching functions which are given by,

$$\psi_{js} = -\beta_{js} \frac{Y_{js}^T S_{js}}{\| Y_{js}^T S_{js} \|} \tag{198}$$

where $\beta_{js} \geq \| \alpha_{js} \|$ is upperbound of α_{js} which is known though it could be conservatively selected.

6.4.1.1 Stability analysis

The exponential stability of the closed loop system described by (186) and (197) is achieved as shown in the following analysis.

Differentiating the sliding surface (196) with respect to time gives,

$$\dot{S}_{js} = \ddot{q}_d - \ddot{q}_r \tag{199}$$

Mutiplying both sides of (199) by M_{js} and using (186), (199) can be rewritten as,

$$M_{js}\dot{S}_{js} = \tau_{js} - C_{js}\dot{q} - G_{js} - M_{js}\ddot{q}_r \tag{200}$$

Adding and subtracting $C_{js}\dot{q}_r$ in (200)

$$M_{js}\dot{S}_{js} = \tau_{js} - (M_{js}\ddot{q}_r + C_{js}\dot{q}_r + G_{js}) + C_{js}\dot{q}_r - C_{js}\dot{q} \tag{201}$$

By using (196), (201) can be rewritten as,

$$M_{js}\dot{S}_{js} = \tau_{js} - Y_{js}(\ddot{q}_r, \dot{q}_r, q) - C_{js}S_{js} \tag{202}$$

where,

$$(M_{js}\ddot{q}_r + C_{js}\dot{q}_r + G_{js}) = Y_{js}(\ddot{q}_r, \dot{q}_r, q)\alpha_{js}$$

Consider a Lyapunov function candidate as,

$$V_6(t, S_{js}) = \frac{1}{2}S_{js}^T M_{js} S_{js} \tag{203}$$

Differentiating (203) with respect to time gives,

$$\dot{V}_6(t, S_{js}) = S_{js}^T M_{js}\dot{S}_{js} + \frac{1}{2}S_{js}^T \dot{M}_{js} S_{js} \tag{204}$$

Substituting (202) into (204) and also using property 2 in JS given in (188), above equation yields,

$$\dot{V}_6(t,S_{js}) = S_{js}^T[\tau - Y_{js}(\ddot{q}_r,\dot{q}_r,q)\alpha_{js}] \tag{205}$$

Substituting the control law given in (197) and (198) into (205) one can have,

$$\leq -S_{js}^T K_{D1} S_{js} - \beta_{js}\|Y_{js}^T\, S_{js}\| + \|S_{js}^T Y_{js}\|\|\alpha_{js}\| \tag{206}$$

Taking transpose of $\|S_{js}^T Y_{js}\|$ and also $\beta_{js} \geq \|\alpha_{js}\|$ results in,

$$\dot{V}_6(t,S_{js}) \leq -S_{js}^T K_{D1} S_{js} \tag{207}$$

It is known that [89] $K_{D1} = M_{js}\kappa_1$ where κ_1 can be considered as a least eigenvalue. Using (203), (207) can be rewritten as,

$$\frac{dV_6(t,S_{js})}{dt} \leq -2\kappa_1 V_6(t,S_{js}) \tag{208}$$

The solution of the above equation is,

$$V_6(t,S_{js}) \leq V_6(0,S_{js}(0))e^{-2\kappa_1 t} \tag{209}$$

It is evident from the above equation that the sliding surface will converge exponentially to zero. Thus the sliding surface is related to the tracking error e_{rr} in (196) which also converges exponentially to zero.

6.4.2 Feedback control for fast subsystem in joint space

Since the fast subsystem is similar in structure both in joint space as well as Cartesian space, the proposed control algorithm for the fast subsystem in Chapter 4 as a part of the

composite control law is still valid here. It can be given by,

$$u_{sf} = (f_{jf}) = -F_{ff}^{\dagger}\Pi\hat{w}_f(v) \tag{210}$$

Then similar arguments on the various operators such as A, Π and Q and also damping relations $QA\hat{w}_f(v)$ and $Q = A^{\beta}$ are also valid. In addition, the exponential stability of fast subsystem presented in Chapter 4 also holds good and hence they are not discussed.

It must be noted that, Tikhnov's theorem is still satisfied due to the exponential convergence of slow and fast subsystem in joint space. Therefore, the singular perturbation analysis is validated to the joint space system as well.

6.4.3 Simulation results

The objective of this composite controller is to move the object from the initial position of center of mass and orientation [103] (0.51m; 0.36m; 90°) to the final position and orientation (0.55 m; 0.36 m; 90°) using two planar manipulators each with three links, while suppressing the vibrations. The object motion corresponds to move each revolute joint of first manipulator from (0°; -45°; -45°) to (-10.35°; -21.5°; -58.2°) and correspondingly the second manipulator from the initial angular position (0°; 45°; 45°) to final position (10.35°; 21.5°; 58.2°). The control parameters are tuned and they are given in Table 7.

Table 5: Parameters of the manipulator

Link	Length (m)	Mass (kg)	Moment of inertia (kgm^2)
1	0.3	1.0	0.30
2	0.3	1.0	0.30
3	0.05	0.4	0.15

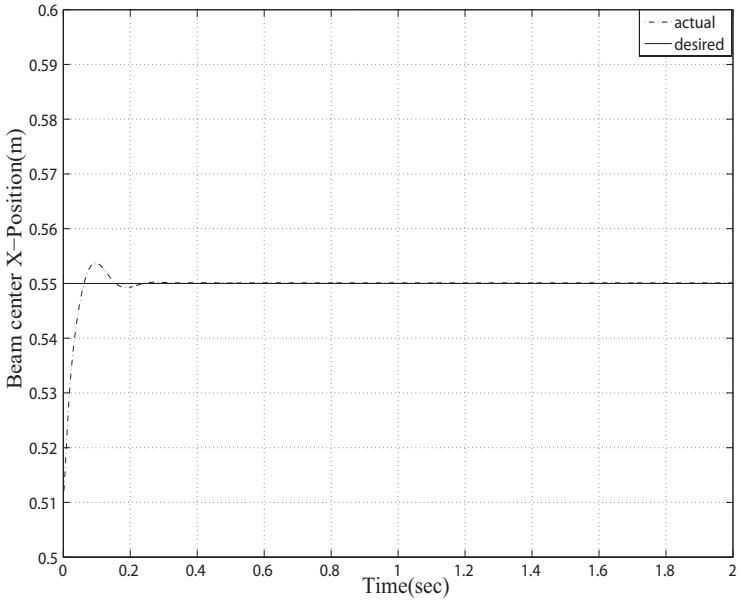

Figure 53: X movement-Sliding control in JS

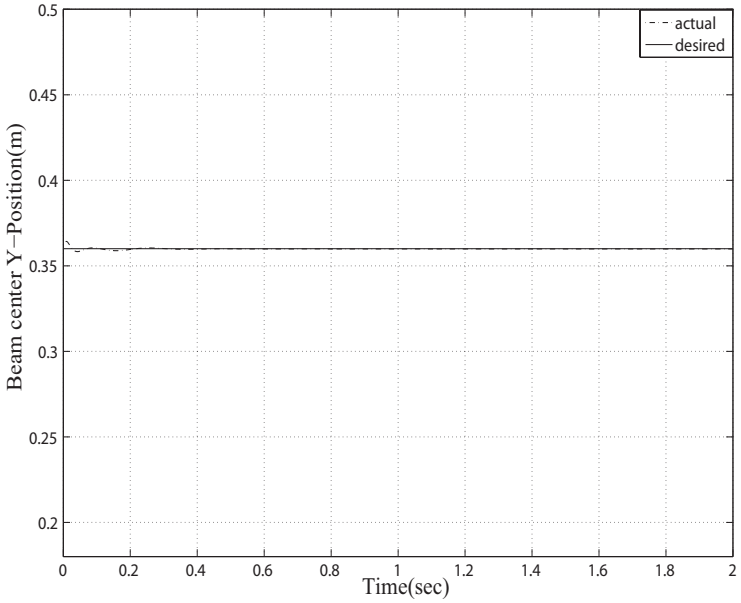

Figure 54: Y movement-Sliding control in JS

Table 6: Parameters of the beam

Parameter	Value
Mass (m)	1.0 kg
Length (L)	0.1 m
Moment of Inertia (I)	0.2 kgm^2

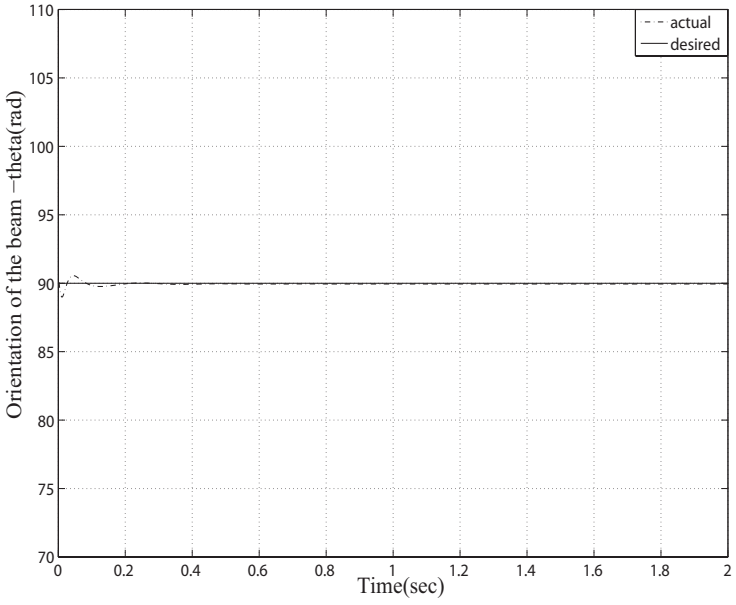

Figure 55: Orientation-Sliding control in JS

It is shown in Fig. 53 that, beam approaches towards its final position along X direction within 0.5 secs. The translation along Y direction and orientation of the beam are also maintained towards their desired values which are shown in Figs. 54 and 55. Due to the highly nonlinear manipulator parameters, a small deviation to the final value occurs initially in Figs. 54 and 55 and after 0.2 secs the beam center has reached its final pose.

Due to the sliding condition given in (198), the control law (197) is discontinuous across the sliding surface and this causes the chattering phenomenon. Chattering is the undesirable phenomenon of oscillations which has finite frequency and amplitude. In the

Table 7: Control parameters-sliding control in JS

Parameter	Value
K_{D1}	diag(20)
λ_{js}	diag(50)
β_{js}	3

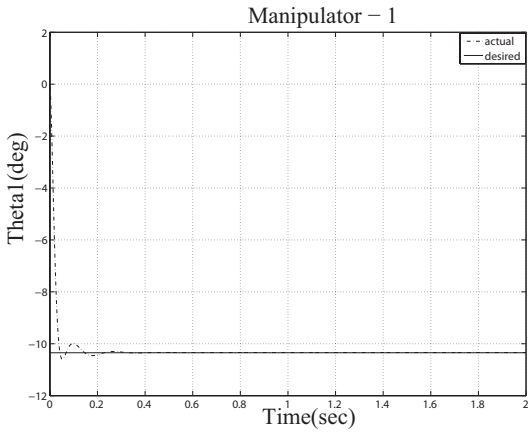

Figure 56: J1M1-Sliding control in JS

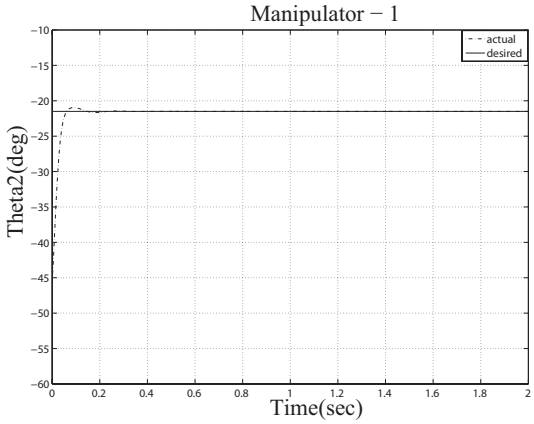

Figure 57: J2M1-Sliding control in JS

case of ideal sliding, infinite switching of frequencies takes place. The chattering leads to high control activity that corresponds to low control accuracy, high wear of moving mechanical parts and also high heat losses in electrical power circuits [104]. It may excite unmodeled high frequency dynamics which are not considered during initial modeling of the systems. This phenomenon is observed in the sliding variables (SV) which are shown in the Figs. 62 - 67 and also in the input control torques (CT) shown in the Figs. 68 - 73.

In order to overcome the chattering, the discontinuous control law can be replaced with continuous one inside the boundary layer [77] and [105]. This can be done by adding a boundary layer thickness ϕ in the switching function which is given by,

$$\psi_{js} = -\beta_{js} \frac{Y_{js}^T S_{js}}{\|Y_{js}^T S_{js}\| + \phi} \tag{211}$$

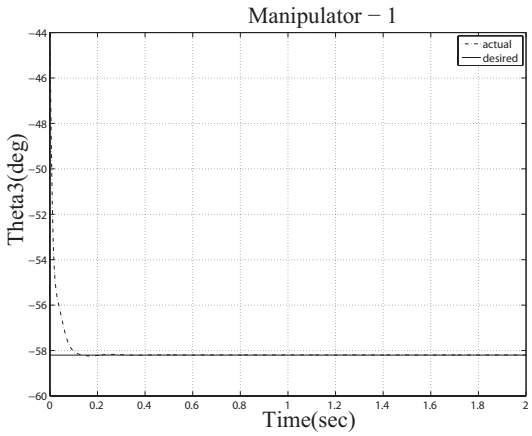

Figure 58: J3M1-Sliding control in JS

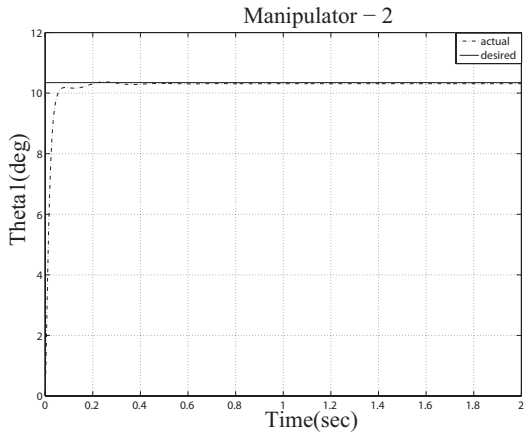

Figure 59: J1M2-Sliding control in JS

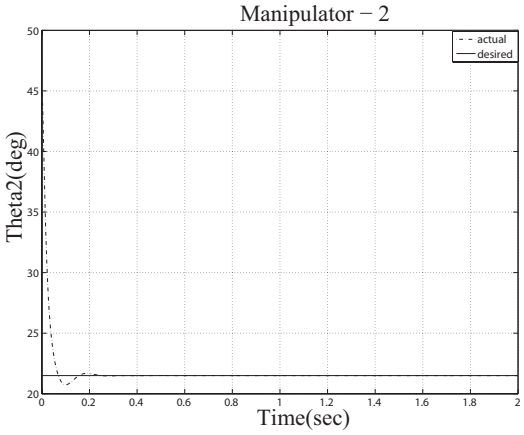

Figure 60: J2M2-Sliding control in JS

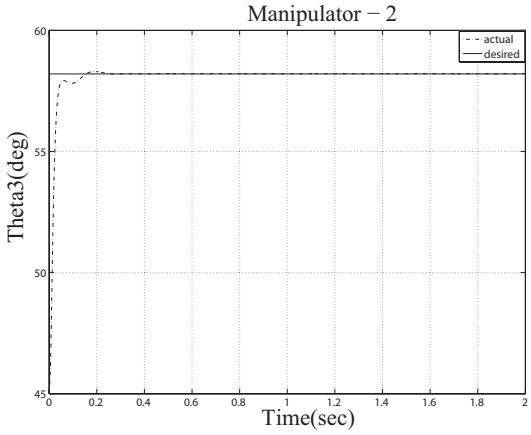

Figure 61: J3M2-Sliding control in JS

It can be seen from the Figs. 74 - 85 that, the chattering is completely reduced by adding the boundary layer thickness $\phi = 0.75$. This will lead us to avoid the problems mentioned earlier due to chattering and also ensure the stability of the system. Since the fast subsystem is analogous in both Cartesian and joint space, simulation results presented in Chapter 4 for the fast subsystem are still valid here and hence they are not presented in this section.

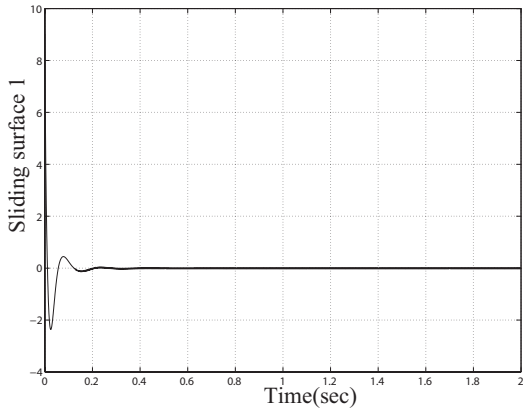

Figure 62: SV 1 with chattering in JS

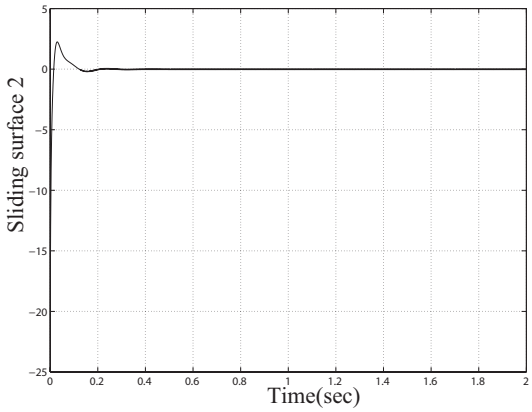

Figure 63: SV 2 with chattering in JS

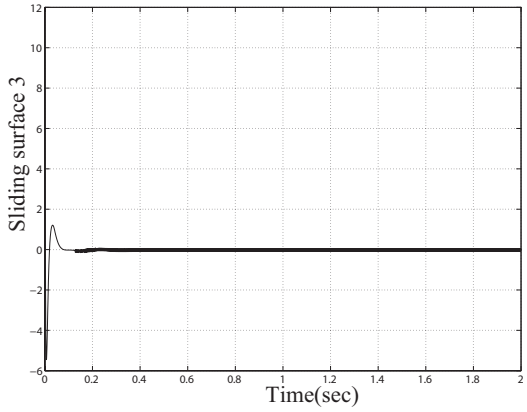

Figure 64: SV 3 with chattering in JS

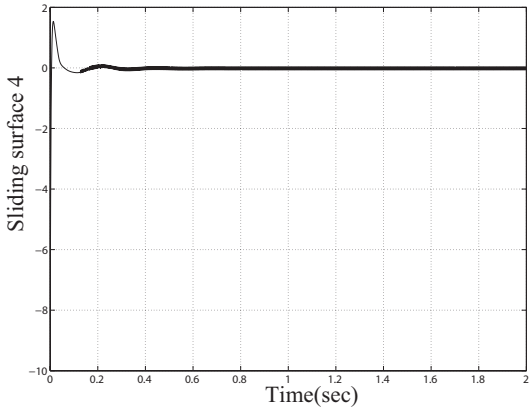

Figure 65: SV 4 with chattering in JS

6.5 Further improvements on the controller design of slow subsystem in joint space

In order to improve the controller design for the joint space slow subsystem, control algorithms presented in Chapter 5 such as an adaptive controller without velocity measurements and non-regressor based adaptive-robust controller can be reformulated and implemented

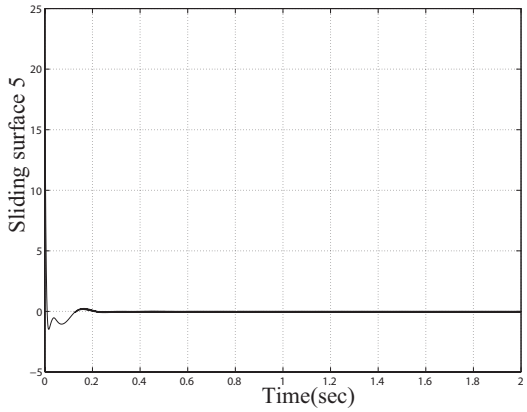

Figure 66: SV 5 with chattering in JS

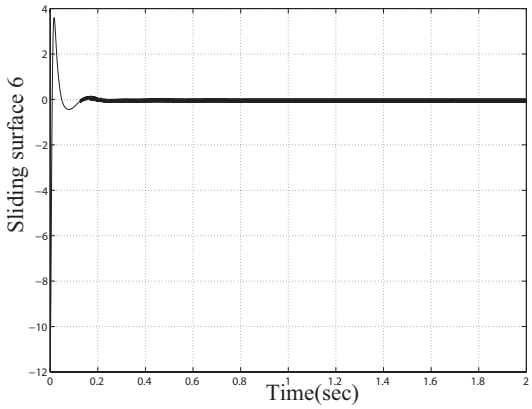

Figure 67: SV 6 with chattering in JS

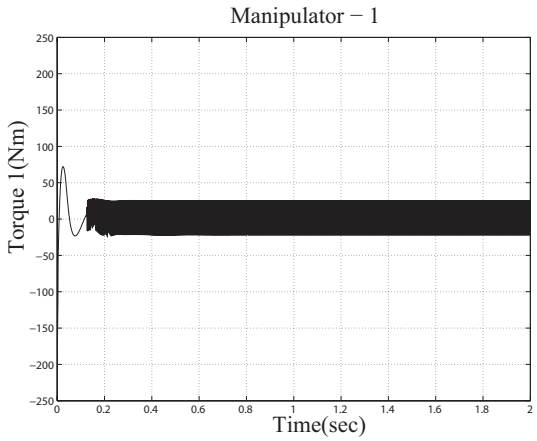

Figure 68: CT of J1M1 with chattering in JS

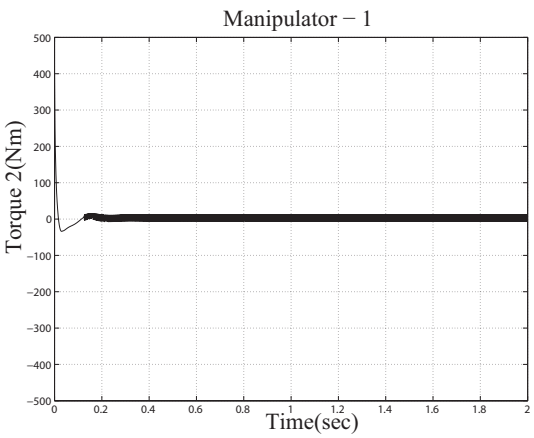

Figure 69: CT of J2M1 with chattering in JS

to the developed slow subsystem (186) in joint space. It should be noted that, the composite control law will be obtained by combining one of the above mentioned slow subsystem control law in joint space and fast subsystem controller given in (104). This composite control signal will be used to track the desired trajectory while simultaneously suppressing the vibration. Since the fast subsystem control is considered to be same in both Cartesian and joint space, in the following sections, the control algorithms presented for the Cartesian space slow subsystem will be modified according to the joint space slow subsystem (186) and corresponding stability analysis and simulations will be carried out.

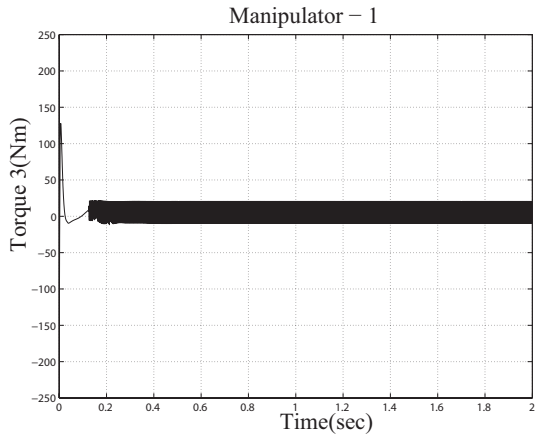

Figure 70: CT of J3M1 with chattering in JS

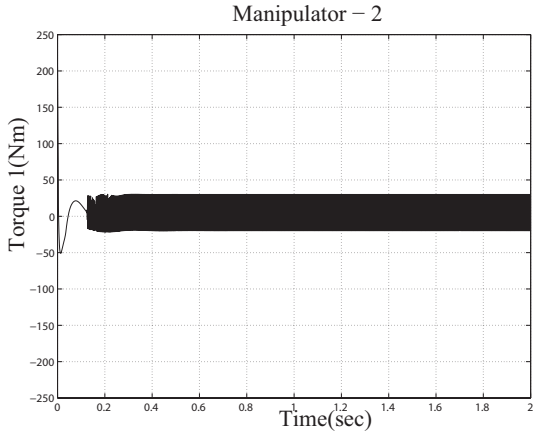

Figure 71: CT of J1M2 with chattering in JS

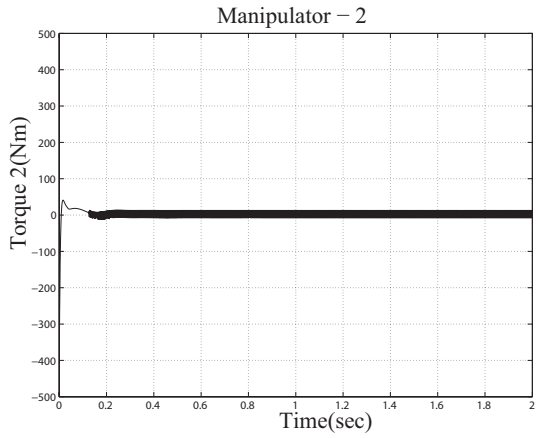

Figure 72: CT of J2M2 with chattering in JS

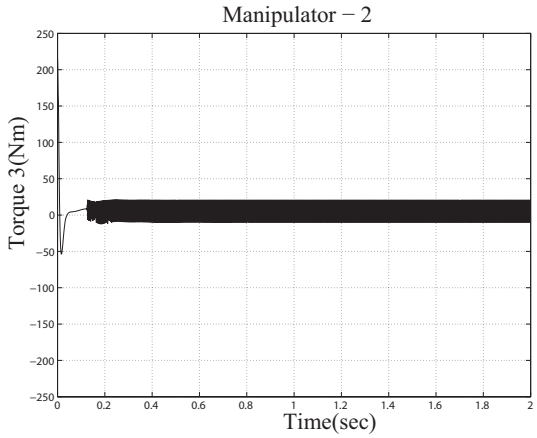

Figure 73: CT of J3M2 with chattering in JS

6.5.1 Controller design without velocity measurements in joint space

Measurement of joint speeds by tachometers may contain undesirable noise and tachometers may not perform at low speeds due to magnetic field discontinuities [106]. In order to avoid such problems, a controller without velocity feedback is necessary. Hence, an adaptive controller without velocity feedback presented in Chapter 5 is formulated again for the case of joint space slow subsystem.

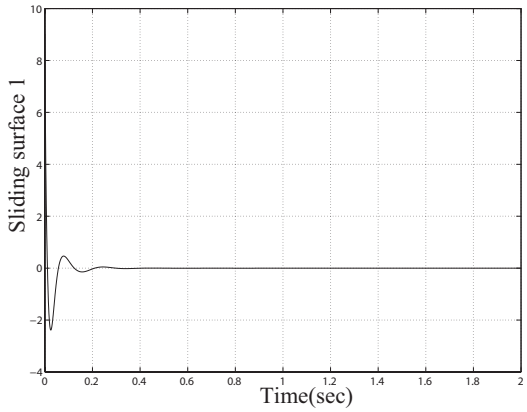

Figure 74: SV 1 without chattering in JS

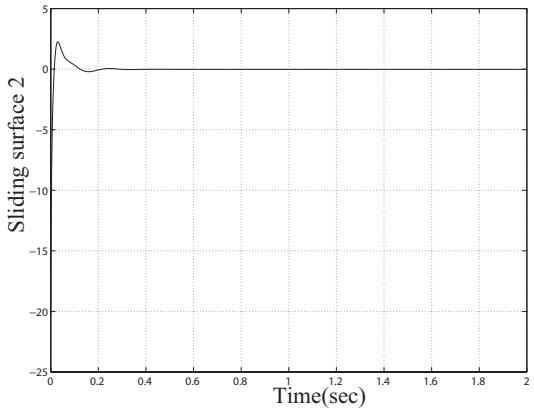

Figure 75: SV 2 without chattering in JS

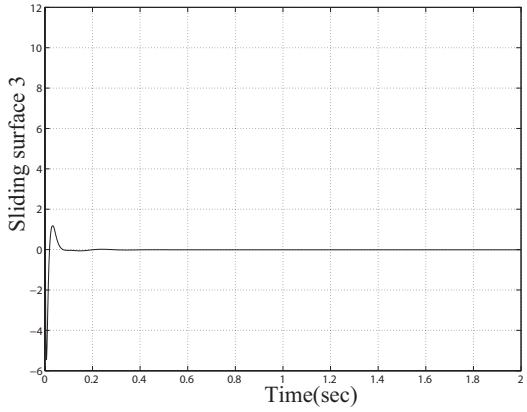

Figure 76: SV 3 without chattering in JS

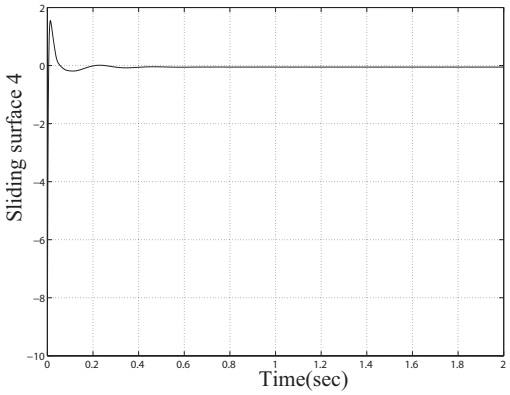

Figure 77: SV 4 without chattering in JS

By using desired velocity and acceleration trajectory of the object, the slow subsystem given in (186) can be expressed based on the parameterizations technique [76] which is given by,

$$M_{js}\ddot{q} + C_{js}\dot{q} + G_{js} = Y_b(q, \dot{q}_d, \ddot{q}_d)\alpha_{js} \tag{212}$$

where $Y_b(q, \dot{q}_d, \ddot{q}_d)$ is the regressor matrix which is dependent of desired set point parameters of the manipulators and also independent of dynamic parameters. α_{js} is the constant vector of manipulator and beam inertia parameters.

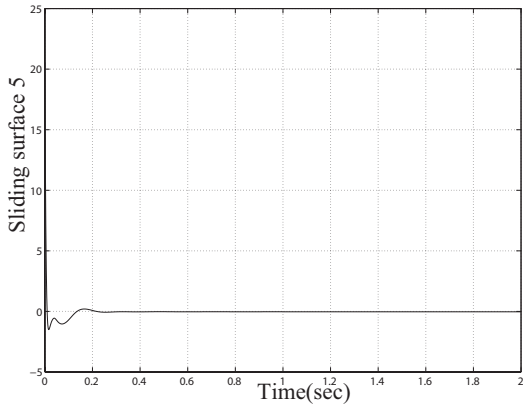

Figure 78: SV 5 without chattering in JS

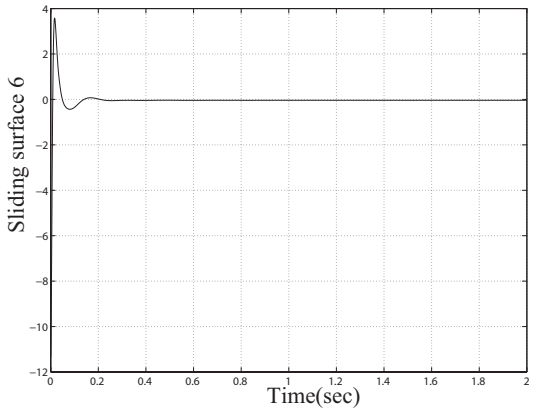

Figure 79: SV 6 without chattering in JS

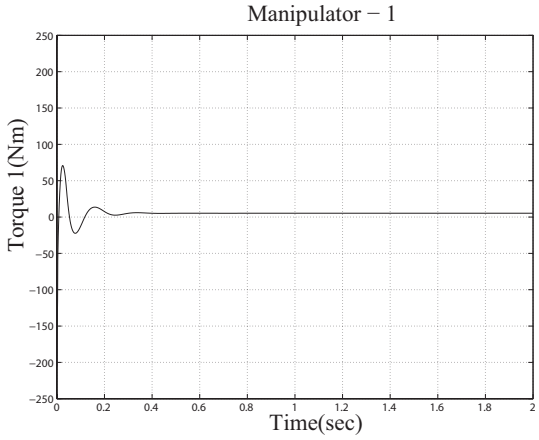

Figure 80: CT of J1M1 without chattering in JS

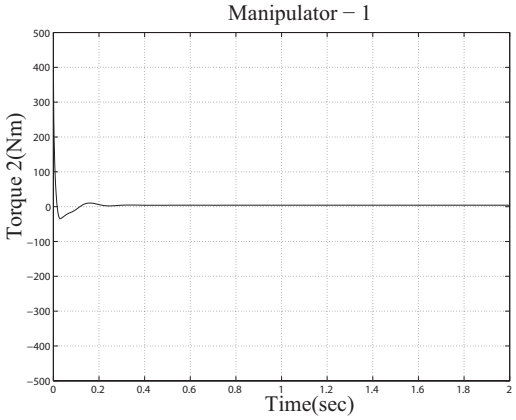

Figure 81: CT of J2M1 without chattering in JS

The control law can be formulated as,

$$\tau_{js} = u_{ss} = Y_b(q, \dot{q}_d, \ddot{q}_d)\check{\alpha}_{js} - \Omega_1^2 \Upsilon_1(\omega_1 + \rho_1 e_{rr}) \tag{213}$$

and the intermediate vectors ω_1 and $\bar{\omega}_1$ can be calculated by,

$$\omega_1 = \bar{\omega}_1 + \Omega_1^2 e_{rr} \tag{214}$$

$$\dot{\bar{\omega}}_1 = -2\Omega_1 \bar{\omega}_1 - 2\Omega_1^3 e_{rr} \tag{215}$$

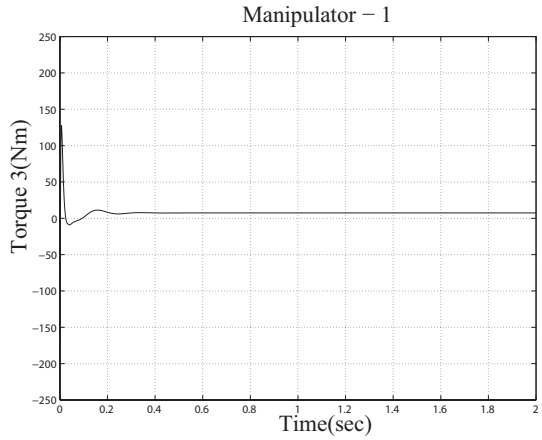

Figure 82: CT of J3M1 without chattering in JS

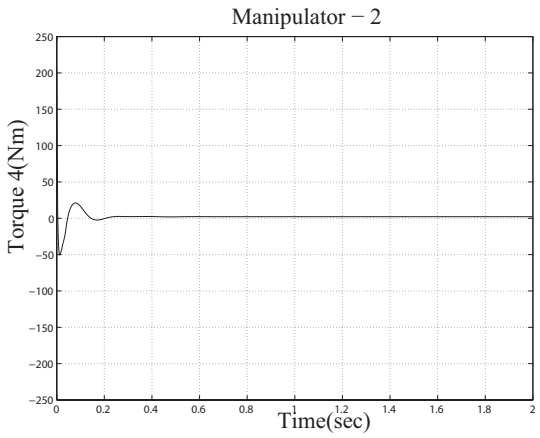

Figure 83: CT of J1M2 without chattering in JS

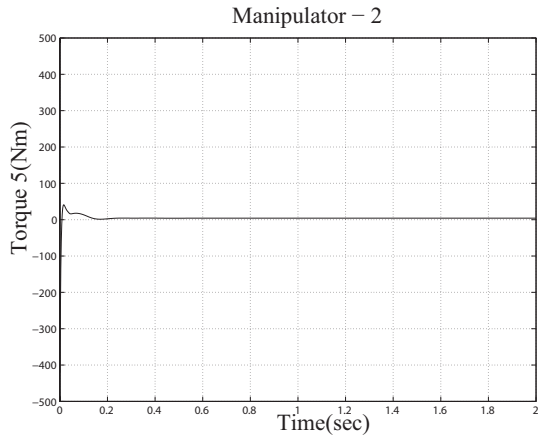

Figure 84: CT of J2M2 without chattering in JS

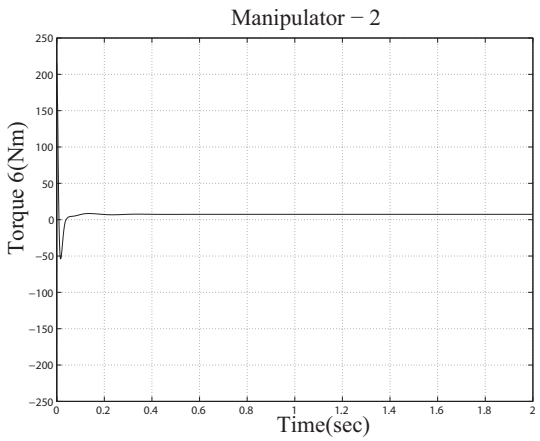

Figure 85: CT of J3M2 without chattering in JS

Also, the adaptive law is given by,

$$\dot{\breve{\alpha}}_{js} = \dot{\tilde{\alpha}}_{js} = -\zeta_1 Y_b^T z_1 \tag{216}$$

and z_1 can be given as,

$$z_1 \;=\; \dot{e}_{rr} - \frac{\omega_1}{\Omega_1} + \frac{\rho_1}{\Omega_1} e_{rr} \tag{217}$$

where $e_{rr} = q - q_d$ is the tracking error; $\breve{\alpha}_{js}$ is the estimate of α_{js}. Then, the parameter error vector can be defined as $\tilde{\alpha}_{js} = \breve{\alpha}_{js} - \alpha_{js}$; Υ_1 is constant positive definite matrix; Ω_1,

ρ_1 and ζ_1 are positive constants. It should be noted here that the control law given in (213) and also the adaptive parameter $\breve{\alpha}_{js}$ can be found using adaptive law given in (216) and does not involve any velocity signal as feedback. Thus, it avoids the velocity sensors and the controller needs only position measurements.

Substituting (213) into (186) gives,

$$\ddot{e}_{rr} = M_{js}^{-1}(-\Omega_1^2\Upsilon_1\omega_1 - \rho_1\Omega_1^2\Upsilon_1 e_{rr} - C_{js}\dot{e}_{rr} + Y_b\tilde{\alpha}_{js} - C_e\dot{e}_{rr}) \tag{218}$$

where $C_e\dot{e}_{rr} = C_{js}(q,\dot{q})\dot{q}_d - C_{js}(q,\dot{q}_d)\dot{q}_d$.

With the introduction of state vector $x_1^T = [\dot{e}_{rr}^T, \omega_1^T, {e_{rr}}^T]$, using (214), (215) and (218), the state space form of closed-loop equation is given by,

$$\dot{x}_1 = -A_1x_1 + C_1(-C_{js}\dot{e}_{rr} - C_e\dot{e}_{rr} + Y_b\tilde{\alpha}_{js}) \tag{219}$$

where the matrix A_1 and C_1 are,

$$A_1 = \begin{bmatrix} 0 & \Omega_1^2 M_{js}^{-1}\Upsilon_1 & \rho_1\Omega_1^2 M_{js}^{-1}\Upsilon_1 \\ -\Omega_1^2 \mathrm{I_d} & 2\Omega_1 \mathrm{I_d} & 0 \\ -\mathrm{I_d} & 0 & 0 \end{bmatrix}; C_1 = \begin{bmatrix} M_{js}^{-1} \\ 0 \\ 0 \end{bmatrix}$$

By arbitrarily selecting the matrices P_1 and Q_1, one can show that $1/2(P_1A_1 + A_1^TP_1) = Q_1$. One of the possible choice for the symmetric positive definite matrices P_1 and Q_1 are given by [95],

$$P_1 = \begin{bmatrix} M_{js} & -\frac{1}{\Omega_1}M_{js} & \frac{\rho_1}{\Omega_1}M_{js} \\ -\frac{1}{\Omega_1}M_{js} & \Upsilon_1 & 0 \\ \frac{\rho_1}{\Omega_1}M_{js} & 0 & \rho_1\Omega_1^2\Upsilon_1 \end{bmatrix}; Q_1 = \begin{bmatrix} (\Omega_1 - \frac{\rho_1}{\Omega_1})M_{js} & -M_{js} & 0 \\ -M_{js} & \Omega_1\Upsilon_1 & 0 \\ 0 & 0 & \rho_1^2\Omega_1\Upsilon_1 \end{bmatrix}$$

Also, the eigenvalues of P_1 and Q_1 and satisfies the following bounds,

$$\lambda_{p1} \parallel x_1 \parallel^2 \leq x_1^TP_1x_1 \qquad and \qquad \Omega_1\lambda_{q1} \parallel x_1 \parallel^2 \leq x_1^TQ_1x_1 \tag{220}$$

6.5.1.1 Stability analysis

The stability of the closed loop system described by (219) and (216) is obtained from the following theorem.

Theorem: If the input control torque given by (213) are applied to the system (186), then all the closed loop signals are bounded and $lim_{t\to\infty}\ x_1 = 0$, provided the following condition satisfied,

$$\Omega_1\lambda_{q1} > 3 \parallel C_e \parallel +2\vartheta_1[sup \parallel \dot{q}_d \parallel +\sqrt{\frac{2V_6(t)}{\lambda_{p1}}}] \tag{221}$$

where λ_{p1} and λ_{q1} are the positive eigenvalues of P_1 and Q_1 and $V_7(t)$ is a function defined in (222).

Proof:

Consider a Lyapunov function candidate

$$V_7(t) = \frac{1}{2}x_1^T P_1 x_1 + \frac{1}{2\zeta_1}\tilde{\alpha}_{js}^T\tilde{\alpha}_{js} \tag{222}$$

Differentiating (222) gives,

$$\dot{V}_7(t) = x_1^T P_1\dot{x}_1 + \frac{1}{2}x_1^T\dot{P}_1 x_1 + \frac{1}{\zeta_1}\dot{\tilde{\alpha}}_{js}^T\tilde{\alpha}_{js} \tag{223}$$

Using (219), the above equation can be rewritten as,

$$\dot{V}_7(t) = -x_1^T Q_1 x_1 + x_1^T P_1 C_1(-C_{js}\dot{e}_{rr} - C_e\dot{e}_{rr} + Y_b\tilde{\alpha}_{js}) + \frac{1}{2}x_1^T\dot{P}_1 x_1 + \frac{1}{\zeta_1}\dot{\tilde{\alpha}}_{js}^T\tilde{\alpha}_{js} \tag{224}$$

when $\Omega_1 \geq max(1,\rho_1)$, one can have the following,

$$\begin{aligned} -x_1^T P_1 C_1 C_e\dot{e}_{rr} &= -(\dot{e}_{rr} - \frac{\omega_1}{\Omega_1} + \frac{\rho_1}{\Omega_1}e_{rr})^T C_e\dot{e}_{rr} \\ &\leq 3 \parallel C_e \parallel\parallel x_1 \parallel^2 \end{aligned} \tag{225}$$

$$\frac{1}{2}x_1^T\dot{P}_1x_1 - x_1^TP_1C_1C_{js}\dot{e}_{rr} = \frac{1}{2}\dot{e}_{rr}^T\dot{M}_{js}\dot{e}_{rr} + \dot{e}_{rr}\frac{\rho_1}{\Omega_1}\dot{M}_{js}{e_{rr}}^T - \dot{e}_{rr}\frac{1}{\Omega_1}\dot{M}_{js}\omega_1^T$$
$$-(\dot{e}_{rr} - \frac{\omega_1}{\Omega_1} + \frac{\rho_1}{\Omega_1}e_{rr})^TC_{js}\dot{e}_{rr} \qquad (226)$$

Using the property $\dot{e}_{rr}^T(1/2\dot{M}_{js} - C_{js})\dot{e}_{rr} = 0$, above equation can be rewritten as,

$$\begin{aligned}\frac{1}{2}x_1^T\dot{P}_1x_1 - x_1^TP_1C_1C_{js}\dot{e}_{rr} &= \frac{1}{\Omega_1}[\rho_1e_{rr} - \omega_1][\dot{M}_{js} - C_{js}]\dot{e}_{rr} \\ &\leq 2\vartheta_1 \parallel \dot{q} \parallel \parallel x_1 \parallel^2 \end{aligned} \qquad (227)$$

where $\vartheta_1 \parallel \dot{q} \parallel = \parallel \dot{M}_{js} - C_{js} \parallel$.

Substituting (220), (225) and (227) into (224) yields,

$$\begin{aligned}\dot{V}_7(t) &\leq -(\Omega_1\lambda_{q1} - 3 \parallel C_e \parallel -2\vartheta_1 \parallel \dot{q} \parallel) \parallel x_1 \parallel^2 + (z_1^TY_b + \frac{1}{\zeta_1}\dot{\tilde{\alpha}}_{js}^T)\tilde{\alpha}_{js} \\ &= -f(\parallel \dot{q} \parallel) \parallel x_1 \parallel^2 \end{aligned} \qquad (228)$$

where $f(\parallel \dot{q} \parallel) = \Omega_1\lambda_{q1} - 3 \parallel C_e \parallel -2\vartheta_1 \parallel \dot{q} \parallel$ and $x_1^TP_1C_1 = z_1^T$ and also (216) is used to obtain the above equation. The right hand side of (228) is negative if $f(\parallel \dot{q} \parallel) > 0$, which is true if (221) is satisfied.

When $\Omega_1\lambda_{q1}$ is sufficiently large, (221) is satisfied and also $V_7(t) < 0$. By induction with respect to t, $V_7(t)$ will be decreasing until $\parallel x_1 \parallel = 0$ which shows that the closed-loop system (219) is asymptotically stable and hence the given theorem is proved.

6.5.1.2 Simulation results

The simulation is carried out by considering the similar parameters of manipulators and beam given in Table 5 and 6. The beam is moved from the initial position of center of mass and orientation [103] (0.51m; 0.36m; 90°) to final position and orientation (0.55 m; 0.36 m; 90°) is considered for the simulation. Correspondingly, the first manipulator is moved

Table 8: Control parameters-without velocity measurements in JS

Parameter	Value
Ω_1	23
ρ_1	20
Υ_1	diag(0.027)
ζ_1	0.1

from (0°; -45°; -45°) to (-10.35°; -21.5°; -58.2°) and also the second manipulator is moved from the initial joint angles (0°; 45°; 45°) to final joint angles (10.35°; 21.5°; 58.2°). The initial values of $\check{\alpha}_{js}(0)$ = [0.96; 0.08; 0.003; 0.003; 0.51; 0.15; 1.46; 2.65; 0.098; 0.96; 0.08; 0.003; 0.003; 0.51; 0.15; 1.46; 2.65; 0.098; 1.5; 0.13]^T. The initial value of $\bar{\omega_1}(0)$ is chosen as zero. The control parameters are tuned and given in Table 8.

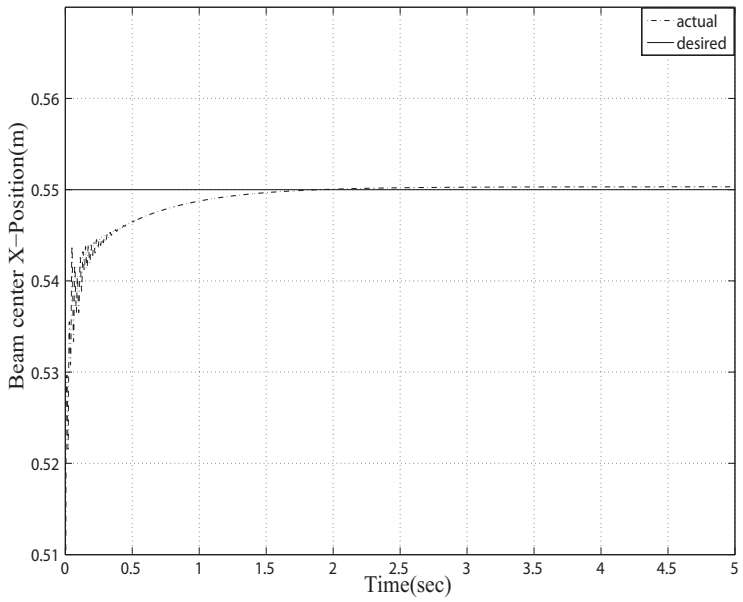

Figure 86: X movement-Without velocity measurement in JS

The motion of beam along X direction reaches its desired value around 2 sec with a small steady state error, that can be observed from the Fig. 86. In the Y direction, after

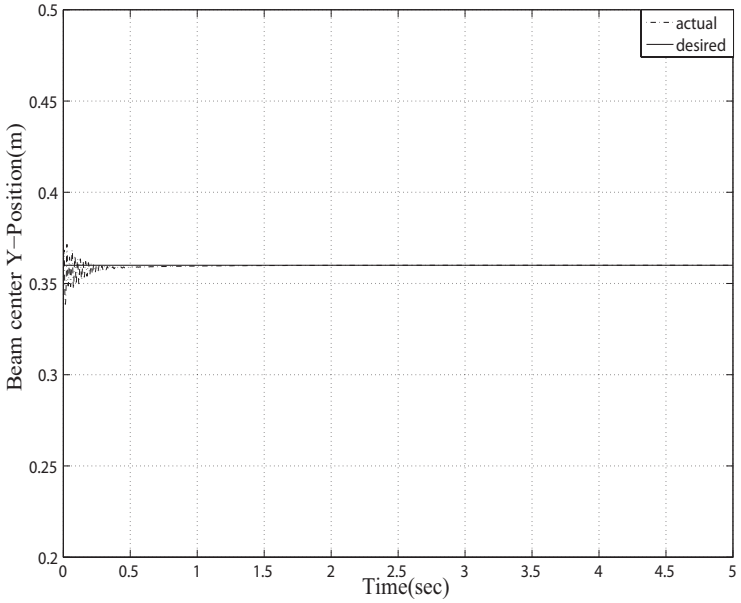

Figure 87: Y movement-Without velocity measurement in JS

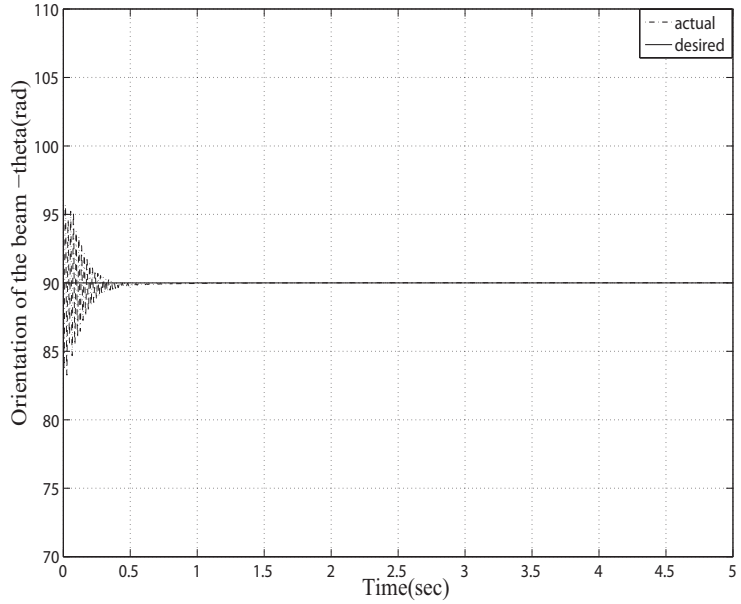

Figure 88: Orientation-Without velocity measurement in JS

small oscillation for about 0.5 sec, the beam approaches the desired value which is shown in Fig. 87. It is evident from the Fig. 88 that, the orientation of the beam has more oscillation initially and after 0.5 sec it maintains the final set value. Figs. 89 - 94 shows the angular positions of each joints of the manipulators. They have attained their desired value within 1 sec. However, compared with the Cartesian space results here in the joint space, all the joint angular motions have initial oscillations and reach their desired values after few seconds.

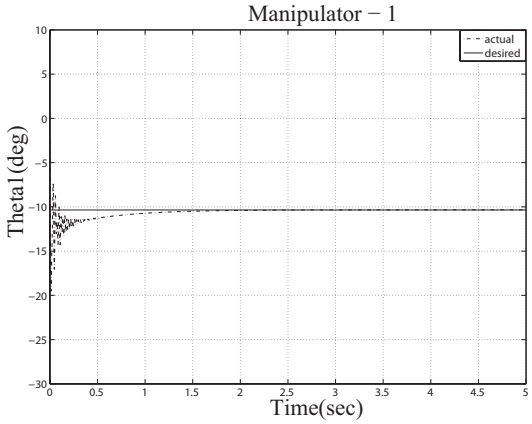

Figure 89: J1M1-Without velocity measurement in JS

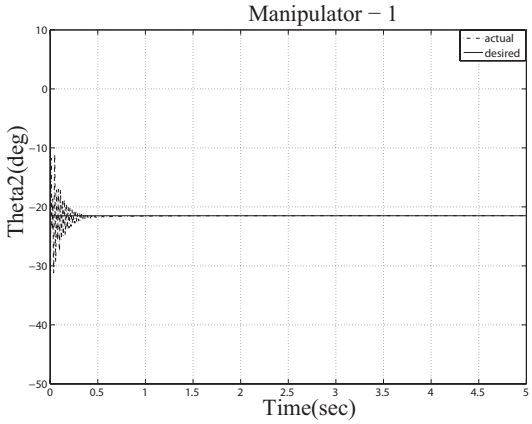

Figure 90: J2M1-Without velocity measurement in JS

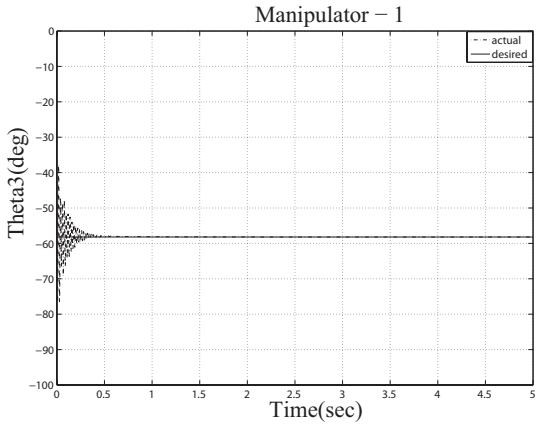

Figure 91: J3M1-Without velocity measurement in JS

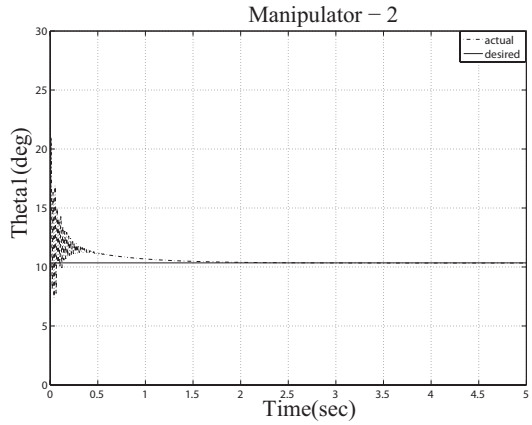

Figure 92: J1M2-Without velocity measurement in JS

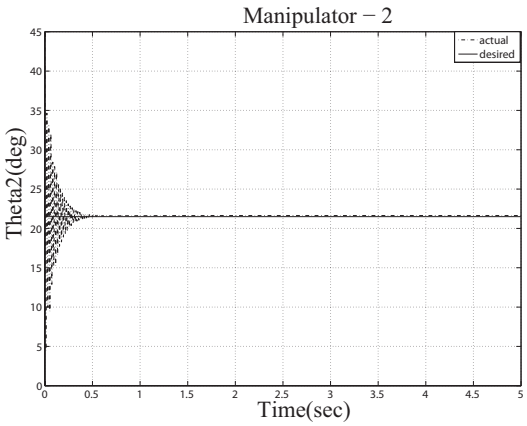

Figure 93: J2M2-Without velocity measurement in JS

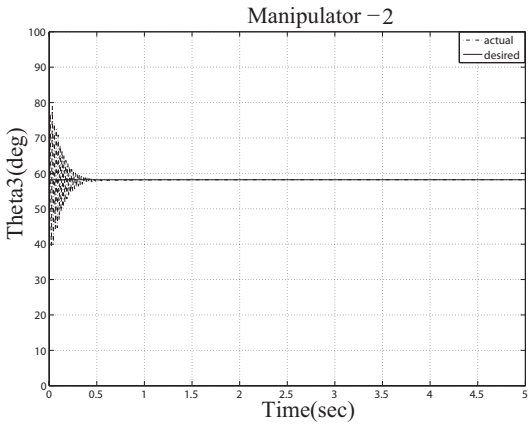

Figure 94: J3M2-Without velocity measurement in JS

6.5.2 Controller design without regressor in joint space

In order to control the motion of manipulators and the object in the joint space without involving complex regressor matrix calculations, a non-regressor based control algorithm presented in Chapter 5 is reformulated according to the slow subsystem in joint space (186). The robust adaptive control law is given by,

$$\tau_{js} = u_{ss} = -K_{dd}M_{js}S_{\phi 1} - (\check{\rho}_{11} \parallel \ddot{q}_r \parallel + \check{\rho}_{22} \parallel \dot{q} \parallel \parallel \ddot{q}_r \parallel + \check{\rho}_{33} + \check{\rho}_{44} \parallel \dot{q} \parallel) sat(\frac{S_{js}}{\phi}) \quad (229)$$

where K_{dd} is the positive definite matrix and $\check{\rho}_{ii}$, i=1,2,3,4, are the adaptive control gains, respectively.

$S_{\phi 1} = S_{js} - \phi\ sat(S_{js}/\phi)$ is the measure of the algebraic distance of the current state to the boundary layer, $\phi > 0$ is boundary layer thickness.

The adaptive parameters are given by,

$$\dot{\check{\rho}}_{11} = \beta_{11} \parallel S_{\phi 1} \parallel \parallel \ddot{q}_r \parallel \quad (230)$$

$$\dot{\check{\rho}}_{22} = \beta_{22} \parallel S_{\phi 1} \parallel \parallel \dot{q} \parallel \parallel \ddot{q}_r \parallel \quad (231)$$

$$\dot{\check{\rho}}_{33} = \beta_{33} \parallel S_{\phi 1} \parallel \tag{232}$$

$$\dot{\check{\rho}}_{44} = \beta_{44} \parallel S_{\phi 1} \parallel\parallel \dot{q} \parallel \tag{233}$$

where $\beta_{ii} > 0$ (i=1, 2, 3, 4) are the arbitrary constants which determines the rates of adaptation.

6.5.2.1 Stability analysis:

To carry out the stability analysis, the closed loop system (186) will be expressed in terms of the sliding variable S_{js}.

Mutiplying both sides of (199) by M_{js} and using (186), (199) can be rewritten as,

$$M_{js}\dot{S}_{js} = \tau_{js} - C_{js}\dot{q} - G_{js} - M_{js}\ddot{q}_r \tag{234}$$

Adding and subtracting $C_{js}\dot{q}_r$ in (234) gives,

$$M_{js}\dot{S}_{js} = \tau_{js} - M_{js}\ddot{q}_r - C_{js}S_{js} - G_{js} - C_{js}\dot{q}_r \tag{235}$$

Consider a Lyapunov function candidate,

$$V_8(t) = \frac{1}{2}S_{\phi 1}^T M_{js} S_{\phi 1} + \frac{1}{2}\Sigma\frac{(\rho_{ii} - \check{\rho}_{ii})^2}{\beta_{ii}} \tag{236}$$

Since $\dot{S}_{\phi 1} = \dot{S}_{js}$, differentiating (236) with respect to time gives ,

$$\dot{V}_8(t) = S_{\phi 1}^T M_{js}\dot{S}_{js} + \frac{1}{2}S_{\phi 1}^T \dot{M}_{js} S_{\phi 1} + \Sigma\frac{(\rho_{ii} - \check{\rho}_{ii})(-\dot{\check{\rho}}_{ii})}{\beta_{ii}} \tag{237}$$

Using (229) and (235), (237) becomes,

$$\begin{aligned}\dot{V}_8(t) = {} & S_{\phi 1}^T[-K_{dd}M_{js}S_{\phi 1} - (\check{\rho}_{11} \parallel \ddot{q}_r \parallel + \check{\rho}_{22} \parallel \dot{q} \parallel\parallel \ddot{q}_r \parallel + \check{\rho}_{33} + \check{\rho}_{44} \parallel \dot{q} \parallel)]sat(\frac{S_{js}}{\phi}) \\ & + S_{\phi 1}^T(-M_{js}\ddot{q}_r - C_{js}S_{js} - G_{js} - C_{js}\dot{q}_r) + \frac{1}{2}S_{\phi 1}^T\dot{M}_{js}S_{\phi 1} + \Sigma\frac{(\rho_{ii} - \check{\rho}_{ii})(-\dot{\check{\rho}}_{ii})}{\beta_{ii}}\end{aligned} \tag{238}$$

Since $\| S_{\phi 1} \| = S_{\phi 1}^T sat(S_{js}/\phi)$, using property 6 and after some manipulation, (238) results in,

$$\dot{V}_8(t) \leq -S_{\phi 1}^T K_{dd} M_{js} S_{\phi 1} - (\check{\rho}_{11} \| \ddot{q}_r \| + \check{\rho}_{22} \| \dot{q} \| \| \ddot{q}_r \| + \check{\rho}_{33} + \check{\rho}_{44} \| \dot{q} \|) \| S_{\phi 1} \|$$
$$+ (\rho_{11} \| \ddot{q}_r \| + \rho_{22} \| \dot{q} \| \| \ddot{q}_r \| + \rho_{33}) \| S_{\phi 1} \|$$
$$+ \frac{1}{2} S_{\phi 1}^T \dot{M}_{js} S_{\phi 1} + \Sigma \frac{(\rho_{ii} - \check{\rho}_{ii})(-\dot{\check{\rho}}_{ii})}{\beta_{ii}} - S_{\phi 1}^T C_{js} S_{\phi 1} + \phi \rho_{22} \| \dot{q} \| \| S_{\phi 1} \| \quad (239)$$

Since $S_{\phi 1}^T (\dot{M}_{js} - 2C_{js}) S_{\phi 1} = 0$ and defining $\rho_{44} = \phi \rho_{22}$ and also using the adaptive parameters (230-233), (239) yields into,

$$\dot{V}_8(t) = -S_{\phi 1}^T K_{dd} M_{js} S_{\phi 1} \quad (240)$$

Since $K_{dd} M_{js}$ is symmetric positive definite matrix then, there exists a constant γ such that $\gamma I_d \leq K_{dd} M_{js}$. Then (240) can be rewritten as,

$$\dot{V}_8(t) \leq -\gamma \| S_{\phi 1} \|_2^2 \leq 0 \quad (241)$$

In order to achieve the stability it is necessary to show that $S_{\phi 1} \rightarrow 0$ as $t \rightarrow \infty$. This can be achieved by applying Barbalat's lemma to the following continuous non-negative function,

$$\begin{aligned} \dot{V}_9(t) &= V_8(t) - \int_0^t (\dot{V}_8(\tau) + \gamma \| S_{\phi 1}(\tau) \|_2^2) d\tau \quad \text{with} \\ \dot{V}_9(t) &= -\gamma \| S_{\phi 1}(\tau) \|_2^2 \end{aligned} \quad (242)$$

Since S_{js} is bounded and correspondingly e_{rr} and $\dot{e}_{rr}$ are bounded. Thus, all the feedback signals q, $\dot{q}$ and $\dot{q}_r$ are bounded. Therefore, it can seen from (235) that, $\dot{S}_{js}$ is also bounded because M_{js} is already given as bounded property (property4 in JS) which proves $\dot{V}_9(t)$ to be uniformly continuous function of time. Since V_9 is bounded below by 0 and $\dot{V}_9(t) \leq 0$ for all t, use of Barbalat's lemma proves that $\dot{V}_9(t) \rightarrow 0$ and from (242) that $\| S_{\phi 1} \| \rightarrow 0$ as $t \rightarrow \infty$.

6.5.2.2 Simulation results

In order to validate the above presented controller, simulations are performed. Similar set of parameters for the manipulators and beam given in Table 5 and 6 are considered. The control parameters are chosen as K_{dd} = 500 and λ_{js} = 20. The adaptive gains are chosen as β_{11}=β_{22}=β_{33}=β_{44}=0.01. The initial adaptive parameters are taken as $\check{\rho}_{11}(0)$=$\check{\rho}_{22}(0)$=$\check{\rho}_{33}(0)$=$\check{\rho}_{44}(0)$=1. In order to reduce the chattering effect, the boundary layer thickness is chosen as ϕ=0.05. The position of the object along X direction is shown in Fig. 95 where it reaches desired value within 0.5secs. It can be seen from the Figs. 96 and 97 that the motion of object along Y direction and orientation about Z axis is maintained at its desired value. Each joint of the manipulators are reached towards its set point value within 0.5secs which are shown in Figs. 98 - 103. It can be concluded from these results that the, controller without regressor has achieved better control performance than the controller without velocity measurement in joint space.

The following conclusions are made by analyzing the slow subsystem in joint space as compared to the Cartesian space slow subsystem:

1. The regressor for joint space slow subsystem has less computation burden than that of the Cartesian space slow subsystem.

2. The regressor based sliding mode control law achieved good control performance in the regulation problem as well.

3. It can be observed from the simulation results of the controller without velocity measurement in the joint space that, there are some oscillations at the beginning to

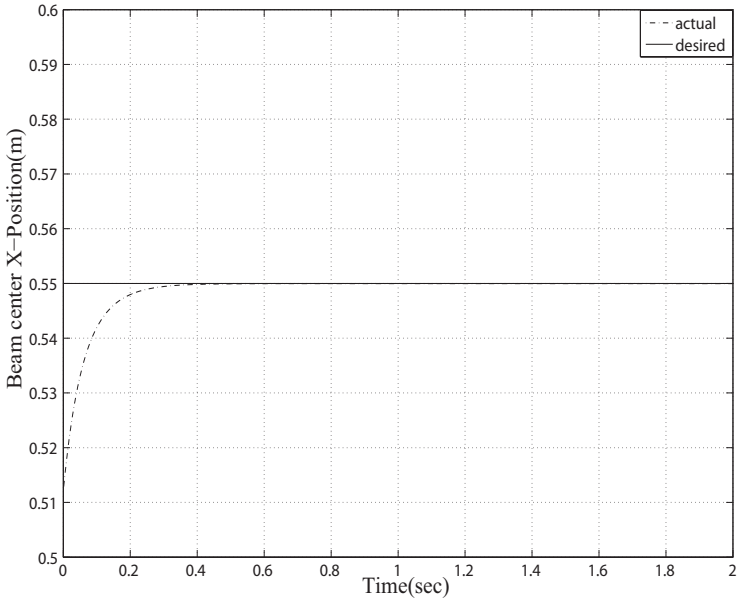

Figure 95: X movement-Without regressor in JS

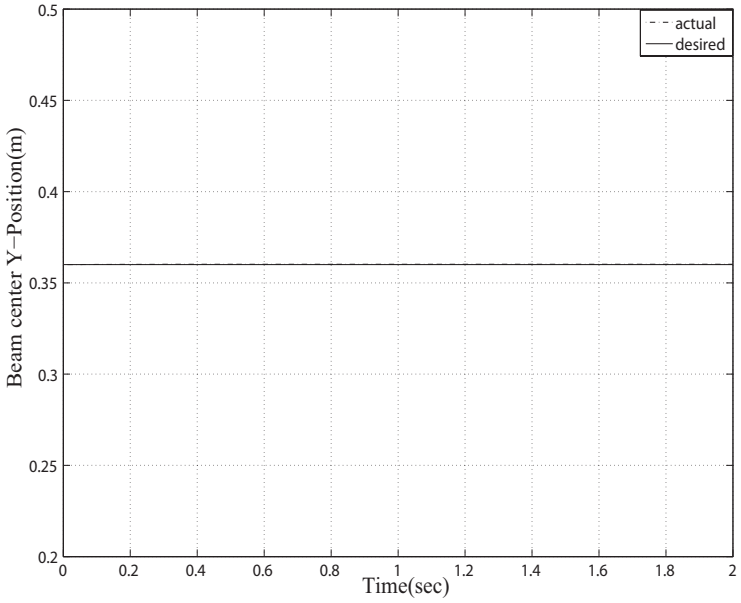

Figure 96: Y movement-Without regressor in JS

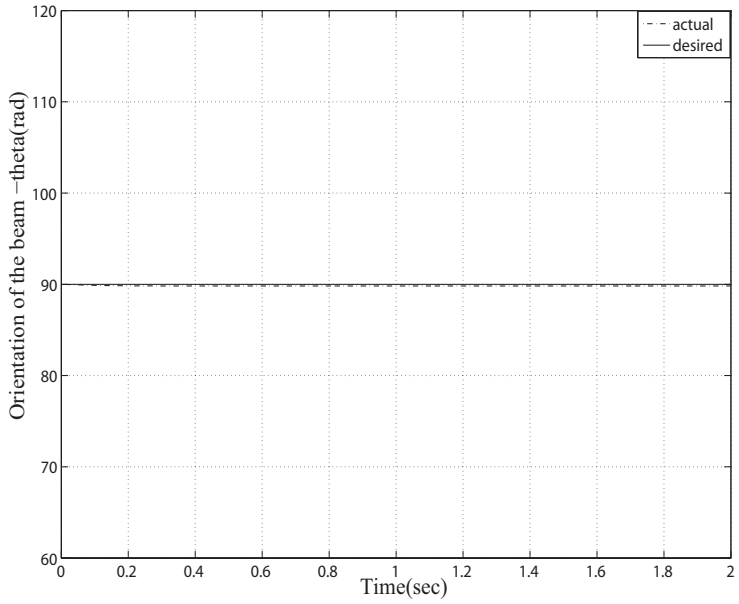

Figure 97: Orientation-Without regressor in JS

achieve the set point value of manipulators joint angles and beam pose. These kinds of oscillations are not seen from the Cartesian space slow subsystem simulation results of similar controller.

4. The non regressor based control approach yield comparatively better results than those by other control schemes in both Cartesian and joint spaces.

6.6 Summary

In this Chapter, complete systems of dynamic equations have been developed in joint space. The two subsystems, namely, slow and fast were identified by using the singular perturbation approach. Furthermore, the composite control algorithms presented for the

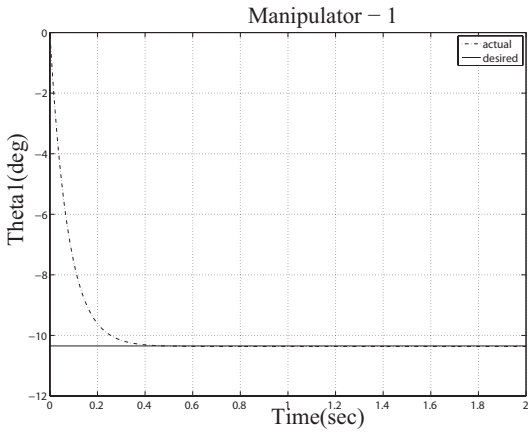

Figure 98: J1M1-Without regressor in JS

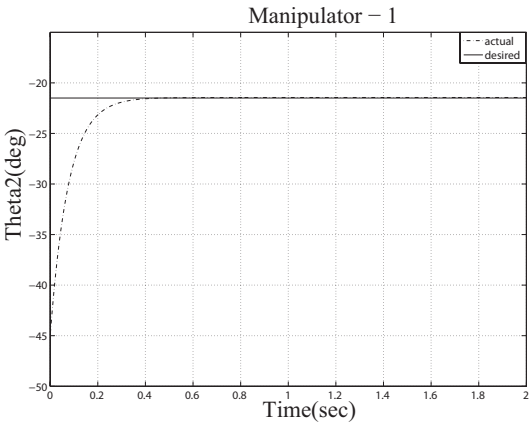

Figure 99: J2M1-Without regressor in JS

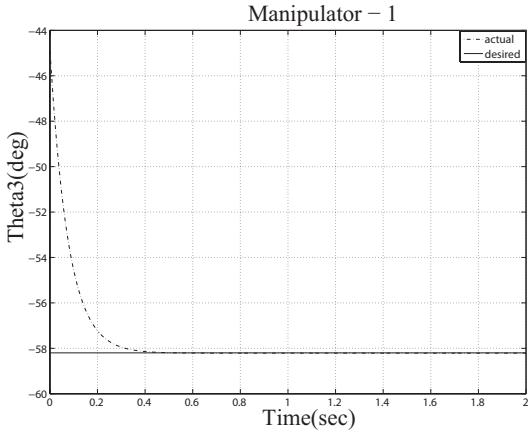

Figure 100: J3M1-Without regressor in JS

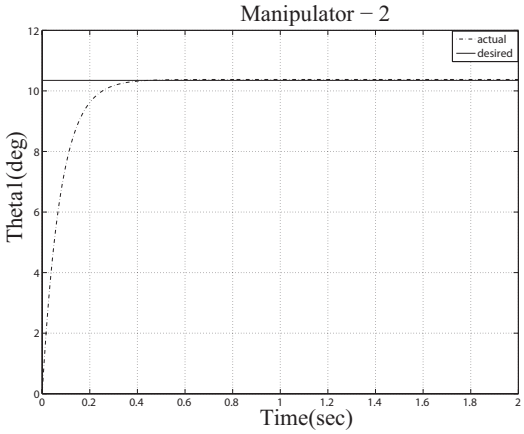

Figure 101: J1M2-Without regressor in JS

Cartesian space system was implemented to the joint space system as well. Stability analysis and simulation results were discussed. In the next Chapter, conclusions and some of the possible extensions to this thesis will be given.

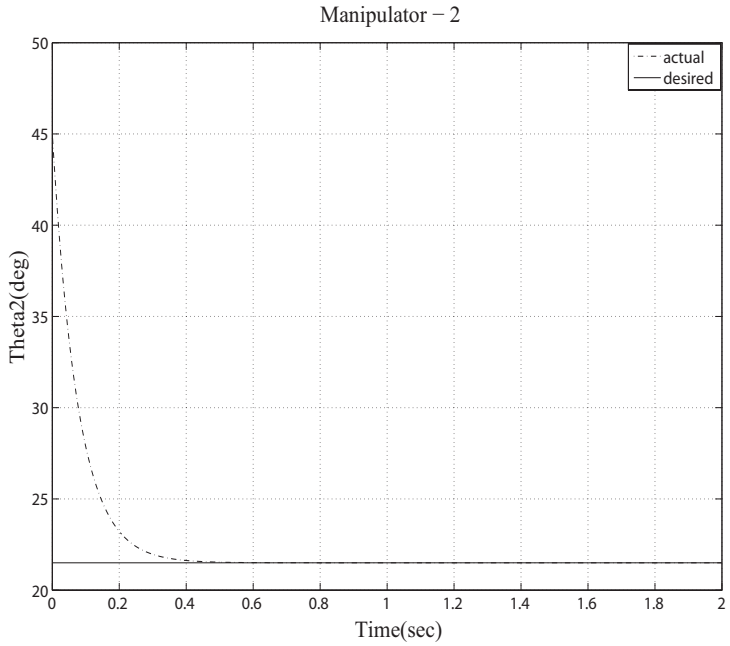

Figure 102: J2M2-Without regressor in JS

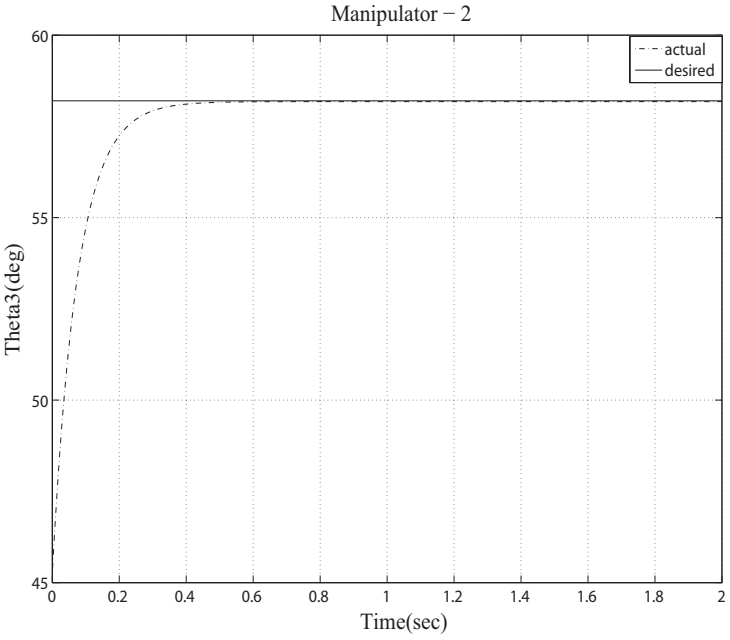

Figure 103: J3M2-Without regressor in JS

Chapter 7

Conclusions and Recommendations for Future Works

7.1 Summary

Maneuvering of flexible objects by robot arms has wide applications in various industries and in space. Especially solving the complete system of dynamic equations without using any approximate methods, correspondingly developing the robust control algorithms and also satisfying the necessary stability criteria are challenging problems. This dissertation research has addressed these problems by implementing collaborative manipulation of two planar rigid manipulators moving a flexible object in a prescribed trajectory while suppressing the vibration of the flexible object being handled. A brief summary of this research is provided in the following:

The flexible object being handled by two rigid arm manipulators is a beam. From the kinematics of the flexible beam, the relation between the velocities of end-effectors and

the object are obtained. In order to alleviate problems associated with truncating the infinite degrees-of-freedom flexible beam to a finite dimensional model, dynamic equations of motion of the beam are derived in PDE form. Furthermore, by utilizing the established kinematic relations of manipulators as well as beam, the dynamic equations of manipulators are formulated in Cartesian space. Then, the resulting manipulator dynamics were combined to the beam dynamics to yield a combined system dynamics in Cartesian space without utilizing any approximate or discretiation methods.

The derived systems of dynamic equations are coupled with rigid and flexible parameters. Without the aid of the assumed modes, the coupled rigid-felxible dynamics has been separated into slow subsystem, which signifies the rigid body motion and the fast subsystem that considers the vibration of the flexible object by using singular perturbation technique. The method of separation is considered under two different time scales that permits designing of the control signal for each subsystem. The challenge in the design of control systems lies in the fact that, they should be robust against parameter uncertainties and also guarantees the exponential convergence. Hence, for the slow subsystem, regressor based sliding mode control algorithm is developed. This method avoids the need of parameter estimation unlike in the case of adaptive control. Moreover, the method also gives the desired transient response while achieving robustness to uncertainties. In the case of fast subsystem, as a part of the composite control scheme, a simple feedback control algorithm is designed with a special damping term. The exponential stability results for slow and fast subsystems validate the singular perturbation analysis by satisfying the Tikhnov's theorem. Simulation results of the composite control strategy confirmed that, the proposed controller achieved very good tracking performance while suppressing the

vibration. In addition, switching function in the sliding mode control algorithm may cause chattering which is an undesirable phenomenon in real time applications. Hence, a suitable smoothing control law is suggested. As a special case, the combined dynamic model for the two manipulators handling a rigid object is derived which validate the developed slow subsystem in the Cartesian space.

Further improvement in the design of control algorithm for the slow subsystem is achieved by avoiding the measurement of velocity feedback. An adaptive control law with only position feedback is proposed. The stability analysis and simulations results are presented to illustrate the tracking performance of the controller. In addition to this, to avoid the online computation of complex regressor, a non-regressor based adaptive robust control algorithm is implemented to the slow subsystem and corresponding stability analysis has been carried out. Simulation results demonstrate the effectiveness of the suggested control scheme.

The earlier analysis has been extended to the joint space to avoid the complex inverse kinematics solutions of Cartesian trajectories and singularity problems. In order to rectify these issues, the complete system of dynamic equations is derived in joint space. By following the typical steps of singular perturbation approach, slow and fast subsystems are obtained in joint space. It is observed that, fast subsystem has similar structure in both Cartesian and joint space. Based upon these subsystems, composite controllers have been developed and corresponding simulations are performed. It is evident from the simulation results that, the proposed composite controllers achieved good control performance.

7.2 Major Contributions

1. A complete system of dynamic equations with respect to Cartesian space and joint space in PDE form was developed. This avoids the problems associated with approximation techniques which are mentioned in Chapter 1.

2. A composite control algorithm for the PDE based model satisfying the Tikhnov's theorem to achieve the tracking and regulation control performance and also suppressing the vibration of the flexible object was designed.

3. A regressor for the Cartesian space and joint space manipulators-beam system dynamics was formulated.

7.3 Conclusions

The major conclusions drawn from this dissertation study are summarized below:

- When the complete system of dynamic equations for the manipulator and the flexible object is solved using modal approximation techniques, it is not clear as to how many modes should be considered while developing the model. Further, neglecting higher order modes may cause instabilities in the system. This thesis primarily attempts to avoid such problems by developing the system of dynamic equations in PDE form.

- Validation of singular perturbation approach necessitates satisfying the Tikhnov's theorem wherein, both slow and fast subsystems should achieve the exponential convergence. Furthermore, in real time applications parameters of the manipulators and

flexible object will be varying and hence robust control algorithm is necessary. This thesis addressed these problems by developing a composite robust control algorithm and corresponding exponential stability analysis of each subsystem, which is as a whole, not found in the literature.

- The proposed feedback control algorithm for the fast subsystem suppresses the vibration only with velocity feedback and it also reduces the need for more sensors unlike in the available control algorithms in the literature. As a result, the measurement cost is minimized.

- For the slow subsystem, in order to avoid velocity measurements, a controller without velocity feedback is proposed. The simulation results show that, the proposed controller does not affect the tracking performance of the slow subsystem.

- Further improvement in the control law for the slow subsystem is made to avoid the complex computational burden of the regressor. A non-regressor based adaptive robust control algorithm is developed. Simulation studies demonstrate that, the desired tracking is achieved as in the other proposed control algorithms.

- Further studies have been carried out by developing the complete system of dynamics in joint space, to avoid the singularity problems and also complex inverse kinematic calculations of online trajectories. The simulation results show that, the proposed controller does not affect the tracking performance of the slow subsystem.

7.4 Future Works

There are some recommended studies related to this domain that needs further investigations are listed below:

- Vibration free motion is necessary in many of the deformable structural components such as in aircraft wings, shiphulls, space antennas and aircraft skins. The dynamic equations of motion can also be derived by assuming these structures as plates or shells instead of beam. The development of system of dynamic equations without using any approximate methods and establishing the slow and fast subsystem is a complex problem. Developing these subsystems and implementing the proposed robust control algorithms is very important.

- The proposed control algorithms in this thesis can be implemented through experiments. Performing experimental studies will be an added advantage.

- In this thesis, the two manipulators grasping the flexible object was considered as rigid grasping. In the literature, different grasping configurations are available [107]. According to the types of objects to be grasped and transported, one can consider the required grasping configuration and perform the detailed analysis.

- In general manipulators are considered to be rigid. Now-a-days flexible manipulators are used in medical and aerospace applications. They have low mass, and require less power and ultimately saves the cost. However, mathematical modeling of flexible object needs special attention and also coupling with the flexible object can be a

complex problem. In addition, suppressing the vibration of manipulators as well as the flexible object is critical too.

- The interaction between the external environment such as any obstacles or collision between manipulators are not considered in this thesis. This scenario occurs in real time applications such as assembly, material handling and pick and place operations. When the object is constrained, the dynamic modeling and deriving the control law becomes more tedious.

Bibliography

[1] R. C. Goertz, " Fundamentals of general-purpose remote manipulators," *Nucleonics*, vol. 10, pp. 36-42, 1952.

[2] E. Nakano, S. Ozaki, S. Isida and I. Kato, "Cooperation control of the anthropomorphous manipulator MELARM," in *Proc. 4th Int. Conf. on Industrial Robots*, 1974, pp. 251-260.

[3] J. Y. S. Luh and Y. F. Zheng, "Constrained relations between two coordinated industrial robots for motion control," *Int. J. of Robotics Research*, vol. 6, pp. 60-70, 1987.

[4] J. K. Mills, "Multi-manipulator control for fixtureless assembly of elastically deformable parts," in *Proc. Japan - U.S.A. Sym. on Flexible Automation*, 1992, pp. 1565-1572.

[5] T. Ishida, "Force control in coordination of two arms," in *Proc. 5th Int. Conf. on Artificial Intelligence*, 1977, pp. 717-722.

[6] C. O. Alford and S. M. Belyeu, "Coordinated control of two robot arms," in *Proc. IEEE Int. Conf. on Robotics and Automation*, 1984, pp. 468-473.

[7] Y. F. Zheng and F. R. Sias, “Two robots arms in assembly,” in *Proc. IEEE Int. Conf. on Robotics and Autonomous System*, 1986, pp. 1230-1235.

[8] T. J. Tarn, A. K. Bejczy and X. Yun, “Co-ordinated control of two robot arms,” in *Proc. IEEE Int. Conf. on Robotics and Automation*, 1986, pp. 1193-1202.

[9] T. J. Tarn, A. K. Bejczy and X. Yun, “Dynamic coordination of two robot arms,” in *Proc. IEEE Int. Conf. on Decision and Control*, 1986, pp. 1267-1270.

[10] M. H. Raibert and J. J. Craig, “Hybrid position/force control of manipulators,” *ASME J. of Dynamic Systems, Measurement, and Control*, vol. 120, pp. 126-133, 1981.

[11] S. Hayati, “Hybrid position/force control of multi-arm cooperating robots,” in *Proc. IEEE Int. Conf. on Robotics and Automation*, 1986, pp. 82-89.

[12] M. Uchiyama, N. Iwasawa and K. Hakomori, “Hybrid position/force control for co-ordination of a two arm robot,” in *Proc. IEEE Int. Conf. on Robotics and Automation*, 1987, pp. 1242-1247.

[13] M. Uchiyama and P. Dauchez, “A symmetric hybrid position/force control scheme for the coordination of two robots,” in *Proc. IEEE Int. Conf. on Robotics and Automation*, 1988, pp. 350-356.

[14] P. Dauchez, A. Fournier and R. Jordon, “Hybrid control of a two-arm robot for complex tasks,” *IEEE J. of Robotics and autonomous Systems*, vol. 5, pp. 323-332, 1989.

[15] J. Wang, S. J. Dodds and W. N. Bailey, “Co-ordinated control of multiple robotic manipulators handling a common object - theory and experiments,” in *Proc. IEEE Control Theory Applications*, 1997, pp. 73-84.

[16] C. D. Kopf and T. Yabuta, “Experimental comparison of master/slave and hybrid two-arm position/force control,” in *Proc. IEEE Int. Conf. on Robotics and Automation*, 1989, pp. 425-430.

[17] J. Duffy, “The fallacy of modern hybrid control theory that is based on orthogonal c omplements of twist and wrench spaces,” *J. of Robotic systems*, vol. 7, no. 2, pp. 139-144, 1990.

[18] Y. R. Hu and A. A. Goldenberg, “An adaptive approach to motion and force control of multiple coordinated robots,” in *Proc. IEEE Int. Conf. on Robotics and Automation*, 1988, pp. 1633-1637.

[19] M. W. Walker, D. Kim, and J. Dionise, “Adaptive coordinated motion control of two manipulator arms,” in *Proc. IEEE Int. Conf. on Robotics and Automation*, 1989, pp. 1084-1090.

[20] B. Yao and M. Tomizuka, “Adaptive coordinated control of multiple manipulators handling a constrained object,” in *Proc. IEEE Int. Conf. on Robotics and Automation*, 1993, pp. 624-629.

[21] S. Arimoto, Y.H. Liu, and T. Naniwa, “Model-based adaptive hybrid control for geometrically constrained robots,” in *Proc. IEEE Int. Conf. on Robotics and Automation*, 1993, pp. 618-623.

[22] R. G. Bonitz and T. C. Hsia, “Intemal force-based impedance control for cooperating manipulators,” *IEEE Trans. on Robotics and Automation*, vol. 12, no. 1, pp. 78-89, 1996.

[23] R. G. Bonitz and T. C. Hsia, “Robust internal force-based impedance control for cooperating manipulators - theory and experiments,” in *Proc. IEEE Int. Conf. on Robotics and Automation*, 1996, pp. 622-628.

[24] I. Uzmaya, R. Burkan and H. Sarikaya, “Application of robust and adaptive control techniques to cooperative manipulation,” *Control Engineering Practice*, vol. 12, pp. 139-148, 2004.

[25] W. Gueaieb, F. Karray and S. Al-Sharhan, “A Robust hybrid intelligent position/force control scheme for cooperative manipulators,” *IEEE/ASME Transactions on Mechatronics*, vol. 12, no. 2, pp. 109-125, 2007.

[26] F. Caccavale, P. Chiacchio, A. Marino and L. Villani, “Six-DOF impedance control of dual-Arm cooperative manipulators,” *IEEE/ASME Transactions on Mechatronics*, vol. 13, no. 5, pp. 576-586, 2008.

[27] S. A. A. Moosavian and E. Papadopoulos, “Cooperative object manipulation with contact impact using multiple impedance control,” *Int. J. of Control, Automation, and Systems*, vol. 8, pp. 314-327, 2010.

[28] N. Yagiz, Y. Hacioglu and Y. Z. Arslan,“Load transportation by dual arm robot using sliding mode control,” *J. of Mechanical Science and Technology*, vol. 24, pp. 1177-1184, 2010.

[29] J. K. Mills, “Fixtureless assembly: Multi-robot manipulation of distributed parameter payloads,” in *IMAC/SICE Int. Sym. on Robotics, Mechatronics and Manufacturing Systems*, 1992.

[30] J. K. Mills and J. G. L. Ing, “Robotic fixtureless assembly of sheet metal parts using dynamic finite element models:Modeling and simulation,” in *Proc. IEEE Int. Conf. on Robotics and Automation*, 1995, pp. 2530-2537.

[31] Y. F. Zheng, R. Pei and C. Chen, “Strategies for automatic assembly of deformable objects,” in *Proc. IEEE Int. Conf. on Robotics and Automation*, 1991, pp. 2708-2715.

[32] Y. F. Zheng and M. Z. Chen, “Trajectory planning for two manipulators to deform flexible beams,” in *Proc. IEEE Int. Conf. on Robotics and Automation*, 1993, pp. 1109-1024.

[33] W. F. Dellinger and J. N. Anderson, “Interactive force dynamics of two robot manipulators grasping a non-rigid object,” in *Proc. IEEE Int. Conf. on Robotics and Automation*, 1992, pp. 2205-2210.

[34] T. Yukawa, M. Uchiyama and H. Hooka, “Cooperative control of a vibrating flexible object by a rigid dual-arm robot,” in *Proc. IEEE Int. Conf. on Robotics and Automation*, 1995, pp. 1820-1825.

[35] K. Kosuge, H. Yoshida, T. Fukuda, M. Sakai and K. Kanitani, “Manipulation of sheet metal by dual manipulators based on finite element model,” in *Proc. IEEE Int. Conf. on Robotics and Automation*, 1995, pp. 199-204.

[36] W. Nguyen and J. K. Mills, “Multi-robot control for flexible fixtureless assembly of flexible sheet metal auto body parts,” in *Proc. IEEE Int. Conf. on Robotics and Automation*, 1996, pp. 2340-2345.

[37] W. Kraus Jr. and B. McCarragher, “Control of flexible load deformations and environment contact forces in dual-arm manipuiation,” in *Proc. 13th IFAC World Congress*, 1996, pp. 61-67.

[38] W. Kraus Jr. and B. McCarragher, “Force fields in the manipulation of flexible materials,” in *Proc. IEEE Int. Conference on Robotics and Automation*, 1996, pp. 2352-2357.

[39] W. Kraus Jr. and B. McCarragher, “Case studies in the manipulation of flexible parts using a Hybrid position/force approach,” in *Proc. IEEE Int. Conf. on Robotics and Automation*, 1997, pp. 367-372.

[40] T. Yukawa, M. Uchiyama, D. N. Nenchev and H. Inooka, “Stability of control system in handling of a flexible object by rigid arm robots,” in *Proc. IEEE Int. Conf. Robotics and Automation*, 1996, pp. 2332-2339.

[41] D. Sun, J. K. Mills and Y. Liu, “Position control of multiple robots manipulating a flexible payload,” in *Proc. American Control Conference*, 1998, pp. 456-460.

[42] D. Sun and Y. H. Liu, “Modeling and impedance control of a two-manipulator system handling a flexible beam,” *ASME J. of Dynamic Systems, Measurement, and control*, pp. 736-742, 1997.

[43] Y. Liu and D. Sun, “Stabilizing a flexible beam handled by two manipulators via PD feedback,” *IEEE Trans. on Automatic Control*, vol. 45, no. 11, pp. 2159-2164, 2000.

[44] D. Sun and Y. Liu, “Position and force tracking of a two manipulator system manipulating a flexible beam,” *J. of Robotic Systems*, vol. 18, no. 4, pp. 197-212, 2001.

[45] D. Sun, “Cooperative control of two-manipulator systems handling a flexible object,” Ph.D. dissertation, The Chienese Univ. of Hong Kong, China, 1997.

[46] Y. C. Ji and Y. Park, “Optimal input design for a cooperating robot to reduce vibration when carrying flexible objects,” *Robotica*, vol. 19, pp. 209-215, 2001.

[47] Z. Doulgeri and J. Peltekis, “Modeling and dual manipulation of a flexible object,” in *Proc. IEEE Int. Conf. on Robotics and Automation*, 2004, pp. 1700-1705.

[48] A. S. Al-Yahmadi and T. C. Hsia, “Internal force-based impedance control of dual arm manipulation of flexible objects,” in *Proc. IEEE Int. Conf. on Robotics and Automation*, 2000, pp. 3296-3301.

[49] A. S. Al-Yahmadi and T. C. Hsia, “Modeling and control of two manipulators handling a flexible object,” *J. of the Franklin Institute*, vol. 344, pp. 349-361, 2007.

[50] A. Tavasoli, M. Eghtesad and H. Jafarian, “Two-time scale control and observer design for trajectory tracking of two robot manipulators moving a flexible beam,” *J. of Robotics and Autonomous systems*, vol. 57, pp. 212-221, 2009.

[51] Z. Tang and Y. Li, "Modeling and control of two manipulators handling a flexible payload based on singular perturbation," in *Proc. IEEE Int. Conf. on Advanced Computer Control*, 2010, pp. 558-562.

[52] S. S. Ge, T. H. Lee and G. Zhu, "Improving regulation of a single-link-flexible manipulator with strain feedback," *IEEE Trans. on Robotics and Automation*, vol. 14, pp. 179-185, 1998.

[53] D. T. Greenwood, *Classical Dynamics*. Dover publications, Prentice Hall, 1997.

[54] J. J. Craig, *Introduction to Robotics:Mecahnics and Control*. Prentice Hall, Third edition, 2004.

[55] M. W. Spong, S. Hutchinson and M. Vidyasagar, "Robot modeling and control," John Wiley and Sons, First Edition, 2006.

[56] F. L. Lewis, D. M. Dawson and C. T. Abdallah, *Robot Manipulator Control Theory and Practice*, Prentice-Hall, Second edition, 2006.

[57] R. Ortega and M. W. Spong, "Adaptive motion control of rigid robots: A tutorial," *Automatica*, vol. 25, no. 6, pp. 877-888, 1989.

[58] J. J. E. Slotine and W. Li, "On the adaptive control of robot manipulators," *Int. J . Robotics Res.*, vol. 6, no. 3, pp. 49-59, 1987.

[59] C. Y. Su and Y. Stepanenko, "Adaptive sliding mode coordinated control of multiple robot arms handling one constrained object," *IEEE Transactions on Systems, Man, and Cybernetics*, vol. 25, no. 5, pp. 871-878, 1995.

[60] P. V. Kokotovic, R. E. O'Malley and P. Sannutiti, "Singular perturbations and order reduction in control theory an overview," *Automatica*, vol. 12, no. 2, pp. 123-132, 1976.

[61] V. R. Saksena, J. O'Reily and P. V. Kokotovic, "Singular perturbations and time-scale methods in control theory: Survey 1976-1983," *Automatica*, vol. 20, no. 3, pp. 273-293, 1984.

[62] D. Subbaram Naidu and A. J. Calise, "Singular perturbations and time-scales in guidance and control of aerospace systems: A survey," *J. of Guidance, Control, and Dynamics*, vol. 24, no. 6, pp. 1057-1078, 2001.

[63] D. Subbaram Naidu, "Singular perturbations and time-scales in control theory and applications:An overview," *J. of Dynamics, Continuous and Discrete Impulsive Systems: series-B; applications and algorithms*, vol. 9, pp. 233-278, 2002.

[64] P. Kokotovic, H. K. Khalil and J. O'Reilly, *Singular Perturbation Methods in Control:Analysis and Design*. SIAM, 1999.

[65] H. K. Khalil, *Nonlinear Systems*. Prentice Hall, New Jersey, 2002.

[66] A. Lotfazar, M. Eghtesad and A. Najafi, "Vibration control and trajectory tracking for general in-plane motion of Euler-Bernoulli beam via two-time scale and boundary control methods," *ASME J. of Vibrations and Acoustics*, vol. 130, 051009-1-11, 2008.

[67] M. W. Spong, "Adaptived control of flexible joint manipulators:Comments on two papers," *Automatica*, pp. 585-590, 1995.

[68] M. Zribi, M. Karkoub and L. Huang, “Modelling and control of two robotic manipulators handling a constrained object,” *Applied Mathematical Modelling*, vol. 24, no. 12, pp. 881-898, 2000.

[69] T. P. Leung and C. Y. Su, “Adaptive control for a constrained robot without using a regressor,” *Transactions of the Institute of Measurement and Control*, vo1. 18, no. 5, pp. 267-275, 1996.

[70] Z. H. Luo, “Direct strain feedback control of flexible robot arms:New theoretical and experimental results,” *IEEE Trans. on Auomatic Control*, vol. 38, no. 11, pp. 1610-1622, 1993.

[71] Z. H. Luo and B. Guo, “Further theoretical results on direct strain feedback control of flexible robot arms,” *IEEE Trans. on Auomatic Control*, vol. 40, no. 4, pp. 747-751, 1995.

[72] J. L. Soule, *Linear Operators In Hilbert Space*, Gordon and Breach Science Publishers, New York, 1968.

[73] E. Kreyszig, *Introductory Functional Analysis with Applications*, John Wiley and Sons, New York, 1978.

[74] Y. Sakawa and Z. H. Luo, “Modeling and control of cooupled bending and torsional vibrations of flexible beam,” *IEEE Trans. on Auomatic Control*, vol. 34, no. 9, pp. 970-977, 1989.

[75] Y. Sakawa, F. Matsuno and S. Fukushima,“Modeling and feedback control of a flexible arm,” *J. of Robotic Systems*, pp. 453-472, 1985.

[76] J. J. E. Slotine and W. Li, *Applied Nonlinear Control*. Prentice Hall, New Jersey, 1991.

[77] C. Y. Su, T. P. Leung and Y. Stepanenko, "Real-time implementation of regressor-based sliding mode control algorithm for robotic manipulator," *IEEE Transactions on Industrial Electronics*, vol. 40, no. 1, pp. 71-79, 1993.

[78] L. Hsu and R. R. Costa, "Adaptive control with discontinuous u-factor and saturation for improved robustness," *Int. J. of Control*, vol. 45, no. 3, pp. 843-859, 1987.

[79] M. W. Spong, "On the robust control of robot manipulators," *IEEE Transactions on Automatic Control*, vol. 37, no. 11, pp. 1782-1786, 1992.

[80] C. Abdallah, D. Dawson, P. Dorato and M. Jamshidi, "Survey of robust control for rigid robots," *IEEE Control Systems Magazine*, vol. 11, pp. 24-30, 1991.

[81] H. G. Sage, M. F. De Mathelin and E. Ostertag, "Robust control of robot manipulators: a survey," *Int. J. of Control* , vol. 72, no. 6, pp. 1498-1522, 1999.

[82] M. J. Balas, "Direct velocity feedback control of large space strutures," *J. of Guidance and Control*, vol. 2, pp. 252-253, 1979.

[83] P. Gardonio and S. J. Elliott "Modal response of a beam with a sensoractuator pair for the implementation of velocity feedback control," *J. of Sound and Vibration*, vol. 284, pp. 1-22, 2005.

[84] A. Lotfazar, M. Eghtesad and A. Najafi, "Exponential Stabilization of Transverse Vibration and Trajectory Tracking for General In-Plane Motion of an Euler-Bernoulli

Beam Via Two-Time Scale and Boundary Control Methods,"*ASME J. of Vibrations and Acoustics*, vol. 131, pp. 054503-1-7, 2009.

[85] G. Chen and D. L. Russell, "A Mathematical model for linear elastic systems with structural damping," *Quarterly Applied Mathematics*, vol. 39, pp. 433-454, 1981.

[86] F. Huang,"On the mathematical model for linear elastic systems with analytic damping," *SIAM J. of Control and Optimization*, vol. 26, pp. 714-724, 1988.

[87] S. Chen and R. Triggiani, "Gevrey class semigroups arising from elastic systems with gentle dissipation:The case $0 < \alpha < \frac{1}{2}$," *Proc. of the American Mathematical Society*, vol. 110, no.2, pp. 401-415, 1990.

[88] J. A. Burns and B. B. King, "A note on mathematical modeling of damped second order systems," *J. of Mathematical Systems, Estimation and Control*, vol. 8, no. 2, pp. 1-12, 1998.

[89] W. T. Thomson, *Theory of vibration with applications*. Prentice Hall, United Kingdom, 1993.

[90] A. Pazy, *Semigroups of linear operators and applications to partial differential equations*. Springer-Verlag, New york, 1983.

[91] M. Hattori, S. Tadokoro and T. Takamori, "Robust stablization of flexible structures using static output feedback," in *Proc. 2nd World Congress Nonlinear Analysis, Theory, Methods and Applications*, 1997, pp. 2215-2220.

[92] J. H. Yang, “Adaptive Tracking Control for Manipulators with Only Position Feedback”, in *Proc. IEEE Canadian Conf. on Electrical and Computer Engineering*, 1999, pp. 1740-1745.

[93] M. A. Arteaga, “Robot control and parameter estimation with only joint position measurements,” *Automatica*, vol. 39, no. 1, pp. 67-73, 2003.

[94] C. Y. Su and Y. Stepanenko, “Redesign of hybrid adaptive/robust motion control of rigid-link electrically-driven robot manipulators,” *IEEE Transactions on Robotics and Automation*, vol. 14, no. 4, pp. 651-655, 1998.

[95] C. Y. Su and Y. Stepanenko, “Hybrid adaptive/robust motion control of rigid-link electrically-driven robot manipulators,” *IEEE Transactions on Robotics and Automation*, vol. 11, no. 3, pp. 426-432, 1995.

[96] J. H. Jean and L. C. Fu, “An adaptive control scheme for coordinated multi-manipulator system,” *IEEE Transaction on Robotics and Automation*,” vol. 9, no. 2, pp. 226-231, 1993.

[97] Y. D. Song, “Adaptive motion tracking control of robot manipulators: non-regressor based approach,” in *Proc. IEEE Int. Conf. on Robotics and Automation*, 1994, pp. 3008-3013.

[98] N. Sadegh and R. Horowitz, “Stability and robustness analysis of a class of adaptive controller for robotic manipulators,” *Int. J. of Robotics Research*, vol. 9, no. 3, pp. 74-92, 1990.

[99] Y. Stepanenko and J. Yuan, “Robust adaptive control of robotic manipulators without the regressor matrix,” *Int. J. of Adaptive Control and Signal Processing*, vol. 6, pp. 111-126, 1992.

[100] R. Colbaugh and K. Glass, “Adaptive regulation of rigid-link electrically-driven manipulators,” in *Proc. IEEE Int. Conf. on Robotics and Automation*, 1995, pp. 293-299.

[101] J. X. Liu, *Robotic Manipulators: New Research*. Nova Science Pub. Inc., 2005.

[102] S. Arimoto, F. Miyazaki, “Stability and robustness of PID feedback control for robot manipulators of sensory capability,” in *Robotics Research:Proc. First Int. Symp.*, 1984, pp. 783-799.

[103] S. Ahmad and M. Zribi, “Lyapunov based control design for multiple robots handling a common object,” *J. of Dynamics and Control*, vol. 3, no. 2, pp. 127-157, 1993.

[104] V. Utkin and H. Lee, “Chattering problem in sliding mode control systems,” in *Proc. International Workshop on Variable Structure Systems*, 2006, pp. 346-350.

[105] M. Oya, C. Y. Su and R. Katoh, “Robust adaptive motion/force tracking control of uncertain nonholonomic mechanical systems,” *IEEE Transactions on Robotics and Automation*, vol. 19, no. 1, pp. 175-181, 2003.

[106] L. Hsu and F. Lizarralde, “Experimental results on variable structure adaptive robot control without joint velocity measurement,” in *Proc. American Control Conf.*, 1995, pp. 2317-2321.

[107] B. Mishra and N. Silver, “Some discussions of static gripping and its stability,” *IEEE Transactions on Systems, Man, and Cybernetics*, vol. 19, no. 4, pp. 783-796, 1989.

Appendix A

Dynamics of Beam

Kinetic energy with respect to fixed coordinate frame in Cartesian space is given by,

$$\begin{aligned} K.E &= \frac{1}{2}\int_{\frac{-L}{2}}^{\frac{L}{2}} \rho[\dot{x}_0^2+\dot{y}_0^2+\dot{\theta}^2\eta^2+(x\dot{\theta}+\dot{\eta})^2-2\dot{\theta}\eta(\dot{x}_0 cos\theta+\dot{y}_0 sin\theta) \\ &\quad +2(\dot{\theta}x+\dot{\eta})(\dot{y}_0 cos\theta-\dot{x}_0 sin\theta)]dx \end{aligned}$$

Variational principle is applied to the kinetic energy terms which are illustrated for some of the terms as follows:

$$\begin{aligned} \delta(\frac{1}{2}\dot{x_0}^2) &= \int_{t_1}^{t_2} \dot{x}_0\delta(\dot{x}_0) \\ &= \dot{x}_0\delta(x_0)\,|_{t_2}^{t_1} - \int_{t_1}^{t_2} \ddot{x}_0\delta(x_0) \\ &= \int_{t_1}^{t_2} -\ddot{x}_0\delta(x_0) \\ \delta(\frac{1}{2}\dot{y_0}^2) &= \int_{t_1}^{t_2} \dot{y}_0\delta(\dot{y}_0) \\ &= \int_{t_1}^{t_2} -\ddot{y}_0\delta(y_0) \\ \delta(\frac{1}{2}\dot{\theta}^2\eta^2) &= \int_{t_1}^{t_2} -\ddot{\theta}\eta^2\delta\theta, \quad for\ variation\ of\ \theta \\ &= \int_{t_1}^{t_2} \dot{\theta}^2\eta\,\delta\eta, \quad for\ variation\ of\ \eta \end{aligned}$$

$$\begin{aligned}
\delta[\frac{1}{2}(x\dot{\theta}+\dot{\eta})^2] &= (x\dot{\theta}+\dot{\eta})[x\delta\dot{\theta}+\delta\dot{\eta}] \\
&= x^2\dot{\theta}\delta\dot{\theta}+x\dot{\theta}\delta\dot{\eta}+x\dot{\eta}\delta\dot{\theta}+\dot{\eta}\delta\dot{\eta} \\
&= -x^2\ddot{\theta}\delta\theta-x\ddot{\theta}\delta\eta-x\ddot{\eta}\delta\theta-\ddot{\eta}\delta\eta \\
&= \int_{t_1}^{t_2}[(-x^2\ddot{\theta}-x\ddot{\eta})\delta\theta-(x\ddot{\theta}+\ddot{\eta})\delta\eta]
\end{aligned}$$

Similarly, variations on the other kinetic energy terms are also performed.

Potential energy is given by

$$\begin{aligned}
U_e &= \frac{1}{2}\int_{\frac{-L}{2}}^{\frac{L}{2}}\left[EI\eta''^2\right]dx \\
U_g &= mgy_0
\end{aligned}$$

Variation of potential energy:

$$\begin{aligned}
\delta(\frac{1}{2}\int_{\frac{-L}{2}}^{\frac{L}{2}}\left[EI\eta''^2\right]dx) &= \frac{1}{2}\left[EI2\eta''\delta(\eta'')\right]=EI\eta''\delta(\eta')-EI\eta'''\delta(\eta)+\int_{t_1}^{t_2}EI\eta^{iv}\delta(\eta) \\
\delta(mgy_0) &= mg\delta y_0
\end{aligned}$$

Work done due to the external forces is given by,

$$W=F_{1x}(x_0-\frac{L}{2}\cos\theta)+F_{1y}(y_0-\frac{L}{2}\sin\theta)+F_{2x}(x_0+\frac{L}{2}\cos\theta)+F_{2y}(y_0+\frac{L}{2}\sin\theta)+$$
$$(F_{2y}+F_{1y})\eta\cos\theta-(F_{1x}+F_{2x})\eta\sin\theta$$

Variation of external forces:

1. $F_{1x}\delta x_0$
2. $-F_{1x}\frac{L}{2}\delta\cos\theta=F_{1x}\frac{L}{2}\sin\theta\delta\theta$
3. $F_{1y}\delta y_0$

4. $-F_{1y}\frac{L}{2}\delta\sin\theta = -F_{1y}\frac{L}{2}\cos\theta\delta\theta$

5. $F_{2x}\delta x_0$

6. $F_{2x}\frac{L}{2}\delta\cos\theta = -F_{2x}\frac{L}{2}\sin\theta\delta\theta$

7. $F_{2y}\delta y_0$

8. $F_{1y}\frac{L}{2}\delta\sin\theta = F_{2y}\frac{L}{2}\cos\theta\delta\theta$

9. $-F_{1x}\eta\delta(\sin\theta) = -F_{1x}\eta\cos\theta\delta\theta$

10. $-F_{1x}\sin\theta\delta(\eta)$

11. $F_{1y}\eta\delta(\cos\theta) = -F_{1y}\eta\sin\theta\delta\theta$

12. $F_{1y}\cos\theta\delta(\eta)$

13. $-F_{2x}\eta\delta(\sin\theta) = -F_{2x}\eta\cos\theta\delta\theta$

14. $-F_{2x}\sin\theta\delta(\eta)$

15. $F_{2y}\eta\delta(\cos\theta) = -F_{2y}\eta\sin\theta\delta\theta$

16. $F_{2y}\cos\theta\delta(\eta)$

Separating δx_0 components

$$\begin{aligned} -\ddot{x}_0 + \ddot{\theta}\eta\cos\theta + \dot{\theta}\dot{\eta}\cos\theta - \eta\sin\theta\dot{\theta}^2 + x\ddot{\theta}\sin\theta & \\ +x\dot{\theta}^2\cos\theta + \ddot{\eta}\sin\theta + \dot{\eta}\cos\theta\dot{\theta} &= F_{2x} - F_{1x} \end{aligned}$$

Integrating all the terms in δx_0 ($\rho \int_{\frac{-L}{2}}^{\frac{L}{2}} dx$)

$$-\rho \ddot{x}_0 \int_{\frac{-L}{2}}^{\frac{L}{2}} dx = -\ddot{x}_0 \frac{m}{L} L = -m\ddot{x}_0$$

$$\rho \ddot{\theta} \cos\theta \int_{\frac{-L}{2}}^{\frac{L}{2}} \eta dx$$

$$2\rho \dot{\theta}\dot{\eta} \cos\theta \int_{\frac{-L}{2}}^{\frac{L}{2}} \dot{\eta} dx$$

$$-\rho \sin\theta \dot{\theta}^2 \int_{\frac{-L}{2}}^{\frac{L}{2}} \eta dx$$

$$\rho \int_{\frac{-L}{2}}^{\frac{L}{2}} x\ddot{\theta} \sin\theta dx = 0$$

$$\rho \int_{\frac{-L}{2}}^{\frac{L}{2}} x\dot{\theta}^2 \cos\theta dx = 0$$

$$\rho \int_{\frac{-L}{2}}^{\frac{L}{2}} \ddot{\eta} \sin\theta dx = \rho \sin\theta \int_{\frac{-L}{2}}^{\frac{L}{2}} \ddot{\eta} dx$$

Separating δy_0 components

$$-\ddot{y}_0 + \ddot{\theta}\eta \sin\theta + \dot{\theta}\dot{\eta} \sin\theta + \eta \cos\theta \dot{\theta}^2 - x\ddot{\theta} \cos\theta$$

$$-x\dot{\theta}^2 \sin\theta - \ddot{\eta} \cos\theta + \dot{\eta} \sin\theta \dot{\theta} + mg = F_{2y} - F_{1y}$$

Integrating all the terms in δy_0 ($\rho \int_{\frac{-L}{2}}^{\frac{L}{2}} dx$)

$$-\rho \ddot{y}_0 \int_{\frac{-L}{2}}^{\frac{L}{2}} dx = -\ddot{y}_0 \frac{m}{L} L = -m\ddot{y}_0$$

$$\rho \ddot{\theta} \sin\theta \int_{\frac{-L}{2}}^{\frac{L}{2}} \eta dx$$

$$2\rho \dot{\theta}\dot{\eta} \sin\theta \int_{\frac{-L}{2}}^{\frac{L}{2}} \dot{\eta} dx$$

$$\rho \cos\theta \dot{\theta}^2 \int_{\frac{-L}{2}}^{\frac{L}{2}} \eta dx$$

$$-\rho \int_{\frac{-L}{2}}^{\frac{L}{2}} x\ddot{\theta} \cos\theta dx = 0$$

$$\rho \int_{\frac{-L}{2}}^{\frac{L}{2}} x\dot{\theta}^2 \sin\theta dx = 0$$

$$-\rho \int_{\frac{-L}{2}}^{\frac{L}{2}} \ddot{\eta} \cos\theta dx = -\rho \cos\theta \int_{\frac{-L}{2}}^{\frac{L}{2}} \ddot{\eta} dx$$

Separating $\delta\theta$ components

$$-\ddot{\theta}\eta^2 - (x^2\ddot{\theta} + x\ddot{\eta}) + \dot{\eta}\dot{x}_0 \cos\theta + \eta\ddot{x}_0 \cos\theta - \eta\dot{x}_0 \sin\theta\dot{\theta} + \eta\dot{x}_0 \sin\theta\dot{\theta} + \dot{\eta}\dot{y}_0 \sin\theta$$

$$+\eta\ddot{y}_0 \sin\theta + \eta\dot{y}_0 \cos\theta\dot{\theta} - \dot{\theta}\eta\dot{y}_0 \cos\theta + x\ddot{x}_0 \sin\theta + x\dot{x}_0 \cos\theta\dot{\theta} - x\dot{x}_0 \cos\theta\dot{\theta} - x\ddot{y}_0 \cos\theta$$

$$+x\dot{y}_0 \sin\theta\dot{\theta} - x\dot{y}_0 \sin\theta\dot{\theta} - \dot{\eta}\dot{y}_0 \cos\theta - \dot{\eta}\dot{x}_0 \cos\theta =$$

$$F_{1x}(\frac{L}{2}\sin\theta - \eta\cos\theta) + F_{1y}(-\frac{L}{2}\cos\theta - \eta\sin\theta)$$

$$+F_{2x}(-\frac{L}{2}\sin\theta - \eta\cos\theta) + F_{2y}(\frac{L}{2}\cos\theta - \eta\sin\theta)$$

$$-\ddot{\theta}\eta^2 - (x^2\ddot{\theta} + x\ddot{\eta}) + \ddot{x}_0\eta\cos\theta + \ddot{y}_0\eta\sin\theta + \ddot{x}_0 x\sin\theta - \ddot{y}_0 x\cos\theta =$$

$$F_{1x}(\frac{L}{2}\sin\theta - \eta\cos\theta) + F_{1y}(-\frac{L}{2}\cos\theta - \eta\sin\theta)$$

$$+F_{2x}(-\frac{L}{2}\sin\theta - \eta\cos\theta) + F_{2y}(\frac{L}{2}\cos\theta - \eta\sin\theta)$$

Integrating all the terms in $\delta\theta$ ($\rho \int_{\frac{-L}{2}}^{\frac{L}{2}} dx$)

$$-\rho\ddot{\theta} \int_{\frac{-L}{2}}^{\frac{L}{2}} \eta^2 dx$$

$$-\rho\ddot{\theta} \int_{\frac{-L}{2}}^{\frac{L}{2}} x^2 dx = -\frac{mL^2}{12}\ddot{\theta}$$

$$\rho\ddot{x}_0 \cos\theta \int_{\frac{-L}{2}}^{\frac{L}{2}} \eta dx$$

$$\rho\ddot{y}_0 \sin\theta \int_{\frac{-L}{2}}^{\frac{L}{2}} \eta dx$$

$$\rho \int_{\frac{-L}{2}}^{\frac{L}{2}} x\ddot{y}_0 \cos\theta dx = 0$$

$$\rho \int_{\frac{-L}{2}}^{\frac{L}{2}} x\ddot{x}_0 \sin\theta dx = 0$$

Separating $\delta\eta$ components

$$\dot{\theta}^2\eta - (x\ddot{\theta} + \ddot{\eta}) - \dot{x}_0\dot{\theta}\cos\theta - \dot{y}_0\dot{\theta}\sin\theta - \ddot{y}_0\cos\theta + \dot{y}_0\dot{\theta}\sin\theta + \ddot{x}_0\sin\theta + \dot{x}_0\dot{\theta}\cos\theta + \frac{EI}{\rho}\eta^{iv}$$
$$= -F_{1x}\sin\theta + F_{1y}\cos\theta - F_{2x}\sin\theta + F_{1y}\cos\theta$$

Appendix B

Regressor for Manipulator - Flexible Object System in Cartesian Space

B.1 Time dependent parameters

$$Y_{cs} = \begin{bmatrix} Y_{cs}^{a1} & Y_{cs}^{a2} & Y_{cs}^{a3} & Y_{cs}^{a4} & Y_{cs}^{a5} & .... & Y_{cs}^{a16} & Y_{cs}^{a17} & Y_{cs}^{a18} & Y_{cs}^{a19} & Y_{cs}^{a20} \\ Y_{cs}^{b1} & Y_{cs}^{b2} & Y_{cs}^{b3} & Y_{cs}^{b4} & Y_{cs}^{b5} & .... & Y_{cs}^{b16} & Y_{cs}^{b17} & Y_{cs}^{b18} & Y_{cs}^{b19} & Y_{cs}^{b20} \\ Y_{cs}^{c1} & Y_{cs}^{c2} & Y_{cs}^{c3} & Y_{cs}^{c4} & Y_{cs}^{c5} & .... & Y_{cs}^{c16} & Y_{cs}^{c17} & Y_{cs}^{c18} & Y_{cs}^{c19} & Y_{cs}^{c20} \end{bmatrix}$$

$$\begin{aligned} Y_{cs}^{a1} &= \frac{\cos(q_1+q_2)^2\ddot{x}_0}{\sin(q_2)^2} + \frac{\sin(2q_1+2q_2)\ddot{y}_0}{2\sin(q_2)^2} - \frac{\cos(q_1+q_2)\ddot{\theta}[\sin(q_1+q_2-\theta)-2\sin(q_3)]}{2\sin(q_2)^2} \\ &\quad + \frac{\cos(\theta)\dot{\theta}^2+\cos(2q_1+2q_2-\theta)\dot{\theta}^2}{4\sin(q_2)^2} - \frac{\sin(2q_1+2q_2)\dot{x}_0}{2\sin(q_2)^2\dot{q}_1} + \frac{\cos(2q_1+2q_2)\dot{y}_0}{\sin(q_2)^2\dot{q}_1} \\ &\quad + \frac{\cos(2q_1+2q_2)[\sin(q_3)\dot{q}_1-0.5\cos(q_1+q_2-\theta)+\sin(q_3)\dot{q}_2+\sin(q_3)\dot{q}_3]\dot{\theta}}{\sin(q_2)^2\dot{q}_1} \\ Y_{cs}^{b1} &= -\frac{\sin(q_1+q_2)^2\ddot{y}_0}{\sin(q_2)^2} + \frac{\sin(2q_1+2q_2)\ddot{x}_0}{2\sin(q_2)^2} - \frac{\sin(q_1+q_2)[\sin(q_1+q_2-\theta)-2\sin(q_3)]\ddot{\theta}}{2\sin(q_2)^2} \end{aligned}$$

$$
\begin{aligned}
&-\frac{\sin(\theta)\dot{\theta}^2+\sin(2q_1+2q_2-\theta)\dot{\theta}^2}{4\sin(q_2)^2}+\frac{\sin(2q_1+2q_2)\dot{y}_0}{2\sin(q_2)^2\dot{q}_1}-\frac{\sin(2q_1+2q_2)\dot{x}_0}{\sin(q_2)^2\dot{q}_1}\\
&+\frac{\sin(2q_1+2q_2)[\sin(q_3)\dot{q}_1-0.5\cos(q_1+q_2-\theta)+\sin(q_3)\dot{q}_2+\sin(q_3)\dot{q}_3]\dot{\theta}}{\sin(q_2)^2\dot{q}_1}
\end{aligned}
$$

$$
\begin{aligned}
Y_{cs}^{c1} \;=\;& \frac{[2\sin(q_3)+\cos(q_1+q_2)\sin(\theta)-\sin(q_1+q_2)\cos(\theta)]^2\ddot{\theta}}{4\sin(q_2)^2}\\
&-\frac{\cos(q_1+q_2)[\sin(q_1+q_2-\theta)-2\sin(q_3)]\ddot{x}_0}{2\sin(q_2)^2}\\
&-\frac{\sin(q_1+q_2)[\sin(q_1+q_2-\theta)+2\sin(q_3)]\ddot{y}_0}{2\sin(q_2)^2}\\
&+\frac{\sin(q_1+q_2)[\sin(q_1+q_2-\theta)-2\sin(q_3)]\ddot{x}_0}{2\sin(q_2)^2\dot{q}_1}\\
&-\frac{[0.5\sin(q_1+q_2-\theta)-2\sin(q_3)][\sin(q_3)\dot{q}_1-0.5\cos(q_1+q_2-\theta)}{\sin(q_2)^2\dot{q}_1}\\
&-\frac{[0.5\sin(q_1+q_2-\theta)-2\sin(q_3)][\sin(q_3)\dot{q}_2+\sin(q_3)\dot{q}_3]}{\sin(q_2)^2\dot{q}_1}\\
&-\frac{\cos(q_1+q_2)[\sin(q_1+q_2-\theta)-2\sin(q_3)]\dot{y}_0}{2\sin(q_2)^2\dot{q}_1}\\
&-\frac{\cos(q_1+q_2-\theta)[\sin(q_1+q_2-\theta)-2\sin(q_3)]\dot{\theta}^2}{4\sin(q_2)^2}
\end{aligned}
$$

$j11=\sin(q_1+2q_2+q_3);\quad j12=\sin(q_1+q_3);\quad j13=\sin(2q_1+q_2-\theta);$

$j14=\cos(q_1+q_2)\sin(q_2+q_3);\quad j15=\cos(q_1)\sin(q_3);\quad j16=[\cos(q_1+q_2)]\cos(q_1)\cos(\theta);$

$j17=\sin(q_1)\sin(\theta);\quad j18=[\sin(q_1+q_2)]\cos(q_1)\sin(\theta);\quad j19=\cos(q_1)sin(q_3);$

$j20=\cos(q_1+2q_2+q_3);\quad j21=\cos(2q_1+q_2-\theta);\quad j22=\cos(q_2+\theta);$

$j23=\sin(q_1+q_2)\sin(q_2+q_3);\quad j24=\sin(q_1)\sin(q_3);\quad j25=\cos(q_1+q_2)\cos(\theta)\sin(q_1);$

$j26=\sin(q_1+q_2)\cos(\theta)\cos(q_1);\quad j27=\sin(q_1+q_2)\sin(\theta)\sin(q_1);\quad j28=\sin(2q_1+q_2);$

$j29=\sin(q_2)^2\dot{q}_1(\dot{q}_1+\dot{q}_2);\quad j30=\cos(q_1+2q_2+q_3);$

$j31=\cos(2q_1+q_2-\theta);\quad j32=\sin(q_1+2q_2+q_3);\quad j33=\sin(2q_1+q_2-\theta);$

$j34=\cos(q_1+q_2)\sin(\theta);\quad j35=\sin(q_1+q_2)\cos(\theta);\quad j36=\frac{\sin(q_1+q_2-\theta)}{2\sin(q_2)}-\frac{\sin(q_3)}{\sin(q_2)};$

$j37=2\cos(q_1+q_2)\cos(q_2);\quad j38=\cos(q_2)[\cos(q_1+q_2)\dot{q}_1+\cos(q_1+q_2)\dot{q}_2+\cos(q_1)\dot{q}_1];$

$j39=2\sin(q_1+q_2)\cos(q_2);\quad j40=\cos(q_2)[\sin(q_1+q_2)\dot{q}_1+\sin(q_1+q_2)\dot{q}_2+\sin(q_1)\dot{q}_1];$

$$j41 = 2\cos(q_2)\sin(q_3)(\dot{q}_1+\dot{q}_2+\dot{q}_3);$$

$$j42 = [\sin(q_2+q_3)\dot{q}_1+\sin(q_3)\dot{q}_1+\sin(q_3)\dot{q}_2]\cos(q_2)(\dot{q}_1+\dot{q}_2+\dot{q}_3)$$

$$j43 = \cos(q_1+q_2)\cos(q_2)\cos(\theta); \quad j44 = \cos(q_2)\sin(q_3)(\dot{q}_1+\dot{q}_2+\dot{q}_3);$$

$$j45 = \sin(q_1+q_2)\cos(q_2)\sin(\theta); \quad j46 = \sin(q_2+q_3)+\sin(q_3);$$

$$j47 = \sin(\theta)[\cos(q_1+q_2)+\cos(q_1)]; \quad j48 = \frac{j_{43}}{2\sin q_2\dot{q}_1} - \frac{j_{44}}{\sin q_2\dot{q}_1} + \frac{j_{45}}{2\sin q_2\dot{q}_1};$$

$$j49 = \frac{j_{46}}{\sin q_2} + \frac{j_{47}}{2\sin q_2} - \frac{j_{47}}{2\sin q_2}; \quad j50 = \frac{\sin(q_1+q_2-\theta)}{2\sin(q_2)} - \frac{\sin(q_3)}{\sin(q_2)};$$

$$j51 = \cos(q_1+q_2)\dot{q}_1+\cos(q_1+q_2)\dot{q}_2+\cos(q_1)\dot{q}_1; \quad j52 = \sin(q_2+q_3)+\sin(q_3);$$

$$j53 = \sin(\theta)[\cos(q_1+q_2)+\cos(q_1)]; \quad j54 = \cos(\theta)[\sin(q_1+q_2)+\sin(q_1)];$$

$$j55 = 2\cos(q_1+q_2)\cos(q_2); \quad j56 = 2\sin(q_1+q_2)\cos(q_2);$$

$$j57 = \sin(q_1+q_2)\dot{q}_1+\sin(q_1+q_2)\dot{q}_2+\sin(q_1)\dot{q}_1; \quad j58 = \sin(q_2)\dot{q}_1;$$

$$j59 = \sin(q_2)\dot{q}_1(\dot{q}_1+\dot{q}_2); \quad j60 = \frac{j_{52}}{\sin(q_2)} + \frac{j_{53}}{2\sin(q_2)} - \frac{j_{54}}{2\sin(q_2)}; \quad j61 = \sin(q_1+2q_2+q_3);$$

$$j62 = \sin(q_1+q_3); \quad j63 = \sin(2q_1+q_2-\theta); \quad j64 = \sin(q_2-\theta);$$

$$j65 = \cos(q_1+2q_2+q_3); \quad j66 = \cos(q_1+q_3); \quad j67 = \cos(2q_1+q_2-\theta);$$

$$j68 = \cos(q_2-\theta); \quad j69 = \frac{\sin(2q_1+2q_2-2\theta)}{8}; \quad j70 = \frac{\sin(q_1+q_2-q_3-\theta)}{4};$$

$$j71 = \frac{\sin(q_1-q_2+q_3-\theta)}{8}; \quad j72 = \frac{\sin(q_1+3q_2+q_3-\theta)}{8};$$

$$j73 = \frac{\sin(2q_1-2\theta)}{8}; \quad j74 = \frac{\sin(q_1-q_2-q_3-\theta)}{4}; \; j75 = \frac{\sin(q_1+q_2+q_3-\theta)}{4}; \quad j76 = \cos(q_1+q_2)\sin(\theta);$$

$$j77 = \sin(q_1+q_2)\cos(\theta); \quad j78 = \cos(q_1)\sin(\theta); \quad j79 = \sin(q_1)\cos(\theta);$$

$$\begin{aligned} Y_{cs}^{a2} \;=\; & -\frac{[\sin(2q_1)+\sin(2q_1+2q_2)]\ddot{y}_0}{2\sin(q_2)^2} \\ & -\frac{[2\sin(q_1-q_3)+0.5\sin(q_2-\theta)-j11-j12-0.5\sin(q_2+\theta)+j13]\cos(q_2)\ddot{\theta}}{2(\cos(q_2)^2-1)} \\ & -\frac{2[\cos(q_1+q_2)\cos(q_1)\cos(q_2)]\ddot{x}_0}{\sin(q_2)^2} \\ & +\frac{[2j_{11}\dot{q}_1+2j_{11}\dot{q}_2-2j_{12}\dot{q}_1+\sin(q_2+\theta)\dot{q}_1+\sin(q_2+\theta)\dot{q}_2-j_{13}\dot{q}_2]\dot{\theta}}{4\sin(q_2)} \end{aligned}$$

$$
\begin{aligned}
&+\frac{[\sin(q_2-\theta)\dot{q}_1 - j_{13}\dot{q}_2 - 2\sin(q_1-q_3)\dot{q}_2 + \sin(q_2-\theta)\dot{q}_1]\dot{\theta}}{4\sin(q_2)} \\
&-\frac{[2\dot{q}_1+\dot{q}_2]\dot{y}_0}{2} - \frac{\cot(q_2)[\cot(q_2)\cos(\theta) - \sin(2q_1-\theta) + \cos(2q_1-\theta)\cot(q_2)]\dot{\theta}^2}{2} \\
&+\frac{\sin(2q_1+q_2)\dot{q}_1\dot{y}_0}{2\sin(q_2)} + \frac{\cos(q_1+q_2)\dot{q}_2\cos(q_1)\dot{x}_0}{\sin(q_2)} \\
&+\frac{[2j_{14}\dot{q}_1^2 + 2j_{15}\dot{q}_1^2 + 2j_{15}\dot{q}_2^2 - 2j_{16}\dot{q}_1 - j_{16}\dot{q}_2]\cos(q_2)\dot{\theta}}{\sin(q_2)^2\dot{q}_1(\dot{q}_1+\dot{q}_2)} \\
&+\frac{[-j_{17}\dot{q}_1 - j_{18}\dot{q}_1 - j_{18}\dot{q}_2 + 2j_{14}\dot{q}_1\dot{q}_2 - 2j_{19}\dot{q}_1\dot{q}_3 + 2j_{19}\dot{q}_2\dot{q}_2]\cos(q_2)\dot{\theta}}{\sin(q_2)^2\dot{q}_1(\dot{q}_1+\dot{q}_2)} \\
&-\frac{[\cos(q_1+q_2)\cos(q_1)\cos(q_2)](2\dot{q}_1+\dot{q}_2)\dot{y}_0}{\sin(q_2)^2\dot{q}_1(\dot{q}_1+\dot{q}_2)}
\end{aligned}
$$

$$
\begin{aligned}
Y_{cs}^{b2} \quad = \quad & -\frac{\sin(2q_1)+\sin(2q_1+2q_2)\ddot{x}_0}{2\sin(q_2)^2} - \frac{2\sin(q_1+q_2)\cos(q_2)\sin(q_1)\ddot{y}_0}{\sin(q_2)^2} + 2\frac{[\dot{q}_1+\dot{q}_2]\dot{x}_0}{2} \\
&-\frac{0.5\cos(q_2-\theta) - 2\sin(q_1-q_3) + j20 + \cos(q_1+q_3) + 0.5\cos(q_2+\theta) - j21}{2(\cos(q_2)^2-1)} \\
&-\frac{[2j_{20}\dot{q}_1 + 2j_{20}\dot{q}_2 + 2\cos(q_1+q_3)\dot{q}_1 + j_{22}\dot{q}_1 + j_{22}\dot{q}_2 - j_{21}\dot{q}_2]\dot{\theta}}{4\sin(q_2)} \\
&-\frac{[2\cos(q_1-q_3)\dot{q}_2 - \cos(q_2-\theta)\dot{q}_1]\dot{\theta}}{4\sin(q_2)} \\
&-\frac{[\cos(2q_1-\theta) + \cot(q_2)\sin(\theta) + \sin(2q_1-\theta)\cot(q_2)]\cot(q_2)\dot{\theta}^2}{2} \\
&+\frac{\sin(q_1+q_2)\sin(q_1)\dot{q}_2\dot{y}_0}{\sin(q_2)} + \frac{\sin(2q_1+q_2)\dot{q}_2\dot{x}_0}{2\sin(q_2)} \\
&-\frac{2j_{23}\dot{q}_1^2 + 2j_{24}\dot{q}_1^2 + 2j_{24}\dot{q}_2^2 - j_{25}\dot{q}_1 - j_{26}\dot{q}_1 - j_{25}\dot{q}_2 - 2j_{27}\dot{q}_1}{2\sin(q_2)^2\dot{q}_1(\dot{q}_1+\dot{q}_2)} \\
&-\frac{j_{27}\dot{q}_2 + 2j_{23}\dot{q}_1\dot{q}_2 + 2j_{23}\dot{q}_1\dot{q}_3 + 4j_{24}\dot{q}_1\dot{q}_2 + 2j_{24}\dot{q}_1\dot{q}_3 + 2j_{24}\dot{q}_2\dot{q}_3}{2j_{29}} \\
&-\frac{[j_{28}\dot{q}_1 - 0.5\sin(q_2)\dot{q}_2 + 0.5j_{28}\dot{q}_2]\cos(q_2)\dot{y}_0}{j_{29}} \\
&+\frac{\sin(q_1+q_2)\cos(q_2)\sin(q_1)[2\dot{q}_1+\dot{q}_2]\dot{x}_0}{j_{29}}
\end{aligned}
$$

$$
\begin{aligned}
Y_{cs}^{c2} \quad = \quad & -\frac{[0.5\cos(q_2-\theta) - 2\cos(q_1-q_3) + j_{30} + \cos(q_1+q_3)]\cos(q_2)\ddot{y}_0}{2(\cos(q_2)^2-1)} \\
&-\frac{[0.5\cos(q_2+\theta) - j_{31}]\cos(q_2)\ddot{y}_0}{2(\cos(q_2)^2-1)} \\
&-\frac{[2\sin(q_1-q_3) + 0.5\sin(q_2-\theta) - j_{32} - \sin(q_1+q_3) - 0.5\sin(q_2+\theta)]\cos(q_2)\ddot{x}_0}{2(\cos(q_2)^2-1)}
\end{aligned}
$$

$$
\begin{aligned}
&-\frac{[2\sin(q_3)+j_{34}-j_{35}][2\sin(q_2+q_3)+\cos(q_1)\sin(\theta)-\cos(\theta)\sin(q_1)]\cos(q_2)\ddot{\theta}}{2\sin(q_2)^2}\\
&+\{(0.5\cos(\theta)[\frac{j_{37}}{j_{58}}-\frac{j_{38}}{j_{59}}]+0.5\sin(\theta)[\frac{j_{39}}{j_{58}}-\frac{j_{40}}{j_{59}}]-\frac{j_{41}}{j_{58}}+\frac{j_{42}}{j_{59}})j_{36}+j_{48}j_{49}\}\dot{\theta}\\
&-\{[\frac{j_{55}}{j_{58}}-\frac{\cos(q_2)j_{51}}{j_{59}}]j_{50}+\frac{\cos(q_1+q_2)\cos(q_2)j_{60}}{j_{58}}\}\dot{y}_0\\
&+\{[\frac{j_{56}}{j_{58}}-\frac{\cos(q_2)j_{57}}{j_{59}}]j_{50}+\frac{\sin(q_1+q_2)\cos(q_2)j_{60}}{j_{58}}\}\dot{x}_0\\
&-\frac{[2j_{61}\dot{q}_1-2j_{62}\dot{q}_1-2j_{62}\dot{q}_2+\sin(q_2+\theta)\dot{q}_1+j_{63}\dot{q}_2+2\sin(q_1-q_3)\dot{q}_2+j_{64}\dot{q}_1]\dot{x}_0}{4\sin(q_2)}\\
&+\frac{[2j_{65}\dot{q}_1-2j_{66}\dot{q}_1-2j_{66}\dot{q}_2+\cos(q_2+\theta)\dot{q}_1+j_{67}\dot{q}_2+2\cos(q_1-q_3)\dot{q}_2-j_{68}\dot{q}_1]\dot{y}_0}{4\sin(q_2)}\\
&+\frac{[j_{69}+j_{70}-j_{71}-j_{72}+j_{73}+j_{74}-j_{75}]\dot{\theta}^2}{\sin(q_2)^2}\\
&+\frac{[2\sin(q_3)+j_{76}-j_{77}][2\sin(q_2+q_3)+j_{78}-j_{79}]\dot{q}_2\dot{\theta}}{4\sin(q_2)}
\end{aligned}
$$

$k11=\sin(q_1-\theta)-2\sin(q_2+q_3);\quad k12=\cos(q_1)\cos(q_3);\quad k13=\cos(q_3)\sin(q_1);$

$k14=\cos(q_1-\theta)\cos(q_3);\quad k15=\sin(q_1)\sin(q_3);\quad k16=\sin(q_2+q_3);$

$k17=\sin(q_1-\theta);\quad k18=\sin(q_2)\dot{q}_1+\sin(q_2)\dot{q}_2$

$$
\begin{aligned}
Y_{cs}^{a3} &= -\frac{\cos(q_1)\cos(q_3)\ddot{\theta}}{\sin(q_2)}+\frac{\cos(q_1)\sin(q_3)(\dot{q}_1+\dot{q}_2+\dot{q}_3)\dot{\theta}}{\sin(q_2)}-\frac{\cos(q_1)\cos(q_3)\dot{\theta}}{\sin(q_2)}\\
Y_{cs}^{b3} &= -\frac{\cos(q_3)\sin(q_1)\ddot{\theta}}{\sin(q_2)}+\frac{\sin(q_1)\cos(q_3)(\dot{q}_1+\dot{q}_2+\dot{q}_3)\dot{\theta}}{\sin(q_2)}-\frac{\cos(q_3)\sin(q_1)\dot{\theta}}{\sin(q_2)}\\
Y_{cs}^{c3} &= -\frac{\cos(q_3)k_{11}\ddot{\theta}}{\sin(q_2)}-\frac{k_{12}\ddot{x}_0}{\sin(q_2)}-\frac{k_{13}\ddot{y}_0}{\sin(q_2)}+\frac{k_{13}\dot{x}_0}{k_{18}}-\frac{k_{12}\dot{y}_0}{k_{18}}-\frac{k_{14}\dot{\theta}^2}{2\sin(q_2)}-\frac{k_{15}(\dot{q}_1+\dot{q}_2)\dot{y}_0}{\sin(q_2)}\\
&\quad -\frac{\sin(q_3)k_{11}\dot{q}_3\dot{\theta}}{2\sin(q_2)}-\frac{k_{13}(\dot{q}_1+\dot{q}_2)\dot{x}_0}{\sin(q_2)}\\
&\quad +\frac{\cos(q_3)[\cos(q_1-\theta)-4k_{16}\dot{q}_1-4k_{16}\dot{q}_2-2k_{16}\dot{q}_3+k_{17}\dot{q}_1+k_{17}\dot{q}_2]\dot{\theta}}{2\sin(q_2)(\dot{q}_1+\dot{q}_2)}
\end{aligned}
$$

$n11=\cos(q_1+q_2)\cos(q_2+q_3);\quad n12=\cos(q_1+q_2)\sin(q_2+q_3);$

$n13=\cos(q_2+q_3)\sin(q_1+q_2);\quad n14=\sin(q_1+q_2)\sin(q_2+q_3);$

$n15=\sin(q_1+q_2-q_3-\theta);\quad n16=\sin(q_1+3q_2+q_3-\theta);$

$n17=\sin(q_1-q_2-q_3-\theta);\quad n18=\sin(q_1+q_2+q_3-\theta);\quad n19=\cos(q_1+q_2-q_3-\theta);$

$n20 = \cos(q_1 + 3q_2 + q_3 - \theta)$; $n21 = \cos(2q_2 + 2q_3)$; $n22 = \cos(q_1 - q_2 - q_3 - \theta)$;

$n23 = \cos(q_1 + q_2 + q_3 - \theta)$; $n24 = \cos(2q_2)$; $n25 = \cos(2q_3)$.

$$
\begin{aligned}
Y_{cs}^{a4} &= \frac{n_{11}\ddot{\theta}}{\sin(q_2)} + \frac{n_{11}\dot{\theta}}{\sin(q_2)} - \frac{n_{12}(\dot{q}_1 + \dot{q}_2 + \dot{q}_3)\dot{\theta}}{\sin(q_2)} \\
Y_{cs}^{b4} &= \frac{n_{13}\ddot{\theta}}{\sin(q_2)} + \frac{n_{13}\dot{\theta}}{\sin(q_2)} - \frac{n_{14}(\dot{q}_1 + \dot{q}_2 + \dot{q}_3)\dot{\theta}}{\sin(q_2)} \\
Y_{cs}^{c4} &= \frac{n_{11}\ddot{x}_0}{\sin(q_2)} + \frac{n_{13}\ddot{y}_0}{\sin(q_2)} - \frac{\cos(q_2 + q_3)[\sin(q_1 + q_2 - \theta) - 2\sin(q_3)]\ddot{\theta}}{\sin(q_2)} \\
&\quad + \frac{0.5\cos(q_1 + 2q_2 + q_3)\dot{y}_0 + 0.5\cos(q_1 - q_3)\dot{y}_0}{\sin(q_2)\dot{q}_1} \\
&\quad + \frac{[\cos(q_1 + 2q_2 + q_3 - \theta) + \cos(q_1 - q_3 - \theta)]\dot{\theta}^2}{4\sin(q_2)} \\
&\quad - \frac{[4\dot{q}_1 + 2\dot{q}_2 + 2\dot{q}_3 + n_{15} + n_{16} - n_{17} - n_{18} - n_{19}\dot{q}_1 - n_{20}\dot{q}_1 + 4n_{21}\dot{q}_1 + 2n_{21}\dot{q}_2]\dot{\theta}}{8\sin(q_2)^2\dot{q}_1} \\
&\quad + \frac{[n_{22}\dot{q}_1 + n_{23}\dot{q}_1 - 4n_{24}\dot{q}_1 - 2n_{24}\dot{q}_2 - 2n_{24}\dot{q}_3 - 4n_{25}\dot{q}_1 - 2n_{25}\dot{q}_2 - 2n_{25}\dot{q}_3]\dot{\theta}}{8\sin(q_2)^2\dot{q}_1} \\
&\quad - \frac{[\sin(q_1 - q_3) + \sin(q_1 + 2q_2 + q_3)]\dot{x}_0}{2\sin(q_2)\dot{q}_1} \\
&\quad + \frac{\sin(q_2 + q_3)(\dot{q}_2 + \dot{q}_3)[\sin(q_1 + q_2 - \theta) - 2\sin(q_3)]\dot{\theta}}{2\sin(q_2)} \\
&\quad + \frac{\cos(q_1 + q_2)\sin(q_2 + q_3)\dot{q}_1\dot{x}_0}{\sin(q_2)} + \frac{\sin(q_1 + q_2)\sin(q_2 + q_3)\dot{q}_1\dot{y}_0}{\sin(q_2)}
\end{aligned}
$$

$q31 = \sin(q_1 + q_2)^2 - \sin(q_1)^2$; $q32 = \sin(2q_1) - \sin(2q_1 + 2q_2)$;

$q33 = \sin(2q_1 + 2q_2 - \theta)$; $q34 = \sin(2q_1 - \theta)$; $q35 = \sin(q_1 + q_2 - q_3)$;

$q36 = \sin(q_1 - q_2 - q_3)$; $q37 = \cos(2q_1 + 2q_2 - \theta)$; $q38 = \cos(2q_1 - \theta)$;

$q39 = \cos(q_1 + q_2)^2$; $q40 = \sin(q_1 + q_2 + q_3)$; $q41 = \sin(2q_1 + 2q_2)$; $q42 = \sin(q_1 + q_2)^2$;

$q43 = \cos(q_1 + q_2 + q_3)$; $q44 = \cos(q_1 + q_2 - q_3)$; $q45 = \cos(q_1 - q_2 - q_3)$;

$q46 = \cos(2q_1 + 2q_2 - 2\theta)$; $q47 = \cos(q_1 + q_2 - q_3 - \theta)$; $q48 = \cos(q_1 - q_2 - q_3 - \theta)$;

$q49 = \sin(q_1 + q_2 - q_3 - \theta)$; $q50 = \sin(q_1 - q_2 - q_3 - \theta)$;

$q51 = \sin(q_1+q_2-\theta)$; $q52 = \sin(q_2+q_3)$; $q53 = \cos(q_1+q_2-\theta)$.

$$
\begin{aligned}
Y_{cs}^{a5} &= \frac{q_{31}\ddot{x}_0}{\sin(q_2)^2} + \frac{q_{32}\ddot{y}_0}{2\sin(q_2)^2} + \frac{[q_{33}-q_{34}+2q_{35}-2q_{36}]\ddot{\theta}}{4\sin(q_2)^2} \\
&\quad - \frac{[q_{37}-q_{38}]\dot{\theta}^2}{4\sin(q_2)^2} - \frac{[q_{39}\dot{q}_1+q_{39}\dot{q}_2]\dot{y}_0}{\sin(q_2)^2\dot{q}_1(\dot{q}_1+\dot{q}_2)} \\
&\quad - \frac{[\cos(\theta)\dot{q}_2 - q_{38}\dot{q}_1 - 2q_{40}\dot{q}_2^2]\dot{\theta}}{2\cos(2q_2-1)\dot{q}_1(\dot{q}_1+\dot{q}_2)} - \frac{[2q_{36}\dot{q}_1^2+2q_{35}\dot{q}_1^2+2q_{35}\dot{q}_2^2]\dot{\theta}}{2\cos(2q_2-1)\dot{q}_1(\dot{q}_1+\dot{q}_2)} \\
&\quad + \frac{[q_{37}\dot{q}_1+q_{37}\dot{q}_2-2q_{36}\dot{q}_1\dot{q}_2-2q_{36}\dot{q}_1\dot{q}_3-2q_{40}\dot{q}_1\dot{q}_2-2q_{40}\dot{q}_2\dot{q}_3+4q_{35}\dot{q}_1\dot{q}_2]\dot{\theta}}{2\cos(2q_2-1)\dot{q}_1(\dot{q}_1+\dot{q}_2)} \\
&\quad + \frac{[2q_{40}\dot{q}_1\dot{q}_3+2q_{35}\dot{q}_2\dot{q}_3]\dot{\theta}}{2\cos(2q_2-1)\dot{q}_1(\dot{q}_1+\dot{q}_2)} - \frac{[q_{41}\dot{q}_1-\sin(2q_1)\dot{q}_1+q_{41}\dot{q}_2]\dot{x}_0}{\cos(2q_2-1)\dot{q}_1(\dot{q}_1+\dot{q}_2)}
\end{aligned}
$$

$$
\begin{aligned}
Y_{cs}^{b5} &= \frac{[\sin(2q_1)-q_{41}]}{2\sin(q_2)^2} - \frac{[q_{37}-q_{38}+2q_{44}-2q_{45}]\ddot{\theta}}{4\sin(q_2)^2} - \frac{q_{31}\ddot{y}_0}{\sin(q_2)^2} \\
&\quad - \frac{[q_{33}\dot{q}_1+q_{33}\dot{q}_2+2q_{43}\dot{q}_2^2-q_{34}\dot{q}_1-2q_{44}\dot{q}_1^2-2q_{44}\dot{q}_2^2+\sin(\theta)\dot{q}_2+2q_{45}\dot{q}_1^2]\dot{\theta}}{2\cos(2q_2-1)\dot{q}_1\dot{q}_1\dot{q}_2} \\
&\quad + \frac{[2q_{43}\dot{q}_2\dot{q}_3-4q_{44}\dot{q}_1\dot{q}_2-2q_{44}\dot{q}_1\dot{q}_3-2q_{44}\dot{q}_2\dot{q}_3+2q_{45}\dot{q}_1\dot{q}_2+2q_{45}\dot{q}_1\dot{q}_3]\dot{\theta}}{2\cos(2q_2-1)\dot{q}_1(\dot{q}_1+\dot{q}_2)} \\
&\quad - \frac{[q_{33}-q_{34}]\dot{\theta}^2}{4\sin(q_2)^2} - \frac{[q_{41}\dot{q}_1-\sin(2q_1)\dot{q}_1+q_{41}\dot{q}_2]\dot{y}_0}{\cos(2q_2-1)\dot{q}_1(\dot{q}_1+\dot{q}_2)} + \frac{[q_{42}\dot{q}_1-\sin(q_1)^2\dot{q}_1+q_{42}\dot{q}_2]\dot{x}_0}{\sin(q_2)^2\dot{q}_1(\dot{q}_1+\dot{q}_2)}
\end{aligned}
$$

$$
\begin{aligned}
Y_{cs}^{c5} &= \frac{[\sin(2q_1)-q_{41}]\ddot{x}_0}{2\sin(q_2)^2} - \frac{[q_{37}-q_{38}+2q_{44}-2q_{45}]\ddot{\theta}}{4\sin(q_2)^2} - \frac{q_{31}\ddot{y}_0}{\sin(q_2)^2} \\
&\quad + \frac{[q_{42}\dot{q}_1-\sin(q_1)^2\dot{q}_1+q_{42}\dot{q}_2]\dot{x}_0}{\sin(q_2)^2\dot{q}_1(\dot{q}_1+\dot{q}_2)} \\
&\quad - \frac{[0.5\sin(q_1-\theta)+0.5q_{51}-q_{52}][q_{52}\dot{q}_1-0.5\cos(q_1-\theta)+q_{52}\dot{q}_2+q_{52}\dot{q}_3]\dot{\theta}}{\sin(q_2)^2(\dot{q}_1+\dot{q}_2)} \\
&\quad - \frac{[0.5q_{51}-\sin(q_3)][\sin(q_3)\dot{q}_1^2+\sin(q_3)\dot{q}_2^2-0.5q_{53}\dot{q}_1-0.5q_{53}\dot{q}_2]\dot{\theta}}{\sin(q_2)^2\dot{q}_1(\dot{q}_1+\dot{q}_2)} \\
&\quad - \frac{[0.5q_{51}-\sin(q_3)][-0.5\cos(q_1-\theta)\dot{q}_1+q_{54}\dot{q}_1^2]}{\sin(q_2)^2\dot{q}_1(\dot{q}_1+\dot{q}_2)} \\
&\quad + \frac{[0.5q_{51}-\sin(q_3)][2\sin(q_3)\dot{q}_1\dot{q}_2+\sin(q_3)\dot{q}_1\dot{q}_3+\sin(q_3)\dot{q}_2\dot{q}_3]\dot{\theta}}{\sin(q_2)^2\dot{q}_1(\dot{q}_1+\dot{q}_2)} \\
&\quad + \frac{[\sin(q_2+q_3)\dot{q}_1\dot{q}_2+\sin(q_2+q_3)\dot{q}_1\dot{q}_3]\dot{\theta}}{\sin(q_2)^2\dot{q}_1(\dot{q}_1+\dot{q}_2)} \\
&\quad + \frac{[q_{38}\dot{q}_1-2q_{44}\dot{q}_1-2q_{44}\dot{q}_2+2q_{45}\dot{q}_1+\cos(\theta)\dot{q}_2+2q_{43}\dot{q}_2-q_{37}\dot{q}_1-q_{37}\dot{q}_2]\dot{x}_0}{2\cos(2q_2-1)\dot{q}_1(\dot{q}_1+\dot{q}_2)} \\
&\quad - \frac{[q_{33}\dot{q}_1+q_{33}\dot{q}_2-q_{34}\dot{q}_1+2q_{35}\dot{q}_1+2q_{35}\dot{q}_2-2q_{36}\dot{q}_1-\sin(\theta)\dot{q}_2-2q_{40}\dot{q}_2]\dot{y}_0}{2\cos(2q_2-1)\dot{q}_1(\dot{q}_1+\dot{q}_2)}
\end{aligned}
$$

$r11 = \sin(q_1 - \theta);\quad r12 = \sin(q_2 + q_3);\quad r13 = \cos(2q_1 - \theta);\quad r14 = \cos(q_1 - \theta);$

$r15 = \sin(2q_1 - \theta);\quad r16 = \sin(2q_1 - 2\theta);\quad r17 = \sin(q_1 - q_2 - q_3 - \theta);$

$r18 = \sin(q_1 + q_2 + q_3 - \theta);\quad r19 = \cos(2q_2 + 2q_3);\quad r20 = \cos(q_1 - q_2 - q_3 - \theta);$

$r21 = \cos(q_1 + q_2 + q_3 - \theta);\quad r22 = \sin(q_1 + q_2 + q_3);\quad r23 = \sin(q_1 - q_2 - q_3);$

$$
\begin{aligned}
Y_{cs}^{a6} &= \frac{[r_{11} - 2r_{12}]\cos(q_1)\ddot{\theta}}{\sin(q_2)^2} - \frac{\sin(2q_1)\ddot{y}_0}{2\sin(q_2)^2} - \frac{\cos(q_1)^2\ddot{x}_0}{\sin(q_2)^2} + \frac{\sin(2q_1)\dot{x}_0}{2\sin(q_2)^2(\dot{q}_1 + \dot{q}_2)} \\
&\quad - \frac{\cos(q_1)^2\dot{y}_0}{\sin(q_2)^2(\dot{q}_1 + \dot{q}_2)} - \frac{[r_{13} + \cos(\theta)]\dot{\theta}^2}{4\sin(q_2)^2} - \frac{[2r_{12}\dot{q}_1 - r_{14} + 2r_{12}\dot{q}_2 + 2r_{12}\dot{q}_3]\cos(q_1)\dot{\theta}}{2\sin(q_2)^2(\dot{q}_1 + \dot{q}_2)} \\
Y_{cs}^{b6} &= \frac{[r_{11} - 2r_{12}]\sin(q_1)\ddot{\theta}}{2\sin(q_2)^2} - \frac{\sin(q_1)^2\ddot{y}_0}{\sin(q_2)^2} - \frac{\sin(2q_1)\ddot{x}_0}{2\sin(q_2)^2} \\
&\quad - \frac{[2r_{12}\dot{q}_1 - r_{14} + 2r_{12}\dot{q}_2 + 2r_{12}\dot{q}_3]\sin(q_1)\dot{\theta}}{2\sin(q_2)^2(\dot{q}_1 + \dot{q}_2)} \\
&\quad + \frac{\sin(q_1)^2\dot{x}_0}{\sin(q_2)^2(\dot{q}_1 + \dot{q}_2)} - \frac{[r_{15} + \sin(\theta)]\dot{\theta}^2}{4\sin(q_2)^2} - \frac{\sin(2q_1)\dot{y}_0}{\sin(q_2)^2(\dot{q}_1 + \dot{q}_2)} \\
Y_{cs}^{c6} &= \ddot{\theta} - \frac{[2r_{12} + \cos(q_1)\sin(\theta) - \cos(\theta)\sin(q_1)]^2\ddot{\theta}}{4\sin(q_2)^2} + \frac{[r_{11} - 2r_{12}]\cos(q_1)\ddot{x}_0}{2\sin(q_2)^2} \\
&\quad + \frac{[r_{11} - 2r_{12}]\sin(q_1)\ddot{y}_0}{2\sin(q_2)^2} + \frac{[r_{16} + 2r_{17} - 2r_{18}]\dot{\theta}^2}{8\sin(q_2)^2} \\
&\quad + \frac{[4\dot{q}_3 + r_{16} + 2r_{17} - 2r_{18} - 4r_{19}\dot{q}_1 - 4r_{19}\dot{q}_2 - 4r_{19}\dot{q}_3 - 2r_{20}\dot{q}_1 - 2r_{20}\dot{q}_2]\dot{\theta}}{4\cos(2q_2 - 1)(\dot{q}_1 + \dot{q}_2)} \\
&\quad - \frac{[2r_{20}\dot{q}_3 + 2r_{21}\dot{q}_1 + 2r_{21}\dot{q}_2 + 2r_{21}\dot{q}_3 + 4\cos(2q_2)\dot{q}_1 + 4\cos(2q_2)\dot{q}_2]\dot{\theta}}{4\cos(2q_2 - 1)(\dot{q}_1 + \dot{q}_2)} \\
&\quad + \frac{[2r_{22} - r_{11} - 2r_{23} + \sin(\theta)]\dot{y}_0}{2\cos(2q_2 - 1)(\dot{q}_1 + \dot{q}_2)} \\
&\quad - \frac{[r_{11} - 2r_{12}]\sin(q_1)\dot{x}_0}{2\sin(q_2)^2(\dot{q}_1 + \dot{q}_2)} \\
Y_{cs}^{a7} &= \frac{\cos(q_1 + q_2)\cos(q_1)}{\sin(q_2)} \\
Y_{cs}^{b7} &= \frac{\sin(q_1 + q_2)\cos(q_1)}{\sin(q_2)} \\
Y_{cs}^{c7} &= -\frac{[\sin(q_1 + q_2 - \theta) - 2\sin(q_3)]\cos(q_1)}{2\sin(q_2)} \\
Y_{cs}^{a8} &= -\frac{\cos(q_1 + q_2)\cos(q_1)}{\sin(q_2)} \\
Y_{cs}^{b7} &= -\frac{\sin(q_1 + q_2)\sin(q_1)}{\sin(q_2)}
\end{aligned}
$$

$$Y_{cs}^{c8} = -\frac{[\sin(q_1-\theta)-2\sin(q_2+q_3)]\cos(q_1+q_2)}{2\sin(q_2)}$$

$$Y_{cs}^{a9} = 0$$

$$Y_{cs}^{b9} = 0$$

$$Y_{cs}^{c9} = \cos(q_1+q_2+q_3)$$

$s11 = \cos(q_4+q_5)^2$; $s12 = \sin(2q_4+2q_5)$; $s13 = \sin(q_4+q_5-\theta)$;

$s14 = \cos(\theta-2q_4)$; $s15 = \sin(\theta-2q_4)$; $s16 = \cos(q_4+q_5-\theta)$; $s17 = \sin(q_4+q_5)^2$;

$s18 = \sin(2q_4+2q_5-\theta)$; $s19 = \sin(2q_4-\theta)$; $s20 = \sin(\theta-q_5-q_4)$;

$$\begin{aligned}
Y_{cs}^{a10} = {} & \frac{s_{11}\ddot{x}_0}{\sin(q_5)^2} + \frac{s_{12}\ddot{y}_0}{2\sin(q_5)^2} + \frac{\cos(q_4+q_5)[s_{13}+2\sin(q_6)]\ddot{\theta}}{2\sin(q_5)^2} + \frac{s_{11}\dot{y}_0}{\dot{q}_4\sin(q_5)^2} - \frac{s_{12}\dot{x}_0}{2\dot{q}_4\sin(q_5)^2} \\
& - \frac{[\cos(\theta)-s_{14}+2s_{15}\cot(q_5)+\cot(q_5)^2\cos(\theta)+s_{14}\cot(q_5)^2]\dot{\theta}^2}{4} + \frac{s_{14}\cot(q_5)^2}{4} \\
& + \frac{\cos(q_4+q_5)[0.5s_{16}+\sin(q_6)\dot{q}_4+\sin(q_6)\dot{q}_5+\sin(q_6)\dot{q}_6]\dot{\theta}}{\dot{q}_4\sin(q_5)^2}
\end{aligned}$$

$$\begin{aligned}
Y_{cs}^{b10} = {} & \frac{s_{17}\ddot{y}_0}{\sin(q_5)^2} + \frac{s_{12}\ddot{x}_0}{2\sin(q_5)^2} + \frac{\sin(q_4+q_5)[s_{13}+2\sin(q_6)]\ddot{\theta}}{2\sin(q_5)^2} + \frac{s_{12}\dot{y}_0}{2\dot{q}_4\sin(q_5)^2} \\
& - \frac{\dot{\theta}^2\sin(\theta)+0.75s_{15}\dot{\theta}^2+s_{18}\dot{\theta}^2+0.753s_{19}\dot{\theta}^2}{4\sin(q_5)^2} \\
& - \frac{s_{17}\dot{x}_0}{\dot{q}_4\sin(q_5)^2} + \frac{\sin(q_4+q_5)[0.5s_{16}+\sin(q_6)\dot{q}_4+\sin(q_6)\dot{q}_5+\sin(q_6)\dot{q}_6]\dot{\theta}}{\dot{q}_4\sin(q_5)^2}
\end{aligned}$$

$$\begin{aligned}
Y_{cs}^{c10} = {} & \frac{(2\sin(q_6)-\cos(q_4+q_5)\sin(\theta)+\sin(q_4+q_5)\cos(\theta))^2\ddot{\theta}}{4\sin(q_5)^2} \\
& + \frac{\cos(q_4+q_5)[s_{13}+2\sin(q_6)]\ddot{x}_0}{2\sin(q_5)^2} \\
& + \frac{\sin(q_4+q_5)[s_{13}+2\sin(q_6)]\ddot{x}_0}{2\sin(q_5)^2} \\
& + \frac{[0.5s_{13}+\sin(q_6)][0.5s_{16}+\sin(q_6)\dot{q}_4+\sin(q_6)\dot{q}_5+\sin(q_6)\dot{q}_6]\dot{\theta}}{\dot{q}_4\sin(q_5)^2} \\
& - \frac{s_{16}[2\sin(q_6)-s_{20}]\dot{\theta}^2}{4\sin(q_5)^2} + \frac{\cos(q_4+q_5)[2\sin(q_6)-s_{20}]\dot{y}_0}{2\sin(q_5)^2\dot{q}_4} \\
& - \frac{\sin(q_4+q_5)[2\sin(q_6)-s_{20}]\dot{x}_0}{2\sin(q_5)^2\dot{q}_4}
\end{aligned}$$

$t11 = \sin(q_5 - \theta);\quad t12 = \sin(q_4 - q_6);\quad t13 = \sin(q_4 + 2q_5 + q_6);\quad t14 = \sin(q_4 + q_6);$

$t15 = \sin(q_5 + \theta);\quad t16 = \sin(2q_4 + q_5 - \theta);\quad t17 = \sin(2q_4 + 2q_5);$

$t18 = \cos(q_4 + q_5);\quad t19 = \sin(2q_4 - \theta);\quad t20 = \cos(2q_4 - \theta);\quad t21 = \sin(2q_4 + q_5);$

$t22 = \cos(q_4 + q_5);\quad t23 = \sin(q_5 + q_6);\quad t24 = \sin(q_4 + q_5);\quad t25 = \sin(2q_4 + q_5);$

$t26 = \cos(q_4 - q_6);\quad t27 = \cos(q_5 - \theta);\quad t28 = \cos(q_4 + 2q_5 + q_6);\quad t29 = \cos(q_4 + q_6);$

$t30 = \cos(q_5 + \theta); t31 = \cos(2q_4 + q_5 - \theta);\quad t32 = \sin(\theta - q_5 - q_4);\quad t33 = (\dot{q}_4 + \dot{q}_5 + \dot{q}_6);$

$t34 = \sin(2q_4 + 2q_5 - 2\theta);\quad t35 = \sin(q_4 + q_5 - q_6 - \theta);\quad t36 = \sin(q_4 - q_5 + q_6 - \theta);$

$t37 = \sin(q_4 + 3q_5 + q_6 - \theta);\quad t38 = \sin(2q_4 - 2\theta);\quad t39 = \sin(q_4 - q_5 - q_6 - \theta);$

$t40 = \sin(q_4 + q_5 + q_6 - \theta);\quad t41 = \cos(q_4)\sin(q_6);\quad t42 = \cos(q_4)\cos(\theta);$

$t43 = \sin(q_4)\sin(\theta);\quad t44 = \cos(q_4)\sin(\theta);\quad t45 = \cos(q_4)\cos(q_5);\quad t46 = \cos(q_5)\sin(q_4);$

$t47 = \sin(q_4)\sin(q_6);\quad t48 = \cos(\theta)\sin(q_4);\quad t49 = \sin(q_4)\sin(q_6);$

$$
\begin{aligned}
t50 &= \frac{\sin(q_6)}{\sin(q_5)} - \frac{\sin(\theta - q_5 - q_4)}{2\sin(q_5)} \\
t51 &= \frac{2t_{18}t_{50}\cos(q_5)}{\dot{q}_4\sin(q_5)} \\
t52 &= \frac{t_{18}t_{50}(\dot{q}_4 + \dot{q}_5) + \cos q_4\dot{q}_4}{\sin q_5(\dot{q}_4 + \dot{q}_5)\dot{q}_4} \\
t53 &= \frac{t_{50}[t_{23} + \sin(q_6)]}{\sin(q_5)} - \frac{t_{50}\sin(\theta)[t_{18} + \cos(q_4)]}{2\sin(q_5)} \\
t54 &= \frac{t_{50}\cos(\theta)[t_{24} + \sin(q_4)]}{2\sin(q_5)} \\
t55 &= \frac{2t_{50}t_{24}\cos(q_5)}{\sin(q_5)\dot{q}_4} \\
t56 &= \frac{t_{50}t_{24}(\dot{q}_4 + \dot{q}_5) + \sin q_4\dot{q}_4}{\sin q_5(\dot{q}_4 + \dot{q}_5)\dot{q}_4} \\
t57 &= \frac{2t_{50}\cos(q_5)\sin(q_6)t_{33}}{\sin q_5\dot{q}_4} \\
t58 &= \frac{\cos(q_5)\sin(q_6)t_{33}}{\sin q_5\dot{q}_4} + \frac{t_{22}\cos(q_5)\cos(\theta)}{2\sin q_5\dot{q}_4} \\
t59 &= \frac{\cos(q_5)\sin(\theta)t_{24}}{2\sin q_5\dot{q}_4\dot{q}_4 + \dot{q}_5)\dot{q}_4}
\end{aligned}
$$

$$
\begin{aligned}
t60 &= \frac{2\cos(q_5)\sin(q_6)t_{33}}{\sin q_5 \dot{q}_4} \\
t61 &= \frac{t_{23}+\sin(q_6)}{\sin(q_5)} - \frac{\sin(\theta)[t_{22}+\cos(q_4)]}{2\sin q_5} + \frac{\cos(\theta)[t_{24}+\sin(q_4)]}{2\sin q_5} \\
t62 &= \frac{2t_{24}\cos(q_5)}{\sin q_5 \dot{q}_4} - \frac{\cos(q_5)[t_{24}\dot{q}_4+t_{24})\dot{q}_5+\sin q_4 \dot{q}_4]}{\sin(q_5)\dot{q}_4(\dot{q}_4+\dot{q}_5)} \\
t63 &= \frac{\sin(q_6)}{\sin(q_5)} - \frac{t_{32}}{2\sin q_5} \\
t64 &= \frac{t_{23}+\sin(q_6)}{\sin(q_5)} - \frac{\sin(\theta)[t_{18}+\cos(q_4)]}{2\sin(q_5)} + \frac{\cos(\theta)[t_{24}+\sin(q_4)]}{2\sin(q_5)} \\
t65 &= [2\sin(q_6) - t_{18}\sin(\theta) + t_{24}\cos(\theta)][2t_{23} - \cos(q_4)\sin(\theta) + \cos(\theta)\sin(q_4)]
\end{aligned}
$$

$$
\begin{aligned}
Y_{cs}^{a11} &= \frac{\cos(q_5)[0.5t_{11} - 2t_{12} + t_{13} + t_{14} - 0.5t_{15} + t_{16}]\ddot{\theta}}{2\cos(q_5)^2 - 1} - \frac{[\sin(2q_4) + t_{17}]\ddot{y}_0}{2\sin(q_5)^2} \\
&\quad - \frac{2t_{18}\cos(q_4)\cos(q_5)\ddot{x}_0}{\sin(q_5)^2} + \frac{\cot(q_5)[\cot(q_5)\cos(\theta) - t_{19} + t_{20}\cot(q_5)]\dot{\theta}^2}{2} \\
&\quad - \frac{[2t_{14}\dot{q}_4 - 2t_{13}\dot{q}_5 - 2t_{13}\dot{q}_4 + t_{15}\dot{q}_4 + t_{15}\dot{q}_5 - t_{16}\dot{q}_5 + 2t_{12}\dot{q}_5 + t_{11}\dot{q}_4]\dot{\theta}}{4\sin(q_5)} \\
&\quad - \frac{[2\dot{q}_4 + \dot{q}_5]\dot{y}_0}{2} + \frac{t_{21}\dot{q}_5\dot{y}_0}{2\sin(q_5)} + \frac{t_{18}\cos(q_4)\dot{q}_5\dot{x}_0}{\sin(q_5)} \\
&\quad - \frac{\cos(q_5)[2t_{18}t_{23}\dot{q}_4^2 + 2t_{41}\dot{q}_4^2 + 2t_{41}\dot{q}_5^2 + 2t_{18}t_{42}\dot{q}_4 + t_{18}t_{42}\dot{q}_5]\dot{\theta}}{2\sin(q_5)^2\dot{q}_4(\dot{q}_4+\dot{q}_5)} \\
&\quad + \frac{\cos(q_5)[t_{18}t_{43}\dot{q}_4 + t_{24}t_{44}\dot{q}_4 + t_{24}t_{44}\dot{q}_5 + 2t_{18}t_{23}\dot{q}_4\dot{q}_5]\dot{\theta}}{2\sin(q_5)^2\dot{q}_4(\dot{q}_4+\dot{q}_5)} \\
&\quad + \frac{\cos(q_5)[2t_{18}t_{23}\dot{q}_4\dot{q}_6 + 4t_{41}\dot{q}_4\dot{q}_5 + 2t_{41}\dot{q}_4\dot{q}_6 + 2t_{41}\dot{q}_5\dot{q}_6]\dot{\theta}}{2\sin(q_5)^2\dot{q}_4(\dot{q}_4+\dot{q}_5)} \\
&\quad + \frac{\cos(q_5)[0.5\sin q_5\dot{q}_5 + t_{25}\dot{q}_4 + 0.5t_{25}\dot{q}_5]\dot{x}_0}{\sin(q_5)^2\dot{q}_4(\dot{q}_4+\dot{q}_5)} - \frac{t_{18}t_{45}[2\dot{q}_4+\dot{q}_5]\dot{y}_0}{\sin(q_5)^2\dot{q}_4(\dot{q}_4+\dot{q}_5)} \\
Y_{cs}^{b11} &= \frac{\cos q_5[2t_{26} + 0.5t_{27} - t_{28} - t_{29} + 0.5t_{30} - t_{31}]\ddot{\theta}}{2\cos(q_5)^2 - 1} - \frac{[\sin(2q_4) + t_{17}]\ddot{x}_0}{2\sin(q_5)^2} \\
&\quad - \frac{2t_{24}t_{46}\ddot{y}_0}{\sin(q_5)^2} + \frac{[2\dot{q}_4 + \dot{q}_5]\dot{x}_0}{2} \\
&\quad - \frac{[2t_{28}\dot{q}_4 + 2t_{28}\dot{q}_5 - 2t_{29}\dot{q}_4 - t_{30}\dot{q}_4 - t_{30}\dot{q}_5 + t_{31}\dot{q}_5 - 2t_{26}\dot{q}_5 + t_{27}\dot{q}_4]\dot{\theta}}{4\sin(q_5)} \\
&\quad + \frac{\cot(q_5)[t_{22} + \cot(q_5)\sin(\theta) + t_{19}\cot(q_5)]\dot{\theta}^2}{2} + \frac{t_{25}\dot{q}_5\dot{x}_0}{2\sin(q_5)} + \frac{t_{24}\sin(q_4)\dot{q}_5\dot{y}_0}{\sin(q_5)} \\
&\quad - \frac{\cos q_5[2t_{24}t_{23}\dot{q}_4^2 + 2t_{47}\dot{q}_4^2 + 2t_{47}\dot{q}_5^2 + t_{18}t_{48}\dot{q}_4 + 2t_{24}t_{42}\dot{q}_4 + t_{18}t_{48}\dot{q}_5 + 2t_{24}t_{43}\dot{q}_4]\dot{\theta}}{2\sin(q_5)^2\dot{q}_4(\dot{q}_4+\dot{q}_5)}
\end{aligned}
$$

$$
\begin{aligned}
& + \frac{\cos q_5[2t_{24}t_{23}\dot{q}_4 + 2t_{24}t_{23}\dot{q}_4\dot{q}_6 + 4t_{49}\dot{q}_4\dot{q}_5 + 2t_{47}\dot{q}_4\dot{q}_6 + 2t_{47}\dot{q}_5\dot{q}_6]\dot{\theta}}{2\sin(q_5)^2\dot{q}_4(\dot{q}_4+\dot{q}_5)} \\
& - \frac{\cos q_5[t_{21}\dot{q}_4 - 0.5\sin(q_5)\dot{q}_5 + 0.5t_{21}\dot{q}_5]\dot{y}_0}{\sin(q_5)^2\dot{q}_4(\dot{q}_4+\dot{q}_5)} + \frac{t_{24}t_{46}[2\dot{q}_4+\dot{q}_5]\dot{x}_0}{\sin(q_5)^2\dot{q}_4(\dot{q}_4+\dot{q}_5)} \\
Y_{cs}^{c11} = & \frac{\cos q_5[0.5t_{11} - 2t_{12} + t_{13} + t_{14} - 0.5t_{15} + t_{16}]\ddot{x}_0}{2\cos(q_5)^2 - 1} \\
& + \frac{\cos q_5[2t_{26} + 0.5t_{27} - t_{28} - t_{29} + 0.5t_{30} - t_{31}]\ddot{y}_0}{2\cos(q_5)^2 - 1} \\
& - \frac{\cos q_5[2\sin(q_6) - t_{22}\sin(\theta) + t_{24}\cos(\theta)][2t_{23} - t_{44} + t_{18}]\ddot{\theta}}{2\sin(q_5)^2} \\
& + \frac{0.5\cos(\theta)[t_{51} - \cos(q_5)[t_{18}\dot{q}_4 + t_{18}\dot{q}_5 + \cos(q_4)\dot{q}_4]\dot{y}_0}{\sin(q_5)\dot{q}_4(\dot{q}_4+\dot{q}_5)} \\
& + \frac{0.5\sin(\theta)[t_{51} - \cos(q_5)[t_{18}\dot{q}_4 + t_{18}\dot{q}_5 + \cos(q_4)\dot{q}_4]\dot{y}_0}{\sin(q_5)\dot{q}_4(\dot{q}_4+\dot{q}_5)} \\
& + [t_{51} - t_{52}\cos(q_5)] - \frac{t_{18}\cos(q_5)[t_{53}+t_{54}]}{\sin(q_5)\dot{q}_4} + 0.5\cos(\theta)[t_{51} - t_{52}\cos(q_5)]\dot{\theta} \\
& + 0.5\sin(\theta)[t_{54} - t_{55}\cos(q_5)]\dot{\theta} - \frac{t_{50}\cos(q_5)[t_{23}\dot{q}_4 + \sin(q_6)\dot{q}_4 + \sin(q_6)\dot{q}_5]t_{33}}{\sin(q_5)\dot{q}_4(\dot{q}_4+\dot{q}_5)} \\
& - ([t_{58}+t_{59}]t_{61})\dot{\theta} - t_{62}t_{63}\dot{x}_0 + \frac{t_{63}\dot{x}_0}{\sin(q_5)\dot{q}_4} \\
& + \frac{[2t_{14}\dot{q}_4 - 2t_{13}\dot{q}_4 + 2t_{14}\dot{q}_5 + t_{15}\dot{q}_4 + t_{16}\dot{q}_5 - 2t_{12}\dot{q}_5 + t_{11}\dot{q}_4 + t_{11}\dot{q}_5]\dot{x}_0}{4\sin(q_5)} \\
& + \frac{[2t_{28}\dot{q}_4 - 2t_{29}\dot{q}_4 - 2t_{29}\dot{q}_5 - t_{30}\dot{q}_4 - t_{31}\dot{q}_5 + 2t_{26}\dot{q}_5 + t_{27}\dot{q}_4 + t_{27}\dot{q}_5]\dot{y}_0}{4\sin(q_5)} \\
& + \frac{[0.13t_{34} - 0.25t_{35} + 0.13t_{36} + 0.13t_{37} + 0.13t_{38} - 0.25t_{39} + 0.25t_{40}]\dot{\theta}^2}{\sin(q_5)^2} + \frac{t_{65}\dot{q}_5\dot{\theta}}{4\sin(q_5)} \\
Y_{cs}^{a12} = & -\frac{\cos(q_4)\cos(q_6)\ddot{\theta}}{\sin(q_5)} + \frac{\cos(q_4)\sin(q_6)(\dot{q}_4 + \dot{q}_5\dot{\theta} + \dot{q}_6)}{\sin(q_5)} - \frac{\cos(q_4)\cos(q_6)\dot{\theta}}{\sin(q_5)} \\
Y_{cs}^{b12} = & -\frac{\cos(q_6)\sin(q_4)\ddot{\theta}}{\sin(q_5)} + \frac{\sin(q_4)\sin(q_6)(\dot{q}_4 + \dot{q}_5\dot{\theta} + \dot{q}_6)}{\sin(q_5)} - \frac{\cos(q_6)\sin(q_4)\dot{\theta}}{\sin(q_5)} \\
Y_{cs}^{c12} = & -\frac{\cos(q_6)[\sin(q_4-\theta) + 2\sin(q_5+q_6)]\ddot{\theta}}{\sin(q_5)} - \frac{\cos(q_4)\cos(q_6)\ddot{x}_0}{\sin(q_5)} - \frac{\cos(q_6)\sin(q_4)\ddot{y}_0}{\sin(q_5)} \\
& + \frac{\cos(q_6)\cos(q_4-\theta)\dot{\theta}^2}{2\sin(q_5)} - \frac{\cos(q_4)\cos(q_6)\dot{y}_0}{\sin(q_5)\dot{q}_4 + \sin(q_5)\dot{q}_5} + \frac{\cos(q_6)\sin(q_4)\dot{x}_0}{\sin(q_5)\dot{q}_4 + \sin(q_5)\dot{q}_5} \\
& - \frac{\sin(q_4)\sin(q_6)(\dot{q}_4+\dot{q}_5)\dot{y}_0}{\sin(q_5)} + \frac{[\sin(q_4-\theta) + 2\sin(q_5+q_6)]\sin(q_6)\dot{q}_6\dot{\theta}}{2\sin(q_5)} \\
& - \frac{\cos(q_4)\sin(q_6)(\dot{q}_4+\dot{q}_5)\dot{x}_0}{\sin(q_5)} \\
& - \frac{\cos(q_6)[\cos(q_4-\theta) + 4\sin(q_5+q_6)\dot{q}_4 + 4\sin(q_5+q_6)\dot{q}_5 + 2\sin(q_5+q_6)\dot{q}_6]\dot{\theta}}{2\sin(q_5)(\dot{q}_4+\dot{q}_5)}
\end{aligned}
$$

$$+\frac{[\sin(q_4-\theta)\dot{q}_4+\sin(q_4-\theta)\dot{q}_5]\dot{\theta}}{2\sin(q_5)(\dot{q}_4+\dot{q}_5)}$$

$u11=\cos(q_4+q_5);\quad u12=\cos(q_5+q_6);\quad u13=\sin(q_5+q_6);\quad u14=(\dot{q}_4+\dot{q}_5+\dot{q}_6);$

$u15=\sin(q_4+q_5);\quad u16=\sin(q_4+q_5-\theta);\quad u17=\cos(q_4+2q_5+q_6);$

$u18=\cos(q_4-q_6);\quad u19=\cos(q_4+2q_5+q_6-\theta);\quad u20=\cos(q_4-q_6-\theta);$

$u21=\sin(q_4+q_5-q_6-\theta);\quad u22=\sin(q_4+3q_5+q_6-\theta);$

$u23=\sin(q_4-q_5-q_6-\theta);\quad u24=\sin(q_4+q_5+q_6-\theta);\quad u25=\cos(q_4+q_5-q_6-\theta);$

$u26=\cos(q_4+3q_5+q_6-\theta);\quad u27=\cos(2q_5+2q_6);\quad u28=\cos(q_4-q_5-q_6-\theta);$

$u29=\cos(q_4+q_5+q_6-\theta);\quad u30=\sin(q_4+2q_5+q_6);$

$$\begin{aligned}
Y_{cs}^{a13} &= -\frac{u_{11}u_{12}\ddot{\theta}}{\sin(q_5)}+\frac{u_{11}u_{12}\dot{\theta}}{\sin(q_5)}-\frac{u_{11}u_{13}u_{14}\dot{\theta}}{\sin(q_5)}\\
Y_{cs}^{b13} &= -\frac{u_{12}u_{15}\ddot{\theta}}{\sin(q_5)}+\frac{u_{11}u_{12}\dot{\theta}}{\sin(q_5)}-\frac{u_{11}u_{13}u_{14}\dot{\theta}}{\sin(q_5)}\\
Y_{cs}^{c13} &= -\frac{u_{11}u_{12}\ddot{x}_0}{\sin(q_5)}+\frac{u_{12}u_{15}\ddot{y}_0}{\sin(q_5)}+\frac{u_{12}[u_{16}+2\sin(q_6)]\ddot{\theta}}{\sin(q_5)}+\frac{[0.5u_{17}+0.5u_{18}]\dot{y}_0}{\dot{q}_4\sin(q_5)}\\
&\quad -\frac{[u_{19}+u_{20}]\dot{\theta}^2}{4\sin(q_5)}\\
&\quad -\frac{[4\dot{q}_4+2\dot{q}_5+2\dot{q}_6-u_{21}-u_{22}+u_{23}+u_{24}+u_{25}\dot{q}_4+u_{26}\dot{q}_4+4u_{27}\dot{q}_4+2u_{27}\dot{q}_5]\dot{\theta}}{8\sin(q_5)^2\dot{q}_4}\\
&\quad +\frac{[2u_{27}\dot{q}_6-u_{28}\dot{q}_4-u_{29}\dot{q}_4-4\cos(2q_5)\dot{q}_4-2\cos(2q_5)\dot{q}_5]\dot{\theta}}{8\sin(q_5)^2\dot{q}_4}\\
&\quad -\frac{[2\cos(2q_5)\dot{q}_6-4\cos(2q_6)\dot{q}_4-2\cos(2q_6)\dot{q}_5-2\cos(2q_6)\dot{q}_6]\dot{\theta}}{8\sin(q_5)^2\dot{q}_4}\\
&\quad -\frac{u_{13}[u_{16}+2\sin(q_6)](\dot{q}_5+\dot{q}_6)}{2\sin(q_5)}-\frac{[\sin(q_4-q_6)+u_{30}]\dot{x}_0}{2\sin(q_5)\dot{q}_4}\\
&\quad +\frac{u_{11}u_{13}\dot{q}_4\dot{x}_0}{\sin(q_5)}+\frac{u_{15}u_{13}\dot{q}_4\dot{y}_0}{\sin(q_5)}
\end{aligned}$$

$v11=\sin(q_4+q_5)^2;\quad v12=\sin(2q_4+2q_5);\quad v13=\sin(2q_4+2q_5-\theta);$

$v14=\sin(2q_4-\theta);\quad v15=\sin(q_4+q_5-q_6);\quad v16=\sin(q_4-q_5-q_6);$

$v17=\cos(\theta-2q_5-2q_4);\quad v18=\cos(\theta-2q_4);\quad v19=\cos(2q_4+2q_5-\theta);$

$v20=\cos(2q_4-\theta);$

$v21 = \cos(q_4+q_5)^2$; $v22 = \sin(q_4+q_5+q_6)$; $v23 = \cos(q_4+q_5-q_6)$;

$v24 = \cos(q_4-q_5-q_6)$; $v25 = \cos(q_4+q_5+q_6)$; $v26 = \cos(2q_4+2q_5-2\theta)$;

$v27 = \cos(q_4+q_5-q_6-\theta)$; $v28 = \cos(2q_5+2q_6)$;

$v29 = \cos(2q_4-2\theta)$; $v30 = \sin(q_5+q_6)$;

$v31 = \sin(q_4+q_5-\theta)$; $v32 = \cos(q_4+q_5-\theta)$; $v33 = \sin(2q_4+2q_5-2\theta)$;

$v34 = \sin(q_4+q_5-q_6-\theta)$; $v35 = \sin(2q_4-2\theta)$; $v36 = \sin(q_4-q_5-q_6-\theta)$.

$$
\begin{aligned}
Y_{cs}^{a14} &= \frac{[v_{11}-\sin(q_4)^2]\ddot{x}_0-}{\sin(q_5)^2} + \frac{[\sin(2q_4)-v_{12}]\ddot{y}_0-}{2\sin(q_5)^2} - \frac{[v_{13}-v_{14}-2v_{15}+2v_{16}]\dot{\theta}}{4\sin(q_5)^2} \\
&+ \frac{[0.25v_{17}-0.25v_{18}+0.75v_{19}-0.75v_{20}]\dot{\theta}^2}{4\sin(q_5)^2} - \frac{[v_{21}\dot{q}_4+v_{21}\dot{q}_5-\cos(q_4)^2\dot{q}_4]\dot{y}_0}{\sin(q_5)^2\dot{q}_4(\dot{q}_4+\dot{q}_5)} \\
&+ \frac{[2v_{16}\dot{q}_4^2-v_{20}\dot{q}_4+2v_{22}\dot{q}_5^2+\cos(\theta)\dot{q}_5-2v_{15}\dot{q}_4^2-2v_{15}\dot{q}_5^2+v_{19}\dot{q}_4]\dot{\theta}}{2[\cos(2q_5)-1]\dot{q}_4(\dot{q}_4+\dot{q}_5)} \\
&+ \frac{[v_{19}\dot{q}_5+2v_{16}\dot{q}_4\dot{q}_5+2v_{16}\dot{q}_4\dot{q}_6]\dot{\theta}}{2[\cos(2q_5)-1]\dot{q}_4(\dot{q}_4+\dot{q}_5)} \\
&+ \frac{[2v_{22}\dot{q}_4\dot{q}_5+2v_{22}\dot{q}_5\dot{q}_6-4v_{15}\dot{q}_4\dot{q}_5-2v_{15}\dot{q}_4\dot{q}_6-2v_{15}\dot{q}_5\dot{q}_6]\dot{\theta}}{2[\cos(2q_5)-1]\dot{q}_4(\dot{q}_4+\dot{q}_5)} \\
&- \frac{[v_{12}\dot{q}_4-\sin(2q_4)\dot{q}_4+v_{12}\dot{q}_5]\dot{x}_0}{[\cos(2q_5)-1]\dot{q}_4(\dot{q}_4+\dot{q}_5)} \\
Y_{cs}^{b14} &= \frac{[v_{19}-v_{20}-2v_{23}+2v_{24}]\ddot{\theta}}{4\sin(q_5)^2} - \frac{[v_{11}-\sin(q_4)^2]\ddot{y}_0}{\sin(q_5)^2} + \frac{[\sin(2q_4)-v_{12}]\ddot{x}_0}{2\sin(q_5)^2} \\
&+ \frac{1.75\sin(\theta-2q_4)+v_{13}+0.75v_{14}}{4\sin(q_5)^2} \\
&+ \frac{[v_{13}\dot{q}_4+v_{13}\dot{q}_5-2v_{25}\dot{q}_5^2-v_{14}\dot{q}_4+2v_{23}\dot{q}_4^2+2v_{23}\dot{q}_5^2]\dot{\theta}}{2[\cos(2q_5)-1]\dot{q}_4(\dot{q}_4+\dot{q}_5)} \\
&+ \frac{[\sin(\theta)\dot{q}_5-2v_{24}\dot{q}_4^2-2v_{25}\dot{q}_4\dot{q}_5-2v_{25}\dot{q}_5\dot{q}_6+4v_{23}\dot{q}_4\dot{q}_5+2v_{23}\dot{q}_4\dot{q}_6]\dot{\theta}}{2[\cos(2q_5)-1]\dot{q}_4(\dot{q}_4+\dot{q}_5)} \\
&+ \frac{[2v_{23}\dot{q}_5\dot{q}_6-2v_{24}\dot{q}_4\dot{q}_5-2v_{24}\dot{q}_5\dot{q}_6]\dot{\theta}}{2[\cos(2q_5)-1]\dot{q}_4(\dot{q}_4+\dot{q}_5)} \\
&+ \frac{[v_{11}\dot{q}_4-\sin(q_4)^2\dot{q}_4+v_{11}\dot{q}_5]\dot{x}_0}{\sin(q_5)^2\dot{q}_4(\dot{q}_4+\dot{q}_5)} \\
&+ \frac{[v_{12}\dot{q}_4-\sin(2q_4)\dot{q}_4+v_{12}\dot{q}_5]\dot{y}_0}{\sin(q_5)^2\dot{q}_4(\dot{q}_4+\dot{q}_5)} \\
Y_{cs}^{c14} &= \frac{[4\cos(2q_6)+v_{26}-4v_{27}-4v_{28}-v_{29}+4v_{27}]\ddot{\theta}}{8\sin(q_5)^2} + \frac{[v_{19}-v_{20}-2v_{23}+2v_{24}]\ddot{y}_0}{2\sin(q_5)^2}
\end{aligned}
$$

$$
\begin{aligned}
&-\frac{[v_{13}-v_{14}-2v_{15}+2v_{16}]\ddot{x}_0}{2\sin(q_5)^2}\\
&+\frac{[0.5\cos(q_4-\theta)+v_{30}\dot{q}_4+v_{30}\dot{q}_5+v_{30}\dot{q}_6][0.5\sin(q_4-\theta)-0.5v_{31}+v_{30}]\dot{\theta}}{\sin(q_5)^2(\dot{q}_4+\dot{q}_5)}\\
&+\frac{[0.5v_{31}+\sin(q_6)][2\sin(q_6)\dot{q}_4^2+2\sin(q_6)\dot{q}_5^2+v_{32}\dot{q}_4+v_{32}\dot{q}_5+\cos(q_4-\theta)\dot{q}_4]\dot{\theta}}{\sin(q_5)^2(\dot{q}_4+\dot{q}_5)}\\
&+\frac{[\sin(q_6)][2v_{30}\dot{q}_4^2+4\sin(q_6)\dot{q}_4\dot{q}_5+2\sin(q_6)\dot{q}_4\dot{q}_6+2\sin(q_6)\dot{q}_5\dot{q}_6+2v_{30}\dot{q}_4\dot{q}_5]\dot{\theta}}{\sin(q_5)^2(\dot{q}_4+\dot{q}_5)}\\
&+\frac{[0.125v_{33}-0.25v_{34}-0.125v_{35}+v_{36}]\dot{\theta}^2}{\sin(q_5)^2}\\
-\quad&\frac{[v_{20}\dot{q}_4+2v_{23}\dot{q}_4+2v_{23}\dot{q}_5-2v_{24}\dot{q}_4+\cos(\theta)\dot{q}_5-2v_{25}\dot{q}_5-v_{19}\dot{q}_4-v_{19}\dot{q}_5]\dot{x}_0}{2[\cos(2q_5)-1]\dot{q}_4(\dot{q}_4+\dot{q}_5)}\\
&-\frac{[v_{13}\dot{q}_4+v_{13}\dot{q}_5-v_{14}\dot{q}_4-2v_{15}\dot{q}_4-2v_{15}\dot{q}_5+2v_{16}\dot{q}_4-\sin(\theta)\dot{q}_5+2v_{22}\dot{q}_5]\dot{y}_0}{2[\cos(2q_5)-1]\dot{q}_4(\dot{q}_4+\dot{q}_5)}
\end{aligned}
$$

$w11=\sin(q_4-\theta);\quad w12=\sin(q_5+q_6);\quad w13=\cos(\theta-2q_4);\quad w14=\cos(q_4-\theta);$

$w15=\sin(\theta-2q_4);\quad w16=\sin(2q_4-2\theta);\quad w17=\sin(q_4-q_5-q_6-\theta);$

$w18=\sin(q_4+q_5+q_6-\theta);\quad w19=\cos(2q_5+2q_6);\quad w20=\cos(q_4-q_5-q_6-\theta);$

$w21=\cos(q_4+q_5+q_6-\theta);\quad w22=\sin(q_4+q_5+q_6);\quad w23=\sin(2q_4-\theta);$

$w24=\sin(q_4-q_5-q_6);\quad w25=\cos(q_4+q_5+q_6);\quad w26=\cos(2q_4-\theta);$

$w27=\cos(q_4-q_5-q_6).$

$$
\begin{aligned}
Y_{cs}^{a15} &= \frac{-\cos(q_4)^2\ddot{x}_0}{\sin(q_5)^2}-\frac{\sin(2q_4)\ddot{y}_0}{2\sin(q_5)^2}-\frac{\cos(q_4)[w_{11}+2w_{12}]\ddot{\theta}}{2\sin(q_5)^2}+\frac{[w_{13}+\cos(\theta)]\dot{\theta}^2}{4\sin(q_5)^2}\\
&\quad-\frac{\cos(q_4)^2\dot{y}_0}{\sin(q_5)^2(\dot{q}_4+\dot{q}_5)}+\frac{\sin(2q_4)\dot{x}_0}{2\sin(q_5)^2(\dot{q}_4+\dot{q}_5)}\\
&\quad-\frac{\cos(q_4)[w_{14}+2w_{12}\dot{q}_4+2w_{12}\dot{q}_5+2w_{12}\dot{q}_6]\dot{\theta}}{2\sin(q_5)^2(\dot{q}_4+\dot{q}_5)}\\
Y_{cs}^{b15} &= \frac{-\sin(2q_4)\ddot{x}_0}{\sin(q_5)^2}-\frac{\sin(q_4)^2\ddot{y}_0}{2\sin(q_5)^2}-\frac{\sin(q_4)[w_{11}+2w_{12}]\ddot{\theta}}{2\sin(q_5)^2}+\frac{\sin(q_4)^2\dot{x}_0}{\sin(q_5)^2(\dot{q}_4+\dot{q}_5)}\\
&\quad-\frac{[w_{15}-\sin(\theta)]\dot{\theta}^2}{4\sin(q_5)^2}-\frac{\sin(2q_4)\dot{y}_0}{2\sin(q_5)^2(\dot{q}_4+\dot{q}_5)}\\
&\quad-\frac{\sin(q_4)[w_{14}+2w_{12}\dot{q}_4+2w_{12}\dot{q}_5+2w_{12}\dot{q}_6]\dot{\theta}}{2\sin(q_5)^2(\dot{q}_4++\dot{q}_5)}\\
Y_{cs}^{c15} &= \ddot{\theta}-\frac{(\ddot{\theta}[w_{11}+2w_{12}]^2)}{4\sin(q_5)^2}-\frac{\cos(q_4)[w_{11}+2w_{12}]\ddot{x}_0}{4\sin(q_5)^2}-\frac{\sin(q_4)[w_{11}+2w_{12}]\ddot{y}_0}{4\sin(q_5)^2}
\end{aligned}
$$

$$
\begin{aligned}
&+\frac{[w_{16}-2w_{17}+2w_{18}]\dot{\theta}^2}{8\sin(q_5)^2}\\
&+\frac{[4\dot{q}_6+w_{16}-2w_{17}+2w_{18}-4w_{19}\dot{q}_4-4w_{19}\dot{q}_5-4w_{19}\dot{q}_6+2w_{20}\dot{q}_4]\dot{\theta}}{2[\cos(2q_5)-1]\dot{q}_4(\dot{q}_4+\dot{q}_5)}\\
&+\frac{[2w_{20}\dot{q}_5+2w_{20}\dot{q}_6-2w_{21}\dot{q}_4-2w_{21}\dot{q}_5-2w_{21}\dot{q}_6+4\cos(2q_5)\dot{q}_4]\dot{\theta}}{2[\cos(2q_5)-1]\dot{q}_4(\dot{q}_4+\dot{q}_5)}\\
&+\frac{[2w_{22}+w_{23}-2w_{24}-\sin(\theta)]\dot{y}_0}{2[\cos(2q_5)-1]\dot{q}_4(\dot{q}_4+\dot{q}_5)}-\frac{[2w_{25}+w_{26}-2w_{27}-\cos(\theta)]\dot{x}_0}{2[\cos(2q_5)-1]\dot{q}_4(\dot{q}_4+\dot{q}_5)}
\end{aligned}
$$

$$
\begin{aligned}
Y_{cs}^{a16} &= \frac{\cos(q_4+q_5)\cos(q_4)}{\sin(q_5)}\\
Y_{cs}^{b16} &= \frac{\sin(q_4+q_5)\cos(q_4)}{\sin(q_5)}\\
Y_{cs}^{c16} &= -\frac{[\sin(q_4+q_5-\theta)+2\sin(q_6)]\cos(q_4)}{2\sin(q_5)}\\
Y_{cs}^{a17} &= -\frac{\cos(q_4+q_5)\cos(q_4)}{\sin(q_5)}\\
Y_{cs}^{b17} &= -\frac{\cos(q_4+q_5)\sin(q_4)}{\sin(q_5)}\\
Y_{cs}^{c17} &= -\frac{[\sin(q_4-\theta)+2\sin(q_5+q_6)]\cos(q_4+q_5)}{2\sin(q_5)}\\
Y_{cs}^{a18} &= 0\\
Y_{cs}^{b18} &= 0\\
Y_{cs}^{c18} &= \cos(q_4+q_5+q_6)\\
Y_{cs}^{a19} &= \ddot{x}_0\\
Y_{cs}^{b19} &= \ddot{y}_0\\
Y_{cs}^{c19} &= 0\\
Y_{cs}^{a20} &= 0\\
Y_{cs}^{b20} &= 0\\
Y_{cs}^{c20} &= \ddot{\theta}
\end{aligned}
$$

B.2 Time independent parameters

$$\alpha_{cs} = [\alpha_{cs}^1 \;\; \alpha_{cs}^2 \;\; \alpha_{cs}^3 \;\; \alpha_{cs}^4 \;\; \alpha_{cs}^5 \;\ldots\ldots\; \alpha_{cs}^{16} \;\; \alpha_{cs}^{17} \;\; \alpha_{cs}^{18} \;\; \alpha_{cs}^{19} \;\; \alpha_{cs}^{20}]^T$$

$a1 = l_{12}^2 l_{21}^2 l_{22}^2$; $a2 = l_{11}^2 l_{12}^2 l_{22}^2$; $a3 = l_{11}^2 l_{12}^2 l_{21}^2$; $a4 = l_{11}^2 l_{21}^2 l_{22}^2$; $a5 = l_{11} l_{12} l_{21}^2 l_{22}^2$;

$a6 = l_{11}^2 l_{12}^2 l_{21} l_{22}$; $a7 = l_{11}^2 l_{12}^2 l_{21}^2 l_{22}^2$.

$b1 = l_{11}^2 l_{13} l_{21}^2 l_{22}^2$; $b2 = l_{12}^2 l_{13} l_{21}^2 l_{22}^2$; $b3 = l_{11}^2 l_{12}^2 l_{22}^2 l_{23}$; $b4 = Ll_{12}^2 l_{21}^2 l_{22}^2$; $b5 = Ll_{11}^2 l_{12}^2 l_{22}^2$;

$b6 = Ll_{11}^2 l_{12}^2 l_{21}^2$; $b7 = Ll_{11}^2 l_{21}^2 l_{22}^2$; $b8 = l_{11} l_{12}^2 l_{21}^2 l_{22}^2$; $b9 = l_{11}^2 l_{12}^2 l_{21} l_{22}^2$; $b10 = l_{11}^2 l_{12} l_{21}^2 l_{22}^2$;

$b11 = l_{11}^2 l_{12}^2 l_{21}^2 l_{22}$; $b12 = l_{11} l_{12} l_{13} l_{21}^2 l_{22}^2$; $b13 = l_{11}^2 l_{12}^2 l_{21} l_{22} l_{23}$; $b14 = Ll_{11} l_{12} l_{21}^2 l_{22}^2$;

$b15 = Ll_{11}^2 l_{12}^2 l_{21} l_{22}$; $b16 = l_{11}^2 l_{12}^2 l_{21}^2 l_{23}$.

$c1 = l_{11}^2 l_{13}^2 l_{21}^2 l_{22}^2$; $c2 = l_{11}^2 l_{12}^2 l_{21}^2 l_{23}^2$; $c3 = l_{11}^2 l_{12}^2 l_{21}^2 l_{22}^2$; $c4 = l_{12}^2 l_{13}^2 l_{21}^2 l_{22}^2$; $c5 = l_{11}^2 l_{12}^2 l_{22}^2 l_{23}^2$;

$c6 = L^2 l_{12}^2 l_{21}^2 l_{22}^2$; $c7 = L^2 l_{11}^2 l_{12}^2 l_{22}^2$; $c8 = L^2 l_{11}^2 l_{12}^2 l_{21}^2$; $c9 = L^2 l_{11}^2 l_{21}^2 l_{22}^2$; $c10 = Ll_{12}^2 l_{13} l_{21}^2 l_{22}^2$;

$c11 = Ll_{11}^2 l_{13} l_{21}^2 l_{22}^2$; $c12 = Ll_{11}^2 l_{12}^2 l_{22}^2 l_{23}$; $c13 = Ll_{11}^2 l_{12}^2 l_{21}^2 l_{23}$; $c14 = l_{11} l_{12} l_{13}^2 l_{21}^2 l_{22}^2$;

$c15 = l_{11}^2 l_{12} l_{13}^2 l_{21}^2 l_{22}^2$; $c16 = l_{11} l_{12}^2 l_{13} l_{21}^2 l_{22}^2$; $c17 = l_{11}^2 l_{12}^2 l_{21} l_{22} l_{23}^2$; $c18 = l_{11}^2 l_{12}^2 l_{21}^2 l_{22} l_{23}^2$;

$c19 = l_{11}^2 l_{12}^2 l_{21} l_{22}^2 l_{23}^2$; $c20 = Ll_{11} l_{12}^2 l_{21}^2 l_{22}^2$; $c21 = Ll_{11}^2 l_{12}^2 l_{21} l_{22}^2$; $c22 = Ll_{11}^2 l_{12} l_{21}^2 l_{22}^2$;

$c23 = Ll_{11}^2 l_{12}^2 l_{21}^2 l_{22}^2$; $c24 = L^2 l_{11} l_{12} l_{21}^2 l_{22}^2$; $c25 = L^2 l_{11}^2 l_{12}^2 l_{21} l_{22}^2$; $c26 = Ll_{11} l_{12} l_{13} l_{21}^2 l_{22}^2$;

$c27 = Ll_{11}^2 l_{12}^2 l_{13} l_{21} l_{22} l_{23}$.

$d1 = l_{11} l_{13} l_{21} l_{22}$; $d2 = l_{11} l_{12} l_{22} l_{23}$; $d3 = l_{11} l_{12} l_{21} l_{22}$; $d4 = l_{11} l_{13} l_{21} l_{22}$; $d5 = l_{11} l_{12} l_{21} l_{23}$;

$d6 = Ll_{11} l_{21} l_{22}$; $d7 = Ll_{12} l_{21} l_{22}$; $d8 = Ll_{11} l_{12} l_{21}$; $d9 = Ll_{11} l_{12} l_{22}$

$e1 = \frac{1}{l_{11}}; \;\; e2 = \frac{1}{l_{12}}; \;\; e3 = \frac{1}{l_{21}}; \;\; e4 = \frac{1}{l_{22}}.$

$$
\begin{aligned}
\alpha_{cs}^{1} &= \frac{p_{11}(4a1+4b2-8b4+c4-3c6-2c10)a7d3}{20} \\
\alpha_{cs}^{2} &= \frac{p_{12}(6a5+8b12+12b14+c14-4c24-4c26)a7d3}{20} \\
\alpha_{cs}^{3} &= \frac{p_{13}(4b10+c15-2c22)a7d3}{20} \\
\alpha_{cs}^{4} &= \frac{p_{14}(4b8+c16-2c20)a7d3}{20} \\
\alpha_{cs}^{5} &= \frac{p_{15}(4a1+4a4+4b1+4b2+8b4-8b7+d1+c4+3c6+3c9-2c10-2c11)a7d3}{20} \\
\alpha_{cs}^{6} &= \frac{p_{16}(4a4+4b1+8b7+d1+c3+3c9+2c11)a7d3}{20} \\
\alpha_{cs}^{7} &= \frac{p_{17}(e1-4d1-8d7)a7d3}{20} \\
\alpha_{cs}^{8} &= \frac{p_{18}(e2-4d4-8d6)a7d3}{20} \\
\alpha_{cs}^{9} &= \frac{p_{19}a7d3}{20} \\
\alpha_{cs}^{10} &= \frac{p_{21}(4a2+4b3-8b5+c5-3c7-2c12)a7d3}{20} \\
\alpha_{cs}^{11} &= \frac{p_{22}(6a6+8b13+12b15+c17-4c25-4c27)a7d3}{20} \\
\alpha_{cs}^{12} &= \frac{p_{23}(4b11+c18-2c23)a7d3}{20} \\
\alpha_{cs}^{13} &= \frac{p_{24}(4b9+c19-2c21)a7d3}{20} \\
\alpha_{cs}^{14} &= \frac{p_{25}(4a2+4a3+4b3+8b5-8b6+4b16+c2+c5+3c7+3c8-2c12-2c13)a7d3}{20} \\
\alpha_{cs}^{15} &= \frac{p_{26}(4a3+8b6+4b16+c2+c3+3c8+2c13)a7d3}{20} \\
\alpha_{cs}^{16} &= \frac{p_{27}(e3-4d2-8d9)a7d3}{20} \\
\alpha_{cs}^{17} &= \frac{p_{28}(e4-4d5-8d8)a7d3}{20}
\end{aligned}
$$

$$\alpha_{cs}^{18} = \frac{p_{29}a7d3}{20}$$
$$\alpha_{cs}^{19} = \frac{p_{31}a7d3}{20}$$
$$\alpha_{cs}^{20} = \frac{p_{32}a7d3}{20}$$

where, $p31 = m$; $p32 = I$

Appendix C

Regressor for Manipulators - Flexible Object System in Joint Space

C.1 Time dependent parameters

$$Y_{js} = \begin{bmatrix} Y_{js}^{d1} & Y_{js}^{d2} & Y_{js}^{d3} & Y_{js}^{d4} & Y_{js}^{d5} & .... & Y_{js}^{d17} & Y_{js}^{d18} & Y_{js}^{d19} & Y_{js}^{d20} \\ Y_{js}^{e1} & Y_{js}^{e2} & Y_{js}^{e3} & Y_{js}^{e4} & Y_{js}^{e5} & .... & Y_{js}^{e17} & Y_{js}^{e18} & Y_{js}^{e19} & Y_{js}^{e20} \\ Y_{js}^{f1} & Y_{js}^{f2} & Y_{js}^{f3} & Y_{js}^{f4} & Y_{js}^{f5} & .... & Y_{js}^{f17} & Y_{js}^{f18} & Y_{js}^{f19} & Y_{js}^{f20} \\ Y_{js}^{g1} & Y_{js}^{g2} & Y_{js}^{g3} & Y_{js}^{g4} & Y_{js}^{g5} & .... & Y_{js}^{g17} & Y_{js}^{g18} & Y_{js}^{g19} & Y_{js}^{g20} \\ Y_{js}^{h1} & Y_{js}^{h2} & Y_{js}^{h3} & Y_{js}^{h4} & Y_{js}^{h5} & .... & Y_{js}^{h17} & Y_{js}^{h18} & Y_{js}^{h19} & Y_{js}^{h20} \\ Y_{js}^{i1} & Y_{js}^{i2} & Y_{js}^{i3} & Y_{js}^{i4} & Y_{js}^{i5} & .... & Y_{js}^{i17} & Y_{js}^{i18} & Y_{js}^{i19} & Y_{js}^{i20} \end{bmatrix}$$

$Y_{js}^{d1} = \ddot{q}_1$; $Y_{js}^{d2} = \cos(q_2)(2\ddot{q}_1 + \ddot{q}_2) - \dot{q}_2 \sin(q_2)(2\dot{q}_1 + \dot{q}_2)$;

$Y_{js}^{d3} = \cos(q_3)(2\ddot{q}_1 + 2\ddot{q}_2 + \ddot{q}_3) - \dot{q}_3 \sin(q_3)(2\dot{q}_1 + 2\dot{q}_2 + \dot{q}_3)$;

$Y_{js}^{d4} = \cos(q_2 + q_3)(2\ddot{q}_1 + 2\ddot{q}_2 + \ddot{q}_3) - \sin(q_2 + q_3)(\dot{q}_2 + \dot{q}_3)(2\dot{q}_1 + \dot{q}_2 + \dot{q}_3)$;

$Y_{js}^{d5} = \ddot{q}_2$; $Y_{js}^{d6} = \ddot{q}_3$; $Y_{js}^{d7} = \cos(q_1)$; $Y_{js}^{d8} = \cos(q_1+q_2)$; $Y_{js}^{d9} = \cos(q_1+q_2+q_3)$;

$Y_{js}^{d10} = Y_{js}^{d11} = Y_{js}^{d12} = Y_{js}^{d13} = Y_{js}^{d14} = Y_{js}^{d15} = Y_{js}^{d16} = Y_{js}^{d17} = Y_{js}^{d18} = 0.$

$a_{11} = \sin(q_4+q_5+q_6)$; $a_{12} = \sin(q_1+q_2)$; $a_{13} = \cos(q_4+q_5+q_6)$;

$a_{14} = \sin(q_1+q_2+q_3)$; $a_{15} = \cos(q_1+q_2+q_3)$; $a_{16} = \cos(q_1+q_2)$; $a_{17} = \cos(q_4+q_5)$;

$a_{18} = \sin(q_4+q_5)$; $a_{19} = (\dot{q}_1+\dot{q}_2+\dot{q}_3)$; $a_{20} = (\dot{q}_1+\dot{q}_2)$; $a_{21} = (\dot{q}_4+\dot{q}_5+\dot{q}_6)$;

$a_{22} = (\dot{q}_4+\dot{q}_5)$.

$$
\begin{aligned}
Y_{js}^{d19} \;=\;& \ddot{q}_6[0.25a_{11}a_{12} - 0.25a_{13}a_{12} + 0.25a_{11}\sin(q_1) - 0.25a_{13}a_{14} + 0.25a_{14}a_{11}] \\
& -\ddot{q}_1[(0.25a_{14}+0.25a_{12})(a_{15}+a_{16}+\cos(q_1)) - (a_{14}+a_{12}+\sin(q_1)) \\
& (0.25a_{14}+0.25a_{12}+0.25\sin(q_1)]\ddot{q}_4[(0.25a_{14}+0.25a_{12})(a_{13}+a_{17}+\cos(q_4)) \\
& -(a_{11}+a_{18}+\sin(q_4))(0.25a_{14}+0.25a_{12}+0.25\sin(q_1)] - 0.5g(a_{14}+a_{12}) \\
& -\ddot{q}_3[a_{15}(0.25a_{14}+0.25a_{12}) - a_{14}(0.25a_{14}+0.25a_{12}+0.25\sin(q_1))] \\
& +\dot{q}_2[0.5\{(a_{14}a_{19}+a_{12}a_{20})(0.5a_{14}+0.5a_{12})\} + 0.5\{(a_{15}a_{19}+a_{16}a_{20}) \\
& (0.5a_{14}+0.5a_{12}+0.5\sin(q_1))\}] + \dot{q}_5[0.5\{(a_{11}a_{21}+a_{18}a_{22})(0.5a_{14}+0.5a_{12})\} \\
& +0.5\{(a_{13}a_{21}+a_{17}a_{22})(0.5a_{14}+0.5a_{12}+0.5\sin(q_1))\}] - \ddot{q}_5[(a_{13}+a_{17}) \\
& (0.25a_{14}+0.25a_{12}) - (a_{11}+a_{18})(0.25a_{14}+0.25a_{12}+0.25\sin(q_1))] \\
& \dot{q}_3[0.5\{a_{14}(0.5a_{14}+0.5a_{12})a_{19}\} + 0.5\{a_{15}(0.5a_{14}+0.5a_{12})a_{19}\}] \\
& \dot{q}_6[0.5\{a_{11}(0.5a_{14}+0.5a_{12})a_{21}\} + 0.5\{a_{13}(0.5a_{14}+0.5a_{12})a_{21}\}] \\
& +\dot{q}_1[0.5\{(0.5a_{14}+0.5a_{12})(a_{14}a_{19}+a_{12}a_{20}+\sin(q_1)\dot{q}_1)\} + 0.5\{(a_{12}a_{19} \\
& +a_{16}a_{20}+\cos(q_1)\dot{q}_1)(0.5a_{14}+0.5a_{12}+0.5\sin q_1)\}] \\
& +\dot{q}_4[0.5\{(0.5a_{14}+0.5a_{12})(a_{11}a_{21}+a_{18}a_{22}+\sin(q_4)\dot{q}_4)\} + 0.5\{(a_{13}a_{21} \\
& +a_{17}a_{22}+\cos(q_4)\dot{q}_4)(0.5a_{14}+0.5a_{12}+0.5\sin q_1)\}]
\end{aligned}
$$

$$+0.25[\ddot{q}_2(a_{14}+a_{12})(a_{14}-a_{15}-a_{16}+a_{12}+\sin(q_1))]$$

$a_{23}=\cos(q_1+q_2+\theta)$; $a_{24}=\cos(q_1-\theta)$; $a_{25}=\sin(q_1+q_2+\theta)$;

$a_{26}=\cos(q_1+q_2-\theta)$; $a_{27}=\sin(q_1+q_2-\theta)$; $a_{28}=\cos(q_1+q_2+q_3+\theta)$;

$a_{29}=\sin(q_1+q_2+q_3+\theta)$; $a_{30}=\cos(q_1+\theta)$; $a_{31}=\cos(q_1+q_2+q_3-\theta)$;

$a_{32}=\sin(q_1+q_2+q_3-\theta)$; $a_{33}=\sin(q_4+q_5+q_6-\theta)$; $a_{34}=\sin(q_1-\theta)$;

$a_{35}=\sin(q_4-\theta)$; $a_{36}=\sin(q_4+q_5-\theta)$; $a_{37}=\sin(q_1+q_2-\theta)$;

$a_{38}=\cos(q_4+q_5-\theta)$; $a_{39}=\cos(q_4+q_5+q_6-\theta)$;

$a_{40}=\cos(q_4-\theta)$; $a_{41}=\sin(q_1+\theta)$; $a_{42}=\cos(q_4+q_5+\theta)$; $a_{43}=\sin(q_4+q_5+\theta)$;

$a_{44}=\cos(q_4+q_5+q_6+\theta)$; $a_{45}=\sin(q_4+q_5+q_6+\theta)$;

$a_{46}=\sin(q_4+\theta)$; $a_{47}=\cos(q_4+\theta)$.

$$\begin{aligned}
Y_{js}^{d20} &= 0.04[(0.5a_{23}-0.5a_{24}-2a_{14}+0.5a_{25}-0.5a_{26}+0.5a_{27}+0.5a_{28}+0.5a_{29} \\
&\quad +0.5a30-0.5a_{31}+0.5a_{32})(2\dot{q}_1+2\dot{q}_2+2\dot{q}_3+2\dot{q}_4+2\dot{q}_5+2\dot{q}_6 \\
&\quad +a_{32}\dot{q}_1^2+a_{32}\dot{q}_2^2+a_{32}\dot{q}_3^2-a_{33}\dot{q}_4^2-a_{33}\dot{q}_5^2-a_{33}\dot{q}_6^2+a_{34}\dot{q}_1^2-a_{35}\dot{q}_4^2+a_{27}\dot{q}_1^2 \\
&\quad +a_{27}\dot{q}_2^2-a_{36}\dot{q}_4^2-a_{36}\dot{q}_5^2+2a_{32}\dot{q}_1\dot{q}_2+2a_{32}\dot{q}_1\dot{q}_3+2a_{32}\dot{q}_2\dot{q}_3-2a_{33}\dot{q}_4\dot{q}_5-2a_{33}\dot{q}_4\dot{q}_6 \\
&\quad -2a_{33}\dot{q}_5\dot{q}_6+2a_{37}\dot{q}_1\dot{q}_2-2a_{36}\dot{q}_4\dot{q}_5)]+0.04[(0.5a_{23}-0.5a_{24}-2a_{14}+0.5a_{25} \\
&\quad -0.5a_{26}+0.5a_{27}+0.5a_{28}+0.5a_{29}+0.5a30-0.5a_{31}+0.5a_{32}) \\
&\quad (2\ddot{q}_1+2\ddot{q}_2+2\ddot{q}_3+2\ddot{q}_4+2\ddot{q}_5+2\ddot{q}_6-a_{26}\ddot{q}_1-a_{26}\ddot{q}_2+a_{38}\ddot{q}_4+a_{38}\ddot{q}_5 \\
&\quad -a_{31}\ddot{q}_1-a_{31}\ddot{q}_2-a_{31}\ddot{q}_3+a_{39}\ddot{q}_4+a_{39}\ddot{q}_5+a_{39}\ddot{q}_6-a_{24}\ddot{q}_1+a_{40}\ddot{q}_4)]
\end{aligned}$$

$Y_{js}^{e1}=0$; $Y_{js}^{e2}=\sin(q_2)\dot{q}_1^2+\cos(q_2)\ddot{q}_1$;

$Y_{js}^{e3}=\cos(q_3)(2\ddot{q}_1+2\ddot{q}_2+\ddot{q}_3)-\dot{q}_3\sin(q_3)(2\dot{q}_1+2\dot{q}_2+\dot{q}_3)$;

$Y_{js}^{e4}=\sin(q_2+q_3)\dot{q}_1^2+\cos(q_2+q_3)\ddot{q}_1)$; $Y_{js}^{e5}=\ddot{q}_1+\ddot{q}_2$; $Y_{js}^{e6}=\ddot{q}_3$; $Y_{js}^{e7}=0$;

$Y_{js}^{e8} = \cos(q_1 + q_2);\ \ Y_{js}^{e9} = \cos(q_1 + q_2 + q_3);$

$Y_{js}^{e10} = Y_{js}^{e11} = Y_{js}^{e12} = Y_{js}^{e13} = Y_{js}^{e14} = Y_{js}^{e15} = Y_{js}^{e16} = Y_{js}^{e17} = Y_{js}^{e18} = 0.$

$$
\begin{aligned}
Y_{js}^{e19} \;=\;& \ddot{q}_3[0.25a_{15}(a_{15}+a_{16}) - 0.25a_{14}(a_{15}+a_{16}+\cos q_1)] - \dot{q}_2[0.5\{(a_{14}a_{19}+a_{12}a_{20}) \\
& 0.5(a_{15}+a_{16})\} + 0.5\{(a_{15}a_{19}+a_{16}a_{20})0.5(a_{15}+a_{16}+\cos q_1)\}] - \dot{q}_5[0.5\{(a_{11}a_{21} \\
& +a_{18}a_{22})0.5(a_{15}+a_{16})\} + 0.5\{(a_{13}a_{21}+a_{17}a_{22})0.5(a_{15}+a_{16}+\cos q_1)\}] \\
& 0.25(a_{15}+a_{16}) - (a_{14}+a_{12})0.25(a_{15}+a_{16}+\cos(q_1))] + \ddot{q}_5[(a_{13}a_{17})0.25(a_{15}+a_{16}) \\
& -(a_{11}+a_{18})0.25(a_{15}+a_{16}+\cos(q_1))] - \dot{q}_3[0.25\{a_{15}a_{19}(a_{15}+a_{16}\cos(q_1)\} \\
& +0.25\{a_{14}a_{19}(a_{15}+a_{16})\} - \dot{q}_6[0.25\{a_{13}a_{21} - \dot{(}a_{15}+a_{16}\cos(q_1)\} + 0.25\{a_{11}a_{21} \\
& (a_{15}+a_{16})\} - \dot{q}_1[0.25(a_{15}+a_{16})(a_{14}a_{19}+a_{12}a_{20}+\sin(q_1)\dot{q}_1) + 0.25(a_{15}+a_{16} \\
& +\cos q_1)(a_{15}a_{19}+(a_{16}+a_{20})+\cos(q_1)\dot{q}_1)] - \dot{q}_4[0.25(a_{15}+a_{16})(a_{11}a_{21}+a_{18}a_{22} \\
& +\sin(q_4)\dot{q}_4) + 0.25(a_{15}+a_{16}+\cos q_1)(a_{13}a_{21}+(a_{17}+a_{22})+\cos(q_1)\dot{q}_1)] \\
& +\ddot{q}_4[0.25(a_{14}+a_{16})(a_{13}+a_{17}+\cos q_4) - 0.25(a_{15}+a_{16}+\cos q_1)(a_{11}+a_{18}+\sin q_4)] \\
& +4.98(a_{15}+a_{16}) - \ddot{q}_6[0.25(a_{11}a_{16} - a_{13}a_{16} + a_{11}\cos q_1 - a_{15}a_{13} + a_{11}a_{15})] \\
& -\ddot{q}_1[0.25(a_{15}+a_{16}+\cos q_1)(a_{14} - a_{15} - a_{16} + a_{12} + \sin q_1)]
\end{aligned}
$$

$$
\begin{aligned}
Y_{js}^{e20} \;=\;& 0.04[0.5(a_{34} - 4a_{15} + a_{23} - a_{25} + a_{26} + a_{27} + a_{28} - a_{29} - a_{41} + a_{31} + a_{32}) \\
& 2(\dot{q}_1 + \dot{q}_2 + \dot{q}_3 + \dot{q}_4 + \dot{q}_5 + \dot{q}_6 + a_{32}\dot{q}_1^2 + a_{32}\dot{q}_2^2 + a_{32}\dot{q}_3^2 - a_{33}\dot{q}_4^2 - a_{33}\dot{q}_5^2 - a_{33}\dot{q}_6^2 \\
& +a_{34}\dot{q}_1^2 - a_{35}\dot{q}_4^2 + a_{27}\dot{q}_1^2 + a_{27}\dot{q}_2^2 - a_{36}\dot{q}_4^2 - a_{36}\dot{q}_5^2 + 2a_{32}\dot{q}_1\dot{q}_2 + 2a_{32}\dot{q}_1\dot{q}_3 + 2a_{32}\dot{q}_2\dot{q}_3 \\
& -2a_{33}\dot{q}_4\dot{q}_5 - 2a_{33}\dot{q}_4\dot{q}_6 - 2a_{33}\dot{q}_5\dot{q}_6 + 2a_{27}\dot{q}_1\dot{q}_2 - 2a_{36}\dot{q}_4\dot{q}_5 - 0.5(a_{34} - 4a_{15} + a_{23} \\
& -a_{25} + a_{26} + a_{27} + a_{28} - a_{29} - a_{41} + a_{31} + a_{32})(2\ddot{q}_1 + 2\ddot{q}_2 + 2\ddot{q}_3 + 2\ddot{q}_4 + 2\ddot{q}_5 + 2\ddot{q}_6 \\
& -a_{26}\ddot{q}_1 - a_{26}\ddot{q}_2 + a_{38}\ddot{q}_4 + a_{38}\ddot{q}_5 - a_{31}\ddot{q}_1 - a_{31}\ddot{q}_2 - a_{31}\ddot{q}_3 + a_{39}\ddot{q}_4 + a_{39}\ddot{q}_5
\end{aligned}
$$

$$+a_{39}\ddot{q}_6 - a_{24}\ddot{q}_1 + a_{40}\ddot{q}_4)]$$

$$Y_{js}^{f1} = 0;\ \ Y_{js}^{f2} = 0;\ \ Y_{js}^{f3} = \cos(q_3)(\ddot{q}_1 + \ddot{q}_2 + \ddot{q}_3) + \sin(q_3)(\dot{q}_1 + \dot{q}_2)^2;$$

$$Y_{js}^{f4} = \sin(q_2 + q_3)\dot{q}_1^2 + \cos(q_2 + q_3)\ddot{q}_1);\ \ Y_{js}^{f5} = 0;\ \ Y_{js}^{f6} = \ddot{q}_1 + \ddot{q}_2 + \ddot{q}_3;$$

$$Y_{js}^{f7} = 0;\ \ Y_{js}^{f8} = 0;\ \ Y_{js}^{f9} = \cos(q_1 + q_2 + q_3);$$

$$Y_{js}^{f10} = Y_{js}^{f11} = Y_{js}^{f12} = Y_{js}^{f13} = Y_{js}^{f14} = Y_{js}^{f15} = Y_{js}^{f16} = Y_{js}^{f17};\ \ Y_{js}^{f18} = 0.$$

$$\begin{aligned} Y_{js}^{f19} &= 0.5g + 0.25(a_{16}\ddot{q}_1 + a_{16}\ddot{q}_2 + a_{17}\ddot{q}_4 + a_{17}\ddot{q}_5 - a_{12}\ddot{q}_1 - a_{12}\ddot{q}_2 - a_{18}\ddot{q}_4 - a_{18}\ddot{q}_5 \\ &\quad + \cos(q_4)\ddot{q}_4 - \sin(q_1)\ddot{q}_1 - \sin(q_4)\ddot{q}_4 + a_{15}\ddot{q}_1 + a_{15}\ddot{q}_2 + a_{15}\ddot{q}_3 + a_{13}\ddot{q}_4 - a_{13}\ddot{q}_5 - \\ &\quad a_{14}\ddot{q}_1 - a_{14}\ddot{q}_2 + a_{14}\ddot{q}_3 - a_{11}\ddot{q}_4 - a_{11}\ddot{q}_5 - a_{11}\ddot{q}_6) \end{aligned}$$

$$\begin{aligned} Y_{js}^{f20} &= 0.04[(\sin(\theta) - \cos(\theta) + 2)(2\ddot{q}_1 + 2\ddot{q}_2 + 2\ddot{q}_3 + 2\ddot{q}_4 + 2\ddot{q}_5 + 2\ddot{q}_6 - a_{26}\ddot{q}_1 \\ &\quad - a_{26}\ddot{q}_2 + a_{38}\ddot{q}_4 + a_{38}\ddot{q}_5 - a_{31}\ddot{q}_1 - a_{31}\ddot{q}_2 - a_{31}\ddot{q}_3 + a_{39}\ddot{q}_4 + a_{39}\ddot{q}_5 + a_{39}\ddot{q}_6 \\ &\quad - a_{24}\ddot{q}_1 - a_{40}\ddot{q}_4)] + 0.04[(\sin(\theta) - \cos(\theta) + 2)(2\dot{q}_1 + 2\dot{q}_2 + 2\dot{q}_3 + 2\dot{q}_4 + 2\dot{q}_5 + 2\dot{q}_6 \\ &\quad + a_{32}\dot{q}_1^2 + a_{32}\dot{q}_2 + a_{32}\dot{q}_3^2 - a_{33}\dot{q}_4^2 - a_{33}\dot{q}_5^2 - a_{33}\dot{q}_6^2 + a_{34}\dot{q}_1^2 - a_{35}\dot{q}_4^2 + a_{27}\dot{q}_1^2 + a_{27}\dot{q}_2^2 \\ &\quad - a_{36}\dot{q}_4^2 - a_{36}\dot{q}_5^2 + 2(a_{32}\dot{q}_1\dot{q}_2 + a_{32}\dot{q}_1\dot{q}_3 + a_{32}\dot{q}_2\dot{q}_3 - a_{33}\dot{q}_4\dot{q}_5 - a_{33}\dot{q}_4\dot{q}_6 - a_{33}\dot{q}_5\dot{q}_6 \\ &\quad a_{27}\dot{q}_1\dot{q}_2 - a_{36}\dot{q}_4\dot{q}_5))] \end{aligned}$$

$$Y_{js}^{g1} = Y_{js}^{g2} = Y_{js}^{g3} = Y_{js}^{g4} = Y_{js}^{g5} = Y_{js}^{g6} = Y_{js}^{g7} = Y_{js}^{g8} = Y_{js}^{g9} = 0;$$

$$Y_{js}^{g10} = \ddot{q}_4;\ \ Y_{js}^{g11} = \cos q_5(2\ddot{q}_4 + \ddot{q}_5) - \sin q_5\dot{q}_5(2\dot{q}_4 + \dot{q}_5);$$

$$Y_{js}^{g12} = \cos q_6(2\ddot{q}_4 + 2\ddot{q}_5 + \ddot{q}_6) - \sin q_6\dot{q}_6(2\dot{q}_4 + 2\dot{q}_5 + \dot{q}_6);$$

$$Y_{js}^{g13} = \cos q_5 + q_6(2\ddot{q}_4 + \ddot{q}_5 + \ddot{q}_6) - \sin q_5 + q_6(\dot{q}_5 + \dot{q}_6)(2\dot{q}_4 + \dot{q}_5 + \dot{q}_6);\ \ Y_{js}^{g14} = \ddot{q}_5;$$

$$Y_{js}^{g15} = \ddot{q}_6;\ \ Y_{js}^{g16} = \cos q_4;\ \ Y_{js}^{g17} = \cos q_4 + q_5;\ \ Y_{js}^{g18} = \cos q_4 + q_5 + q_6.$$

$$\begin{aligned} Y_{js}^{g19} &= \ddot{q}_3[0.25(a_{14}a_{18} - a_{15}a_{18} + a_{14}\sin q_4 - a_{15}a_{11} + a_{14}a_{11})] - \ddot{q}_1[0.25(a_{11} + a_{18}) \\ &\quad (a_{15} + a_{16} + \cos q_1) - 0.25(a_{14} + a_{12} + \sin q_1)(a_{11} + a_{18} + \sin q_4) \end{aligned}$$

$$
\begin{aligned}
&-\ddot{q}_4[0.25(a_{11}+a_{18})(a_{13}+a_{17}+\cos q_4)-0.25(a_{11}+a_{18}+\sin q_4)\\
&(a_{11}+a_{18}+\sin q_4)]-0.5g(a_{11}+a_{18})-\ddot{q}_6[0.25a_{13}(a_{11}+a_{18})-0.25a_{11}\\
&(a_{11}+a_{18}+\sin q_4)]+\dot{q}_2[0.5\{(a_{14}a_{19}+a_{12}a_{20})(0.5a_{11}+0.5a_{18})\}]\\
&+0.5\{(a_{15}a_{19}+a_{16}a_{20})(0.5a_{11}+0.5a_{18})+0.5\sin q_4\}+\dot{q}_5[0.5\{(a_{11}a_{21}+a_{18}a_{22})\\
&(0.5a_{11}+0.5a_{18})\}]+0.5\{(a_{13}a_{21}+a_{17}a_{22})(0.5a_{11}+0.5a_{18})+0.5\sin q_4\}\\
&-\ddot{q}_2[0.25(a_{15}a_{16})(a_{11}+a_{18})-0.25(a_{14}+a_{12})(a_{11}+a_{18}+\sin q_4)]\\
&+\dot{q}_3[0.25a_{14}a_{19}(a_{11}+a_{18})+0.25a_{15}a_{19}(a_{11}+a_{18}+\sin q_4)]\\
&+\dot{q}_6[0.25a_{11}a_{21}(a_{11}+a_{18})+0.25a_{13}a_{19}(a_{11}+a_{18}+\sin q_4)]\\
&+\dot{q}_1[0.25(a_{11}+a_{18})(a_{14}a_{19}+a_{12}a_{20}+\sin q_1\dot{q}_1)+0.25(a_{15}a_{19}+a_{16}a_{20}+\cos q_1\dot{q}_1)\\
&(a_{11}+a_{18}+\sin q_4)]+\dot{q}_4[0.25(a_{11}+a_{18})(a_{11}a_{21}+a_{18}a_{22}+\sin q_4\dot{q}_4)+0.25(a_{13}a_{21}\\
&+a_{17}a_{22}+\cos q_4\dot{q}_4)(a_{11}+a_{18}+\sin q_4)]\\
&+0.25\ddot{q}_5[(a_{11}+a_{18})(a_{11}-a_{13}-a_{17}+a_{18}+\sin q_4)]
\end{aligned}
$$

$$
\begin{aligned}
Y_{js}^{g20} = \;& -0.04[0.5(a_{42}-a_{40}+4a_{11}+a_{43}-a_{38}-a_{36}+a_{44}+a_{45}+a_{47}-a_{39}+a_{33})\\
&\{2(\dot{q}_1+\dot{q}_2+\dot{q}_3+\dot{q}_4+\dot{q}_5+\dot{q}_6)+a_{32}\dot{q}_1^2+a_{32}\dot{q}_2^2+a_{32}\dot{q}_3^2-a_{33}\dot{q}_4^2-a_{33}\dot{q}_5^2-a_{33}\dot{q}_6^2\\
&+a_{34}\dot{q}_1^2-a_{35}\dot{q}_4^2+a_{27}\dot{q}_1^2+a_{27}\dot{q}_2^2-a_{36}\dot{q}_4^2-a_{36}\dot{q}_5^2+2a_{32}\dot{q}_1\dot{q}_2+2a_{32}\dot{q}_1\dot{q}_3\\
&+2a_{32}\dot{q}_2\dot{q}_3-2a_{33}\dot{q}_4\dot{q}_5-2a_{33}\dot{q}_4\dot{q}_6-2a_{33}\dot{q}_5\dot{q}_6+2a_{27}\dot{q}_1\dot{q}_2-2a_{36}\dot{q}_4\dot{q}_5\}]\\
&-0.04[0.5(a_{42}-a_{40}+4a_{11}+a_{43}-a_{38}-a_{36}+a_{44}+a_{45}+a_{47}-a_{39}+a_{33})\\
&\{2(\ddot{q}_1+\ddot{q}_2+\ddot{q}_3+\ddot{q}_4+\ddot{q}_5+\ddot{q}_6)-a_{26}\ddot{q}_1-a_{26}\ddot{q}_2+a_{38}\ddot{q}_4+a_{38}\ddot{q}_5\\
&-a_{31}\ddot{q}_1-a_{31}\ddot{q}_2-a_{31}\ddot{q}_3+a_{39}\ddot{q}_4+a_{39}\ddot{q}_5+a_{39}\ddot{q}_6-a_{24}\ddot{q}_1+a_{40}\ddot{q}_4\}]
\end{aligned}
$$

$$Y_{js}^{h1} = Y_{js}^{h2} = Y_{js}^{h3} = Y_{js}^{h4} = Y_{js}^{h5} = Y_{js}^{h6} = Y_{js}^{h7} = Y_{js}^{h8} = Y_{js}^{h9} = 0;$$

$$Y_{js}^{h10} = 0;\ \ Y_{js}^{h11} = \sin q_5 \dot{q}_4^2 + \cos q_5 \ddot{q}_4;$$

$$Y_{js}^{h12} = \cos q_6 (2\ddot{q}_4 + 2\ddot{q}_5 + \ddot{q}_6) - \sin q_6 \dot{q}_6 (2\dot{q}_4 + 2\dot{q}_5 + \dot{q}_6);\ \ Y_{js}^{h13} = \sin q_5 + q_6 \dot{q}_4^2 + \cos q_5 + q_6 \ddot{q}_4;$$

$$Y_{js}^{h14} = \ddot{q}_4 + \ddot{q}_5;\ \ Y_{js}^{h15} = \ddot{q}_6;\ \ Y_{js}^{h16} = 0;\ \ Y_{js}^{h17} = \cos(q_4 + q_5);\ \ Y_{js}^{h18} = \cos(q_4 + q_5 + q_6).$$

$$\begin{aligned}
Y_{js}^{h19} \;=\;& \ddot{q}_6(0.25a_{13}(a_{13}+a_{17}) - 0.25a_{11}(a_{13}+a_{17}+\cos q_4)) - \dot{q}_2[0.5(a_{14}a_{19}+a_{12}a_{20}) \\
& (0.5a_{13}+0.5a_{17}) + (a_{14}a_{19}+a_{12}a_{20})(0.5a_{13}+0.5a_{17}+0.5\cos q_4) \\
& -\dot{q}_5[0.5(a_{11}a_{21}+a_{18}a_{22})(0.5a_{13}+0.5a_{17}) + (a_{13}a_{21}+a_{17}a_{22}) \\
& (0.5a_{13}+0.5a_{17}+0.5\cos q_4) + \ddot{q}_2[(a_{15}+a_{16})(0.25a_{13}+0.25a_{17}) - (a_{14}+a_{12}) \\
& (0.25a_{13}+0.25a_{17}+0.25\cos q_4)] + \ddot{q}_5[(a_{13}+a_{17})(0.25a_{13}+0.25a_{17}) - (a_{11}+a_{18}) \\
& (0.25a_{13}+0.25a_{17}+0.25\cos q_4)] - \dot{q}_3[0.5a_{15}a_{19}(0.5a_{13}+0.5a_{17}+0.5\cos q_4) \\
& +0.5a_{14}a_{19}(0.5a_{13}+0.5a_{17})] - \dot{q}_6[0.5a_{13}a_{21}(0.5a_{13}+0.5a_{17}+0.5\cos q_4) \\
& +0.5a_{11}a_{21}(0.5a_{13}+0.5a_{17})] - \dot{q}_1[0.5(0.5a_{13}+0.5a_{17})(a_{14}a_{19}+a_{12}a_{20}+\sin q_1\dot{q}_1) \\
& +(0.5a_{13}+0.5a_{17}+0.5\cos q_4)(a_{15}a_{19}+a_{16}a_{20}+\cos q_1\dot{q}_1)] - \dot{q}_4[0.5(0.5a_{13}+0.5a_{17}) \\
& (a_{11}a_{21}+a_{18}a_{22}+\sin q_4\dot{q}_4) + (0.5a_{13}+0.5a_{17}+0.5\cos q_4) \\
& (a_{13}a_{21}+a_{17}a_{22}+\cos q_4\dot{q}_4)] + \ddot{q}_1[(0.25a_{13}+0.25a_{17})(a_{15}+a_{16}+\cos q_1) \\
& -(0.25a_{13}+0.25a_{17}+0.25\cos q_4)(a_{14}+a_{12}+\sin q_1)] + 0.5g(a_{13}+a_{17}) \\
& -\ddot{q}_3[0.25a_{14}a_{17} - 0.25a_{15}a_{17} + 0.25a_{14}\cos q_4 - 0.25a_{15}a_{13} + 0.25a_{13}a_{14}] - 0.25\ddot{q}_4 \\
& [(a_{13}+a_{17}+\cos q_4)(a_{11}-a_{13}-a_{17}+a-18+\sin q_4) - 0.25a_{15}a_{13} + 0.25a_{13}a_{14}]
\end{aligned}$$

$$\begin{aligned}
Y_{js}^{h20} \;=\;& 0.04[(2a_{13}+0.5a_{35}+0.5a_{42}-0.5a_{43}+0.5a_{38}+0.5a_{36}+0.5a_{44}-0.5a_{45}+0.5a_{46} \\
& +0.5a_{39}+0.5a_{33})(2\dot{q}_1+2\dot{q}_2+2\dot{q}_3+2\dot{q}_4+2\dot{q}_5+2\dot{q}_6+a_{32}\dot{q}_1^2+a_{32}\dot{q}_2^2+a_{32}\dot{q}_3^2 \\
& -a_{33}\dot{q}_4^2-a_{33}\dot{q}_5^2-a_{33}\dot{q}_6^2+a_{34}\dot{q}_1^2-a_{35}\dot{q}_4^2+a_{27}\dot{q}_1^2+a_{27}\dot{q}_2^2-a_{36}\dot{q}_4^2-a_{36}\dot{q}_5^2+2a_{32}\dot{q}_1\dot{q}_2
\end{aligned}$$

$$+2a_{32}\dot{q}_1\dot{q}_3+2a_{32}\dot{q}_2\dot{q}_3-2a_{33}\dot{q}_4\dot{q}_5-2a_{33}\dot{q}_4\dot{q}_6-2a_{33}\dot{q}_5\dot{q}_6+2a_{27}\dot{q}_1\dot{q}_2-2a_{36}\dot{q}_4\dot{q}_5\}]$$

$$-0.04[(2a_{13}+0.5a_{35}+0.5a_{42}-0.5a_{43}+0.5a_{38}-0.5a_{36}+0.5a_{44}-0.5a_{45}$$

$$-0.5a_{46}+0.5a_{39}+0.5a_{33})\{2(\ddot{q}_1+\ddot{q}_2+\ddot{q}_3+\ddot{q}_4+\ddot{q}_5+\ddot{q}_6)-a_{26}\ddot{q}_1-a_{26}\ddot{q}_2$$

$$+a_{38}\ddot{q}_4+a_{38}\ddot{q}_5-a_{31}\ddot{q}_1-a_{31}\ddot{q}_2-a_{31}\ddot{q}_3+a_{39}\ddot{q}_4+a_{39}\ddot{q}_5+a_{39}\ddot{q}_6-a_{24}\ddot{q}_1+a_{40}\ddot{q}_4\}]$$

$$Y_{js}^{i19} = 0.5g-\dot{q}_3(0.25a_{15}a_{19}+0.25a_{14}a_{19})-\dot{q}_6(0.25a_{13}a_{21}+0.25a_{11}a_{21})$$

$$+0.25(a_{16}\ddot{q}_1+a_{16}\ddot{q}_2+a_{17}\ddot{q}_4+a_{17}\ddot{q}_5-a_{12}\ddot{q}_1-a_{12}\ddot{q}_2-a_{18}\ddot{q}_4a_{18}\ddot{q}_5$$

$$+\cos q_1\ddot{q}_1+\cos q_4\ddot{q}_4)-\dot{q}_5[0.25a_{13}a_{21}+0.25a_{11}a_{21}+0.25a_{17}a_{22}+0.25a_{18}a_{22}]$$

$$-0.25(a_{16}\ddot{q}_1+a_{16}\ddot{q}_2+a_{17}\ddot{q}_4+a_{17}\ddot{q}_5-a_{12}\ddot{q}_1-a_{12}\ddot{q}_2-a_{18}\ddot{q}_4$$

$$-0.25(\sin q_1\ddot{q}_1-\sin q_4\ddot{q}_4+a_{15}\ddot{q}_1+a_{15}\ddot{q}_2+a_{15}\ddot{q}_3+a_{13}\ddot{q}_4+a_{13}\ddot{q}_5+a_{13}\ddot{q}_6)$$

$$-\dot{q}_1[0.25a_{15}a_{19}+0.25a_{14}a_{19}+0.25a_{16}a_{20}+0.25a_{12}a_{20}+0.25\cos q_1\dot{q}_1$$

$$+0.25\sin q_1\dot{q}_1]-\dot{q}_4[0.25a_{13}a_{21}+0.25a_{11}a_{21}+0.25a_{17}a_{22}+0.25a_{18}a_{22}$$

$$+0.25\cos q_4\dot{q}_4+0.25\sin q_4\dot{q}_4]-0.25(a_{14}\ddot{q}_1-a_{14}\ddot{q}_2-a_{14}\ddot{q}_3-a_{11}\ddot{q}_4-a_{11}\ddot{q}_5-a_{11}\ddot{q}_6)$$

$$Y_{js}^{i20} = 0.04[(\cos(\theta)-\sin(\theta)+2)\{2(\ddot{q}_1+\ddot{q}_2+\ddot{q}_3+\ddot{q}_4+\ddot{q}_5+\ddot{q}_6)-a_{26}\ddot{q}_1$$

$$-a_{26}\ddot{q}_2+a_{38}\ddot{q}_4+a_{38}\ddot{q}_5-a_{31}\ddot{q}_1-a_{31}\ddot{q}_2-a_{31}\ddot{q}_3+a_{39}\ddot{q}_4+a_{39}\ddot{q}_5+a_{39}\ddot{q}_6$$

$$-a_{24}\ddot{q}_1+a_{40}\ddot{q}_4\}]+0.04[(\cos(\theta)-\sin(\theta)+2)\{2(\dot{q}_1+\dot{q}_2+\dot{q}_3+\dot{q}_4+\dot{q}_5+\dot{q}_6)$$

$$+a_{32}\dot{q}_1^2+a_{32}\dot{q}_2^2+a_{32}\dot{q}_3^2-a_{33}\dot{q}_4^2-a_{33}\dot{q}_5^2-a_{33}\dot{q}_6^2$$

$$+a_{34}\dot{q}_1^2-a_{35}\dot{q}_4^2+a_{27}\dot{q}_1^2+a_{27}\dot{q}_2^2-a_{36}\dot{q}_4^2-a_{36}\dot{q}_5^2+2a_{32}\dot{q}_1\dot{q}_2+2a_{32}\dot{q}_1\dot{q}_3$$

$$+2a_{32}\dot{q}_2\dot{q}_3-2a_{33}\dot{q}_4\dot{q}_5-2a_{33}\dot{q}_4\dot{q}_6-2a_{33}\dot{q}_5\dot{q}_6+2a_{27}\dot{q}_1\dot{q}_2-2a_{36}\dot{q}_4\dot{q}_5\}]$$

C.2 Time independent parameters

$$\alpha_{js} = [p11 \;\; p12 \;\; p13 \;\; p14 \;\; p15 \;\; p16 \;\; p17 \;\; p18 \;\; p19 \;\; p21 \;\; p22 \;\; p23 \;\; p24$$
$$p25 \;\; p26 \;\; p27 \;\; p28 \;\; p29 \;\; p31 \;\; p32]^T$$

Publications

Journal

1. Balasubramanian Esakki, Rama Bhat, Chun-Yi Su, ”Robust trajectory tracking and vibration control of two planar rigid manipulators moving a flexible object”, (Submitted in IEEE Transaction on Robotics).

Conferences

1. Balasubramanian Esakki, Rama Bhat, Chun-Yi Su, ”Regressor Based Robust Control for Collaborative Manipulators Handling an Object”, (Accepted for publication in 18th International Federation of Automatic Control World Congress, Milan, Italy.)

2. Balasubramanian Esakki, Rama Bhat, Chun-Yi Su, ”Trajectory tracking and vibration control of two planar rigid manipulators moving a flexible object”, (Submitted in International Conference on Intelligent Robotics and Applications, Germany.)